Synthetic receptors for ammonium ions using dynamic combinatorial chemistry

Hamieh, Saleh

Synthetic Receptors for Ammonium Ions Using Dynamic Combinatorial Chemistry

Saleh Hamieh

The work described in this thesis was executed at the Stratingh Institute for Chemistry, University of Groningen, The Netherlands.

university of groningen

This work was financially supported by Marie Curie Actions and University of Groningen

Printed by: Ipskamp Drukkers B. V., Enschede, The Netherlands.

Cover design by: Saleh Hamieh

ISBN: 978-90-367-7579-3 (printed version)

ISBN: 978-90-367-7578-6 (electronic version)

university of groningen

Synthetic Receptors for Ammonium Ions Using Dynamic Combinatorial Chemistry

PhD thesis

to obtain the degree of PhD at the
University of Groningen
on the authority of the
Rector Magnificus Prof. E. Sterken
and in accordance with
the decision by the College of Deans.

This thesis will be defended in public on

Friday 9 January 2015 at 11.00 hours

by

Saleh Hamieh

[redacted]

Supervisor
Prof. S. Otto

Assessment committee
Prof. A.H. Velders
Prof. S. Kubik
Prof. W.R. Browne

To my kind mother and generous father

Contents

Introduction chapter: Molecular recognition of organic ammonium ions using dynamic combinatorial chemistry 1

1.1 The importance of molecular recognition of organic ammonium ions 2

1.2 The main interactions involved in the molecular recognition of organic ammonium ions 2

1.2.1 Protein receptors 2

1.2.2 Synthetic receptors 7

1.3 Requirements for molecular recognition of an organic ammonium ion: (electrostatic and steric) complementarity and preorganization of host-guest interacting groups 10

1.4 Relevant synthetic receptors for organic ammonium ions in water 11

1.4.1 Cucurbit[7]uril: a synthetic receptor with ultra high affinity 11

1.4.2 Sugammadex: a semi-synthetic receptor approved as a therapeutic agent 12

1.5 Merits and disadvantages of synthetic receptors for organic ammonium ions 13

1.6 Dynamic Combinatorial chemisty (DCC) 14

1.6.1 Definition of terms: DCC, building blocks, DCL, amplification and thermodynamic equilibrium 14

1.6.2 Selection approaches in a DCL system, definition of the term template 15

1.6.3 External templating in DCC as an alternative approach to develop synthetic receptors 15

1.6.4 Disulfide exchange for creating DCLs of water soluble synthetic receptors 16

1.6.5 Relevant macrocyclic receptors obtained from a disulfide DCL 17

1.7 References 20

Chapter 2: A synthetic receptor for nicotine from a dynamic combinatorial library 25

2.1 Introduction 26

2.1 Building block design 26

2.2 Results and Discussion 27

2.2.1 Synthesis of building block **1** 27

2.2.2 Dynamic combinatorial libraries 28

2.2.3 Binding Studies 33

2.3 Conclusion and outlook 36

2.4 Experimental section 37

2.4.1 Materials and Methods 37
2.4.2 Synthetic procedures for building block **1** 37
2.4.3 Methods of preparation and analysis of dynamic combinatorial libraries 40
2.5 References 42
Chapter 3: A “dial-a-receptor” dynamic combinatorial library 43
3.1 Introduction 44
3.2 DCL design 44
3.2.1 Choice of building blocks 44
3.2.2 DCL composition 44
LC-MS data of the cyclic disulfide products 47
LC-MS data of the (linear) disulfinic acid side products 50
3.2.3 Choice of the templates 51
3.3 Effect of the chosen templates on the DCL made from **2** and **3** 52
3.3.1 New methodology to compare the amplification factors of the library members 57
3.3.2 Methodology for converting HPLC-UV peak areas of library members into their corresponding concentrations 58
3.3.3 DMSO sample dilution 59
3.3.4 Equation relating HPLC-UV peak areas of library members to their corresponding concentrations 60
3.3.5 Control experiments to test the additivity of the HPLC-UV peak areas of building blocks **2** and **3** 61
3.3.6 Normalized amplification factors 64
3.4 Conclusion 68
3.5 Experimental part 69
3.5.1 DCL preparations 69
3.5.2 HPLC and LC-MS analyseses 69
3.5.3 Analysis of a DCL made from building block **3** 70
3.6 References 73
Chapter 4: Towards selective synthetic receptors for aliphatic α,ω-diamines using dynamic combinatorial chemistry 77
4.1 Introduction 78
4.1.1 Biological importance of aliphatic α,ω-diamines of low molecular weight 78
4.1.2 Ditopic synthetic receptors for selective recognition of α,ω-diamines in organic solvents 78

4.1.3 Synthetic receptors for selective recognition of α,ω-diamines in aqueous medium 83
4.1.4 Evaluation of the binding quality between the reported receptors and α,ω-diamines 85
4.1.5 Features of binding of macrocycle (**3**)$_4$ to α,ω-alkanediammonium ions of n = 4 85
4.1.6 Aim of the research reported in this chapter 86
4.2 DCL studies 87
4.2.1 Methodology of data analysis 87
4.2.2 Effect of α,ω-diamine templates on a DCL made from building block **3** 88
4.2.3 Effect of aliphatic α,ω-diamine templates on a DCL made from **2** 89
4.2.4 Effect of aliphatic α,ω-diamine templates on a DCL made from **2** and **3** 92
4.3 Conclusion 97
4.4 Experimental section 98
4.4.1 Methods of preparation of DCLs 98
4.4.2 HPLC analysis conditions 98
4.4.3 HPLC-UV peak areas (mAU·min) and AFs of the DCL members formed from the combination of building blocks **2** and **3** 99
4.4.4 Concentrations (mM) of the DCL members formed from the combination of building blocks **2** and **3** 100
4.5 References 103
Chapter 5: Estimation of host-guest binding constants from the product distributions of dynamic combinatorial libraries 105
5.1 Introduction 106
5.1.1 How DCLFit works: a general overview 108
5.2 DCL studies and choice of the fitting model 109
5.2.1 DCL studies 109
5.2.2 Model used to fit K_a (**2**)$_n$(**3**)$_m$-template 109
5.3 Fitting results for guests **3.9**-**3.12** 110
5.3.1 Simplification of the model 110
5.3.2 Fitting results for guest **3.9** 110
5.3.3 Fitting results for guest **3.10** 111
5.3.4 Fitting results for guest **3.11** 112
5.3.5 Fitting results for guest **3.12** 113
5.3.6 Evaluation of the quality of the fit of K_a (**2**)$_n$(**3**)$_m$-**3.9**, **3.10**, **3.11** and **3.12** 114

5.4 Validation of some of the fitted affinity constants against their corresponding values obtained using ITC 119

5.5 AF and not AF_n reflects the binding strength of the most amplified library member at substoichiometric template concentration 119

5.6 Range of affinity constants that DCLFit can reliably generate 121

5.7 Conclusion 121

5.8 Experimental section 123

5.8.1 DCL preparations 123

5.8.2 HPLC-UV analysis 123

5.8.3 Quantification of overoxidized species 124

5.8.4 Measured HPLC-UV peak areas 125

5.8.5 Amplification factor (AF) data 127

5.8.6 Fitting details and graphs of the ratio of fitted to observed concentrations of $(\mathbf{3})_4$ and $(\mathbf{2})(\mathbf{3})_3$ in the presence of templates **3.10** and **3.11**, after constraining K_a of binding of $(\mathbf{2})_2(\mathbf{3})_2$ and $(\mathbf{2})_3(\mathbf{3})$ to **3.10** and **3.11** to the values obtained using ITC 129

5.8.7 Variation of observed concentrations of the oligomers as a function of concentrations of the individual templates 131

5.9 References 134

Chapter 6: Dynamic combinatorial chemistry with amino acid derivatized building blocks: towards new structurally diverse and more responsive dynamic combinatorial libraries 137

6.1 Introduction 138

6.1.1 Natural and synthetic amino acid derived macrocycles: structures and applications 138

6.1.2 DCLs of amino acid functionalized macrocycles: structures and applications 142

6.1.3 Intra-molecular interactions in an amino acid derived host may reinforce guest binding 144

6.2 Work motivation 145

6.3 Building block syntheses 147

6.3.1 Synthesis of valine derived naphthalene dithiol building block 147

6.3.2 Synthesis of valine derived benzene dithiol building block 148

6.4 DCL studies 150

6.4.1 DCL made from valine derived naphthalene dithiol building block **4** 150

6.4.2 DCL made from building blocks **1** and **4** 157

6.4.3 DCL made from building blocks **3** and **4** 167

6.4.4 DCL made from building blocks **2** and **5** 174
6.4.5 DCL made from building blocks **4** and **5** 178
6.5 Conclusion and outlook 182
6.6 Experimental section 183
6.6.1 General Points 183
6.6.2 DCL preparations 183
6.6.3 HPLC and HPLC-MS analysis conditions 183
6.6.4 DCL made from building block **5** 184
6.6.5 Synthesis of building blocks **4** and **5** 185
6.7 References 189
Chapter 7: Outlook 191
Summary 195
Samenvatting 199
Synthèse 203
Acknowledgements 205
Curriculum Vitae 209

Introduction chapter: Molecular recognition of organic ammonium ions using dynamic combinatorial chemistry

This chapter is an introduction to the general topic of this dissertation: the development of synthetic receptors for organic ammonium ions in near physiological conditions using dynamic combinatorial chemistry (DCC). The first part of this chapter sheds some light on the biological importance of molecular recognition of organic ammonium ions which explains our interest in developing synthetic receptors for this class of compounds. The second part introduces the main interactions involved in the molecular recognition of organic ammonium ions by proteins and synthetic receptors. This includes their definition, importance, geometry and strength. The third part discusses the general requirements for molecular recognition of organic ammonium ions by synthetic receptors in water. It includes the discussion of the geometry of a successful receptor. This is followed, in the fourth part, by a review of two successful receptors for organic ammonium ions: cucurbit[7]uril with an ultra high affinity and sugammadex with approved therapeutic application.

The fifth part considers the merits and demerits of synthetic receptors for organic ammonium ions. It includes the latest successful applications of these receptors, but also the difficulties associated with their development using the iterative approach: design, synthesis and testing.

The sixth part of the chapter explains the concept of dynamic combinatorial chemistry (DCC) and how this can be used as an alternative approach to develop synthetic receptors able to recognize organic ammonium ions in near physiological conditions, and how this may provide a method superior to the traditional, iterative approach.

1.1 The importance of molecular recognition of organic ammonium ions

The amino group is a widespread functional group in biologically active molecules. For instance, this group exists in amino acids and their derivatives, growth factors,[1] neurotransmitters[2] and many synthetic therapeutic and abused drugs. Biologically active molecules with one or more amino groups (*i.e.* biogenic amines) have always been subjects of ongoing research to supramolecular chemists. Catecholamines such as epinephrine (**1.1**) (Figure 1.1) and naturally occurring polyamines such as spermine (**1.2**) and nicotine (**1.3**) are examples of biogenic amines.

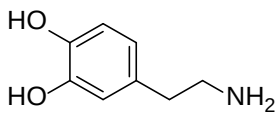

1.1

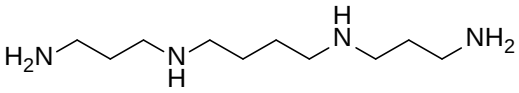

1.2

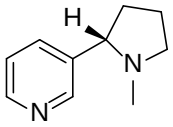

1.3

Figure 1.1: Examples of biogenic amines.

Selective interactions of biogenic amines, usually protonated as ammonium ions under physiological conditions, with protein receptors result in diverse biological signal transduction processes.[3-10] For instance, the binding of epinephrine (**1.1**) to two types of G protein-coupled receptors results in the breakdown of glycogen and triacylglycerol into glucose and fatty acids, respectively.[3] This is particularly important in mediating the body's response to stress when all tissues have an increased need for glucose and fatty acids.[3] Naturally occurring linear polyamines such as spermine (**1.2**) stabilize, upon binding, cellular polynucleic acid structures and protect them against denaturation[4] and shearing.[5] Also, they seem to play a pivotal role in activating protein kinases and transcription factors.[6]
Binding of smoked nicotine (**1.3**) to the nicotinic acetylcholine receptors α4β2 located in the brain,[7] which is strongly associated with nicotine addiction, acutely activates these receptors.[8] This results in cognitive emotional sensitization attributed to negative thoughts and enhancement of emotional states.[9] Nicotine (**1.3**) also acts as an intracellular pharmacological chaperone of α4β2 receptors[8] leading to their up-regulation thought to underlie the effects of chronic nicotine exposure.[10]
Therefore, in view of the important roles played by biogenic ammonium ion compounds in biology,[11] studying their molecular recognition by biological receptors and designing synthetic receptors able to selectively recognize these compounds may lead to a better understanding of many biological processes and is of ongoing interest.

1.2 The main interactions involved in the molecular recognition of organic ammonium ions

1.2.1 Protein receptors

The interactions of organic ammonium ions with protein receptors are achieved through a complex series of non-covalent interactions between functional groups exhibiting electronic complementarity. These interactions constitute the forces that hold the assembled complexes together. Individually, these interactions are typically much weaker than covalent bonds. For instance, in aqueous solution each non-covalent interaction has a typical bond

energy around -3 to -5 kJ mol^{-1}, whereas the typical covalent bond energy is around -350 to -940 kJ mol^{-1}.[12] However, when several non-covalent interactions are combined, robust and specific molecular recognition can be achieved. The binding of organic ammonium ions with protein receptors relies typically on a number of specific non-covalent interactions. Three types of these interactions, mostly acting simultaneously, are usually the most important: hydrogen bonds, cation–π interactions and ion pairs and salt bridges.[13] Herein we define these interactions and discuss their geometries (if relevant), and their strengths and benefits in biological and also synthetic environments.

1.2.1.1 Hydrogen bonds

Definition

A hydrogen bond is an attractive and specific interaction between a hydrogen donor (A-H) and a hydrogen acceptor (B). Hydrogen bonding is attributed to a simple electrostatic attraction between the positive end of the bond dipole of $A^{\delta-}$-$H^{\delta+}$, provided that A is more electronegative than H, and the negative end of the dipole associated with $B^{\delta-}$ (or the negative monopole on B^- if it is an anion or the lone pair of electrons on B).[14] This results in a hydrogen atom attracted by rather strong forces to two atoms (A and B) instead of only one (A). Atoms A and B are usually the highly electronegative such as N, O, and F, which tend to induce large dipole moments.

Importance

Hydrogen bonds are perhaps the most ubiquitous of all non-covalent interactions. They are responsible for the extraordinary properties of water by keeping water in a liquid state at room temperature and a low density solid below 0^oC. They play an important role in maintaining the three-dimensional structures adopted by proteins and nucleic acids (Figure 1.2).[15] Moreover, these interactions contribute favorably to the conformational stabilities of proteins by dictating the folded/unfolded equilibrium.[16] In solution, binding of ammonium ion compounds to synthetic receptors such as crown ethers occurs by hydrogen bonding between oxygen atoms (or nitrogen, sulfur or other free electron pair in hetero crown ethers) and strongly polarized N^+–H bonds. The binding strength decreases in the order primary > secondary > tertiary ammonium ion, depending on the number of H-bonds that can be formed with the guest. Quaternary ammonium ions cannot be bound by hydrogen bonds.

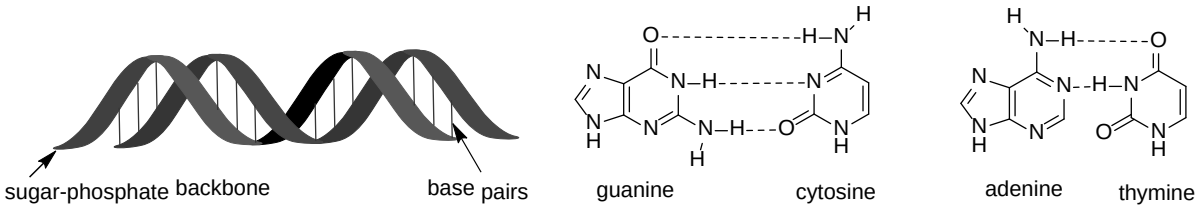

Figure 1.2: Schematic representation of the double-helix structure of DNA and structures of the base pairs linked by hydrogen bonds, as reported by Watson and Crick.[17]

Geometry

The inductive withdrawal of electron density from the hydrogen atom results in the directional nature of hydrogen bonds. The positive dipole extending from the hydrogen atom (in A-H) is in line with the formed B---H hydrogen bond and therefore crystal structures mainly show a linear arrangement of the three atoms.[11] Bifurcated hydrogen bonds can also be observed where a single hydrogen atom participates in two hydrogen bonds rather than one.[18]

Strength

If a solute is exposed to a competing solvent such as polar, hydrogen bond donor or acceptor solvents,[19] a single hydrogen bond cannot contribute with much binding energy. The computed contribution of hydrogen bonding to protein stability averages at about -4.2 kJ mol^{-1} per hydrogen bond.[16] The binding energy of an ammonia molecule to a water molecule is estimate to be about -26.15 kJ mol^{-1}.[20] Gas phase energies range from -22 kJ/mol (neutral hydrogen bonds between water molecules) up to -163 kJ/mol (anionic F–H-----F^- complex).[21] Examples of occurrence of hydrogen bonds in a synthetic host-guest system and their contribution to the binding energy as a function of the molecular environment are discussed in paragraph 1.2.1.3.

1.2.1.2 Cation–π interactions

Definition

Kebarle and co-workers[22] were the firsts to report experimental evidence of interactions between cations and aromatic π-systems. The authors reported that potassium ion (K^+) is able to bind water through ion-induced dipole interactions with a binding energy of -75 kJ mol^{-1} in the gas phase. More interestingly, they reported that K^+ is surprisingly well able to bind the non-polar benzene, which does not have a permanent dipole, with a slightly higher binding energy than water, -78 kJ mol^{-1} in the gas phase. They defined the K^+-benzene interaction as a cation-quadrupole interaction which was later defined by Dougherty and co-workers[23] as a cation-π interaction.

In benzene, the six $C^{\delta-}$-$H^{\delta+}$ bond dipoles combine to produce a region of negative electrostatic potential on the face of the π system. The cation-π interactions occur when the negative electrostatic potential, also called molecular quadrupole moment, is attracted to a cationic species. Other forces such as interactions between induced dipoles and ions-induced dipoles contribute, to significant degrees, to the binding energy of cation-π interactions.[24]

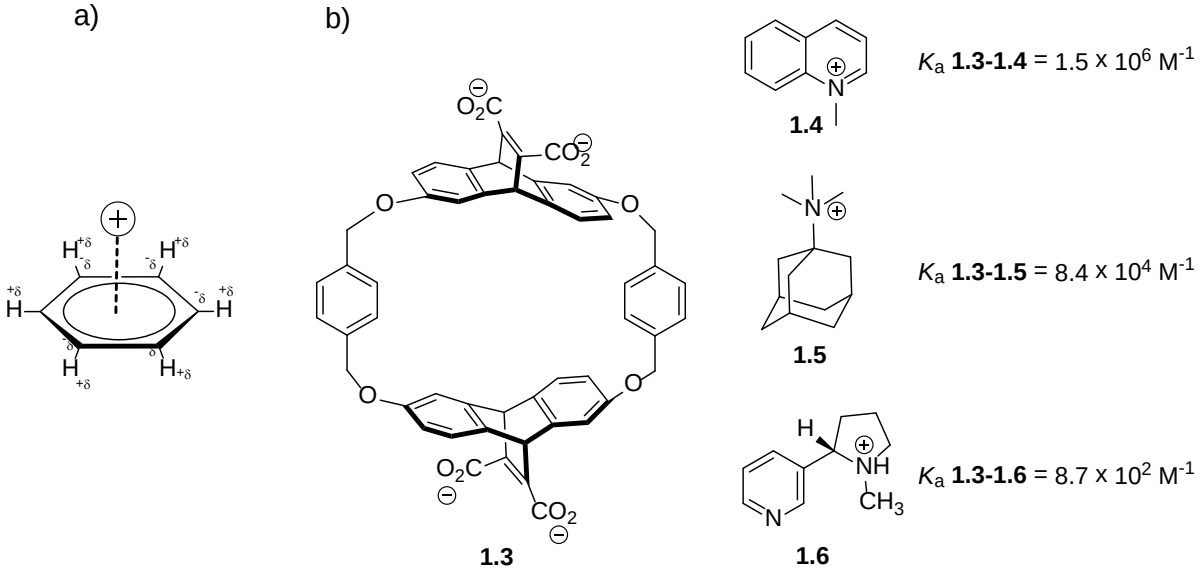

Figure 1.3: a) Schematic representation showing the 6 individual bond dipoles creating the overall electrostatic potential responsible for cation-π interactions; b) cyclophane based receptor **1.3** reported by Dougherty and co-workers,[25] which was found to bind ammonium ion compounds (*e.g.* **1.4**, **1.5** and **1.6**) in borate buffer at pH = 7 mainly through cation-π and hydrophobic interactions.

Importance
Like hydrogen bonding and salt bridges (see paragraph 1.2.1.3), cation-π interactions have been found to play a role in the stability of protein structures.[26] Statistical analyses of protein structures revealed that one fourth of the aromatic indoles of tryptophane side chains interact with proximal arginine residues containing cationic guanidinium groups.[26] The neurotransmitter acetylcholine was found to activate, upon binding, acetylcholinesterase through cation-π interactions.[27] Moreover, cation-π interactions play a critical role in drug binding[28] and neurobiology.[27] For instance, nicotine addiction begins when nicotine activates, upon binding, the nicotinic acetylcholine receptors (nAChRs) α4β2 in the brain through cation-π interactions. Nicotine cannot make this type of interaction with nAChRs in the muscles and therefore it is a weak activator of the latter.[29] Dougherty and co-workers have extensively studied ammonium-π interactions in these systems and they developed many host-guest systems (Figure 1.3) some of which showed catalytic activities.[30] An account on cation-π interactions has recently been published by Dougherty.[31]

Geometry and Strength
A computational study by Sherrill and co-workers[32] showed that cation-π interactions are strongest when the cation is situated perpendicular to the plane of benzene atoms. The strength of cation- π interactions is inversely proportional to the solvent polarity. For the cation-π interactions shown in Figure 1.4, the binding energy in the gas phase is estimated to be around -52 kJ mol^{-1}, while in water it is estimated to -23 kJ mol^{-1}.[33]

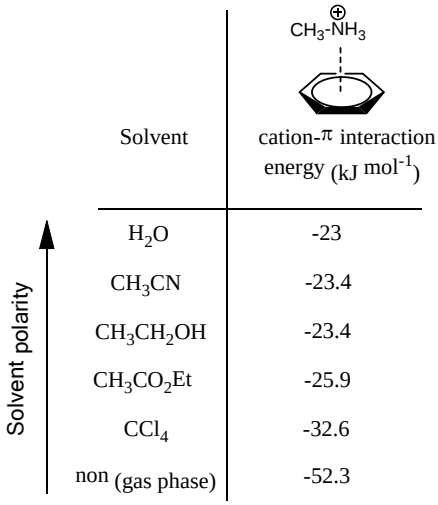

Figure 1.4: Computed cation- π interaction energies between methylammonium ion and benzene in a range of solvents as reported by Dougherty and co-workers.[33]

1.2.1.3 Ion pair and salt bridge interactions

Definition
Ion pair or cation-anion interactions occur between cationic and anionic charges located on fully or partially (*i.e.* on bond dipoles) ionized groups. When additional hydrogen bonds contribute to the cation-anion interactions, these are called salt bridges.[34]

Importance
The salt bridge between protonated guanidinium group of one arginine and the carboxylate of another is responsible for stabilization of charged zwitterionic arginine aggregates in the gas phase.[35] Cation-anion interactions that occur between phosphate oxygens of RNA and

magnesium ions stabilize RNA tertiary structures.[36] Moreover, these interactions are one of the important factors leading to changes in the properties of onium salts such as melting point, density, viscosity, and electrical conductivity.[37]

Strength

The strength of ion pair interactions is inversely proportional to the distance separating the charges[38] and the solvent polarity (Figure 1.5). Particularly, these interactions are weaker in water due to the competition with H_2O molecules and logically are much weaker in water with higher ionic strength. For instance, K_a values between metal cations and cyclic polyethers such as crown ethers are 10^3-10^4 larger in methanol than in water.[39] Dougherty and co-workers[33] estimated that a salt bridge contributes up to -9.2 kJ mol^{-1} to the stability of an ammonium ion-acetate adduct in water, while a cation-π interaction contributes up to -23 kJ mol^{-1} to the stability of an ammonium ion-benzene adduct, as seen in paragraph 1.2.1.2. This difference in binding energy is due to desolvation effects: salt bridge formation has a high desolvation penalty for both charged species whereas the cation–π complex would only pay a significant penalty for the cation. Smith and co-workers[40] have reported that ditopic synthetic receptor **1.7** (Figure 1.6) is able to bind alkylammonium salts such as **1.8**, **1.9** and **1.10** through salt bridges and ion pair interactions, as proved by x-ray crystallography.

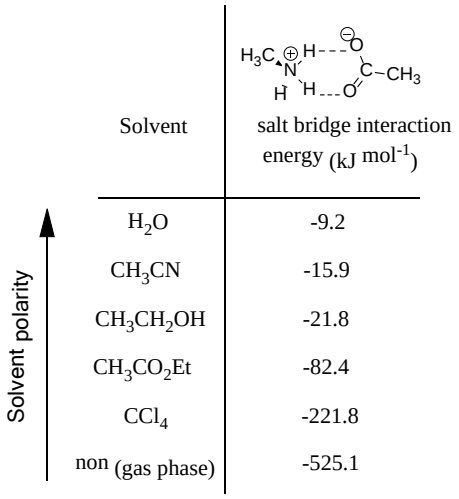

Figure 1.5: Computed salt bridge interaction energies between methylammonium ion and acetate in a range of solvents as reported by Dougherty and co-workers.[33]

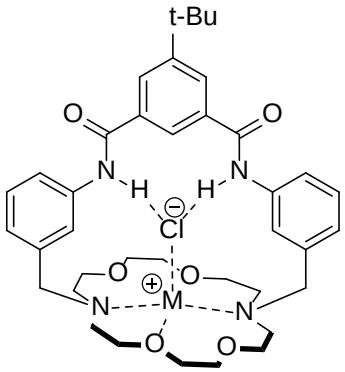

1.7

n-$PrNH_3^{\oplus}$ $Cl^{\ominus}$ **1.8** K_a **1.7-1.8** = 2.0 x 10^4 M^{-1}

i-$PrNH_3^{\oplus}$ $Cl^{\ominus}$ **1.9** K_a **1.7-1.9** = 8.7 x 10^2 M^{-1}

$Bu_4N^{\oplus}$ $Cl^{\ominus}$ **1.10** K_a **1.7-1.10**= 50 M^{-1}

Figure 1.6: Ditopic synthetic receptor (**1.7**), reported by Smith *et al*.,[40] described for the molecular recognition of alkyl ammonium ion salts such as **1.8**, **1.9** and **1.10** in $CHCl_3$-DMSO (85:15). Receptor **1.7** with adjacent anion and cation binding sites is able to binding the ammonium salts as contact ion-pairs following the illustrated model.

1.2.2 Synthetic receptors

Analogous to biological systems, the formation and function of supramolecular host-guest complexes in water solution occurs through a multiplicity of non-covalent forces. In addition to hydrogen bonds, cation–π interactions, ion pairs and salt bridges, other non-covalent interactions are occurring within these complexes. These are mainly the hydrophobic and π–π staking interactions.

1.2.2.1 Hydrophobic interactions

Definition

Hydrophobic interactions differ from all other non-covalent interactions as they do not directly depend on attractive interactions between solute species in the solvent. Rather, they are the indirect result of the collective interactions between water molecules. Water molecules are small and have strong permanent dipoles between their two hydrogens and central oxygens. Therefore their interactions lead to extended hydrogen bond networks and result in a high cohesive density *i.e.* a large number of hydrogen bonds per volume unit.[41,42] Upon interaction with an apolar solute of small volume such as an alkane, the water molecules reorient themselves in a shell around the solute to maintain the maximum number of hydrogen bonds. In this situation hydrophobic hydratation is characterized by a large unfavorable entropy term. For an apolar solute of bigger size such as the hydrophobic cavity of a macrocycle (*e.g.* cyclodextrin), forming a shell around it is no longer possible and hydrogen bonds have to be sacrificed. In this situation water wants to become part of the bulk solvent to regain the broken hydrogen bonds. This often leads to a decrease of the macrocycle solubility. In this situation hydrophobic hydratation is characterized by a large unfavorable enthalpy term.[41,42]

The hydrophobic effect depends on the size and shape[43] of the apolar solute, but also on the temperature and pressure of the solvent and on the presence of co-solutes.[43]

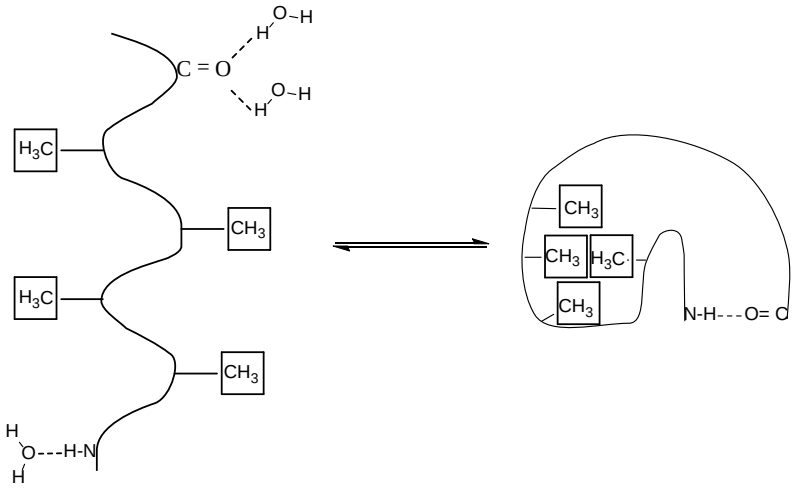

Figure 1.7: Schematic illustration of the formation of hydrogen bond and hydrophobic interactions in the folding of a protein.

Hydrophobic interactions drive the binding of macrocyclic receptors with cavities such as cyclophanes, cyclodextrines and cucurbiturils to organic guests.[44] Upon interaction of these macrocyles with water molecules, the latter reside in their cavities to avoid creating a vacuum. These hosts feature concave or deep cavities that can efficiently prevent the cavity water from contact with the bulk. Cavity water molecules cannot form a stable hydrogen bonded network with their neighbors, and therefore at the first opportunity, they tend to join the bulk of the aqueous medium aiming to restore their hydrogen-bonding ability. This leads to facile release of water from the hydrophobic cavity upon guest binding, as it enables more cohesive water– water interactions, and therefore leads to enthalpy-driven host-guest binding.

Importance and strength

The hydrophobic effect is an important contributor in the ultra high binding constant of up 7 x 10^{17} M^{-1} of cucurbiturils [CB7] to organic guests.[45] Dicationic **1.14** binds to [CB7] with a binding constant of 7 x 10^{15} M^{-1}. Neutral analogue **1.11** has reduced, but still very high binding constant to **1.11** of 3 x 10^{9} M^{-1} (Figure 1.8).[46]

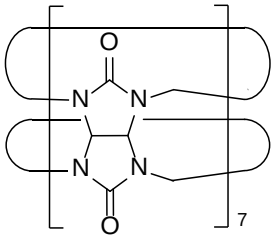

1.11

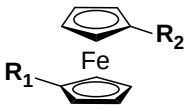

1.12 (**R_1** = CH_2OH); (**R_2** =H) K_a **1.11-1.12** = 3 x 10^{9} M^{-1}

1.13 (**R_1** = $CH_2\overset{\oplus}{N}(CH_3)_3$); (**$R_2$** =H) K_a **1.11-1.13** = 3 x 10^{12} M^{-1}

1.14 (**R_1** = $CH_2\overset{\oplus}{N}(CH_3)_3$); (**$R_2$** = $CH_2\overset{\oplus}{N}(CH_3)_3$) K_a **1.11-1.14** = 3 x 10^{15} M^{-1}

Figure 1.8: Structures of cucurbit[7]uril (host **1.11**) and ferrocene guests: 1-hydroxymethylferrocene (**1.12**), 1-trimethylammoniomethylferrocene (**1.13**), and 1,1'-bis(trimethylammoniomethyl)ferrocene (**1.13**). (To the right) affinity constants of the cucurbit[7]uril-ferrocene complexes.

The assembly of lipids in biological cell membranes and the enzyme-substrate interactions are governed by hydrophobic interactions.[42,47] Moreover, hydrophobic interactions contribute to the conformational stability of proteins (Figure 1.7).[48] They play a crucial role in ligand-protein binding, as is the case for the interactions between the phospholipid acyl chain and membrane protein phospholypase C δ1 resulting in a significant regulation of the protein's function.[49] The use of hydrophobic interaction to drive self-assembly processes[50] is widespread.

1.2.2.2 Aromatic-aromatic (π-π) interactions

Definition

In an aromatic molecule like benzene, three sets of point charges are assigned. The first is at the site of the positively charged carbon atom due to the local $C^{\delta-}$-$H^{\delta+}$ dipole. This point charge is connected to a similar one at the adjacent atom through a positively charged σ-framework. The second and the third are above and below the plane of the σ-framework and these are π point charges of -1/2 each. These form electron clouds that lie above and below the plane of the σ-framework.[51] As defined by Hunter and Sanders, π-π interactions between two π systems, such as two benzenes, are the result of attractive electrostatic interactions between the σ-framework and π-electrons that overcome unfavorable contributions of π-electron repulsion.[52] In addition to the electrostatic interactions, induced dipole-induced dipole forces and solvophobic effects contribute to the overall interactions between aromatic molecules.

Geometry

The geometrical requirements for the interactions between two benzene molecules are as follows. If the benzene dimer is in a sandwich configuration (Figure 1.9 (a)), then the interaction is stabilized by induced dipole-induced dipole forces but destabilized by the π-electron clouds that repel each other. Offsetting one of the benzene rings, resulting in the parallel displaced configuration (Figure 1.9 (b)), reduces these repulsive interactions and allows the positive σ-framework of one benzene ring to interact with the negatively charged π-electron clouds of another one. The T-shaped configuration (Figure 1.9 (c)) features a σ-framework edge of one benzene on a negatively charged π-electron cloud of the other, thus allowing favorable σ- π interaction.[52] The preferred orientations are the parallel displaced and T-shaped ones with a comparable binding energy of -11.3 kJ mol^{-1}.[59]

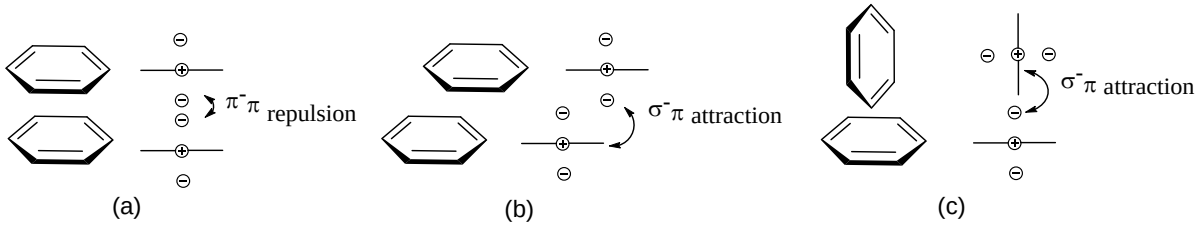

Figure 1.9: Three representative geometries of the benzene dimer, and their proposed σ-π interactions as function of their orientations: (a) The repulsive face-to-face geometry and the two attractive (b) parallel- displaced and (c) T-shaped geometries.

Solvent effect

In water the π-π interactions between aromatic molecules are mainly caused by the hydrophobic effect. In solvents other than water the interactions between solvent molecules are weaker, and therefore, solvophobic forces play a minor role.[53]

Importance

π-π interactions control diverse biological phenomena such as the vertical base-base interactions which stabilize the double helical structure of DNA,[54] the intercalation of drugs into DNA and proteins such as the binding of the anti-Alzheimer's drug Aricept to the active site of acetylcholinesterase. Moreover, π-π interactions play a pivotal role in the stabilization of the tertiary structures of proteins.[52,55] In solution, π-π interactions have been used in drug design,[56] molecular recognition of host-guest systems and self-assembly,[57] and have been implicated in catalytic activities.[58]

Substitution effects

The strength of the interaction can be influenced by substitution. Electron-withdrawing substituents diminish the electron density in the π-cloud of the substituted ring and therefore decrease the electrostatic repulsion with the π-system of the interacting ring. Consequently, the stacking interaction with face-to-face geometry is enhanced relative to the unsubstituted dimer. Conversely, *π*-electron-donating substituents result in weaker *π*-*π* interactions.[59]

1.3 Requirements for molecular recognition of an organic ammonium ion: (electrostatic and steric) complementarity and preorganization of host-guest interacting groups

Molecular recognition of an organic ammonium ion guest by a synthetic receptor (as well as by a protein receptor) occurs if the interacting functional groups of the guest and the receptor exhibit electrostatic complementarity, *i.e* the electrostatic interactions are attractive. Also, the guest and the receptor must exhibit complementary sizes and shapes. Moreover, the functional groups must be positioned in a way allowing their interaction. This complementarity in size, shape and position of the interacting functional groups is called steric complemetarity. Furthermore, molecular recognition of ammonium ion guests depends on the pre-organization of interacting functional groups. Where, as stated by Cram and co-workers,[60] "the more highly hosts and guests are organized for binding and for low solvation prior to their complexation, the more stable will be their complex". In other words, synthetic receptors should be pre-organized, during synthesis, into a conformation that will optimally bind the guest. In this situation the binding is entropically favored since the receptor will hardly any degrees of freedom upon complexation, as the conformational entropy penalty has already been paid for in advance during the synthesis. Therefore, the receptor backbone should be made from rigid parts to avoid its folding which usually occurs to fill its own empty cavity. In addition, the solvent molecules should undergo very little positional reorganization around the host during complexation. In this situation, the binding is enthalpically favorable since the host is less strongly solvated and therefore there are fewer solvent-ligand bonds to break. This implies that in, a general topological sense, cyclic systems are more likely to be pre-organized for binding a guest than acyclic systems. This is because macrocylic hosts have cavities with less solvent accessible areas and feature conformations which are likely to be more rigid and pre-organized than most acyclic systems.

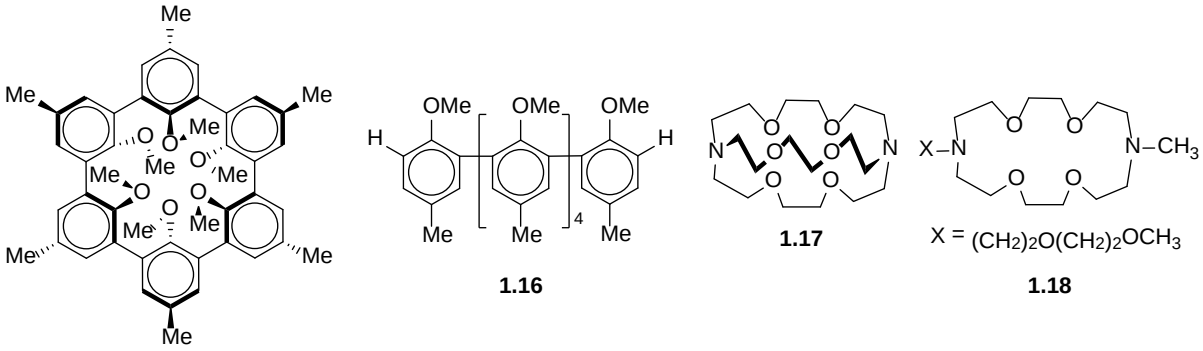

1.15 **1.16** **1.17** **1.18**

Figure 1.10: Prototype hemispherand **1.15** and its acyclic analogue **1.16**. Cryptand **1.17** and its acyclic analogue azacrown ether **1.18**.

Artz and Cram[61] have compared the binding energies of cyclic hemispherands of different sizes and their open-chain analogues towards the alkali metal and ammonium ion compounds (Figure 1.10). Prototype hemispherand **1.15** is designed in such a way that its parts cannot rotate to fill its own cavity, which is too small to be filled with solvent. The authors have found that smaller cycles are stronger binders and are more ion selective than the corresponding bigger cycles and acyclic analogues. For instance hemispherand **1.15** binds to Li^+ and Na^+ by respectively -71 and -54 kJ mol^{-1} more than its open-chain analogue **1.16**. Similarly, Lehn and co-workers[62] have compared the binding strengths of cryptand **1.17** and its open-bridge analogue azacrown ether **1.18** (Figure 1.10) towards the metal alkali and alkaline-earth cations. Cryptand **1.17** differs from azacrown ether **1.18** by an extra bridge that increases its level of preorganization in the system as crown ether cavities often collapse in the absence of a guest. This preorganization has increased the selectivity and the binding constant of cryptand **1.17** towards the metal alkali and alkaline-earth cations by several orders of magnitude over the azacrown ether **1.18**. For instance K_a **1.17**-K^+ = 10^7 M^{-1} vs K_a **1.18**-K^+ = 5.3 x 10^4 M^{-1}, and K_a **1.17**-Na^+ = 10^8 M^{-1} vs K_a **1.18**-Na^+ = 2.25 x 10^4 M^{-1} (in methanol).

1.4 Relevant synthetic receptors for organic ammonium ions in water

1.4.1 Cucurbit[7]uril: a synthetic receptor with ultra high affinity

As seen in paragraph 1.2, the molecular environment determines the stability of a host-guest assembly. In water, the binding of ammonium ion compounds is generally weak since hydrogen bond formation is opposed by competing interactions with solvent molecules. Moreover, water-exposed salt bridges contribute relatively little to the binding energy (-9.2 kJ mol^{-1} per bond).[33] The binding of a non polar moiety of an organic ammonium ion compound is generally stronger in water than in organic solvents, due to the hydrophobic effect. A survey by Houk *et. al.*[63] found that affinities of synthetic receptors for neutral guests were on average one order of magnitude higher in water than in non-aqueous solvents.
The exceptional affinities seen in protein-ligand systems have long represented a challenging research target for supramolecular chemists. The binding of biotin to avidin exemplifies such target well, since it represents the tightest binding in biomolecular systems. In this complex, the noncovalent interactions have achieved an affinity in the order of 10^{15} M^{-1}.[64] This high affinity is attributed to the additional non covalent interactions within the

protein that reinforce the ligand binding, besides the direct protein-ligand interactions.[65] This reinforcement in ligand binding occurs when the ligand binding and the intra-molecular interactions require very similar conformational rearrangement of parts of the protein.[65] In synthetic systems, Isaac and co-workers[66] were the first to discover a water soluble host-guest complex rivaling the affinity of avidin-biotin complex. The authors reported that CB[7] (**1.11**) binds adamantane and ferrocene derivatives such as **1.13** and **1.19** with K_a values corresponding to 3 x 10^{12} M^{-1} and 4.2 x 10^{12} M^{-1}, respectively (Figure 1.8 and Figure 1.11). This record of affinity was later broken when Isaac and co-workers[67] once again reported that K_a for **1.11**-**1.14** corresponds to 3 × 10^{15} M^{-1} in water (Figure 1.8). Later, Gilson and co-workers[68] reported a record K_a for binding between CB[7] **1.11** and adamantane derivative **1.20** corresponding to 5 ×10^{15} M^{-1} in water (Figure 1.11).

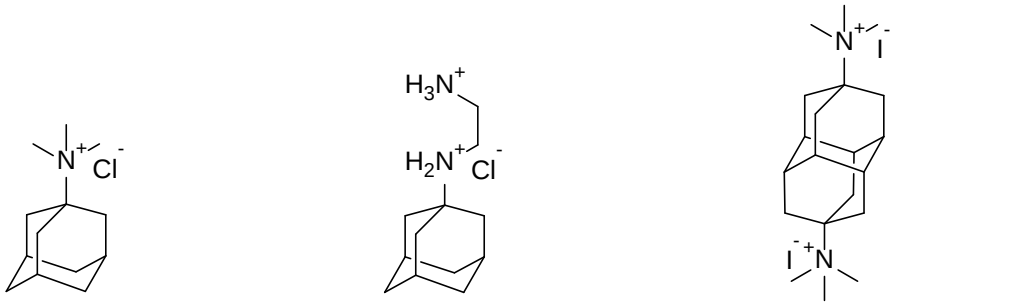

1.19 **1.20** **1.21**

K_a **1.11-1.19** = 4.2 x 10^{12} M^{-1} K_a **1.11-1.20** = 3 x 10^{15} M^{-1} K_a **1.11-1.21** = 7.2 x 10^{17} M^{-1}

Figure 1.11: Structures of adamantane derivatives **1.19**, **1.20** and **1.21** and their affinity towards [CB7] in water.

The tightest non-covalent complex ever reported in water was the one formed between CB[7] and diamantane quaternary diammonium ion derivative **1.21**. The complex reported by Isaac and co-workers reaches a K_a equal to 7.2 x 10^{17} M^{-1} in water.[69] Several reasons are behind this extreme affinity. The host cavity of the barrelshaped (glycoluril-based [CB7]). The cavity of the macrocycle is extremely hydrophobic with no hydrogen bond donor or acceptor pointing inwards. This results in an energetically favorable water desolvation process upon binding. Moreover, the host-guest size-length complementarity allows the maximization of the induced-dipole induced-dipole interactions between the CB[7] inner cavity and the core of **1.21**. Furthermore, the complete inclusion of the **1.21** core in the CB[7] cavity and the almost ideal positioning of each of the trimethylammonium groups allow for high number of ion–dipole interactions between the carbonyl portal of **1.11** and the ammonium ions of **1.21**.

1.4.2 Sugammadex: a semi-synthetic receptor approved as a therapeutic agent

Most of the synthetic drugs are “guest” molecules of their biological “host” macromolecules *i.e.* proteins, while very few synthetic hosts find their way to be accepted as potential[70] or approved[71] therapeutic agents. Sugammadex (**1.22**, Figure 1.12) which is commercialized under the trade name Bridion from Merck & Co, is the first example of a synthetic host molecule used therapeutically to encapsulate an organic guest molecule. Sugammadex is a semi-synthetic derivative of the naturally occurring γ-cyclodextrin reported by Bom and co-workers.[72] It is specially designed to encapsulate the amino-steroid rocuronium (**1.23**) after

the completion of surgery. Rocuronium (**1.23**) operates by blocking, upon binding, acetylcholine receptors resulting in muscle relaxation. Sugammadex is also able to bind two other amino-steroid muscle relaxants, namely vecuronium and pancuroniuim, however with lower affinities than rocuronium. It has a chemically extended hydrophobic cavity capable of full inclusion of the hydrophobic steroidal skeleton of rocuronium, and eight negatively charged carboxylate groups at the rim of the cavity to ensure water solubility, pre-organisation of the cavity entrance by electronic repulsion, and ionic interaction with the positively charged amino group of rocuronium.[73] It has no affinity to other muscle relaxants, like succinylcholine, mivacurium, atracurium, or cisatracurium.[74] The relatively high binding affinity of sugammadex (**1.22**) to rocuronium (**1.23**) (*K*a = 1.8 × 10^7 M^{-1} in water) causes the selective sequestering of rocuronium from the acetylcholine receptors, thereby reversing its effects.

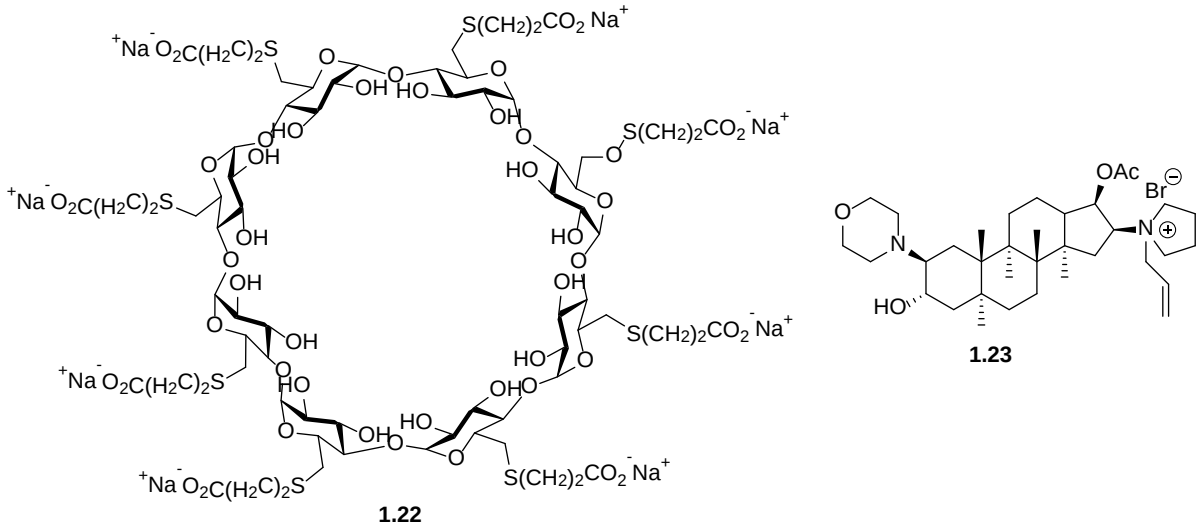

Figure 1.12: Cyclodextrin derivative Sugammadex **1.22**, a reversal agent for neuromuscular blocking agent rocuronium bromide **1.23**.

Sugammadex offers many advantages over the traditional reversal agents such as the acetylcholinesterase (AChE) inhibitors (e.g. neostigamine): it is biologically inactive, well tolerated, it does not alter the acethylcholine levels and the associated cardiovascular side effects and it causes no muscle weakness.[75] However, the price of the drug and the missing evidence of cost efficacy have led to a limited use in clinical anesthesia so far.[74]

1.5 Merits and disadvantages of synthetic receptors for organic ammonium ions

Synthetic receptors for organic ammonium ions have found application as selective chemosensors for the analytical detection of biogenic and non-biogenic amines with relevant biological activities[76] and of metal cations.[77] They have also been used in enantioseparation of racemic primary arylalkyl amines,[78] α-amino acids[79] and amino-acid derivatives.[80] Many of the reported receptors have shown catalytic activities[81] some of which mimic biological enzymes.[82] All of these studies have helped to better understand the individual contributions of the different forces involved in ammonium ion binding. Moreover, these studies have led to a far better understanding of many biological processes. Furthermore, these studies have promoted supramolecular chemistry research by elaborating sophisticated supramolecular structures, such as self-assemblies,[83] mechanically-interlocked molecular architectures (*e.g.*

catenanes and rotaxanes),[84] supramolecular polymers[85] and cages.[86] These supramolecular structures and their recognitions properties have been thoroughly discussed by Spath and Konig in a recent review.[87]
The traditional method followed to obtain an artificial receptor pivots around three steps of an iterative process: design, synthesis and testing. The design step is perhaps the most challenging, as the non-covalent interactions driving the host-guest binding are still insufficiently understood. Moreover, predicting whether the chosen structure and conformation of a given molecule will form a good receptor for a guest molecule with sometimes unknown functional group orientations is extremely difficult. The synthesis of a receptor often involves multiple steps and is therefore time consuming and often of low yield. Additionally, the receptor often has limited water solubility and this requires repeating the synthesis step after introducing new functional groups to increase water solubility. Furthermore, the reported very high affinity constants for receptors **1.11** and **1.22** are the exception rather than the rule. Synthetic receptors are still, on average, several orders of magnitude less efficient in binding than their biological counterparts.[88] Therefore, designing a synthetic receptor able to compete with biological systems remains a significant challenge.
The combination of all these difficulties associated with the iterative character of the process result in the design approach being a rather inefficient method to discover new receptors. In this thesis, we present an alternative approach to obtain synthetic receptors: the dynamic combinatorial chemistry (DCC) approach. This approach may help to solve the mentioned difficulties and will be discussed in the following paragraph.

1.6 Dynamic Combinatorial chemisty (DCC)

1.6.1 Definition of terms: DCC, building blocks, DCL, amplification and thermodynamic equilibrium

Combinatorial chemistry[89] allows quick preparation of a large collection of structurally related oligomers starting by combining a small collection of monomers (*building blocks*). It enables, at a later stage, efficient screening and testing of the generated compounds for biological activities. In comparison with “traditional” chemistry, combinatorial chemistry increases the chance of discovering a biologically active compound.
Dynamic combinatorial chemistry (*DCC*),[90] or combinatorial chemistry under thermodynamic control, is a field of combinatorial chemistry where the building blocks are combined through reversible covalent or non-covalent bonds. Therefore, the building blocks generate a complex mixture of library products which continuously exchange building blocks (*a* dynamic combinatorial library (*DCL*)). As the exchange proceeds, the DCL distribution moves towards the thermodynamic minimum of the system (*thermodynamic equilibrium*) which is determined by the sum of the total thermodynamic stabilities of all species in the library. Since all the components of a DCL are linked through a set of equilibria, the stabilization of one library member will affect the abundance of the others. Therefore, stabilizing a library member leads to the reorganization of the library distribution in order to maximize the thermodynamic stabilities of the DCL members. Such reorganization will ideally lead to an increased production (*amplification*) of the stabilized library member at the expense of the other species in the mixture.

1.6.2 Selection approaches in a DCL system, definition of the term template

Selection of one (or even more) DCL members can be realized through an internal or external templating approach. With the first approach, intramolecular non-covalent interactions occurring inside an oligomer can stabilize, and so amplify, this oligomer generating a foldamer (Figure 1.13 (a)).[91] Also, intermolecular non-covalent interactions occurring between library members and copies of themselves can drive the generation of self-assembled oligomers (Figure 1.13 (b)).[92] External templating is an alternative selection approach to the first: adding an external *template*, *i.e.* a species that cannot take part in the reversible chemistry connecting the building blocks, to the DCL can stabilize an oligomer which can act as a host (Figure 1.13(c)) or as a guest (Figure 1.13 (d)) to that template and so is amplified.[93]

1.6.3 External templating in DCC as an alternative approach to develop synthetic receptors

As we have seen in paragraph 1.5, developing synthetic receptors capable of exhibiting specific molecular recognition capabilities through a straightforward synthetic design approach is difficult. DCC can be used as a powerful alternative approach for developing receptors. In DCC, the building blocks are designed receptor fragments capable of reacting reversibly with one another to form a mixture of interconverting hosts that are at thermodynamic equilibrium (a DCL). Introducing a guest of interest into a DCL of potential hosts should ideally shift the equilibrium in favor of the best receptor(s). Developing synthetic receptors using DCC has several benefits. First, the guest drives the construction of its own receptor from smaller fragments. Therefore it is sufficient to know the functional groups of the target in order to design the receptor fragments, while it is not necessary to know their relative orientations. Moreover, DCC minimizes, in principle, the synthetic effort in that it is sufficient to design a small number of receptor fragments that can lead to a wide range of complex receptors. Another consideration in the building block design is the type of reversible reaction used to generate DCLs. This topic will be discussed in the following paragraph.

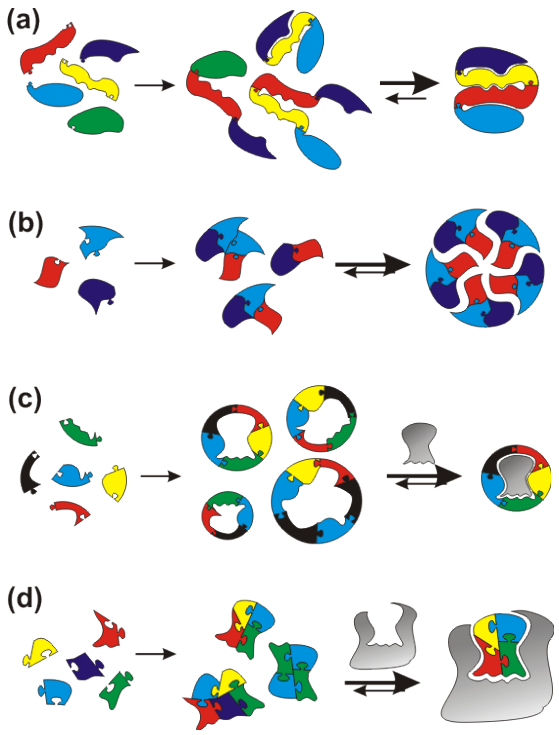

Figure 1.13: Different ways of selection of one (or more) DCl member(s) through non-covalent interactions: (a) intramolecular interactions inside an oligomer lead to the formation of a foldamer, (b) intermolecular interactions between the oligomers lead to the formation of self-assembled oligomers (c) interactions with a separately introduced inert species, an external guest or (d) a separately introduced host lead to the stabilization of the bound library member and therefore its amplification. The figure is reproduced from reference 94.

1.6.4 Disulfide exchange for creating DCLs of water soluble synthetic receptors

To date, many covalent and non-covalent reversible reactions have been used in order to establish DCL systems. These reactions have been extensively reviewed and are summarized in Scheme 1.1.[94]

In our research group, we mostly employ disulfide exchange to establish DCLs of potential synthetic receptors. The disulfide bond is relatively robust but it exchanges under mild conditions. Also, disulfide DCLs allow for the screening of biologically relevant targets under near-physiological conditions, as we will see hereafter. The disulfide exchange mechanism involves four essential steps: initial ionization of the thiol building block(s) to the thiolate anions. In most cases, an aqueous medium with pH in the range of 7–9 produces a sufficient concentration of thiolate for exchange to take place (Scheme 1.2, a)); irreversible oxidation of the thiol building block, in water using air as oxygen source, to form disulfide bonds. This reaction is followed by nucleophilic attack of the thiolate anion on one of the sulfur atoms of the disulfide bond to cleave the original S-S bond and create another. This disulfide exchange reaction is generally efficient under mildly basic conditions (pH = 7-9) and is reversible as long as thiolate anions are present in solution (Scheme 1.2, b and c)). Therefore the disulfide exchange stops after the thiol building blocks are fully oxidized. Also, as the disulfide exchange process depends on the thiolate anion, exchange can be frozen by lowering the pH (Scheme 1.2, d)).

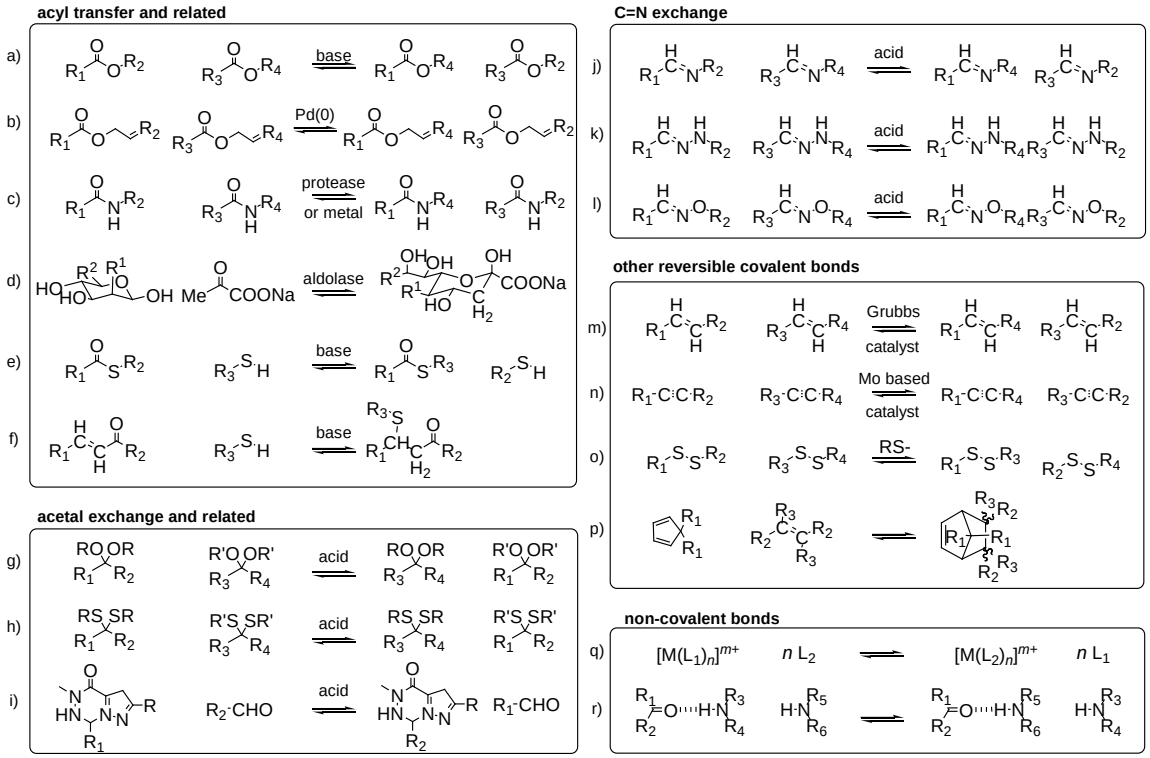

Scheme 1.1: Reversible reactions used for dynamic combinatorial chemistry to date: (a) transesterification; (b) transallylesterification; (c) transamidation; (d) aldol exchange; (e) transthioesterification (f) Michael/retro-Michael reactions; (g) acetal exchange; (h) thioacetal exchange; (i) pyrazolotriazone metathesis; (j) transimination; (k) hydrazone exchange; (l) oxime exchange; (m) alkene metathesis; (n) alkyne metathesis; (o) disulfide exchange; (p) Diels-Alder / retro-Diels-Alder reactions; (q) metal-ligand exchange; and (r) hydrogen bonds exchange. The scheme is reproduced from reference 94.

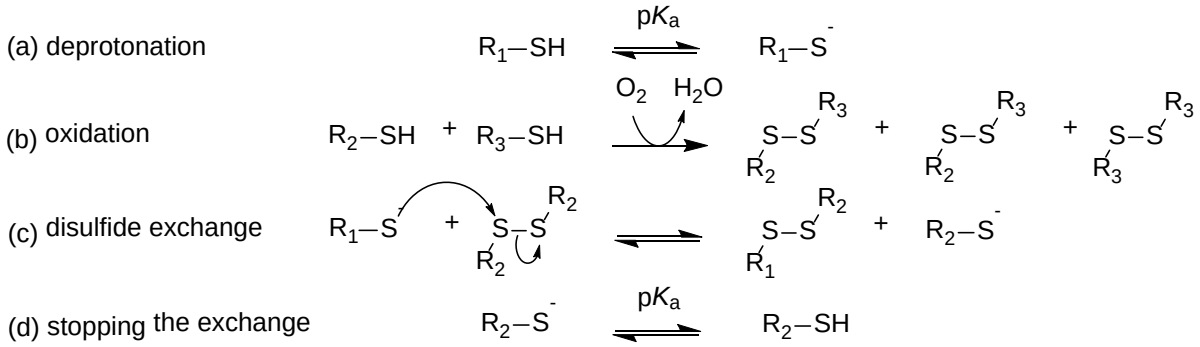

Scheme 1.2: Thiolate mediated disulfide exchange.

1.6.5 Relevant macrocyclic receptors obtained from a disulfide DCL

DCL design

The groups of Sanders and Otto[95] have earlier reported dithiol building blocks such as **1.24**, **1.25** and **1.26** (Scheme 1.3) for establishing of a DCL of macrocyclic hosts. The reported

building block structures were inspired by cyclophane-based macrocycles (*e.g.* **1.12**) published by Dougherty and co-workers.[96]

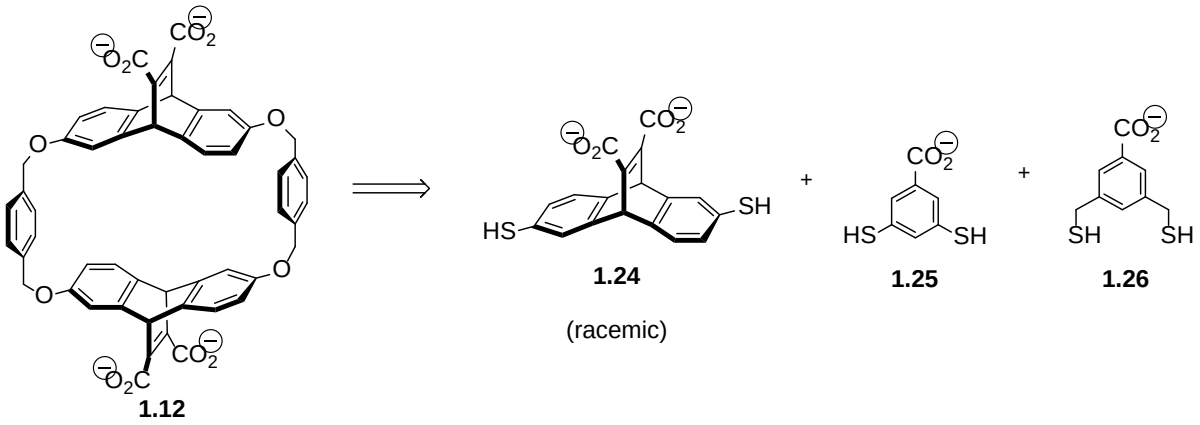

Scheme 1.3: One of the cyclophanes synthesized by Dougherty and co-workers[96] (**1.12**) and the three dithiol building blocks inspired by this receptor (**1.24**, **1.25** and **1.26**) reported by Sanders and Otto.[95]

Dougherty-type receptors are soluble in water and exhibited high affinity towards hydrophobic cationic guests due to their electron rich aromatic hydrophobic cavity and carboxylate groups. Thus, it was to be expected that exposing a DCL made from building blocks **1.24**, **1.25** and **1.26**, prepared in water at pH = 7-9, to separately organic cationic guests will generate diverse macrocyclic receptors some of which are analogues to cyclophane **1.12**.

DCL composition

The DCL was able to generate approximately 45 macrocyclic hosts from only the three chosen building blocks. Moreover, the fact that building block **1.24** was synthesized as a racemic mixture further enriched the DCL diversity and most macrocycles were generated as a mixture of stereomers. Analogous macrocycles to cyclophane **1.22**, *i.e.* macrocyclic heterotetramers made from two units of **1.24** and two other combined units of **1.25** and **1.26**, were not detected in the DCL according to HPLC analysis.

Templating effects and affinity constants

Template **1.27** (Scheme 1.4) is one of the best binders to cyclophane **1.12** with a binding constant equal to 2.3 x 10^5 M^{-1} in borate buffer at pH = 7 (see Figure 1.3 for more binding constant data).[25] Exposing the DCL to template **1.27** did not induce the amplification of an analogue to cyclophane **1.12**. However, it induced the amplification of macrocyclic heterotrimer (**1.24**)$_2$(**1.25**) (Scheme 1.4), which has a smaller cavity than cyclophane **1.12**. The amplified macrocycle was isolated in order to determine its binding constant toward template **1.27** which amounts to 2.5 x 10^5 M^{-1} in borate buffer at pH = 9.

Addition of guest **1.28** to the DCL, as a template with a bigger size than **1.27**, did not induce the amplification of an analogue to cyclophane **1.22** either, but it amplified homotrimer (**1.24**)$_3$. The latter was found to bind to template **1.28** with an affinity constant equal to 7.1 x 10^5 M^{-1} in borate buffer at pH = 9.

Remarkably, exposing the DCL to the smallest template (**1.26**), induced the amplification of the largest macrocycle homotetramer (**1.24**)$_4$. Template **1.26** was found to bind to homotetramer (**1.24**)$_4$ with a high affinity equal to 4 x 10^6 M^{-1} (in borate buffer pH = 9) versus

6.6 x 10^3 M^{-1} for binding of **1.29** to cyclophane **1.22** (in borate buffer pH = 7).[25] This observation seems opposing to conventional host-guest size complementarity. Analysis of the stereochemistry of the amplified receptor (**1.24**)$_4$, based on LC-MS and NMR studies, revealed that it is one of four diastereomers of (**1.24**)$_4$ which are present in the DCL. The selected (RR,SS,RR,SS) meso diastereomer of (**1.24**)$_4$ was found to be the only one that can enable optimum contact with the guest through an induced-fit process, as proven by proton NMR studies. Furthermore, CPK models revealed that host **1.24** could fold into a conformation with a cavity ideally sized to accommodate the guest, while the other three diastereomers could not fold into this conformation.

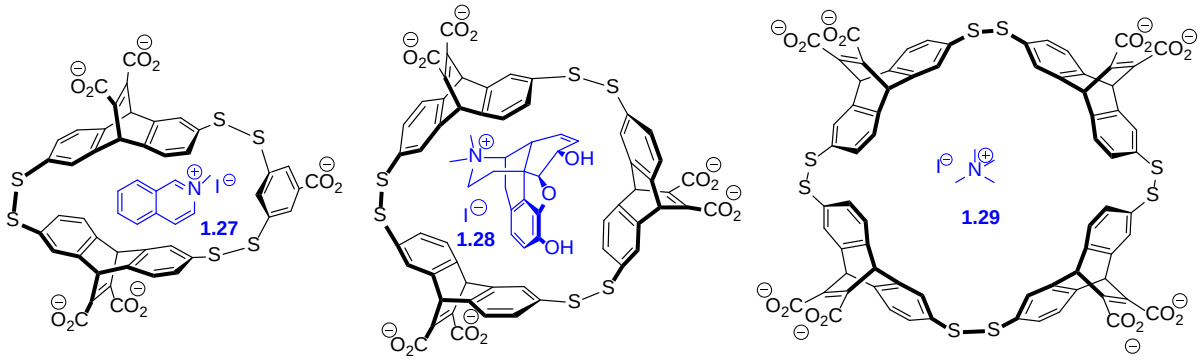

Scheme 1.4: Addition of different hydrophobic cationic guests to a DCL composed of dithiols **1.24-1.26** produces different macrocyclic receptors.

Yield, efficiency and selectivity of the DCC synthesis

The disulfide DCL system presented here provided access to many new and unexpected receptors without the need for long syntheses. The yield of the amplified macrocycles was remarkably high in contrast to the yield of the synthesis of Dougherty-type cyclophanes. Particularly, in the presence of template **1.27** receptor (**1.24**)$_2$(**1.25**) constitutes at equilibrium 60 to 65% of the total material in a biased DCL made from **1.24** and **1.25**. Similarly, receptors (**1.24**)$_3$ and (**1.24**)$_4$ can be produced in 95% and 65 % yield from a DCL solely made from **1.24** in the presence of guests **1.28** or **1.29**, respectively. The affinities of the selected guests towards the DCC receptors were either equal or much higher than their affinities towards Dougherty-type receptors. Also, the DCL was selective where small changes in the template structures are capable of generating very different receptors. This was illustrated in the induced-fit selection of not only one diastereomer but also just one specific conformation upon addition of template **1.29** to the DCL. Supramolecular interactions occurring in disulfide dynamic systems have been recently reviewed by Sanders and co-workers.[97]

1.7 References

[1] Yang, S. Y.; Miah, A.; Pabari, A.; Winslet, M. *Front. Biosci. (Landmark Ed.)* **2011**, *16*, 531.
[2] *Neurohormones and Neurohumors*; Kappers, J. A., Ed.; Springer Berlin Heidelberg: Berlin, Heidelberg, 1969.
[3] *Molecular Cell Biology. 4th edition;* Lodish, H.; Berk, A.; Zipursky, S. L.; Matsudaira, P.; Baltimore, D.; Darnell, J., Eds.; W. H. Freeman: New York, 2000.
[4] Garriga, P.; Garcia-Quintana, D.; Sagi, J.; Manyosa, J. *Biochemstry* **1993**, *32*, 1067.
[5] Tabor, C. W.; Tabor, H. *Annu. Rev. Biochem.* **1976**, *45*, 285.
[6] Bachrach, U.; Wang, Y.-C.; Tabib, A. *News Physiol. Sci.* **2001**, *16*, 106.
[7] Eaton, J. B.; Peng, J-H.; Schroeder, K. M.; George, A. A.; Fryer, J. D.; Krishnan, C.; Buhlman, L.; Kuo, Y-P.; Steinlein, O.; Lukas, R. J. *Mol. Pharmacol*. **2003**, *64*, 1283.
[8] Xiu, X.; Puskar, N. L.; Jai, A. P.; Shanata, J. A. P.; Lester, H. A.; Dougherty, D. A. *Nature* **2009**, *458*, 534.
[9] Vase, L.; Nikolajsen, L.; Christensen, B.; Egsgaard, L. L.; Arendt-Nielsen, L.; Svensson, P.; Staehelin Jensen, T. *Pain* **2011**, *152*, 157.
[10] Nashmi, R.; Xiao, C.; Deshpande, P.; McKinney, S.; Grady, S. R.; Whiteaker, P.; Huang, Q.; McClure-Begley, T.; Lindstrom, J. M.; Labarca, C.; Collins, A. C.; Marks, M. J.; Lester, H. A. *J. Neurosci.* **2007**, *27*, 8202.
[11] Späth, A.; König, B. *Beilstein J. Org. Chem.* **2010**, *6*, 32.
[12] West, K. R. Molecular encapsulation through disulfide dynamic combinatorial chemistry. PhD thesis, University of Cambridge, UK, **2006**.
[13] Lehn, J.-M. *Angew. Chem. Int. Ed.* **1988**, *27*, 89.
[14] Perrin, C. L.; Nielson, J. B. *Annu. Rev. Phys. Chem.* **1997**, *48*, 511.
[15] Pimentel, G. C.; McClellan, A. L. *Annu. Rev. Phys. Chem.* **1971**, *22*, 347.
[16] Pace, C. N.; Fu, H.; Lee Fryar, K.; Landua, J.; Trevino, S. R.; Schell, D.; Thurlkill, R. L.; Imura, S.; Scholtz, J. M.; Gajiwala, K.; Sevcik, J.; Urbanikova, L.; Myers, J. K.; Takano, K.; Hebert, E. J.; Shirley, B. A.; Grimsley, G. R. *Protein Sci.* **2014**, *23*, 652.
[17] Watson, J. D.; Crick, F. H. C. *Nature* **1953**, *171*, 737.
[18] Keutsch, F. N.; Saykally, R. J. *Proc. Natl. Acad. Sci. U. S. A.* **2001**, *98*, 10533.
[19] Spencer, J. N.; Campanella, C. L.; Harris, E. M.; Wolbach, W. S. *J. Phys. Chem.* **1985**, *89*, 1888.
[20] Sánchez-Lozano, M.; Cabaleiro-Lago, E. M.; Hermida-Ramón, J. M.; Estévez, C. M. *Phys. Chem. Chem. Phys.* **2013**, *15*, 18204.
[21] Hibbert, F.; Emsley, J. *Adv. Phys. Org. Chem.* **1990**, 26, 255.
[22] (a) Searles, S. K.; Kebarle, P. *Can. J. Chem*. **1969**, *47*, 2620. (b) Sunner, J.; Kebarle, P. *J. Phys. Chem.* **1981**, *85*, 327. (c) Sunner, J.; Nishizawa, K.; Kebarle, P. *J. Phys. Chem.* **1981**, *85*, 1814.
[23] (a) Stauffer, D. A.; Barrans, R. E.; Dougherty, D. A. *Angew. Chem. Int. Ed.* **1990**, *29*, 915. (b) Stauffer, D. A.; Barrans, R. E.; Dougherty, D. A. *J. Org. Chem.* **1990**, *55*, 2762.
[24] Ma, J. C.; Dougherty, D. A. *Chem. Rev.* **1997**, *97*, 1303.
[25] Kearney, P. C.; Mizoue, L. S.; Kumpf, R. A.; Forman, J. E.; McCurdy, A.; Dougherty, D. A. *J. Am. Chem. Soc.* **1993**, *115*, 9907.
[26] Gallivan, J. P.; Dougherty, D. A. *Proc. Natl. Acad. Sci.* **1999**, *96*, 9459.
[27] Sussman, J. L.; Harel, M.; Frolow, F.; Oefner, C.; Goldman, A.; Toker, L.; Silman, I. *Science* **1991**, *253*, 872.
[28] (a) Ting, A.Y.; Shin, I.; Lucero, C.; Schultz, P. G. *J. Am. Chem. Soc*. **1998**,*120*, 7135. (b) Beene, D. L.; Brandt, G. S.; Zhong, W.; Zacharias, N. M.; Lester, H. A.; Dougherty, D. A. *Biochemistry* **2002**, *41*, 10262.
[29] Xiu, X.; Puskar, N. L.; Shanata, J. A. P.; Lester, H. A.; Dougherty, D. A. *Nature* **2009**, *458*, 534.
[30] (a) McCurdy, A.; Jimenez, L.; Stauffer, D. A.; Dougherty, D. A. *J. Am. Chem. Soc.* **1992**, *114*, 10314. (b) Stauffer, D. A.; Barrans, R. E.; Dougherty, D. A. *Angew. Chem. Int. Ed.* **1990**, *29*, 915.
[31] Dougherty, D. A. *Acc. Chem. Res.* **2013**, *46*, 885.
[32] Marshall, M. S.; Steele, R. P.; Thanthiriwatte, K. S.; Sherrill, C. D. *J. Phys. Chem. A* **2009**, *113*, 13628.
[33] Gallivan, J. P.; Dougherty, D. A. *J. Am. Chem. Soc.* **2000**, *122*, 870.

[34] Burley, S. K.; Petsko, G. A. *Adv. Protein Chem.* **1988**, *39*, 125.
[35] Julian, R. R.; Hodyss, R.; Beauchamp, J. L. *J. Am. Chem. Soc.* **2001**, *123*, 3577.
[36] Draper, D. E. *RNA* **2004**, *10*, 335.
[37] Li, G.; Song, F.; Wu, D.; Lan, J.; Liu, X.; Wu, J.; Yang, S.; Xiao, D.; You, J. *Adv. Funct. Mater.* **2014**, *24*, 747.
[38] Bosshard, H. R.; Marti, D. N.; Jelesarov, I. *J. Mol. Recognit.* **2004**, *17*, 1.
[39] Izatt, R. M.; Bradshaw, J. S.; Nielsen, S. A.; Lamb, J. D.; Christensen, J. J.; Sen, D. *Chem. Rev.* **1985**, *85*, 271.
[40] Mahoney, J. M.; Davis, J. P.; Beatty, A. M.; Smith, B. D. *J. Org. Chem.* **2003**, *68*, 9819–9820.
[41] Otto, S. *Chem. Sci.* **2013**, *4*, 2953.
[42] Otto, S.; Engberts, J. B. F. N. *Org. Biomol. Chem.* **2003**, *1*, 2809.
[43] Southall, N. T.; Dill, K. A.; Haymet, A. D. J. *J. Phys. Chem. B* **2002**, *106*, 521.
[44] Biedermann, F.; Nau, W. M.; Schneider, H.-J. *Angew. Chem. Int. Ed.* **2014**. doi: 10.1002/anie.201310958.
[45] Cao, L.; Sekutor, M.; Zavalij, P. Y.; Mlinarić-Majerski, K.; Glaser, R.; Isaacs, L. *Angew. Chem. Int. Ed.* **2014**, *126*, 1006.
[46] Rekharsky, M. V; Mori, T.; Yang, C.; Ko, Y. H.; Selvapalam, N.; Kim, H.; Sobransingh, D.; Kaifer, A. E.; Liu, S.; Isaacs, L.; Chen, W.; Moghaddam, S.; Gilson, M. K.; Kim, K.; Inoue, Y. *Proc. Natl. Acad. Sci. U. S. A.* **2007**, *104*, 20737.
[47] Blokzijl, W.; Engberts, J. B. F. N. *Angew. Chem. Int. Ed.* **1993**, *32*, 1545.
[48] Pace, C. N.; Shirley, B. A.; McNutt, M.; Gajiwala, K. *FASEB J.* **1996**, *10*, 75.
[49] (a) Kobayashi, M.; Mutharasan, R. K.; Feng, J.; Roberts, M. F.; Lomasney, J. W. *Biochemistry* **2004**, *43*, 7522.
[50] (a) Northrop, B. H.; Zheng, Y.-R.; Chi, K.-W.; Stang, P. J. *Acc. Chem. Res.* **2009**, *42*, 1554. (b) Faul, C. F. J.; Krattiger, P.; Smarsly, B. M.; Wennemers, H. *J. Mater. Chem.* **2008**, *18*, 2962. (c) Cazacu, A.; Tong, C.; van der Lee, A.; Fyles, T. M.; Barboiu, M. *J. Am. Chem. Soc.* **2006**, *128*, 9541.
[51] Hoeben, F. J. M.; Jonkheijm, P.; Meijer, E. W.; Schenning, A. P. H. J. *Chem. Rev.* **2005**, *105*, 1491.
[52] Hunter, C. A.; Sanders, J. K. M. *J. Am. Chem. Soc.* **1990**, *112*, 5525.
[53] Ferguson, S. B.; Sanford, E. M.; Seward, E. M.; Diederich, F. *J. Am. Chem. Soc.* **1991**, *113*, 5410.
[54] Wells, R. A.; Kellie, J. L.; Wetmore, S. D. *J. Phys. Chem. B* **2013**, *117*, 10462.
[55] Brocchieri, L.; Karlin, S. *Proc. Natl. Acad. Sci. U. S. A.* **1994**, *91*, 9297.
[56] Babine, R. E.; Bender, S. L. *Chem. Rev.* **1997**, *97*, 1359.
[57] Sinnokrot, M. O.; Valeev, E. F.; Sherrill, C. D. *J. Am. Chem. Soc.* **2002**, *124*, 10887.
[58] McGaughey, G. B. *J. Biol. Chem.* **1998**, *273*, 15458.
[59] Wheeler, S. E.; McNeil, A. J.; Müller, P.; Swager, T. M.; Houk, K. N. *J. Am. Chem. Soc.* **2010**, *132*, 3304.
[60] (a) Cram, D. J. *Angew. Chem. Int. Ed.* **1988**, *27*, 1009. (b) Kyba, E. P.; Helgeson, R. C.; Madan, K.; Gokel, G. W.; Tarnowski, T. L.; Moore, S. S.; Cram, D. J. *J. Am. Chem. Soc.* **1977**, *99*, 2564. (c) Cram, D. J.; Kaneda, T.; Helgeson, R. C.; Brown, S. B.; Knobler, C. B.; Maverick, E.; Trueblood, K. N. *J. Am. Chem. Soc.* **1985**, *107*, 3645. (d) Koenig, K. E.; Lein, G. M.; Stuckler, P.; Kaneda, T.; Cram, D. J. *J. Am. Chem. Soc.* **1979**, *101*, 3553. (e) Cram, D. *Science* **1988**, *240*, 760–767. (f) Cram, D. J.; Cram, J. M. *Science* **1974**, *183*, 803.
[61] Artz, S. P.; Cram, D. J. *J. Am. Chem. Soc.* **1984**, *106*, 2160.
[62] (a) Lehn, J.-M. *Angew. Chem. Int. Ed.* **1988**, *27*, 89. (b) Lehn, J. M.; Sauvage, J. P. *J. Am. Chem. Soc.* **1975**, *97*, 6700. (c) Dietrich, B.; Lehn, J. M.; Sauvage, J. P. *J. Chem. Soc. Chem. Commun.* **1973**, 15.
[63] Houk, K. N.; Leach, A. G.; Kim, S. P.; Zhang, X. *Angew. Chem. Int. Ed.* **2003**, *42*, 4872–4897.
[64] Green, N. M. *Biochem. J.* **1963**, *89*, 585.
[65] Otto, S. *Dalton Trans.* **2006**, 2861.
[66] Jeon, W. S.; Moon, K.; Park, S. H.; Chun, H.; Ko, Y. H.; Lee, J. Y.; Lee, E. S.; Samal, S.; Selvapalam, N.; Rekharsky, M. V; Sindelar, V.; Sobransingh, D.; Inoue, Y.; Kaifer, A. E.; Kim, K. *J. Am. Chem. Soc.* **2005**, *127*, 12984.
[67] Rekharsky, M. V; Mori, T.; Yang, C.; Ko, Y. H.; Selvapalam, N.; Kim, H.; Sobransingh, D.; Kaifer, A. E.; Liu, S.; Isaacs, L.; Chen, W.; Moghaddam, S.; Gilson, M. K.; Kim, K.; Inoue, Y. *Proc. Natl. Acad. Sci. U. S. A.* **2007**, *104*, 20737.

[68] Moghaddam, S.; Yang, C.; Rekharsky, M.; Ko, Y. H.; Kim, K.; Inoue, Y.; Gilson, M. K. *J. Am. Chem. Soc.* **2011**, *133*, 3570.
[69] Cao, L.; Šekutor, M.; Zavalij, P. Y.; Mlinarić-Majerski, K.; Glaser, R.; Isaacs, L. *Angew. Chem. Int. Ed.* **2014**, *126*, 1006.
[70] Cyclic phenyl disulfide host as an anticancer agent: Vial, L.; Ludlow, R. F.; Leclaire, J.; Pérez-Fernandez, R.; Otto, S. *J. Am. Chem. Soc.* **2006**, *128*, 10253. Calix[4]arenes as inhibitors of binding of protein growth factors to their biological receptors: Sun, J.; Wang, D.-A.; Jain, R. K.; Carie, A.; Paquette, S.; Ennis, E.; Blaskovich, M. A.; Baldini, L.; Coppola, D.; Hamilton, A. D.; Sebti, S. M. *Oncogene* **2005**, *24*, 4701.
[71] Vancomycin derivatives as antimicrobial agents: Lunde, C. S.; Hartouni, S. R.; Janc, J. W.; Mammen, M.; Humphrey, P. P.; Benton, B. M. *Antimicrob. Agents Chemother.* **2009**, *53*, 3375. Sugammadex as a muscle relaxant reversing agent: see reference number 72.
[72] (a) Bom, A.; Bradley, M.; Cameron, K.; Clark, J. K.; Van Egmond, J.; Feilden, H.; MacLean, E. J.; Muir, A. W.; Palin, R.; Rees, D. C.; Zhang, M.-Q. *Angew. Chem. Int. Ed.* **2002**, *41*, 266. (b) Bom, A.; Epemolu, O.; Hope, F.; Rutherford, S.; Thomson, K. *Curr. Opin. Pharmacol.* **2007**, *7*, 298.
[73] Adam, J. M.; Bennett, D. J.; Bom, A.; Clark, J. K.; Feilden, H.; Hutchinson, E. J.; Palin, R.; Prosser, A.; Rees, D. C.; Rosair, G. M.; Stevenson, D.; Tarver, G. J.; Zhang, M.-Q. *J. Med. Chem.* **2002**, *45*, 1806.
[74] Schaller, S. J.; Fink, H. *Core Evid.* **2013**, *8*, 57.
[75] Ming-Qiang, Z. *Drug Discov. Today. Technol.* **2010**, *7*, 95.
[76] (a) Fuji, K.; Tsubaki, K.; Tanaka, K.; Hayashi, N.; Otsubo, T.; Kinoshita, T. *J. Am. Chem. Soc.* **1999**, *121*, 3807. (b) Kim, S. K.; Bang, M. Y.; Lee, S.-H.; Nakamura, K.; Cho, S.-W.; Yoon, J. *J. Incl. Phenom. Macrocycl. Chem.* **2002**, *43*, 71. (c) de Silva, A. P.; Gunaratne, H. Q. N.; McVeigh, C.; Maguire, G. E. M.; Maxwell, P. R. S.; O'Hanlon, E. *Chem. Commun.* **1996**, 2191. (d) Reetz, M. T.; Sostmann, S. *Tetrahedron* **2001**, *57*, 2515. (e) Guilbault, G. G.; Vaughan, A.; Hackney, D. *Anal. Chem.* **1971**, *43*, 721. (f) Gokel, G. W.; Leevy, W. M.; Weber, M. E. *Chem. Rev.* **2004**, *104*, 2723.
[77] (a) Ikeda, A.; Shinkai, S. *Chem. Rev.* **1997**, *97*, 1713. (b) (1) Yordanov, A. T.; Roundhill, D. M. *Coord. Chem. Rev.* **1998**, *170*, 93.
[78] (a) Lakatos, S.; Fetter, J.; Bertha, F.; Huszthy, P.; Tóth, T.; Farkas, V.; Orosz, G.; Hollósi, M. *Tetrahedron* **2008**, *64*, 1012. (b) Horváth, G.; Huszthy, P.; Szarvas, S.; Szókán, G.; Redd, J. T.; Bradshaw, J. S.; Izatt, R. M. *Ind. Eng. Chem. Res.* **2000**, *39*, 3576.
[79] Helgeson, R. C.; Koga, K.; Timko, J. M.; Cram, D. J. *J. Am. Chem. Soc.* **1973**, *95*, 3021.
[80] Gasparrini, F.; Misiti, D.; Villani, C.; Borchardt, A.; Burger, M. T.; Still, W. C. *J. Org. Chem.* **1995**, *60*, 4314.
[81] (a) Chao, Y.; Cram, D. J. *J. Am. Chem. Soc.* **1976**, *98*, 1015–1017. (b) Talma, A. G.; Jouin, P.; De Vries, J. G.; Troostwijk, C. B.; Buning, G. H. W.; Waninge, J. K.; Visscher, J.; Kellogg, R. M. *J. Am. Chem. Soc.* **1985**, *107*, 3981.
[82] Breslow, R.; Czarnik, A. W.; Lauer, M.; Leppkes, R.; Winkler, J.; Zimmerman, S. *J. Am. Chem. Soc.* **1986**, *108*, 1969.
[83] (a) Northrop, B. H.; Zheng, Y.-R.; Chi, K.-W.; Stang, P. J. *Acc. Chem. Res.* **2009**, *42*, 1554. (b) Reczek, J. J.; Kennedy, A. A.; Halbert, B. T.; Urbach, A. R. *J. Am. Chem. Soc.* **2009**, *131*, 2408.
[84] (a) Crowley, J. D.; Goldup, S. M.; Lee, A.-L.; Leigh, D. A.; McBurney, R. T. *Chem. Soc. Rev.* **2009**, *38*, 1530. (b) Niu, Z.; Gibson, H. W. *Chem. Rev.* **2009**, *109*, 6024. (c) Wu, J.; Fang, F.; Lu, W.-Y.; Hou, J.-L.; Li, C.; Wu, Z.-Q.; Jiang, X.-K.; Li, Z.-T.; Yu, Y.-H. *J. Org. Chem.* **2007**, *72*, 2897. (d) Chang, T.; Heiss, A. M.; Cantrill, S. J.; Fyfe, M. C. T.; Pease, A. R.; Rowan, S. J.; Stoddart, J. F.; Williams, D. J. *Org. Lett.* **2000**, *2*, 2943.
[85] (a) Nguyen, T. H.; Ansell, R. J. *Org. Biomol. Chem.* **2009**, *7*, 1211. (b) Che, Y.; Zang, L. *Chem. Commun. (Camb).* **2009**, 5106. (c) Huang, F.; Nagvekar, D. S.; Slebodnick, C.; Gibson, H. W. *J. Am. Chem. Soc.* **2005**, *127*, 484.
[86] Pluth, M. D.; Bergman, R. G.; Raymond, K. N. *J. Am. Chem. Soc.* **2007**, *129*, 11459.
[87] Späth, A.; König, B. *Beilstein J. Org. Chem.* **2010**, *6*, 32.
[88] Houk, K. N.; Leach, A. G.; Kim, S. P.; Zhang, X. *Angew. Chem. Int. Ed.* **2003**, *42*, 4872.
[89] *Combinatorial Chemistry*; Bannwarth, W.; Felder, E., Eds.; Methods and Principles in Medicinal Chemistry; Wiley-VCH Verlag GmbH: Weinheim, Germany, 2000.

[90] *Dynamic Combinatorial Chemistry*; Reek, J. N. H.; Otto, S., Eds.; Wiley-VCH Verlag GmbH & Co. KGaA: Weinheim, Germany, 2010.
[91] Xu, S.; Giuseppone, N. *J. Am. Chem. Soc.* **2008**, *130*, 1826.
[92] Giuseppone, N. *Acc. Chem. Res.* **2012**, *45*, 2178.
[93] (a) Belowich, M. E.; Stoddart, J. F. *Chem. Soc. Rev.* **2012**, *41,* 2003. (b) Klein, J. M.; Saggiomo, V.; Reck, L.; Luning, U.; Sanders, J. K. M. *Org. Biomol. Chem.* **2012**, *10,* 60. (c) Cougnon, F. B. L.; Jenkins, N. A.; Pantos, G. D.; Sanders, J. K. M. *Angew. Chem. Int. Edit.* **2012**, *51,* 1443. (d) Stefankiewicz, A. R.; Sambrook, M. R.; Sanders, J. K. M. *Chem. Sci.* **2012**, *3,* 2326. (e) Beeren, S. R.; Sanders, J. K. M. *J.* Sanders, J. K. M. *Am. Chem. Soc.* **2011**, *133,* 3804. (f) Chung, M-K.; Severin, K.; Lee, S. J.; Waters, M. L.; Gagne, M. R. *Chem. Sci.* **2011**, *2,* 744. (g) Rodriguez-Docampo, Z.; Eugenieva-Ilieva, E.; Reyheller, C. Belenguer, A. M.; Kubik, S.; Otto, S. *Chem. Commun.* **2011**, *47,* 9798. (h) Beeren, S. R. *Chem. Sci.* **2011**, *2,* 1560. (i) Bru, M.; Alfonso, I.; Botle, M.; Burguete, M. I.; Luis, S. V. *Chem. Commun.* **2011**, *47,* 283. (j) Klein, J. M.; Saggiomo, V.; Reck, L.; Mcpartlin, M.; Pantos, G. D.; Luning, U.; Sanders, J. K. M. *Chem. Commun.* **2011**, *47,* 3371. (k) Schleef, F.; Luning, U. *Eur. J. Org. Chem.* **2011**, 2062. (l) Ladame, S. *Org. Biomol. chem* **2008**, *6,* 219. (m) Ludlow, R. F.; Otto, S. *J. Am. Chem. Soc.* **2008**, *130,* 12218. (n) Vial, L.; Ludlow, R. F.; Leclaire, J.; Perez-Fernandez, R.; Otto, S. *J. Am. Chem. Soc.* **2006**, *128,* 10253.
[94] Corbett, P. T.; Leclaire, J.; Vial, L.; West, K. R.; Wietor, J.-L.; Sanders, J. K. M.; Otto, S. *Chem. Rev.* **2006**, *106*, 3652.
[95] (a) Otto, S.; Furlan, R. L. E.; Sanders, J. K. M. *Science* **2002**, *297*, 590. (b) Corbett, P. T.; Tong, L. H.; Sanders, J. K. M.; Otto, S. *J. Am. Chem. Soc.* **2005**, *127*, 8902.
[96] (a) Petti, M. A.; Shepodd, T. J.; Barrans, R. E.; Dougherty, D. A. *J. Am. Chem. Soc.* **1988**, *110*, 6825. (b) Shepodd, T. J.; Petti, M. A.; Dougherty, D. A. *J. Am. Chem. Soc.* **1986**, *108*, 6085. (c) Petti, M. A.; Shepodd, T. J.; Dougherty, D. A. *Tetrahedron Lett.* **1986**, *27*, 807. (d) reference 25
[97] Black, S. P.; Sanders, J. K. M.; Stefankiewicz, A. R. *Chem. Soc. Rev.* **2014**, *43*, 1861.

Chapter 2: A synthetic receptor for nicotine from a dynamic combinatorial library

This chapter focuses on the external template effect in dynamic combinatorial chemistry (DCC), an approach commonly used to generate synthetic receptors for particular guest molecules. It describes the development of a synthetic receptor for nicotine from a dynamic combinatorial library (DCL) in water at near physiological pH.
The first part of the chapter briefly reviews the relevant biological roles of nicotine and the challenge of obtaining a synthetic receptor that binds nicotine under near physiological conditions. Then we describe the design and the synthesis of building blocks soluble at pH 7-9 and able to generate divers DCLs from which nicotine can select its receptor. The use of a DCL to select a nicotine receptor and the binding features of the complex formed between nicotine and the selected receptor are discussed in the last part of this chapter. The work presented here was initiated by Fred Ludlow and Olivier Perraud and was completed by the author and published recently.[1]

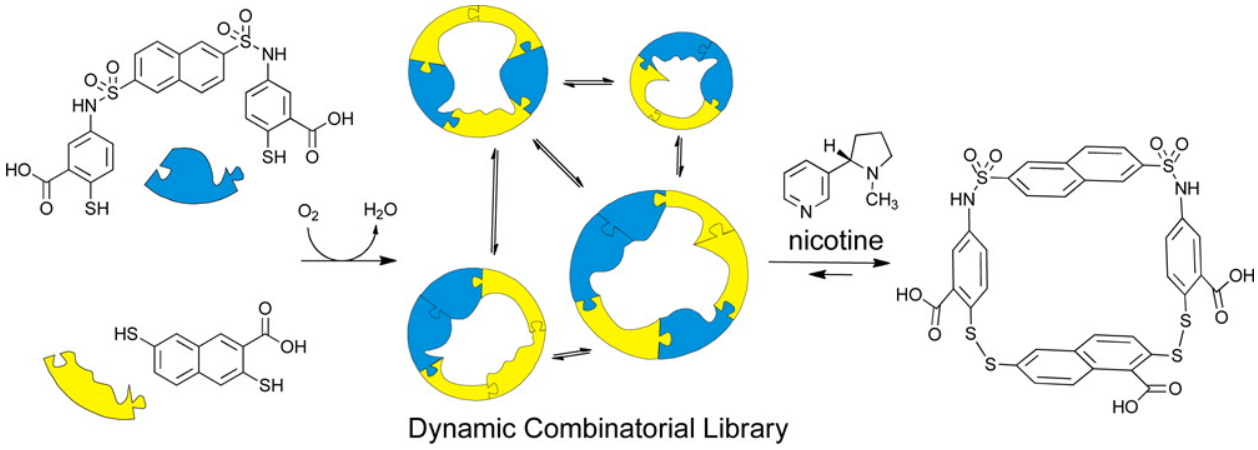

This chapter has been published:

Hamieh, S.; Ludlow, R. F.; Perraud, O.; West, K. R.; Mattia, E.; Otto, S. *Org. Lett.* **2012**, *14*, 5404–5407.

2.1 Introduction

(S)-Nicotine (Scheme 2.1) is a toxic alkaloid produced by the tobacco plant.[2] Nicotine has been used as a natural insecticide,[3] and its potential as a therapeutic agent for treatment of Alzheimer's,[4] Parkinson's[5] and psychiatric diseases[6] and as a pain controller[7] has been investigated. Nicotine acts principally as a potent agonist on the nicotinic acetylcholine receptors such as α4β2[8] and induces the release of several neurotransmitters.[9] Intake of nicotine often gives rise to addiction.[10] At present, smoke cessation treatments include nicotine replacement therapy[11] where nicotine is usually administered in a small quantity as a nicotine β-cyclodextrin complex.[12]

Despite the important biological roles of nicotine, relatively few synthetic receptors for nicotine have been published to date.[13] Indeed, molecular recognition of nicotine in water is challenging given the relatively hydrophilic nature of this alkaloid as measured by the octanol-water partition coefficient log D = 0.41 at pH 7.4.[14]

Despite having only few degrees of freedom, nicotine lacks a well-defined conformation in solution.[15] Therefore designing a receptor for it using classical organic synthesis is challenging.

Dynamic combinatorial chemistry is a powerful alternative approach for providing potential receptors.[16] In this approach it is sufficient to know the functional groups of the target, while it is not necessary to know their relative orientations. As discussed in the first chapter, in a dynamic combinatorial library (DCL), designed receptor fragments (building blocks) react reversibly with one another to form a mixture of interconverting library members that is under thermodynamic control. The libraries are adaptive, *i.e.* introducing nicotine into a DCL of potential hosts should shift the equilibrium in favor of (ideally) the best receptor(s) for the nicotine. Thus, the nicotine should drive the construction of its own receptor from smaller fragments.

2.1 Building block design

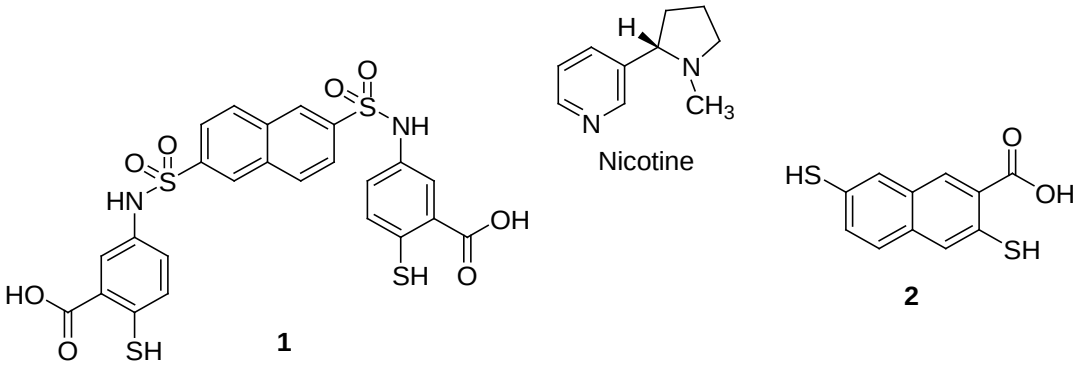

Scheme 2.1: Structure of nicotine, used as a template in the DCL, and building block **1** and **2** selected to generate a DCL able to recognize nicotine under near physiological conditions.

In DCC, a primary consideration in the building block design is the type of reversible reaction used to generate DCLs. We selected building blocks **1** and **2** (Scheme 2.1) capable of reversible covalent associations using thiol-disulfide exchange in water at pH 7-9 and allowing for the screening for nicotine binding under near physiological pH. Another consideration regarding the design of the building block is the structure of the functional groups of the target template and its protonation state under the DCL conditions. Nicotine contains both a hydrophobic moiety (the pyridine ring) and a hydrophilic moiety (the pyrrolidine which is monoprotonated at physiological pH). Building block **1** displays motifs potentially suitable for nicotine recognition, notably the naphthalene and benzene rings that may provide π-π and

cation-π interactions with the guest. The sulfonamide moieties of **1** may be able to interact with the protonated pyrrolidine moiety of nicotine through hydrogen bonding. Additionally, the different conformations related to the two sulfonamide groups of building block **1**, where the naphthalene and benzene rings can be in *cis-cis*, *trans-trans* and *trans-cis* conformations, can play a significant role in the molecular recognition of the template.[17] Carboxylate groups can serve as water solubilizing groups and may interact electrostatically with the protonated nicotine. The backbone structure of building block **1** exhibits a combination of rigidity, provided by the naphthalene core, and conformational flexibility, provided by the rotation around the carbon-sulfur bond of the two sulfonamide arms, which is a desirable combination of features according to Sanders *et. al*.[18] The relatively long flexible arms along with the accessibility of different sulfonamide conformers could allow the host to adapt its shape upon binding nicotine to optimize the interactions between the host and the guest. Also, the relative flexibility of building block **1** should promote the formation of a diverse product distribution.[19]

The naphthalene dithiol building block **2** was reported previously by Kevin West in 2006. In the absence of a good template, a DCL made from this building block consists predominately of a series of isomeric homo-[2]-catenanes $(\mathbf{2})_4$-$(\mathbf{2})_4$,[20] and a minor amount of cyclic homotetramer $(\mathbf{2})_4$ as it was proven later by the author (see Chapter 3). Adding the quaternary ammonium ion **2.1** to the DCL made from building block **2** changes the equilibrium away from the homo-[2]-catenanes $(\mathbf{2})_4$-$(\mathbf{2})_4$ to form exclusively cyclic homo-tetramer $(\mathbf{2})_4$ (Figure 2.1). The homo-tetramer $(\mathbf{2})_4$ was able to host the hydrophobic quaternary ammonium guest **2.1** inside its relatively large hydrophobic cavity and showed a binding affinity K_a of 1 x 10^7 M^{-1},[20] which is unusually high for a host-guest system in water.

Building block **2**, like building block **1**, exhibits motifs that are promising for nicotine recognition such as the naphthalene core and the carboxylate group.

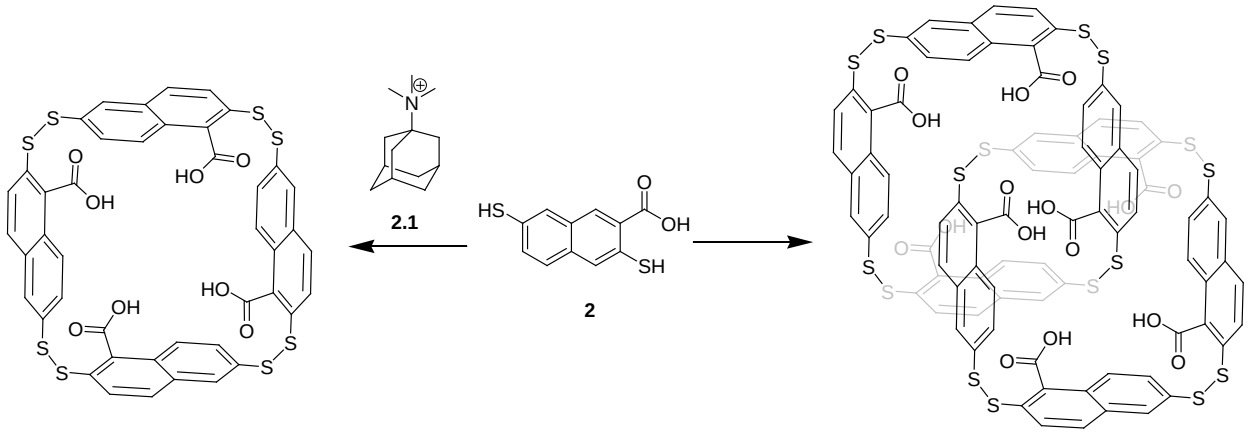

Figure 2.1: Behavior of a DCL made from building block **2**, as described by West *et. al.*[20] Building block **2** forms mixture of isomers of octameric [2]-catenanes $(\mathbf{2})_4$-$(\mathbf{2})_4$ (right) in the untemplated library, while addition of template **2.1** leads to the formation of mixture of isomers of tetramer $(\mathbf{2})_4$ (left).

2.2 Results and Discussion

2.2.1 Synthesis of building block 1

The synthesis of building block **1** is outlined in Scheme 2.2. It starts by the preparation of amine **2.5**, a molecule designed by West *et al.,*[21] which carries protected thiol and carboxylic acid

groups. This compound is a useful intermediate for preparing building blocks for reversible disulfide chemistry, as it may in principle be coupled to any carboxylic acid or sulfonyl chloride, and can be prepared in large scale (15 g).
Amine **2.5** was coupled to bis-sulfonyl chloride **2.7** which was obtained from the conversion of commercially available sodium sulfonate **2.6** in HSO_3Cl/CH_3Cl. The protected building block **2.8** was deprotected to remove the ester and the thiocarbamoyl groups under basic conditions to afford dithiol building block **1** in good purity, but in moderate yield. The synthesis of building block **2** has been reported previously by West *et. al.*[20]

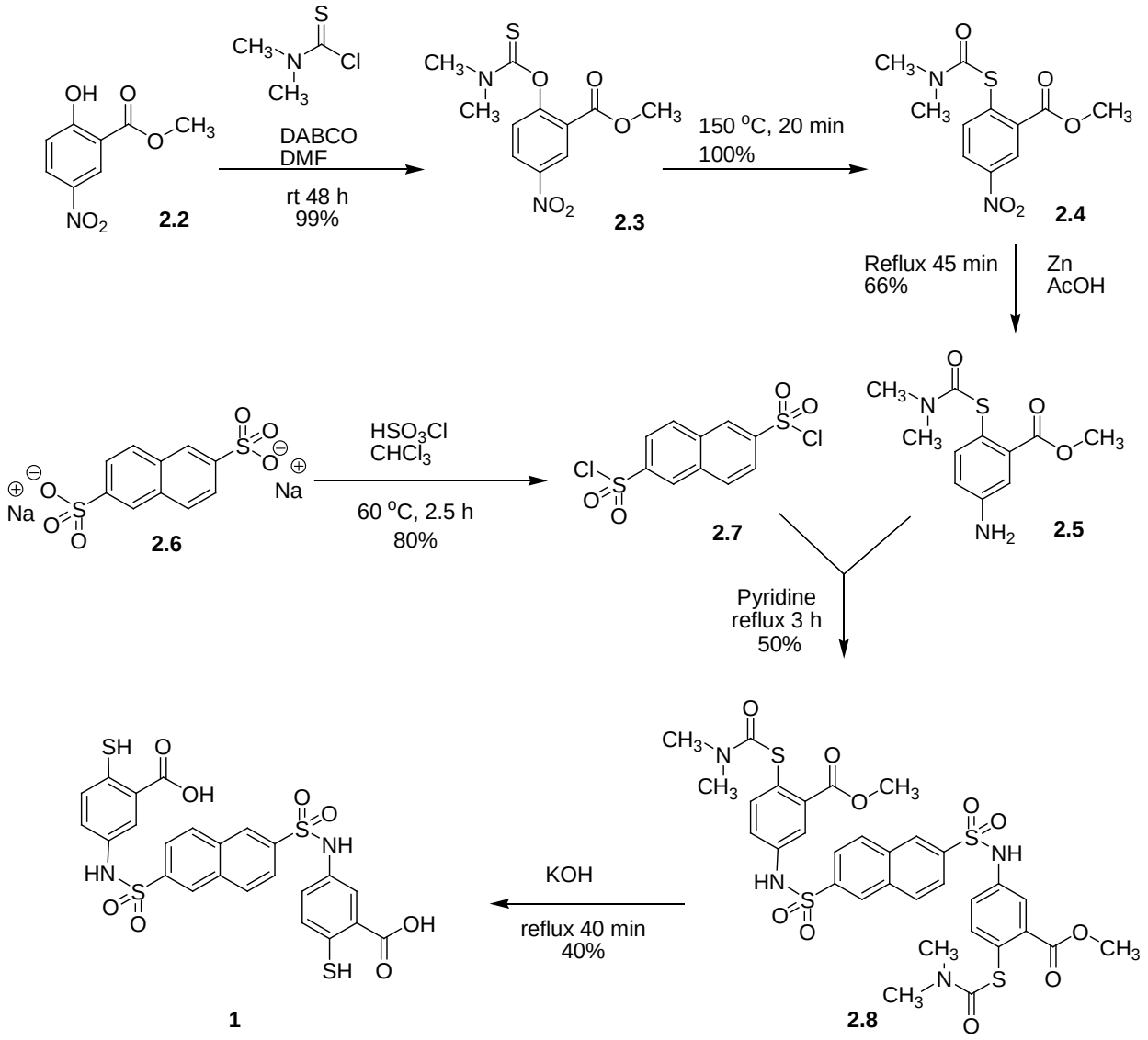

Scheme 2.2: Syntheses of building block **1** as described by R. Fred Ludlow and Kevin West.[20]

2.2.2 Dynamic combinatorial libraries

Two libraries were prepared by mixing equimolar amounts of building blocks **1** and **2** (5.0 mM in total), with and without nicotine, and allowing these to oxidize and equilibrate in aqueous

solution (50 mM borate buffer, pH 8.4) in the presence of air, following standard protocols (see experimental part).
The compositions of the resulting DCLs were analyzed by HPLC and mass spectrometry (Figure 2.2 and Figure 2.4). Cyclic monomer (**1**), homodimer (**1**)$_2$, heterodimer (**1**-**2**), homotetramer (**2**)$_4$, and catenane (**2**)$_4$-(**2**)$_4$ were the major products in the absence of nicotine (Scheme 2.3). Based on the carboxylate substituent arrangements, the asymmetric structure of **2** gives rise to four different isomers of (**2**)$_4$ and many different isomers of catenane (**2**)$_4$-(**2**)$_4$.[20] Cyclic heterodimer (**1**-**2**) is expected to generate only one isomer (Figure 2.3). However, despite the symmetrical structure of building block **1** we could detect three HPLC-MS peaks at the retention times 13.87, 14.1 and 14.65 min with masses corresponding to those of the cyclic heterodimer (**1**-**2**) (m/z = 821.10). We speculate that the different isomers of cyclic heterodimer (**1**-**2**) are due to different conformations of the two sulphonamide groups.[17] The numbers of HPLC peaks corresponding to (**1**-**2**) are consistent with the theoretical possible number of conformation that the two sulfonamide moieties can have: cis-cis, trans-trans and trans-cis. When nicotine was introduced into the DCL, the area of the peak corresponding to one of the isomers of heterodimer (**1**-**2**) increased by an amplification factor of 3.2 relatively to the untemplated DCL, at the expense of most of the other library members, including the other two isomers of (**1**-**2**). Introduction of nicotine drives the conversion of 40% of dithiols **1** and **2** into the formation of this receptor. The fact that one isomer of the homotetramer (**2**)$_4$ was amplified in a library made from building blocks **1** and **2** suggests that it may also have affinity for nicotine. However (**2**)$_4$ aggregates extensively, preventing its use as a synthetic receptor.[20]

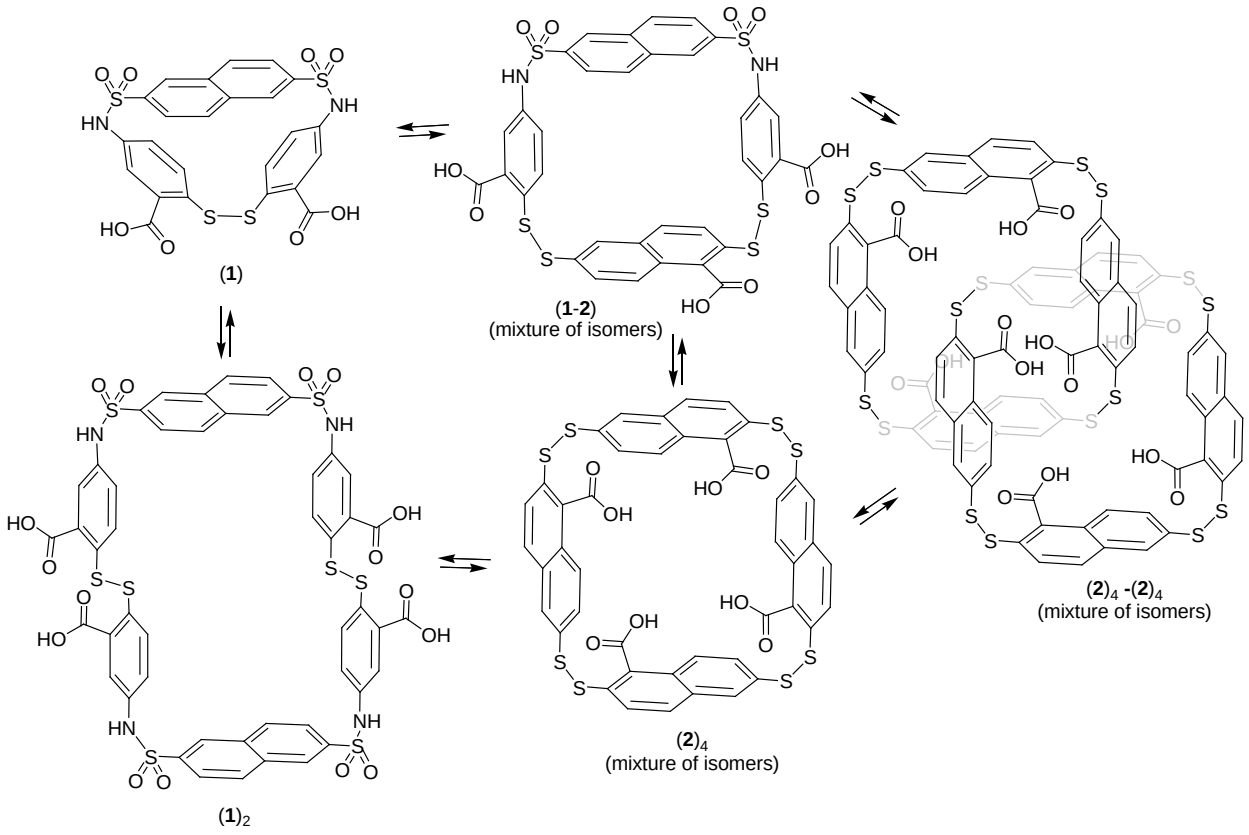

Scheme 2.3: Structure of the main constituents of the dynamic combinatorial library made from building block **1** and **2**, as found in HPLC and MS analyses.

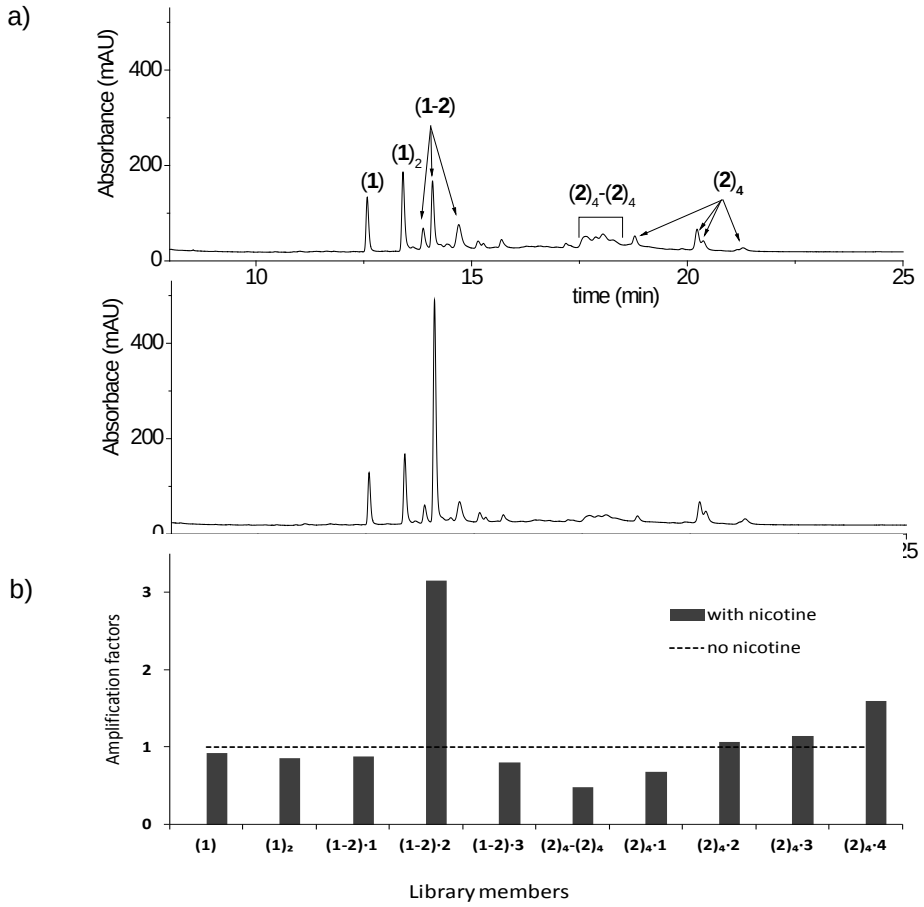

Figure 2.2: HPLC analyses of the libraries made from equimolar amount of dithiols **1** and **2** (5.0 mM in total), (a) in the absence (top) and in the presence (bottom) of nicotine (2.5 mM). (b) Amplification factors for the main library members.

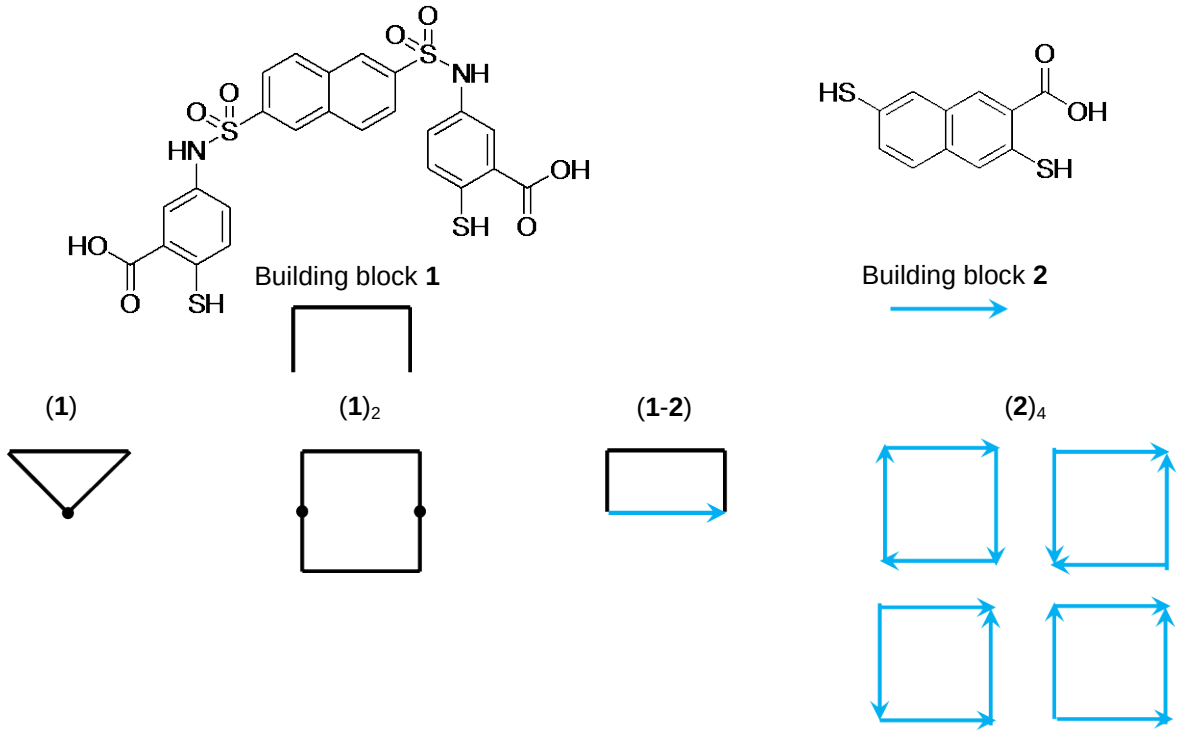

Figure 2.3: Schematic representation of the isomers expected in DCL products formed upon oxidizing a mixture of building blocks **1** and **2** in water at pH 8.4. The possible numbers of isomers of the DCL product are: (from left to right) one isomer for (**1**), (**1**)$_2$ and (**1**-**2**) and four isomers for (**2**)$_4$.

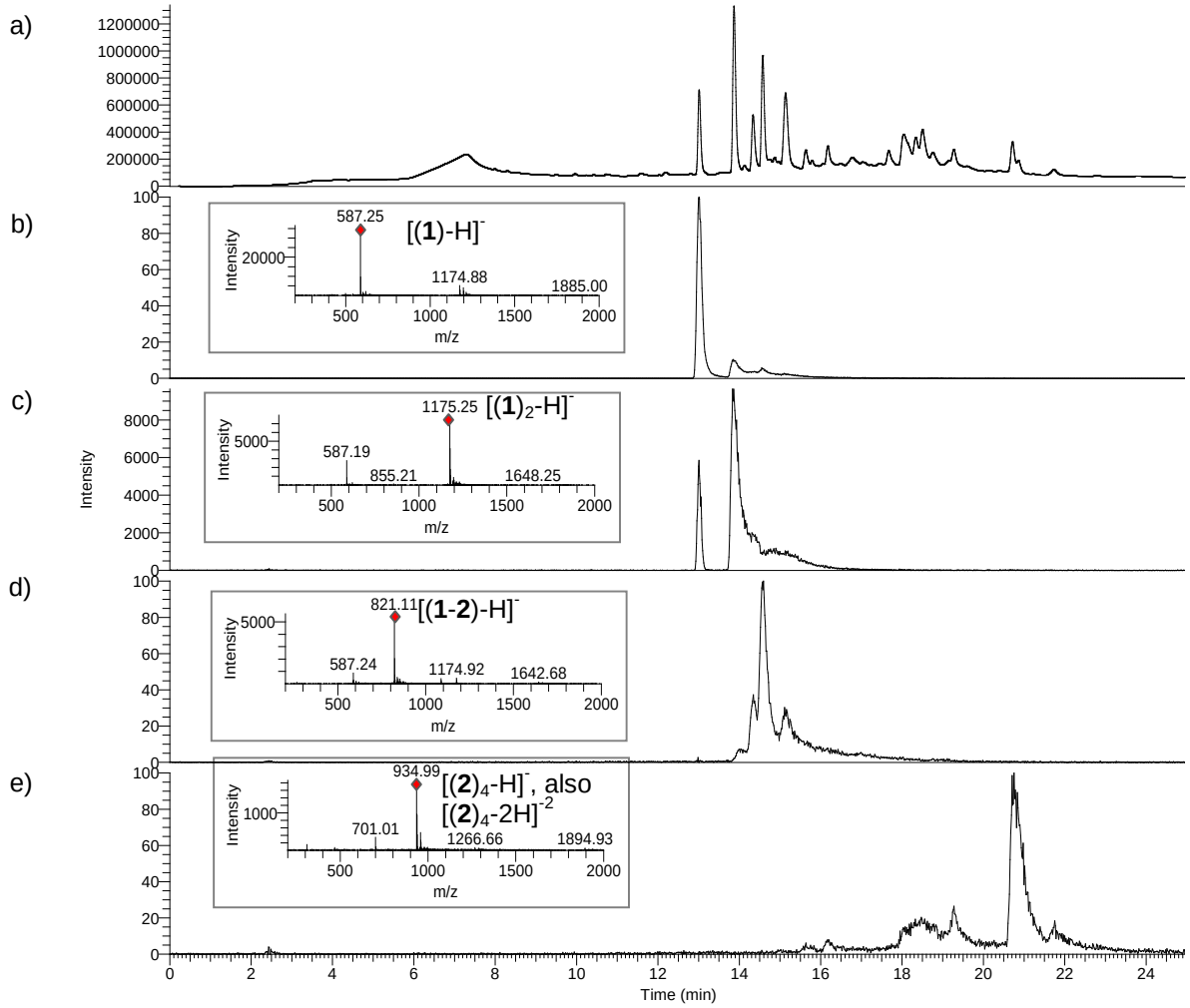

Figure 2.4: HPLC-MS analysis of a DCL prepared in 50.0 mM borate buffer (pH 8.4) and made from equimolar amounts of building blocks **1** and **2** (5.0 mM in total). (a) HPLC-UV chromatogram at 280 nm; (b) Extracted ion chromatogram (negative ion mode) corresponding to cyclic monomer (**1**) (586.5-587.5) with (insert) ESI-MS spectra [m/z 200-2000] summed over the 12.93-13.12 min retention time window, corresponding to cyclic monomer (**1**), showing [(**1**)-H]$^-$ m/z = 587.25 (expected = 586.97); (c) Extracted ion chromatogram (negative ion mode) corresponding to cyclic homodimer (**1**)$_2$ (1174.5-1175.5) with (insert) ESI-MS spectra [m/z 200-2000] summed over the 13.78-13.96 min retention time window, corresponding to cyclic homodimer (**1**)$_2$, showing [(**1**)$_2$-H]$^-$ m/z = 1175.25 (expected = 1174.95); (d) Extracted ion chromatogram (negative ion mode) corresponding to cyclic heterodimer (**1**-**2**) (820.5-821.5) with (insert) ESI-MS spectra [m/z 200-2000] summed over the 14.29-14.41, 14.47-14.73 and 15.08-15.23 min retention time windows, corresponding to three isomers of cyclic heterodimer (**1**-**2**), showing [(**1**-**2**)-H]$^-$ m/z = 821.11 (expected = 820.95); (e) Extracted ion chromatogram (negative ion mode) corresponding to homotetramer (**2**)$_4$ (934.5-935.5) and doubly charged catenane (**2**)$_4$-(**2**)$_4$ (934.5-935.5) with (insert) ESI-MS spectra [m/z 200-2000] summed over the 19.24-19.29, 20.65-20.75, 20.82-20.91 and 21.72-21.82 min retention time windows, corresponding to the four isomers of cyclic homoteramer (**2**)$_4$,[20] showing [(**2**)$_4$-H]$^-$ m/z = 934.99 (expected = 934.92). The ESI-MS spectra [m/z 200-2000] summed over the 17.97-18.88 min retention time window, corresponding to isomers of doubly charged homocatenane (**2**)$_4$-(**2**)$_4$, shows [(**2**)$_4$-(**2**)$_4$-H]$^{-2}$ m/z = 934.89 (expected = 934.92) as proven by 0,5 m/z unit spacing in the isotopic pattern.[20]

2.2.3 Binding Studies

A library made from equimolar amounts of building blocks **1** and **2** and nicotine as a template (7.5 mM in total) gives macrocycle (**1**-**2**) in 40% yield allowing its isolation by preparative HPLC. The isolated isomer of receptor (**1**-**2**) was characterized using HPLC-MS (Figure 2.5), ^{1}H-NMR, and elemental analysis (see experimental part). The structure of the complex formed between host (**1**-**2**) and nicotine as a guest was investigated using proton NMR spectroscopy and CPK models while the host-guest binding affinity was determined using Isothermal Titration Calorimetry (ITC).

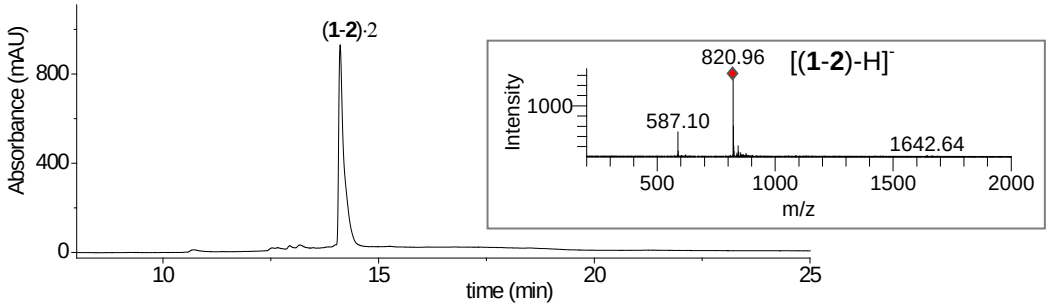

Figure 2.5: HPLC-UV chromatogram at 280 nm of the purified receptor (**1**-**2**) after isolation using preparative HPLC, with (insert) ESI-MS spectra [m/z 200-2000] summed over the 14.47-14.73 min retention time window, corresponding to the second isomer of heterodimer (**1**-**2**), showing [(**1**-**2**)-H]$^{-}$ m/z = 820.96 (expected = 820.95).

2.2.3.1 ^{1}H NMR studies

The binding between the amplified isomer of (**1**-**2**) and nicotine was investigated using ^{1}H-NMR spectroscopy in borate buffer pD 8.4. The signals of the pyridine protons f, g and h of complexed nicotine are notably shielded relative to the corresponding signals for these protons in unbound nicotine (Figure 2.6). The observed shielding ($\Delta\delta \geq 0.29$ ppm) suggests that the pyridine is located in the shielding cones of the aromatic rings of the receptor. In contrast, the protons close to the pyrrolidinyl nitrogen, including the N-methyl protons, show a downfield shift. These observations suggest that the pyridine moiety, and not the pyrrolidine group of nicotine, is located within the cavity of receptor (**1**-**2**); *i.e.* the formation of π-π interactions appears to be favored over cation-π interactions.

2.2.3.2 CPK models

Inspections of CPK models of the free receptor (**1**-**2**) and its complex with nicotine provide further support for the conclusions from the ^{1}H NMR studies in paragraph 2.2.3.1. The results show that only the pyridine moiety of the guest can fit inside the cavity of host (**1**-**2**) allowing mainly π-π interactions to occur (Figure 2.7). Beside, the models of free receptor (**1**-**2**) show a possibility for different sulfonamide-related conformations of (**1**-**2**), resulting in different size cavities. However, the CPK model of host-guest (**1**-**2**)-nicotine complex shows only one conformation of (**1**-**2**) able to locate the pyridine moiety inside its cavity, where the naphthalene

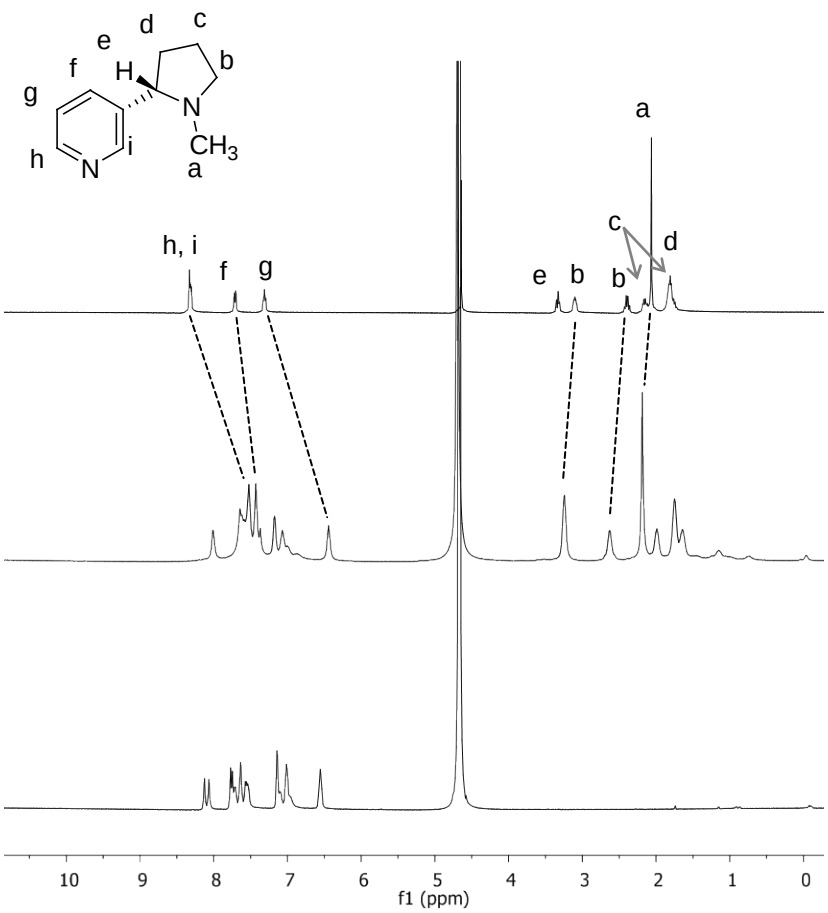

Figure 2.6: ^{1}H-NMR analyses of nicotine (top), receptor (**1**-**2**) (18.2 mM) in the presence of 1 equiv of nicotine (middle) and receptor (**1**-**2**) (18.2 mM) (bottom). Spectra were recorded at 300 K in 200 mM borate buffer (pD 8.4).

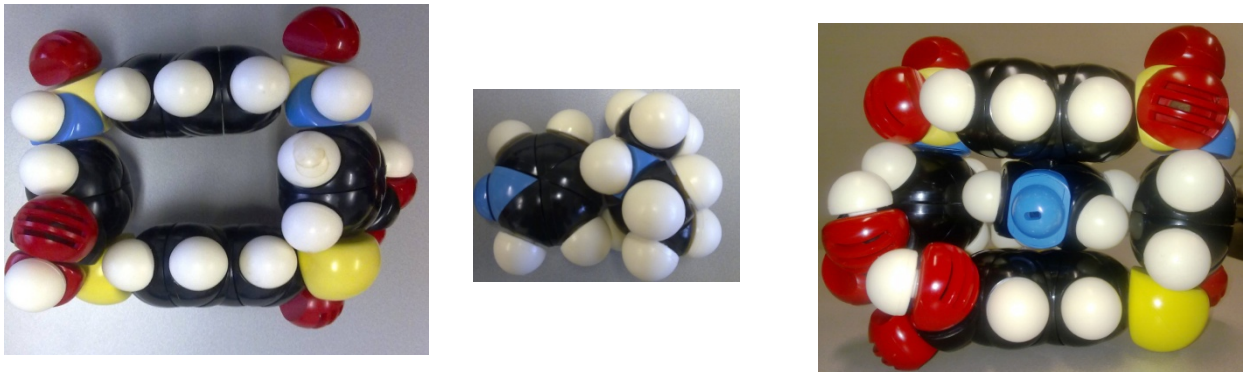

Figure 2.7: CPK models of receptor (**1**-**2**) in a cis-cis conformation (left), nicotine (middle) and the nicotine-(**1**-**2**) complex (right).

and benzene rings of (**1**-**2**) are in cis-cis conformation, providing further support for the conclusions of HPLC-MS studies in paragraph 2.2.2 concerning the amplification of only one of the suggested isomers of (**1**-**2**) after addition of nicotine to the DCL.

2.2.3.3 Isothermal Titration Calorimetry studies

The affinities of receptor (**1**-**2**) for nicotine were measured at three different pHs: 6.9, 8.4 and 9.3 using isothermal titration calorimetry (ITC). The titration data from these experiments are shown in Figure 2.8 and the values obtained are summarized in Table 2.1. The affinity constant for binding of nicotine to receptor (**1**-**2**) at pH 8.4 in 50 mM borate buffer was found to be 1.81 x 10^3 M^{-1}.

Table 2.1: Affinity constants (K_a), stoichiometric coefficients (n), enthalpies (ΔH^o), Gibbs energies (ΔG^o) and entropies $T\Delta S^o$ of the binding of receptor (**1**-**2**) to nicotine at 298 K, in 50 mM borate buffer and at three different pHs: 6.9, 8.4 and 9.3, as determined by isothermal titration calorimetry (ITC).

		Receptor (**1**-**2**)		
		pH 6.9	pH 8.4	pH 9.3
Nicotine	K_a [M^{-1}]	3.43 x 10^3	1.81 x 10^3	3.52 x 10^3
	n	0.82	1.02	0.89
	ΔH^o [KJ·mol^{-1}]	-18.63 x 10^3	-8.81 x 10^3	-18.30 x 10^3
	ΔG^o [KJ·mol^{-1}]	-20.17 x 10^3	-18.57 x 10^3	-20.23 x 10^3
	$T\Delta S^o$ [KJ·mol^{-1}]	1.54 x 10^3	9.76 x 10^3	1.93 x 10^3

This affinity is comparable to that for binding of nicotine to a cyclophane reported by Dougherty *et. al.,* and significantly higher than the affinities of β-cyclodextrin and cucurbit[7]uril for (S)-nicotine (K_a = 20-250 M^{-1} and 360 M^{-1} respectively).[13]
Performing ITC titrations on the binding of receptor (**1**-**2**) to nicotine at pH 6.9 and pH 9.3 led to comparable binding constants: 3.43 x 10^3 M^{-1} and 3.52 x 10^3 M^{-1}, respectively. This indicates that binding affinity is only weakly dependent on the protonation state of nicotine (pK_a = 7.8)[22] supporting the notion that cation-π interactions do not play a major role in the binding. Instead, binding appears to be driven predominantly by π-π interactions and hydrophobic interactions.
While the ΔG values are only weakly dependant on pH, the ΔH and $T\Delta S$ terms show much stronger pH dependence. We currently do not understand the cause of the largely compensating changes of these parameters with pH.

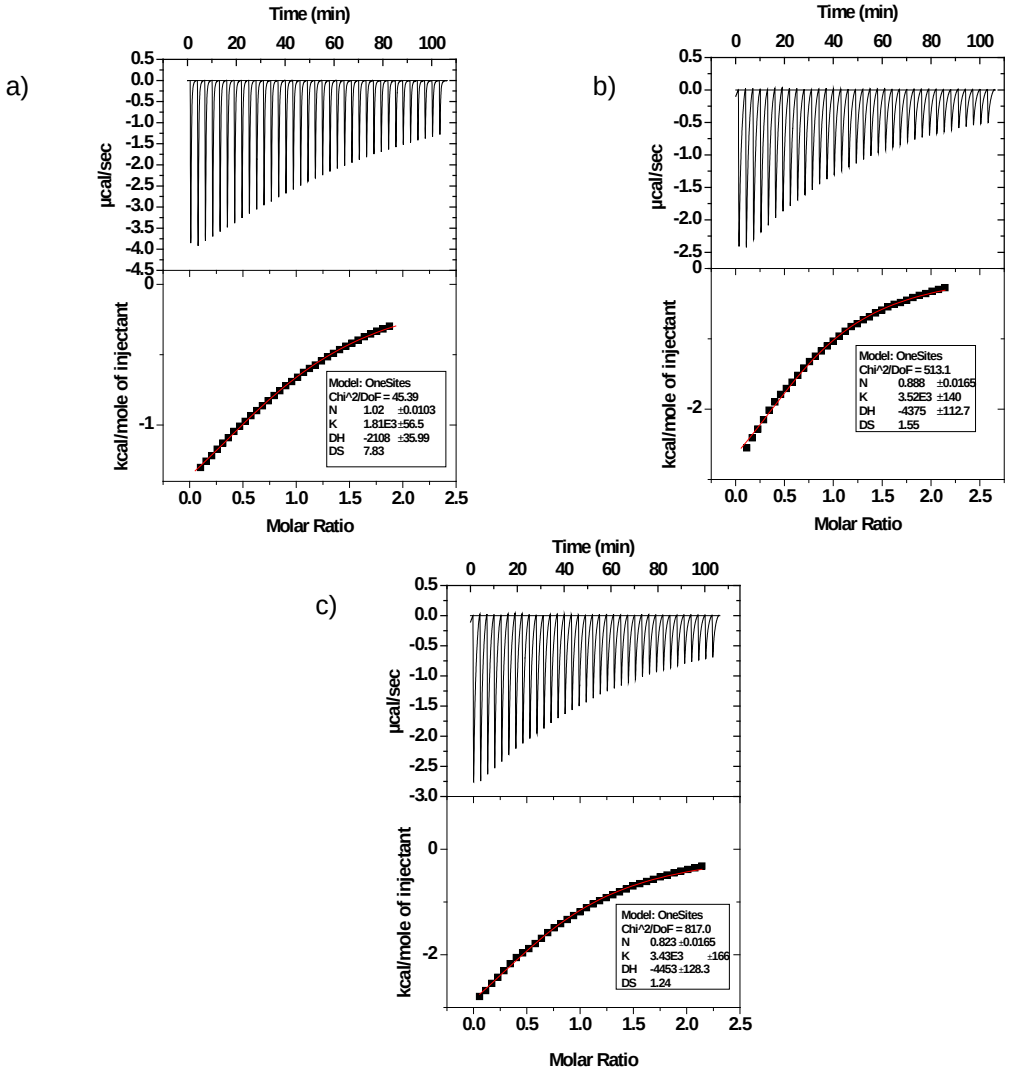

Figure 2.8: ITC traces and binding isotherms for the titrations of (a) receptor (**1**-**2**) (1.00 mM) with 10.00 mM of nicotine at pH 8.4; (b) receptor (**1**-**2**) (0.70 mM) with 7.00 mM of nicotine at pH 9.3 and (c) titration of receptor (**1**-**2**) (0.70 mM) with 7.00 mM of nicotine at pH 6.9.

2.3 Conclusion and outlook

Our results show that it is possible, after the design of only building block receptor fragments, to use dynamic combinatorial chemistry to obtain a receptor that is able to bind nicotine in water at neutral pH. Disulfide-based receptors of this type may find application as a carrier for nicotine that is able to release it upon reduction of disulfide linkages triggered by intracellular glutathione.[23]

While the nicotine receptor we developed has an affinity that is comparable to those reported in the literature, there remains a need to further improve binding affinity. For this purpose a promising strategy is to connect amino-acid residues to the carboxylate groups of the building blocks. These could improve the binding features of the formed receptor since the amino acids will be positioned at the portal of the hydrophobic cavity enabling additional non-covalent interactions. These amino acid derived building blocks will be discussed in more detail in Chapter 6.

2.4 Experimental section

2.4.1 Materials and Methods

Chemicals were purchased from Aldrich or Fluka. NMR analyses were performed using Bruker instruments. Spectra were recorded at 300 K. Elemental analyses were performed using a EuroEA3000-CHNS0-analyser Series from Euro Vector. Details of specialized analytical equipment are provided in the sections dealing with the respective analyses.

2.4.2 Synthetic procedures for building block 1

2-Dimethylthiocarbamoyloxy-5-nitrobenzoic acid methyl ester (**2.3**)

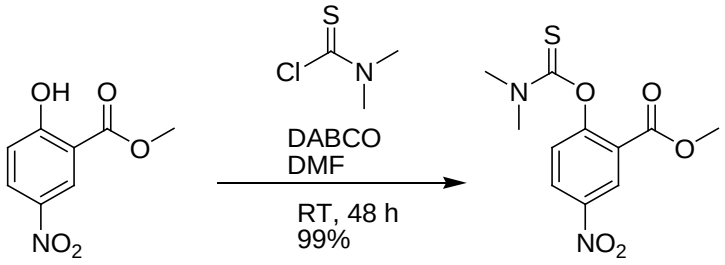

2.2 **2.3**

Methyl 5-nitrosalicylate **2.2** (70 g, 0.355 mol) was dissolved in 700 mL of dry DMF. Dimethylthiocarbamoyl chloride (65.8 g, 0.532 mol, 1.5 eq) was added to the solution followed by the gradual addition of 59.79 g of DABCO (0.533 mol, 1.5 eq) turning the solution yellow. After 20 min of stirring, a precipitate was formed. Stirring was continued for 48 h at which point no starting material could be detected by TLC (3:1 $CHCl_3$/EtOAc). A 50/50 brine/water solution (1.4 L) was added to the reaction mixture causing a large amount of material to precipitate. After stirring for a further 10 min the mixture was filtered. The residue was washed with 2 L of water and thoroughly dried to give 100 g (0.351 mol, 99%) of a pure white solid. ^{1}H NMR (400 MHz, $CDCl_3$) δ (ppm): 8.87 (d, 1H, J=2.7 Hz), 8.41 (dd, 1H, J=2.8, J=8.9 Hz), 7.31 (d, 1H, J=8.8 Hz), 3.89 (s, 3H), 3.47 (s, 3H), 3.40 (s, 3H). ^{13}C NMR (75 MHz, $CDCl_3$) δ (ppm): 186.1, 162.9, 158.2, 145.2, 128.1, 127.2, 126.5, 125.4, 52.9, 43.5, 39.3. MS $[M+H]^+$ found: 285.0552 (expected: 285.0540). Decomposition temperature: 125-126°C.

2-Dimethylcarbamoylsulfanyl-5-nitrobenzoic acid methyl ester (**2.4**)

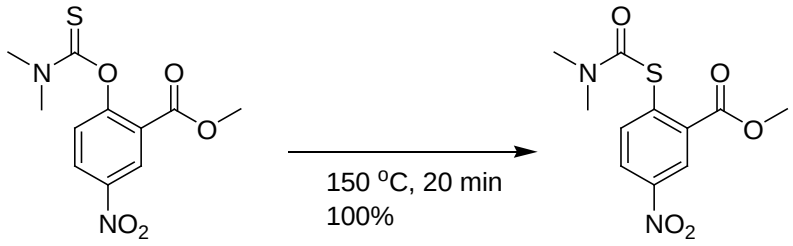

2.3 **2.4**

Carefully dried 2-dimethylthiocarbamoyloxy-5-nitrobenzoic acid methyl ester (**2.3**) (100 g, 0.351 mol) was heated to 150 °C under anhydrous conditions darkening to a brown colour. After 20

min the reaction mixture was allowed to cool and solidified. The product was then ground up to give a yellow solid in quantitative yield (100 g, 0.351 mol). ^{1}H NMR (400 MHz, $CDCl_3$) δ (ppm): 8.72 (d, 1H, J=2.6 Hz), 8.27 (dd, 1H, J=2.6 Hz, J=8.7 Hz), 7.84 (d, 1H, J=8.7 Hz), 3.94 (s, 3H), 3.16 (brs, 3H), 3.04 (brs, 3H). ^{13}C NMR (75 MHz, $CDCl_3$) δ (ppm): 165.5, 164.2, 147.3, 139.1, 137.5, 135.1, 125.5, 53.1, 37.3. MS: $(M+H)^+$found: 285.0552 (expected: 285.0540). Decomposition temperature: 112-113 ^{o}C.

5-Amino-2-dimethylcarbamoylsulfanyl benzoic acid methyl ester (**2.5**)

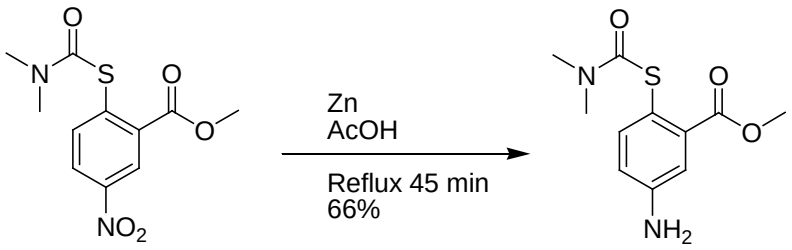

2.4 **2.5**

2-Dimethylcarbamoylsulfanyl-5-nitrobenzoic acid methyl ester (**2.4**) (25.0 g) was dissolved in 1 L of acetic acid. Zinc powder (200 g) was added in portions and the mixture refluxed for 45 min (note: it is important that the product is not left in acetic acid since otherwise the amine will be acetylated). The zinc powder was filtered off and the filtrate washed with acetic acid. The solution was diluted with 750 mL of water and the product extracted into DCM (5 x 200 mL). The DCM layer was washed with 10% NaOH until the aqueous fraction remained basic after washing and the DCM layer was washed a further time with water. The DCM layer was dried over sodium sulfate, filtered and concentrated to a yellow viscous liquid (about 30 mL). Diethyl ether (5 mL) is added and the product crystallized/precipitated overnight to a white solid (0.058 mol, 14.8 g, 66%). ^{1}H NMR (400 MHz, $CDCl_3$) δ (ppm): 7.33 (d, 1H, J=8.3 Hz), 7.14 (d, 1H, J=2.7 Hz), 6.73 (dd, 1H, J=2.7 Hz, J=8.3 Hz), 3.85 (s, 3H), 3.04 (brs, 6H). ^{13}C NMR (75 MHz, $CDCl_3$) δ (ppm): 167.7, 167.3, 147.7, 139.3, 136.6, 117.7, 116.9, 116.2, 52.3, 37.0. MS: $(M+H)^+$ found: 255.0798 (expected: 255.0798). Decomposition temperature: 120-121 ^{o}C.

Naphthalene-2,6-disulfonyl dichloride (**2.7**)

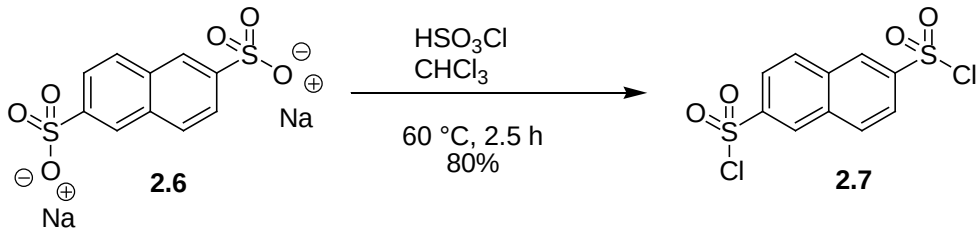

2.6 **2.7**

Chlorosulfonic acid (10 mL) was added dropwise and under a nitrogen atmosphere to 2,6-naphtalenedisulfonic acid disodium salt (1.00 g, 3.01 mmol), using an ice bath to maintain the temperature below 60 ˚C. The viscous solution was stirred during 30 min and 5 mL of chloroform was added. The solution was then heated to 60 ˚C for 2.5 h, cooled and poured into a 10 mL ice/water mixture. The solution was filtered to give a white solid which was dried in vacuum (yield: 740 mg, 80%). ^{1}H NMR ($CDCl_3$, 400 MHz) δ (ppm): 8.73 (s, 1H), 8.32 (d, 1H, J=8 Hz), 8.21 (d, 1H, J=8 Hz). ^{13}C NMR (75 MHz, $CDCl_3$) δ (ppm): 145.7, 132.1, 128.2, 124.2, 123.9. Decomposition temperature: 209-211 ˚C.

Protected building block 2.8

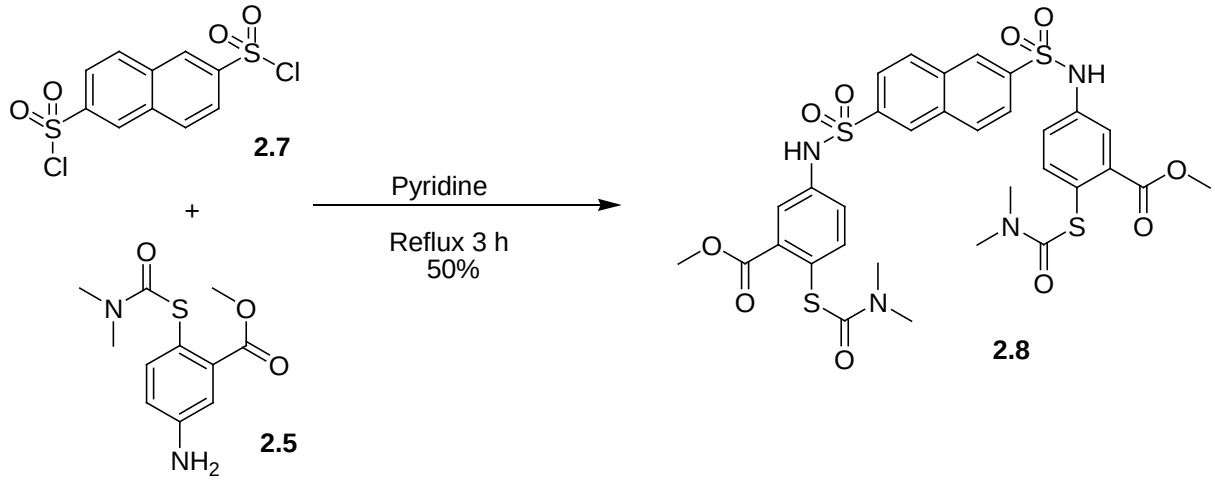

Amine **2.5** (558 mg, 2.19 mmol) was dissolved in pyridine (35 mL) and sulfonyl chloride **2.7** (352 mg, 1.08 mmol) was added in portions to the stirred solution. After 3 h of reflux, 70 mL of ethyl acetate was added and the solution was washed with 3x50 mL of 1 M HCl. The organic phase was separated, dried and then evaporated. The crude product was washed with 4x15 mL of ethanol to give a white solid (yield: 566 mg, 69%). ^{1}H NMR (DMSO, 400 MHz) δ (ppm): 10.99 (s, 1H), 8.59 (s, 1H), 8.36 (d, 1H, J=9 Hz), 7.90 (d, 1H, J=9 Hz), 7.51 (d, 1H, J=2.5 Hz), 7.36 (d, 1H, J=8 Hz), 7.33 (dd, 1H, J=8 Hz, J=2.5 Hz), 3.69 (s, 6H), 2.96-2.84 (bd, 12H). ^{13}C NMR ($(CD_3)_2SO$, 100 MHz) δ (ppm): 165.9, 164.5, 139.1, 138.4, 136.1, 133.2, 131.4, 127.9, 123.5, 123.2, 121.7, 120.5, 52.3, 36.5. Decomposition temperature: 267-271 ˚C. $(M+Na)^+$ found: 783.0848 (expected: 783.0893).

Building block 1

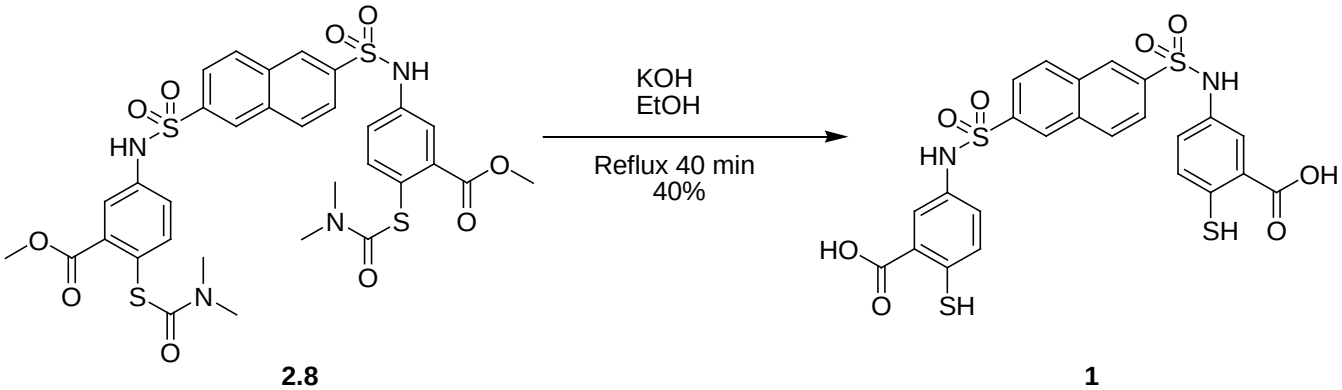

A solution of 7.6 g KOH in 100 mL of EtOH was degassed thoroughly with nitrogen and added under a nitrogen atmosphere to **2.8** (400 mg, 0.53 mmol). The solution was refluxed for 40 min. and then poured into a mixture of 20 mL of conc. HCl and 100 g of ice, forming a precipitate which was filtered and washed with 1 M HCl. The solid was dissolved in 140 mL of ethyl acetate and washed with 3x50 mL of a 10% HCl/brine mixture. The solvent was removed under reduced pressure to give a white solid **1** (Yield: 106 mg, 34.1%). ^{1}H NMR (DMSO, 400 MHz) δ (ppm): 10.53 (s, 1H), 8.46 (d, 1H, J=1 Hz) 8.29 (d, 1H, J=9 Hz), 7.81 (dd, 1H, J=9 Hz, J=1 Hz), 7.66 (d, 1H, J=2 Hz), 7.31 (d, 1H, J=5 Hz), 7.11 (dd, 1H, J=5 Hz, J=2 Hz). ^{13}C NMR (MeOD, 75 MHz) δ

(ppm): 169.1, 140.6, 136.2, 135.3, 134.9, 132.5, 131.7, 129.2, 128.1, 127.2, 126.2, 125.1. Elemental Analysis: C 48.18% (calcd 48.8%) H 3.01% (calcd 3.07%) N 4.29% (calcd 4.74%) Decomposition temperature: 282-286 ˚C. MS: $[M-H]^{-1}$found: 588.9900 (expected: 588.9946).

2.4.3 Methods of preparation and analysis of dynamic combinatorial libraries

2.4.3.1 Dynamic combinatorial library preparations

Stock solutions of single building blocks **1** and **2** and nicotine were freshly prepared at 10 mM concentration by dissolving separately appropriate amounts of **1**, **2** and nicotine in 50 mM borate buffer at pH 8.4. The pH was readjusted to 8.4 by addition of an appropriate volume of a 1 M solution of KOH.
For the untemplated library made from equimolar amounts of building blocks **1** and **2** at 5.0 mM overall building block concentration, 40 µl of each of the stock solutions of the two building blocks were combined with 120 µl of a borate buffer solution (50 mM, pH 8.4).
For the templated library made from equimolar amounts of building blocks **1** and **2** at 5.0 mM overall building block concentration, 40 µl of each of the stock solutions of the two building blocks and nicotine were combined with 80 µl of a borate buffer solution (50 mM, pH 8.4). The resulting nicotine concentration is 2.5 mM.
The mixtures were allowed to oxidize and equilibrate by stirring for 4 days in a closed vial at room temperature.

2.4.3.2 Dynamic combinatorial library analyses

HPLC analyses were performed using Agilent 1100 series and HPLC-MS analyses were performed using a Thermo Scientific HPLC coupled to a LCQ Fleet series mass spectrometer. Acetonitrile was purchased from Biosolve. Formic acid was purchased from Sigma-Aldrich. Analyses were performed using a reversed phase HPLC column (Kromasil C8, 4.6 x 150 mm, 5 µm), using an injection volume of 5 µL, a flow rate of 1 mL/min, and a gradient (5-95% in 30 min) of acetonitrile in doubly distilled water (both containing 0.1% formic acid). Negative ion mass spectra were acquired using electrospray ionization (capillary temperature: 450 °C; sheath gas flow: 40 (arb.); aux. gas flow rate: 1 (arb.); sweep gas flow: 1 (arb.); ionization spray voltage: 5 kV; capillary voltage: -9 V; tube lens: -100 V).

2.4.3.3 Isolation, elemental analysis and ^{1}H NMR characterisation of receptor (1-2)

The amplified isomer of receptor (**1**-**2**) was isolated from a DCL made from building blocks **1** and **2** (5 mM overall concentration) and nicotine (2.5 mM) dissolved in 50 mM borate buffer solution at pH 8.4 using a preparative HPLC from Shimadzu, Reservoir Tray series. Aliquots of 700 µL of this solution were injected into a reversed phase preparative HPLC column (Agilent C8 Zorbax Eclipse XBD, 9.4 x 250 mm, 5 µm) at 300 K. Using a flow rate of 5 mL/min and a gradient (5-95% over 40 min) of acetonitrile in water (both containing 0.1% formic acid), the receptor was collected from 40 runs. The solvents were removed under reduced pressure keeping the temperature below 40 °C. The last traces of solvent were removed using a freeze-dryer for 24 h. The crude host was dissolved in 50 mL of borate buffer (10 mM, pH 9.0) and sonicated for 2 min. The resulting solution was centrifuged and decanted. Hydrochloric acid (3 mL of a 2.0 M solution) was added to the supernatant. The resulting suspension was centrifuged and the pellet resuspended in dilute hydrochloric acid (30 mL of a 40 mM solution)

and centrifuged. The solid (5.2 mg; 9%) was dried using a freeze-dryer overnight. Elemental analysis for $C_{35}H_{22}N_2O_{10}S_6$. $3H_2O$ calcd (%): C 47.93, H 3.19, N 3.19; S 21.94 found C 48.14, H 3.17, N 3.30, S 23.64. ^{1}H NMR (400 MHz, borate buffer pD=8.4) δ (ppm): 8.25 (s, 1H), 8.18 (s, 1H), 7.65-7.89 (m, 7H), 7.08-7.26 (m, 6H), 6.68 (bd, 2H).

2.4.3.4 Isothermal Titration Calorimetry (ITC) experiments

Equilibrium constants, enthalpies and entropies of binding were determined using an isothermal titration calorimetry VP-ITC system from Microcal LLC. The titrations were carried out in a borate buffer solution (50 mM). The ITC experiment involved the titration of a solution of nicotine into a solution of the amplified isomer of receptor (**1**-**2**) at 298 K. The nicotine solution was added in 40 injections of 7 µL, separated by an interval of 180 s between injections. The peak produced by the first injection was discarded during data processing. Binding constants and enthalpies of binding were obtained by curve fitting of the titration data using the one-site binding model. Nicotine and receptor were weighed using an analytical precision balance and dissolved in a known volume of freshly degassed buffer and loaded into the system for immediate analysis. Solutions involved in the same titration experiment were made up from the same batch of buffer.

2.5 References

[1] Hamieh, S.; Ludlow, R. F.; Perraud, O.; West, K. R.; Mattia, E.; Otto, S. *Org. Lett.* **2012**, *14*, 5404.
[2] *Molecules of Death*, 2nd ed.; Waring, R. H., Steventon, G. B., Mitchell, S. C., Eds.; Imperial College Press: London, UK, 2007; Chapter 13, pp 233.
[3] Wink, M. *Theor. Appl. Genet.* **1988**, *75*, 225.
[4] (a) *Oxidative Stress and Age-Related Neurodegeneration*; Luo, Y.; Packer, L., Eds.; CRC Press: Florida, United States, 2005; Chapter 16, pp 265. (b) Ono, K.; Hasegawa, K.; Yamada, M.; Naiki, H. *Biol. Psychiatry* **2002**, *52,* 880.
[5] Powledge, T. M. *PLoS Biol.* **2004**, *2,* 1707.
[6] *Neural Mechanisms of Action of Drugs of Abuse and Natural Reinforcer*; Ubach, M. M.; Mondragón-Ceballos, R., Eds.; research signpost: India, 2008; Chapter 2, pp 121.
[7] Gaigeot, M. P.; Cimas, A.; Seydou, M.; Kim, J. Y.; Lee, S.; Schermann, J. P. *J. Am. Chem. Soc.* **2010**, *132,* 18067.
[8] Xiu, X.; Puskar, N. L.; Shanata, J. A. P.; lester, H. A.; Dougherty, D. A. *Nature* **2009**, *458,* 534
[9] Kauer, J. A.; Malenka, R. C. *Nature Rev. Neurosc.* **2007**, *8,* 844.
[10] Nishioka, T.; Yamamoto, D.; Zhu, T.; Guo, J.; Kim, S.; Chen, C. Y. *PLoS one* **2011**, *4,* e18619.
[11] Navarro, H. A.; Howard, J. L.; Pollard, G. T.; Ivy Carroll, F*. Br. J. Pharmacol.* **2009**, *156,* 1178.
[12] Davaran, S.; Rashidi, M. R.; Khandaghi, R.; Hashemi, M. *Pharmacol. Res***. 2005**, *51,* 233.
[13] (a) Kearney, P. C.; Mizoue, L. S.; Kumpf, R. A.; Forman, J. E.; McCurdy, A.; Dougherty, D. A. *J. Am. Chem. Soc.* **1993**, *115,* 9907. (b) Zhou, Y.; Yu, H.; Zhang, L.; Xu, H.; Wu, L.; Sun, J.; Wang, L. *Microchim. Acta.* **2009**, *164,* 63. (c) Berglund, J.; Cedergren, L.; Andersson, S. B. *Int. J. Pharma.* **1997**, *156,* 195.
[14] Zhu, C.; Jian, L.; Chen, T.-M.; Hwang, K.-K. *Eur. J. Med. Chem.* **2002**, *37*, 399.
[15] Takeshima, T.; Fukumoto, R.; Egawa, T.; Konoka, S. *J. Phys. Chem. A* **2002**, *106,* 8734.
[16] (a) Belowich, M. E.; Stoddart, J. F. *Chem. Soc. Rev.* **2012**, *41,* 2003. (b) Klein, J. M.; Saggiomo, V.; Reck, L.; Luning, U.; Sanders, J. K. M. *Org. Biomol. Chem.* **2012**, *10,* 60. (c) Cougnon, F. B. L.; Jenkins, N. A.; Pantos, G. D.; Sanders, J. K. M. *Angew. Chem. Int. Edit.* **2012**, *51,* 1443. (d) Stefankiewicz, A. R.; Sambrook, M. R.; Sanders, J. K. M. *Chem. Sci.* **2012**, *3,* 2326. (e) Beeren, S. R.; Sanders, J. K. M. *J.* Sanders, J. K. M. *Am. Chem. Soc.* **2011**, *133,* 3804. (f) Chung, M-K.; Severin, K.; Lee, S. J.; Waters, M. L.; Gagne, M. R. *Chem. Sci.* **2011**, *2,* 744. (g) Rodriguez-Docampo, Z.; Eugenieva-Ilieva, E.; Reyheller, C. Belenguer, A. M.; Kubik, S.; Otto, S. *Chem. Commun.* **2011**, *47,* 9798. (h) Beeren, S. R. *Chem. Sci.* **2011**, *2,* 1560. (i) Bru, M.; Alfonso, I.; Botle, M.; Burguete, M. I.; Luis, S. V. *Chem. Commun.* **2011**, *47,* 283. (j) Klein, J. M.; Saggiomo, V.; Reck, L.; Mcpartlin, M.; Pantos, G. D.; Luning, U.; Sanders, J. K. M. *Chem. Commun.* **2011**, *47,* 3371. (k) Schleef, F.; Luning, U. *Eur. J. Org. Chem.* **2011**, 2062. (l) Ladame, S. *Org. Biomol. chem* **2008**, *6,* 219. (m) Ludlow, R. F.; Otto, S. *J. Am. Chem. Soc.* **2008**, *130,* 12218. (n) Vial, L.; Ludlow, R. F.; Leclaire, J.; Perez-Fernandez, R.; Otto, S. *J. Am. Chem. Soc.* **2006**, *128,* 10253.
[17] (a) Senger, *S.; Chan, C.; Convery, M. A.; Hubbard, J. A.; Shah, G. P.; Watson, N. S.; Young. R. J. Bioorg. Med. Chem. Lett.* ***2007****, 17, 2931. (b)* Senger, S.; Convery, M. A.; Chan, C.; Watson, N. S*. Bioorg. Med. Chem. Lett.* ***2006****, 16,* 5731.
[18] Au-Yeung, H. Y.; Pengo, P.; Pantos, G. D., Otto, S.; Sanders, J. K. M. *Chem. Commun*. **2009**, 419.
[19] *Dynamic Combinatorial Chemistry;* Eds; J. N. H. Reek and S. Otto, Wiley-VCH, Weinheim, **2010**.
[20] West, K. R.; Ludlow, R. F.; Corbett, P. T.; Besenius, P. P.; Mansfeld, F. M.; Cormack, P. A. G.; Sherrington, D. C.; Goodman, J. M.; Stuart, M. C. A.; Otto, S. *J. Am. Chem. Soc*. **2008**, *130*, 10834.
[21] West, K. R. Molecular encapsulation through disulfide dynamic combinatorial chemistry. PhD thesis, University of Cambridge, England, **2006**.
[22] Petersson, E. J.; Choi, A.; Dahan, D. S.; Lester, H. A; Dougherty, D. A. *J. Am. Chem. Soc.* **2002**, *124,* 12662.
[23] West, K. R.; Otto, S. *Curr. Drug. Discov. Technol.* **2005**, *2,* 123.

Chapter 3: A “dial-a-receptor” dynamic combinatorial library

While many examples of external template effects in DCC have been reported, these have invariably revealed one or two receptors that bind to one or a few added templates. Thus far, no DCL has been reported where nearly all of the library members are amplified after exposure to a broad range of individual guests. Moreover, DCLs that reliably produce hosts for a specific family of guests have not been reported yet. We now introduce the first example of a ‘dial-a-receptor’ library, where the vast majority of a broad range of 30 amine or ammonium ion guests led to the amplification of one or two receptors with similar cavity sizes, revealing an unprecedentedly large number of six different receptors that constitute nearly all of the most abundant DCL members and cover a continuous range of receptor sizes.
The introduction of this chapter briefly reviews the diverse applications of external templating in DCC and the challenge of extending the number of functions exhibited by one DCL through this approach. In the second part of the chapter, we describe the design of a two dithiol building block DCL from which nearly all of 30 amine and ammonium ion guests can select their receptors at near physiological pH. The introduction of a new methodology to compare the amplification factors of DCL members, the quantification of the library member concentrations and the relation between template size and charge and macrocycle selection are then described in the last parts of the chapter.

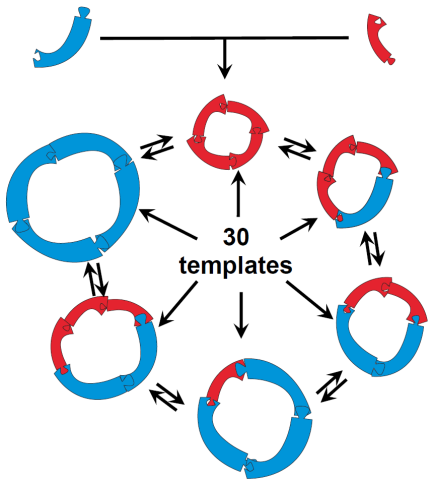

This chapter has been published:

Hamieh, S.; Saggiomo, V.; Nowak, P.; Mattia, E.; Ludlow, R. F.; Otto, S. *Angew. Chem. Int. Ed. Engl.* **2013**.

3.1 Introduction

External templating in DCC is a popular approach widely used to develop synthetic receptors for a wide range of particular guests[1] such as organic cations[2] and anions,[3] inorganic cations[4] and anions,[5] and neutral[6] small molecules.
This approach may also be used to produce elaborate supramolecular structures effective as sensor for analytes,[7] catalysts,[8] mechanically interlocked molecular architectures such as catenanes,[9] cages,[10] capsules,[11] protein folding,[12] ligands and substrates for biological macromolecules such as proteins,[13] DNA,[14] RNA[13a,15] and cytidine,[16] and for assessing molecular similarity.[17]
As described in the first chapter, external template effects in DCC reflect the ability of library members to reorganize and achieve new functions upon addition of a specific template to a DCL. While many examples of external template effects in DCC have been reported,[1-17] usually only one or two library members are amplified upon addition of one or a few individual templates to a DCL, leaving the rest of the library members to serve only as monomer reservoirs. Therefore, the number of functions reported thus far and exhibited by the constituents of one DCL are extremely limited compared to biological systems, where for instance an amino acid residue may exhibit many functions e.g. when incorporated into a protein, used in the biosynthesis of a nucleobase or oxidized to meet an organism's energetic needs.[18] Therefore, designing a DCL able to bridge the gap between a synthetic chemical system and a biological system in terms of number of functions exhibited by its constituents is challenging.

3.2 DCL design

3.2.1 Choice of building blocks

We proceeded to design a library inspired by previously reported DCLs. West *et al.*[2d] reported that exposing a DCL made from naphthalene dithiol building block **2** (Scheme 3.1) to quaternary ammonium ion template **3.29** (Scheme 3.3) is able to disassemble an octameric [2]-catenane $(\mathbf{2})_4$-$(\mathbf{2})_4$ into cyclic receptor $(\mathbf{2})_4$. Additionally, Vial *et al.*[2f] reported that exposing a DCL made from benzene dithiol building block **3** (Scheme 3.1) to polycationic polyamine **3.1** (Scheme 3.3) is able to drive the quantitative conversation of the DCL members into cyclic receptor $(\mathbf{3})_4$. The behavior of this DCL was investigated in more details revealing that the library members, in the absence of a template, were macrocyclic oligomers $(\mathbf{3})_3$, $(\mathbf{3})_4$ and $(\mathbf{3})_5$ (Paragraph 3.5.3). We reasoned that mixing the two dithiol building blocks may generate, in addition to the homotetrameric receptors $(\mathbf{2})_4$ and $(\mathbf{3})_4$, also heteroterameric macrocycles[2c,2f] made from different combinations of building blocks **2** and **3**. Similarly, the resulting DCL may generate heteromacrocycles larger than tetramers.[16]

3.2.2 DCL composition

3.2.2.1 Cyclic disulfide products

We prepared a DCL made from equimolar amounts of dithiol building blocks **2** and **3** (5 mM total) by allowing these to equilibrate in aqueous solution (50 mM borate buffer, pH 8.4) in the presence of air following standard protocols (see experimental section). The composition of the resulting DCL was analyzed by HPLC and mass spectrometry (Figure 3.1, Figure 3.3-Figure 3.7). Homotetrameric $(\mathbf{2})_4$ and $(\mathbf{3})_4$, heterotetrameric $(\mathbf{2})_3(\mathbf{3})$, $(\mathbf{2})_2(\mathbf{3})_2$ and $(\mathbf{2})(\mathbf{3})_3$ and heteropentamer $(\mathbf{2})_2(\mathbf{3})_3$ were the major disulfide macrocycles formed in the DCL. In addition to these macrocycles, two different octameric [2]-catenanes made respectively from two

mechanically interlocked tetramers were detected by LC-MS, the previously reported homo[2]-catenane $(\mathbf{2})_4$-$(\mathbf{2})_4$[2d] and a new hetero[2]-catenane $(\mathbf{2})_3(\mathbf{3})$-$(\mathbf{2})_4$ (Scheme 3.1).

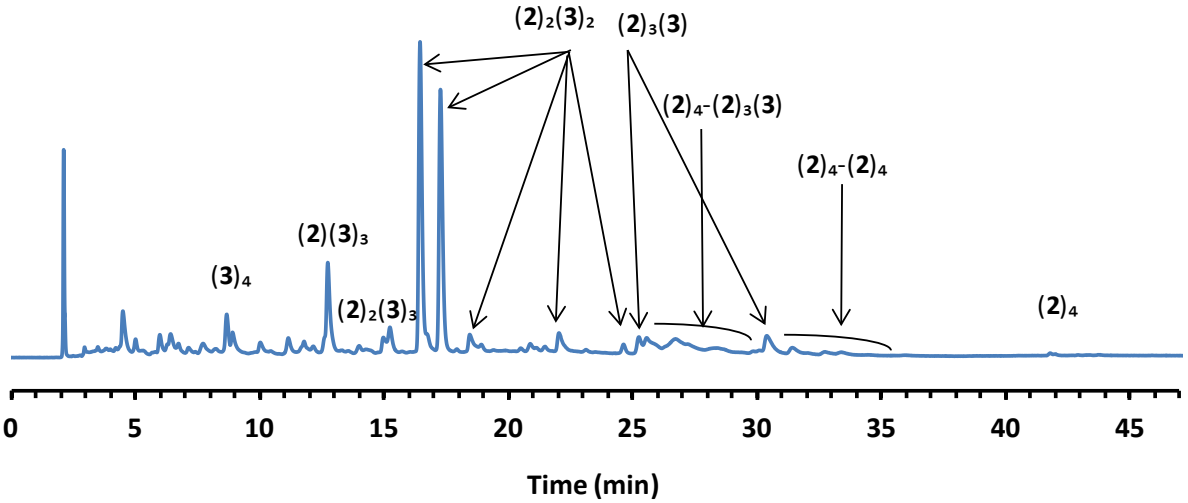

Figure 3.1: HPLC-UV chromatogram showing the cyclic disulfide products including $(\mathbf{3})_4$, $(\mathbf{2})(\mathbf{3})_3$, $(\mathbf{2})_2(\mathbf{3})_2$, $(\mathbf{2})_3(\mathbf{3})$, $(\mathbf{2})_4$, $(\mathbf{2})_2(\mathbf{3})_3$, $(\mathbf{2})_4$-$(\mathbf{2})_4$, $(\mathbf{2})_3(\mathbf{3})$-$(\mathbf{2})_4$. The DCL was prepared in borate buffer (50 mM, pH 8.4) and composed of equimolar amounts (2.5 mM of each) of building blocks **2** and **3**, and analyzed after three to four days of equilibration.

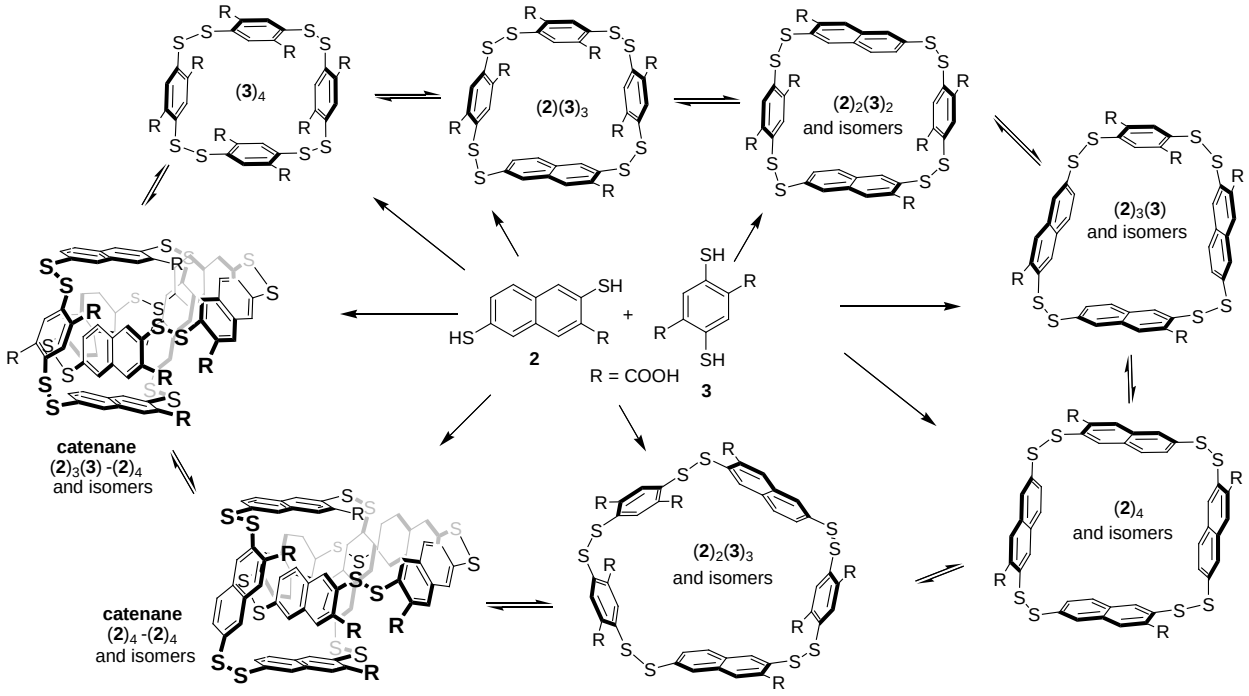

Scheme 3.1: DCL made from building blocks **2** and **3** and composed of several macrocycles including $(\mathbf{2})_4$, $(\mathbf{2})_3(\mathbf{3})$, $(\mathbf{2})_2(\mathbf{3})_2$, $(\mathbf{2})(\mathbf{3})_3$, $(\mathbf{3})_4$, $(\mathbf{2})_2(\mathbf{3})_3$ and two octameric [2]-catenanes $(\mathbf{2})_4$-$(\mathbf{2})_4$ and $(\mathbf{2})_3(\mathbf{3})$-$(\mathbf{2})_4$.

Based on the carboxylate substituent arrangements, the asymmetric structure of **2** gives rise to four different isomers of $(\mathbf{2})_4$, four different isomers of $(\mathbf{2})(\mathbf{3})_3$, five different isomers of $(\mathbf{2})_2(\mathbf{3})_2$ and consequently many isomers of the [2]catenanes $(\mathbf{2})_4$-$(\mathbf{2})_4$ and $(\mathbf{2})_3(\mathbf{3})$-$(\mathbf{2})_4$ (Scheme 3.2).

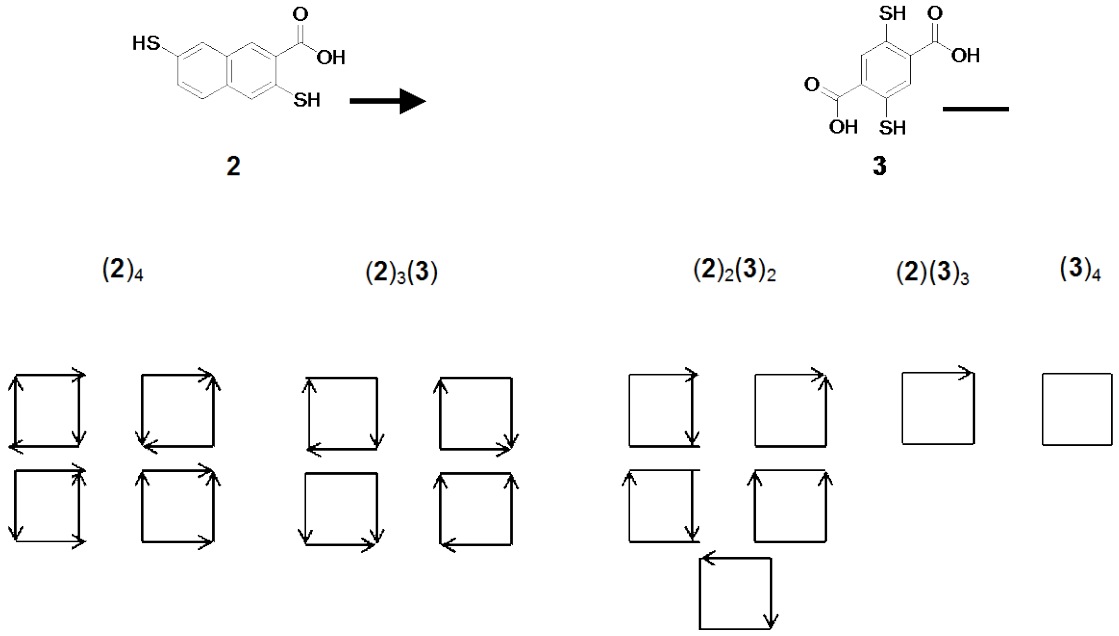

Scheme 3.2: Schematic representation of the possible isomers of the tetrameric macrocyles formed from building blocks **2** and **3**. Asymmetric building block **2** is represented as an arrow and symmetric building block **3** is represented as a straight line. The possible numbers of isomers of tetrameric macrocyles are: four isomers for $(\mathbf{2})_4$ and $(\mathbf{2})_3(\mathbf{3})$, five isomers for $(\mathbf{2})_2(\mathbf{3})_2$ and one isomer for $(\mathbf{2})(\mathbf{3})_3$ and $(\mathbf{3})_4$.

3.2.2.2 (Linear) disulfinic acid side products

In addition to the cyclic disulfide products, which represent the major species in a DCL made from building blocks **2** and **3**, a number of minor peaks are also detected in the HPLC chromatogram of this DCL (Figure 3.2). The masses of these species correspond to linear library members with an extra four oxygen atoms and include heterotrimer $(\mathbf{2})(\mathbf{3})_2$4O, heterodimer (**2**)(**3**)4O, homodimer $(\mathbf{3})_2$4O and homotrimer $(\mathbf{3})_3$4O (Figure 3.7). We assign these species to compounds in which the terminal thiols have been over-oxidized to sulfinic acids (SO_2H).[19] Similar oxidations have been reported for building blocks **2**[20] and **3**[21] however it is not clear what mechanism is operating in this case. In our experience with DCLs of dithiol building blocks, overoxidation occurs most readily in compounds containing two thiols para on a benzene ring or in the 2,6-positions of a naphthalene ring. Adding a good template and increasing its concentration can slow down the rate of overoxidation but again the mechanism for this is not understood. A quantitative study of the effect of a good template on the formation of overoxidized products will be reported in chapter 5.

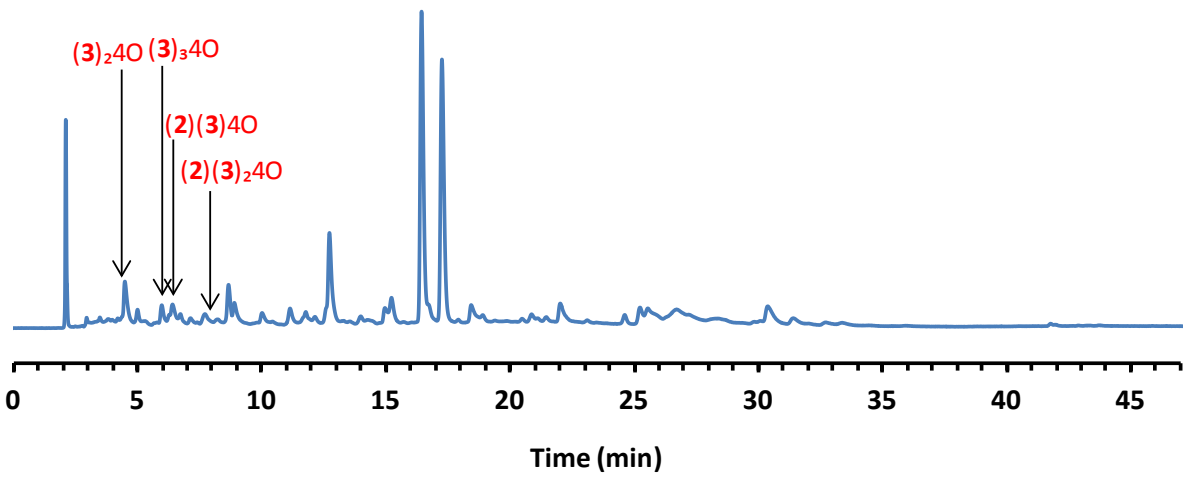

Figure 3.2: HPLC-UV chromatogram showing the disulfinic acid side products including (**3**)$_2$4O, (**3**)$_3$4O, (**2**)(**3**)4O, (**2**)(**3**)$_2$4O. The DCL was prepared in borate buffer (50 mM, pH 8.4) and composed of equimolar amounts (2.5 mM of each) of building blocks **2** and **3**, and analyzed after 3-4 days of equilibration.

LC-MS data of the cyclic disulfide products

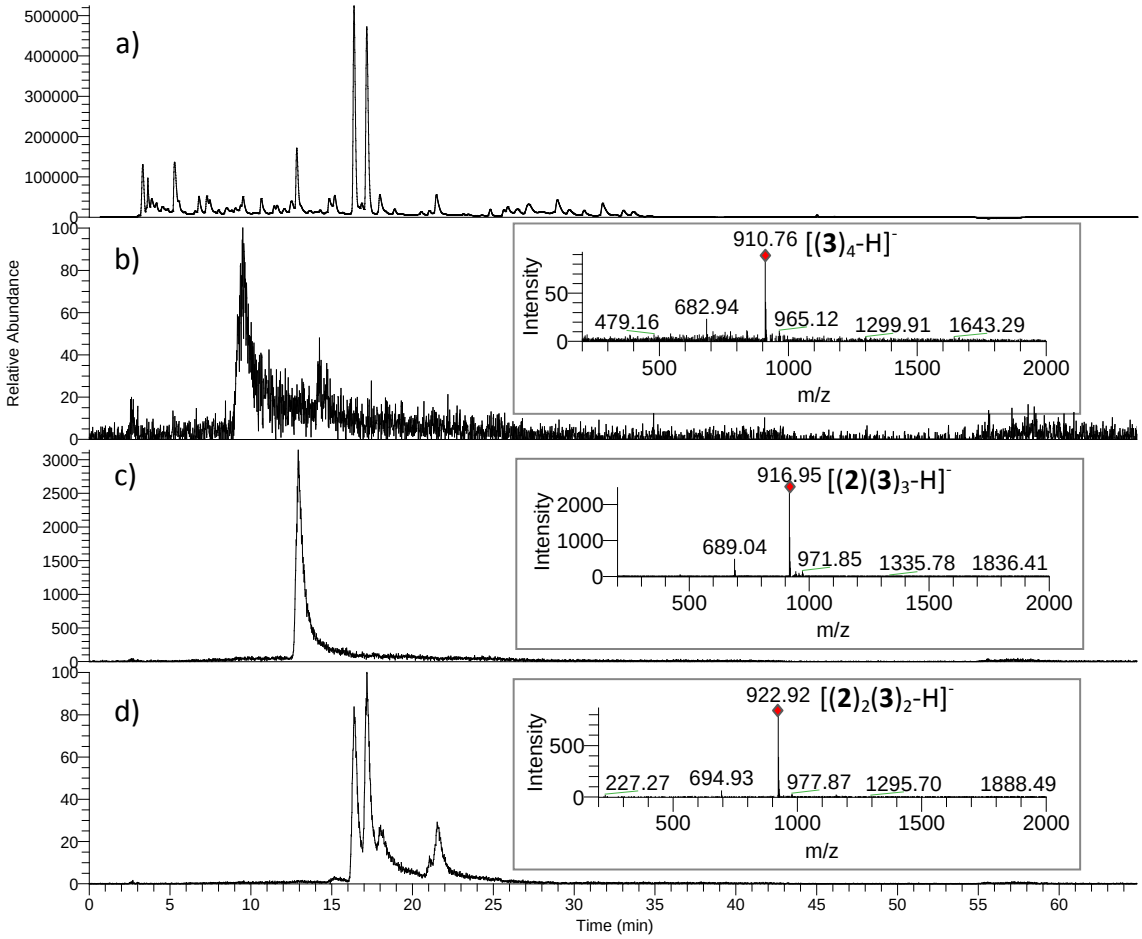

Figure 3.3: Analyses of a DCL prepared in 50 mM borate buffer (pH 8.4) and composed of equimolar amounts (2.5 mM) of building blocks **2** and **3**: (a) HPLC-UV chromatogram at 280 nm; (b) Extracted ion

chromatogram (negative ion mode) corresponding to cyclic homotetramer $(\mathbf{3})_4$ (910.5-911.5) with (insert) ESI-MS spectra [m/z 200-2000] summed over the 9.52-9.70 min retention time window, corresponding to cyclic homotetramer $(\mathbf{3})_4$, showing $[(\mathbf{3})_4\text{-H}]^-$ m/z = 910.76 (expected = 910.81); (c) Extracted ion chromatogram (negative ion mode) corresponding to cyclic heterotetramer $(\mathbf{2})(\mathbf{3})_3$ (916.5-917.5) with (insert) ESI-MS spectra [m/z 200-2000] summed over the 12.90-13.05 min retention time window, corresponding to cyclic heterotetramer $(\mathbf{2})(\mathbf{3})_3$, showing $[(\mathbf{2})(\mathbf{3})_3\text{-H}]^-$ m/z = 916.95 (expected = 916.84); (d) Extracted ion chromatogram (negative ion mode) corresponding to cyclic heterotetramer $(\mathbf{2})_2(\mathbf{3})_2$ (922.5-923.5) with (insert) ESI-MS spectra [m/z 200-2000] summed over the 16.25-16.61, 17.14-17.34, 18.04-18.40, 21.41-21.85 and 25.20-25.60 min retention time windows, corresponding to isomers of cyclic heterotetramer $(\mathbf{2})_2(\mathbf{3})_2$, showing $[(\mathbf{2})_2(\mathbf{3})_2\text{-H}]^-$ m/z = 922.92 (expected = 922.87).

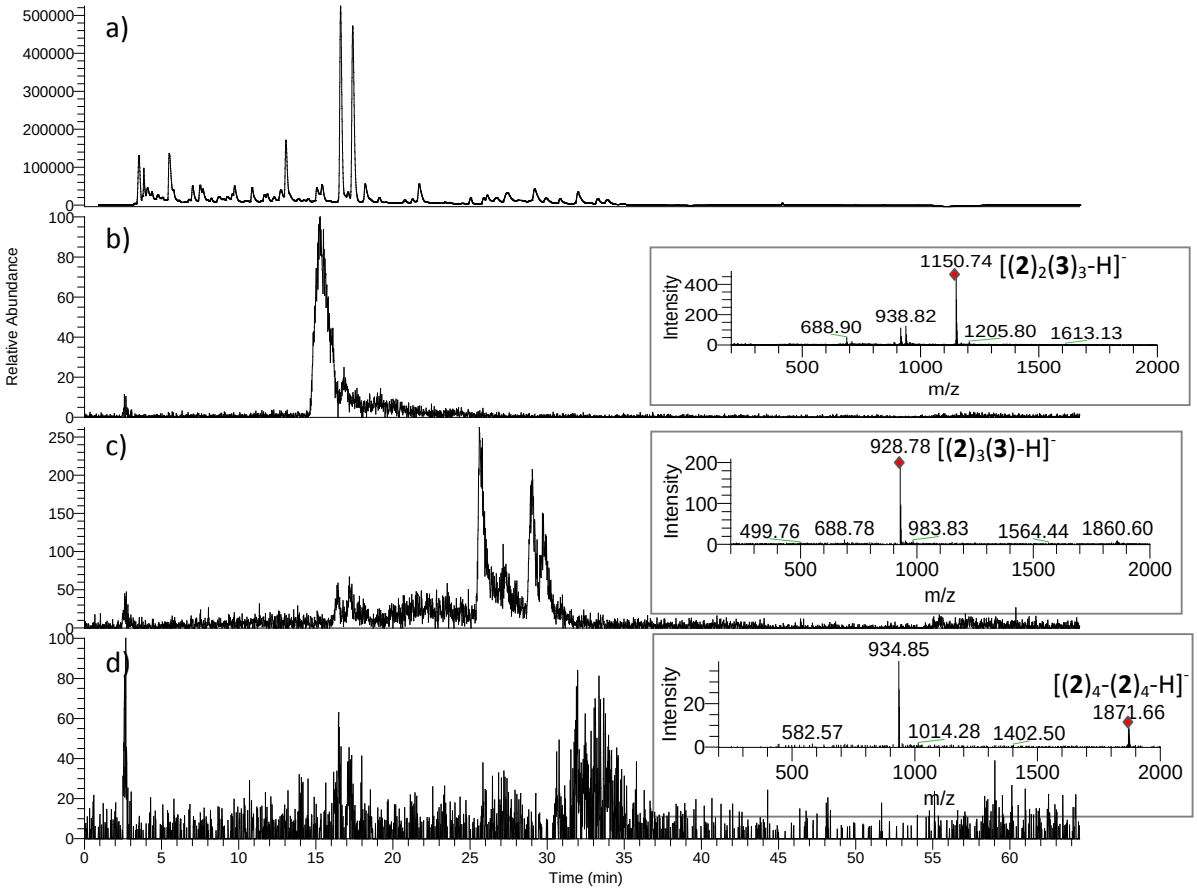

Figure 3.4: Analyses of a DCL prepared in 50 mM borate buffer (pH 8.4) and composed of equimolar amounts (2.5 mM) of building blocks **2** and **3**: (a) HPLC-UV chromatogram at 280 nm; (b) Extracted ion chromatogram (negative ion mode) corresponding to cyclic heteropentamer $(\mathbf{2})_2(\mathbf{3})_3$ (1150.5-1151.5) with (insert) ESI-MS spectra [m/z 200-2000] summed over the 15.28-15.43 min retention time window, corresponding to cyclic heteropentamer $(\mathbf{2})_2(\mathbf{3})_3$, showing $[(\mathbf{2})_2(\mathbf{3})_3\text{-H}]^-$ m/z = 1150.74 (expected = 1150.82); (c) Extracted ion chromatogram (negative ion mode) corresponding to cyclic heterotetramer $(\mathbf{2})_3(\mathbf{3})$ (928.5-929.5) with (insert) ESI-MS spectra [m/z 200-2000] summed over the 25.55-25.81, 28.90-29.10 and 29.64-30.00 min retention time windows, corresponding to isomers of cyclic heterotetramer $(\mathbf{2})_3(\mathbf{3})$, showing $[(\mathbf{2})_3(\mathbf{3})\text{-H}]^-$ m/z = 928.78 (expected = 928.89); (d) Extracted ion chromatogram (negative ion mode) corresponding to homocatenane $[(\mathbf{2})_4\text{-}(\mathbf{2})_4]$ (1870.5-1871.5) with (insert) ESI-MS spectra [m/z 200-2000] summed over the 30.86-34.93 min retention time window, corresponding to isomers of homocatenane $[(\mathbf{2})_4\text{-}(\mathbf{2})_4]$, showing $[(\mathbf{2})_4\text{-}(\mathbf{2})_4\text{-H}]^-$ m/z = 1870.56 (expected 1870.84).

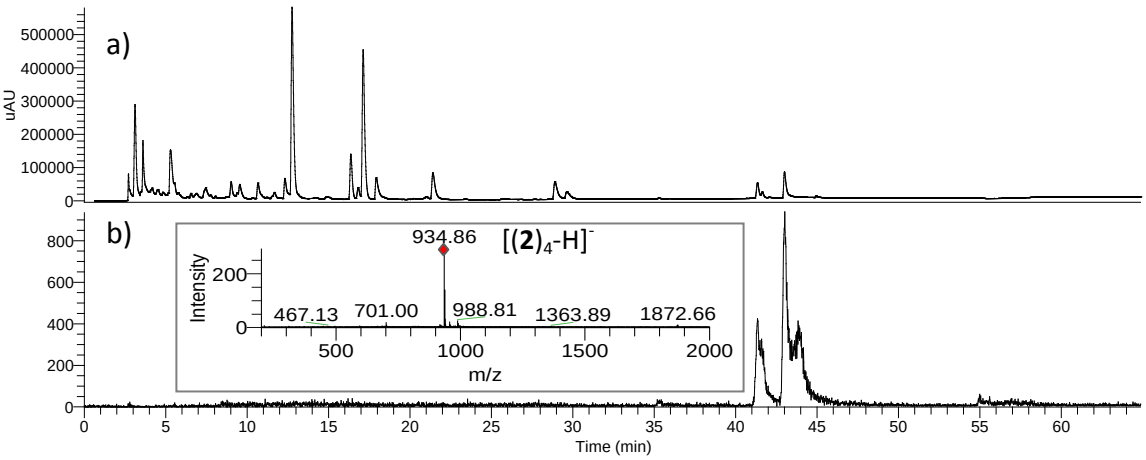

Figure 3.5: Analyses of a DCL prepared in 50 mM borate buffer (pH 8.4) and composed of equimolar amounts (2.5 mM) of building blocks **2** and **3** and template **3.29**: (a) HPLC-UV chromatogram at 280 nm; (b) Extracted ion chromatogram (negative ion mode) corresponding to cyclic homotetramer $(\mathbf{2})_4$ (934.5-935.5) with (insert) ESI-MS spectra [m/z 200-2000] summed over the 35.19-35.50, 41.23-42.17 and 43.07-43.43 min retention time windows, corresponding to isomers of cyclic homotetramer $(\mathbf{2})_4$, showing $[(\mathbf{2})_4\text{-H}]^-$ m/z = 934.86 (expected = 934.92).

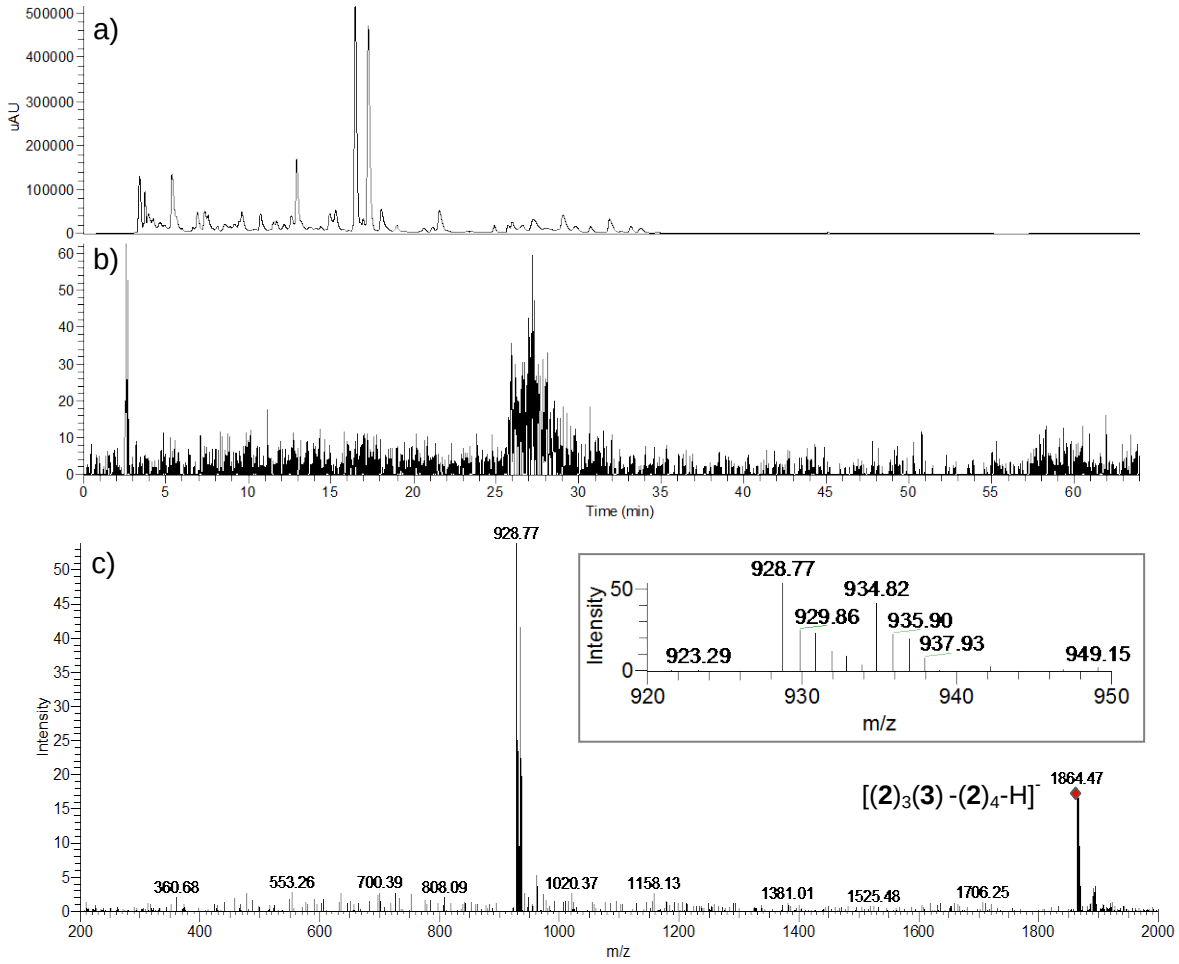

Figure 3.6: Analyses of a DCL prepared in 50 mM borate buffer (pH 8.4) and composed of equimolar amounts (2.5 mM) of building blocks **2** and **3**: (a) HPLC-UV chromatogram at 280 nm; (b) Extracted ion chromatogram (negative ion mode) corresponding to heterocatenane (**2**)$_3$(**3**)-(**2**)$_4$ (1664-1665) and (c) negative mode ESI-MS-MS spectra [m/z 200-2000] summed over the 25.50-28.43 min retention time window, corresponding to heterocatenane (**2**)$_3$(**3**)-(**2**)$_4$, showing singly charged heterocatenane [(**2**)$_3$(**3**)-(**2**)$_4$-H]$^-$ m/z = 1864.48 (expected = 1864.82). The peaks at m/z = 934.85 and m/z = 928.78 (insert) correspond to the daughter ions obtained upon fragmenting the heterocatenane into (singly charged) homotetramer [(**2**)$_4$-H]$^-$ and (singly charged) heterotetramer [(**2**)$_3$(**3**)-H]$^-$ respectively.

LC-MS data of the (linear) disulfinic acid side products

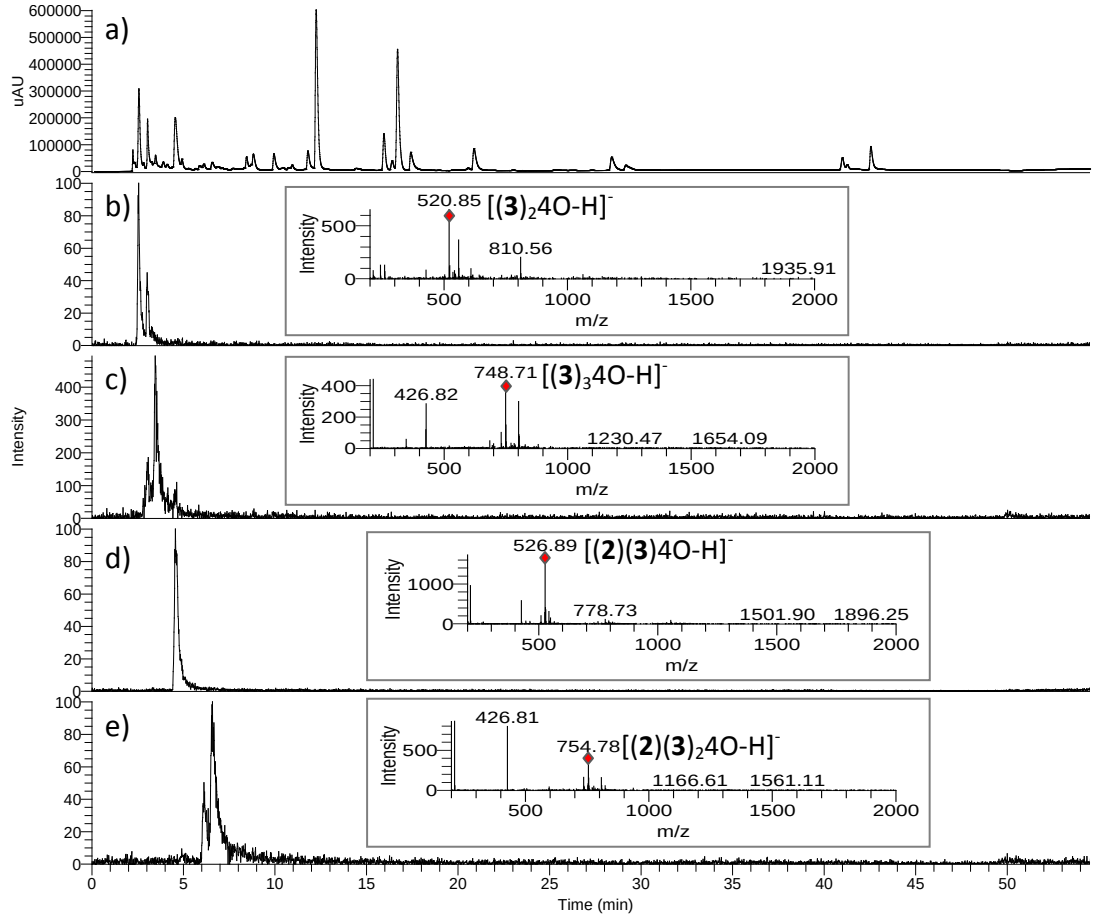

Figure 3.7: Analyses of a DCL prepared in 50 mM borate buffer (pH 8.4) and composed of equimolar amounts (2.5 mM of each) of building blocks **2** and **3** and 1,8-diaminooctane as a template (2.5 mM): (a) HPLC-UV chromatogram at 280 nm; (b) Extracted ion chromatogram (negative ion mode) corresponding to linear homodimer disulfinic acid [(**3**)$_2$4O] (520.5-521.5) with (insert) ESI-MS spectra [m/z 200-2000] summed over the 2.52-2.66 min retention time window, corresponding to linear homodimer disulfinic acid [(**3**)$_2$4O], showing [(**3**)$_2$4O-H]$^-$ m/z = 520.85 (expected = 520.90), (c) Extracted ion chromatogram (negative ion mode) corresponding to linear trimer disulfinic acid [(**3**)$_3$4O] (748.5-749.5) with (insert) ESI-MS spectra [m/z 200-2000] summed over the 2.89-3.28 min retention time window, corresponding to linear trimer disulfinic acid [(**3**)$_3$4O], showing [(**3**)$_3$4O-H]$^-$ m/z = 748.71 (expected = 748.86), (d) Extracted ion chromatogram (negative ion mode) corresponding to linear heterodimer disulfinic acid [(**2**)(**3**)4O] (526.5-527.5) with (insert) ESI-MS spectra [m/z 200-2000] summed over the 4.52-4.63 min retention time window, corresponding to linear heterodimer disulfinic acid [(**2**)(**3**)4O], showing [(**2**)(**3**)4O-H]$^-$ m/z = 526.89 (expected = 526.93); (e) Extracted ion chromatogram (negative ion mode) corresponding to linear heterotrimer disulfinic acids [(**2**)(**3**)$_2$4O] (754.5-755.5) with (insert) ESI-MS spectra [m/z 200-2000]

summed over the 6.55-6.98 min retention time window, corresponding to linear heterotrimer disulfinic acids [(**2**)(**3**)$_2$4O], showing [(**2**)(**3**)$_2$4O-H]$^-$ m/z = 754.78 (expected = 754.88).

3.2.3 Choice of the templates

The macrocycles in the DCL span a range of cavity sizes. They also differ in charge as monomer **3** carries two carboxylate groups versus only one on monomer **2**.[22] With the aim to find templates able to amplify selectively the generated macrocycles we explored a wide variety of compounds of different sizes, shapes and cationic charges but exhibiting common motifs suitable for the recognition of the generated macrocycles under the DCL conditions. Biologically active amines and ammonium ions were selected as these include aromatic and aliphatic cores of different shapes and sizes suitable for π-π and hydrophobic interactions with the aromatic cavities of the various macrocycles. Simultaneously, the protonated amine and ammonium groups of these templates may form salt bridges with the carboxylate groups of the macrocycles or cation-π interactions with the aromatic moieties of the macrocycles. Note that hydrogen bonding, cation-π and ion pair interactions are also responsible for binding between biologically active amines and ammonium ions and their biological targets.[23] The templates consist of four classes of neurotransmitters including nicotinic acetylcholine receptor binders **3.12**, **3.13**, **3.14**, **3.16**, **3.20** and **3.23**,[24] serotonin receptor binder **3.19**,[25] adrenergic receptor binders **3.7**, **3.10**, **3.11**, **3.15**, **3.18**, **3.21** and **3.24**[26] and muscarinic acetylcholine receptor binders **3.26** and **3.27**.[27] Also, spermine **3.1** was used as an aliphatic polycationic polyamine template. This compound plays a key role in many cellular processes required for cell survival and proliferation, at low concentration, while it is cytotoxic inducing apoptosis and cancer at high concentration.[28] Anticancer agent bis(3-aminopropyl)amine **3.2**[29] and reversible inhibitor of protein synthesis L-histidinol **3.7**[30] which has been tested also in chemotherapy cancer treatment,[31] were also used as templates. Aliphatic α,ω-diamines of low molecular weight including **3.3**, **3.4**, **3.5** and **3.30** are positively charged under near physiological conditions and were also used as templates. Their biological activities will be discussed in chapter 4. In addition to these bioactive compounds, many other compounds of unknown biological activities such as polyamine **3.9** and amines **3.6**, **3.8**, **3.17**, **3.22**, **3.25**, **3.28** and **3.29** were also chosen as templates (Scheme 3.3).

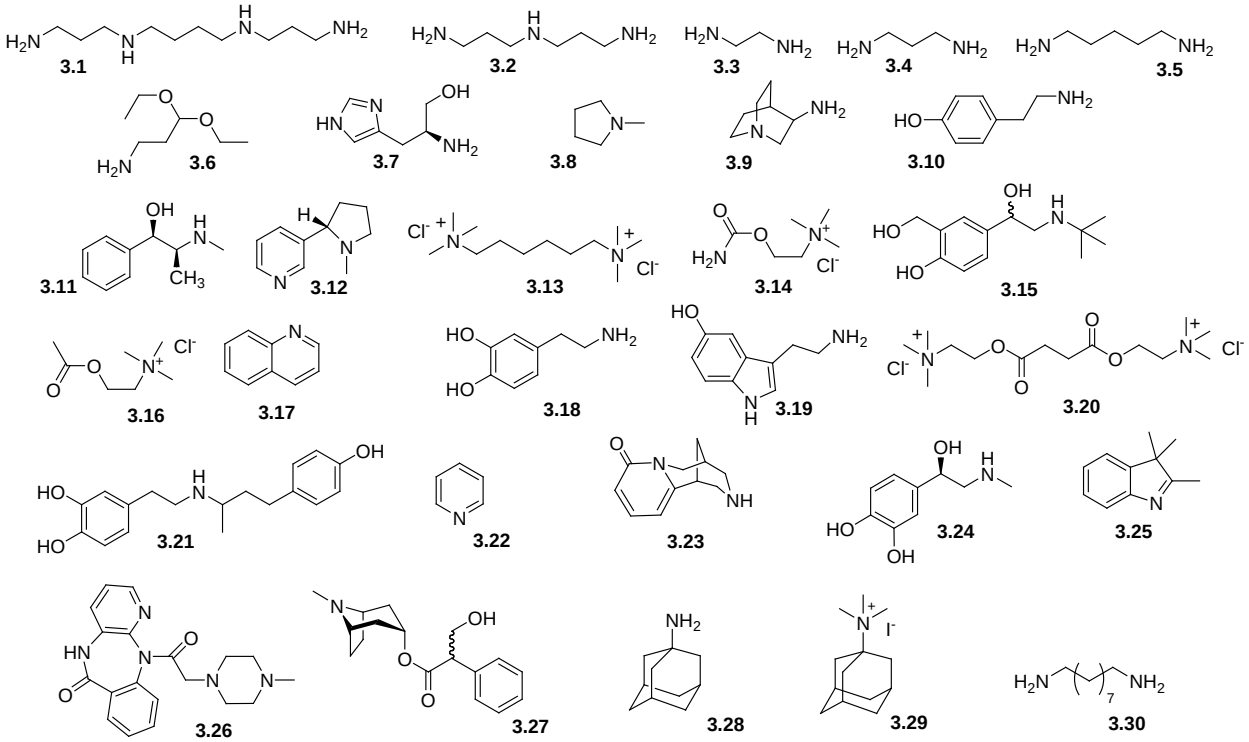

Scheme 3.3: Structure of the 30 investigated amine and ammonium ion templates: spermine **3.1**, bis(3-aminopropyl)amine **3.2**, ethylenediamine **3.3**, trimethylenediamine **3.4**, cadavarine **3.5**, 1-amino-3,3-diethoxypropane **3.6**, histidinol **3.7**, 1-methylpyrrolidine **3.8**, quinuclidin-3-amine **3.9**, tyramine **3.10**, (-) ephedrine **3.11**, nicotine **3.12**, hexamethonium chloride **3.13**, carbamoylcholine **3.14**, isoproterenol **3.15**, acetylcholine chloride **3.16**, quinoline **3.17**, dopamine **3.18**, serotonin **3.19**, succinylcholine chloride dihydrate **3.20**, doputamine **3.21**, pyridine **3.22**, cytisine **3.23**, adrenaline **3.24**, 2,3,3-trimethylindolenine **3.25**, pirenzepine **3.26**, atropine **3.27**, 1-adamantanamine **3.28**, trimethyl adamantanamine iodide **3.29** and 1,9-nanodiamine **3.30**.

3.3 Effect of the chosen templates on the DCL made from 2 and 3

We then proceeded to prepare several DCLs made from building blocks **2** and **3** and templated individually by the chosen amines and ammonium ions. The DCLs were prepared following standard protocols (see experimental part), stirred for three to four days at room temperature and analyzed using HPLC-MS (Figure 3.8). Nearly all of the 30 templates were able to amplify either one or two receptors of similar cavity size. The only exceptions are templates **3.25** and **3.26** which were poorly soluble under the DCL conditions. Moreover, most templates induced a unique response in the DCL.

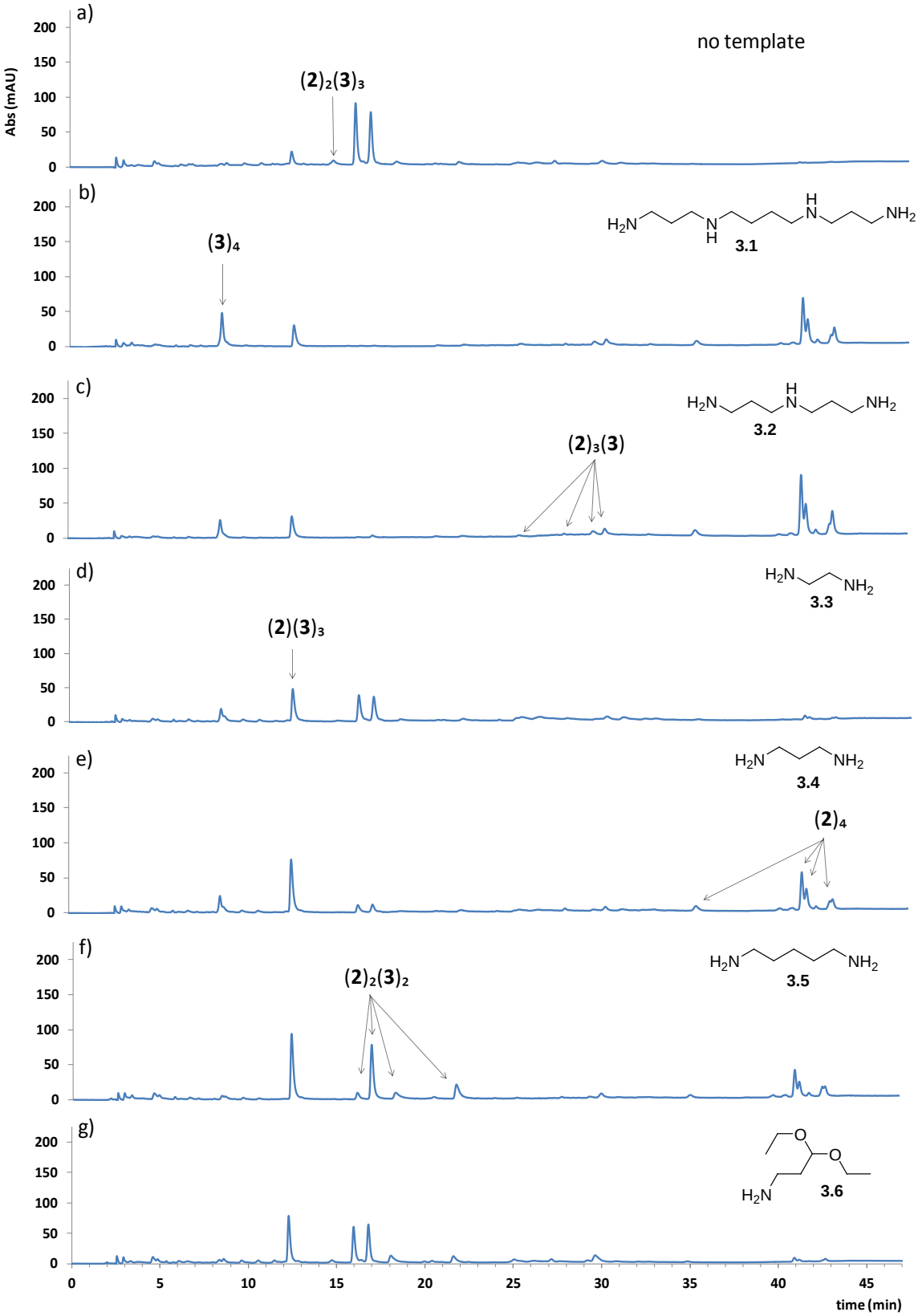
a)
no template
(2)2(3)3
b)
(3)4
3.1
c)
3.2
(2)3(3)
d)
3.3
(2)(3)3
e)
3.4
(2)4
f)
3.5
(2)2(3)2
g)
3.6
Abs (mAU)
time (min)

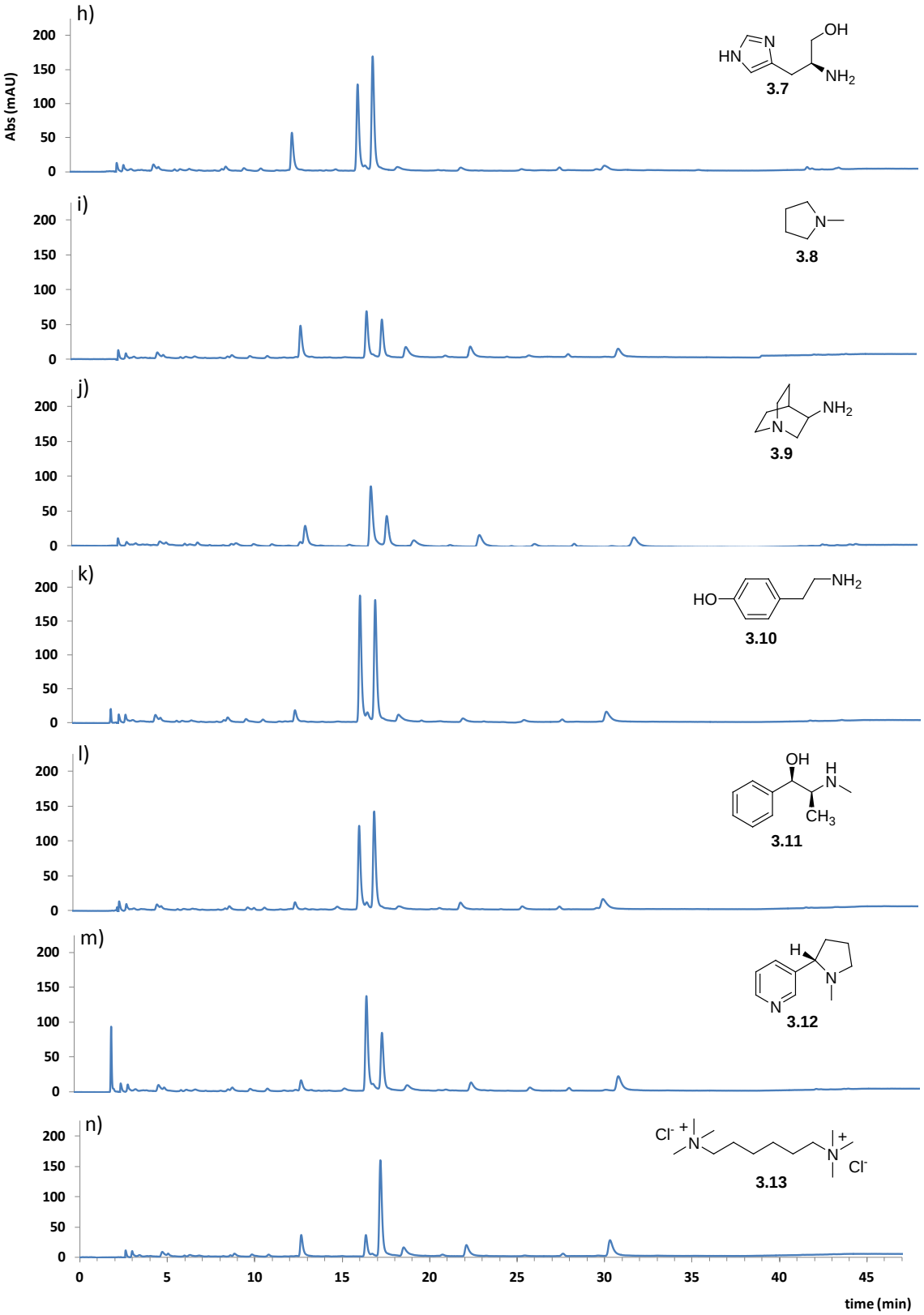
h)
i)
j)
k)
l)
m)
n)
Abs (mAU)
200
150
100
50
0
OH
HN
N
NH2
3.7
N
3.8
NH2
N
3.9
HO
NH2
3.10
OH
H
N
CH3
3.11
H
N
N
3.12
Cl-
+
N
N
+
Cl-
3.13
0
5
10
15
20
25
30
35
40
45
time (min)

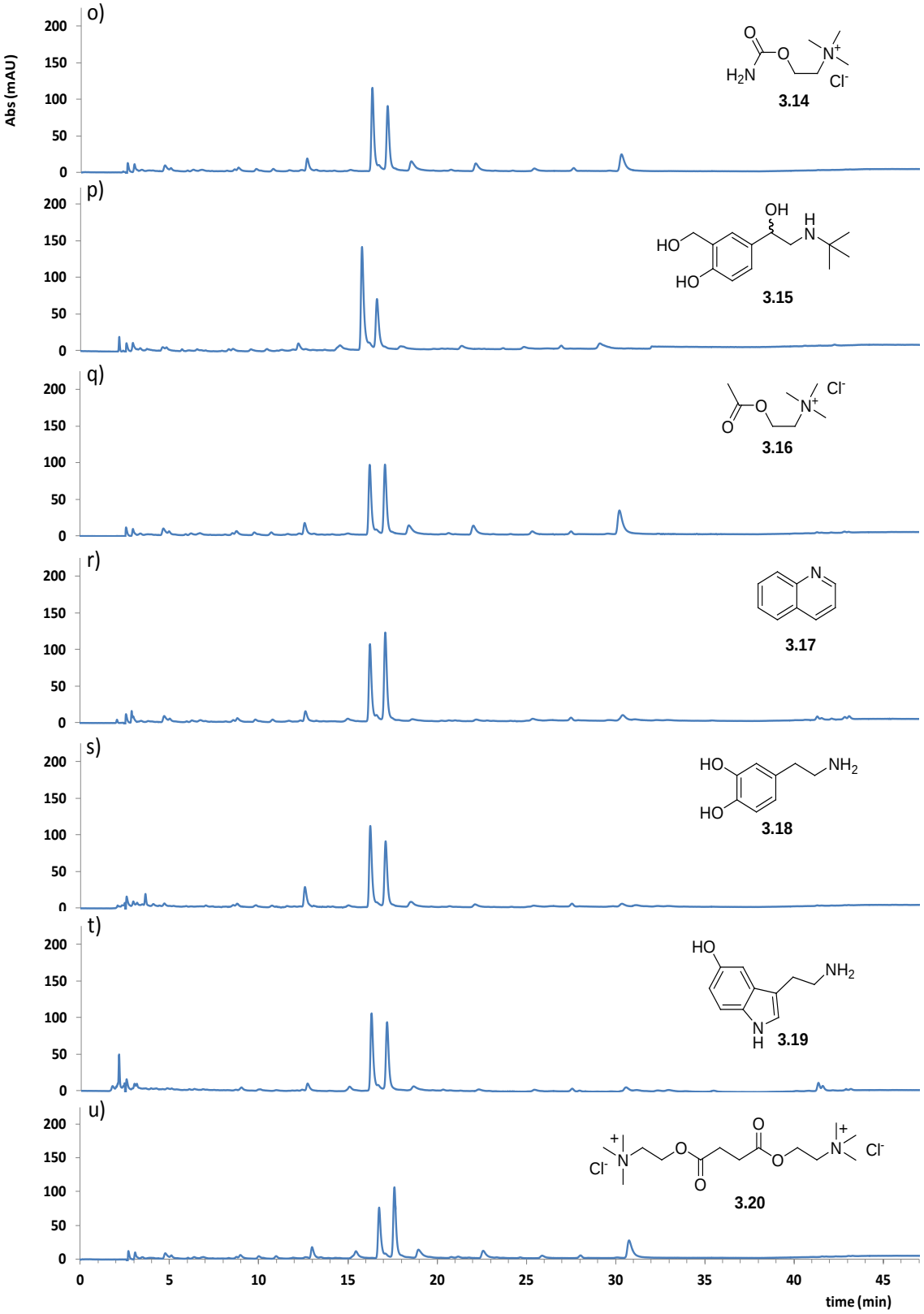
o)
p)
q)
r)
s)
t)
u)
Abs (mAU)
200
150
100
50
0
3.14
3.15
3.16
3.17
3.18
3.19
3.20
0
5
10
15
20
25
30
35
40
45
time (min)

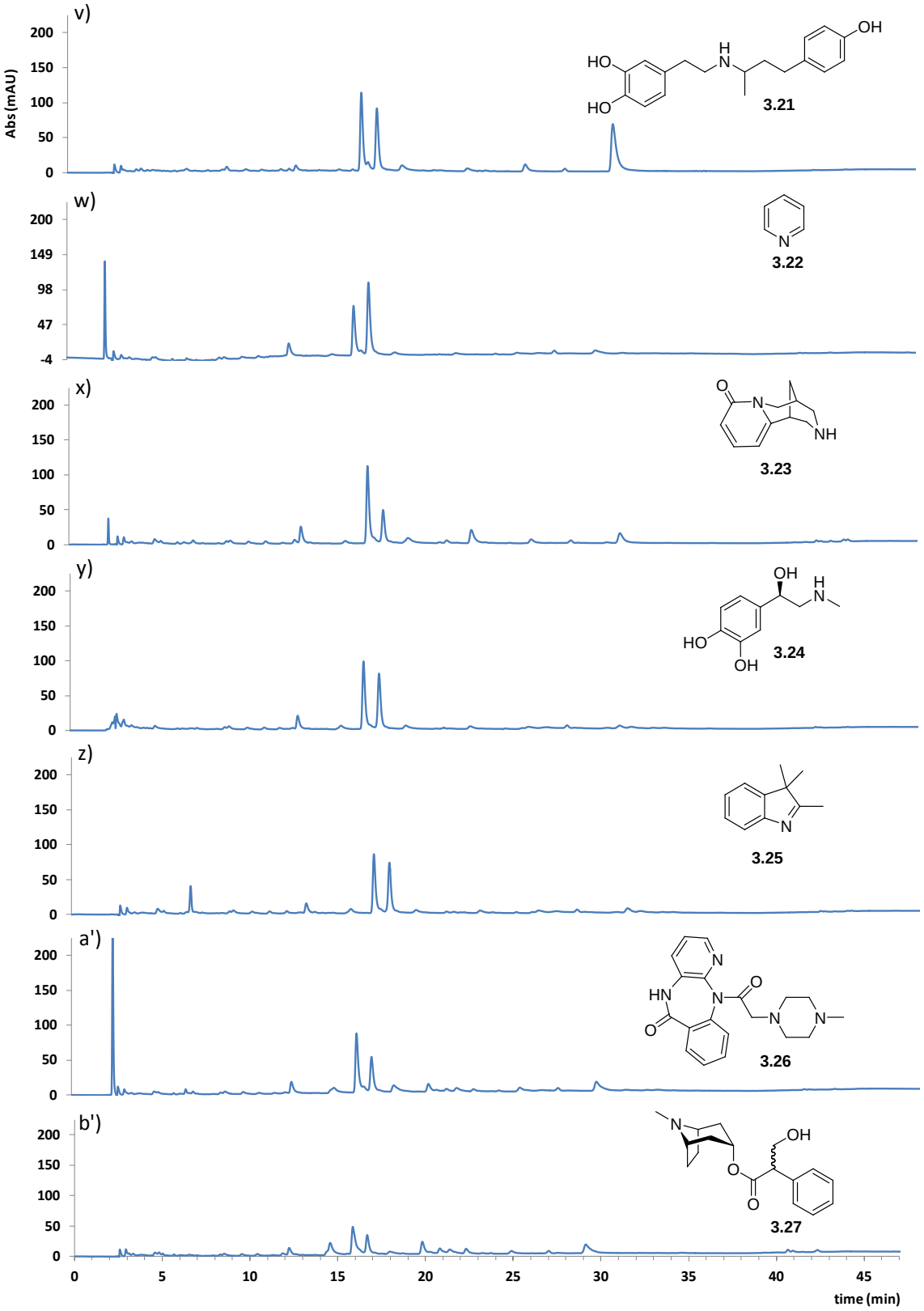
v)
w)
x)
y)
z)
a')
b')
Abs (mAU)
time (min)
3.21
3.22
3.23
3.24
3.25
3.26
3.27

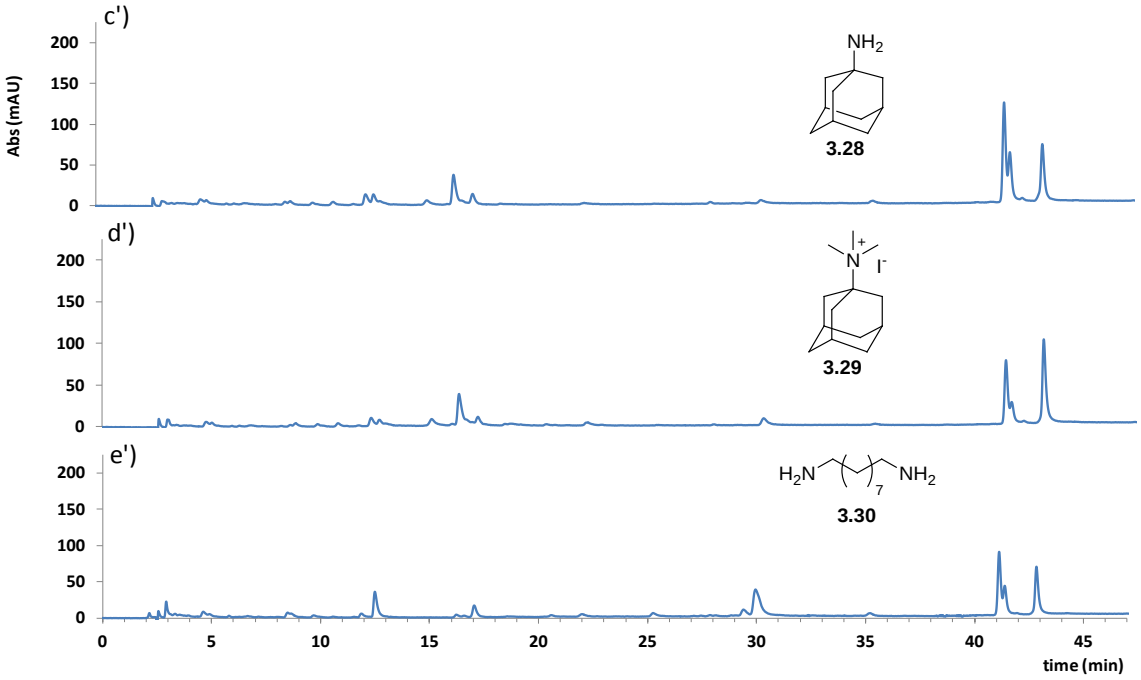

Figure 3.8: HPLC-UV chromatograms (λ_{abs} = 260 nm and λ_{ref} = 550 nm) of DCLs prepared in borate buffer (50 mM, pH 8.4) composed of equimolar amounts (2.5 mM) of building blocks **2** and **3** (a) in the absence of template and (b-e´): in the presence of template **3.1** to **3.30**, respectively. Samples taken from the DCL solutions were diluted with 200% volume DMSO immediately prior to HPLC analyses.

3.3.1 New methodology to compare the amplification factors of the library members

The response of a DCL to a template is routinely analyzed in terms of amplification factors (*AFs*) of the individual receptors. As described in the first chapter, *AFs* are defined as the concentration of the receptor in the presence of the template over the concentration in the absence of the template. However, comparing *AFs* of different receptors within a single library that are present at very different concentration in the absence of the template is not very meaningful. For example, a compound that already contains half of the library material in the absence of the template cannot have an *AF* larger than 2, while a compound that only contains 1% of the untemplated library material can have an *AF* of up to 100. In order to compare amplification factors between different receptors, we introduced a normalized amplification factor (AF_n) defined as:

$$AF_n = ([A]_t-[A]_0)/([A]_{max}-[A]_0)$$

Where $[A]_T$ and $[A]_0$ are the concentration of library member A in the presence and absence of the template, respectively, and $[A]_{max}$ is the maximum possible concentration of A, based on the amounts of available building block(s). The maximum value for AF_n is 1, when $[A]_T = [A]_{max}$ while $AF_n = 0$ corresponds to the case where there is no amplification ($[A]_T = [A]_0$). Values of $AF_n<0$ indicate that the concentration of the library member is reduced in the presence of template. While values of *AF* can be determined directly from the peak areas of HPLC chromatograms based on UV-Vis detection, for AF_n it is necessary to determine the actual concentrations of the species in the library.

3.3.2 Methodology for converting HPLC-UV peak areas of library members into their corresponding concentrations

The concentrations of the macrocylic products formed in a DCL made form building blocks **2** and **3** could be obtained from their corresponding HPLC-UV peak areas after determining the effective absorptivity coefficients of the two building blocks **2** and **3**. We first determined the effective absorptivity coefficient C_2 which relates the HPLC-UV peak area, obtained at λ_{abs} = 260 nm and λ_{ref} = 550 nm, to the building block concentration of a fully oxidized DCL made from **2** (in 50 mM borate buffer pH 8.4) in the presence of template **3.29** (0.25 equivalent with respect to building block). Template **3.29** was added to the DCL to minimize the formation of linear overoxidized products (sulfinic acids). Experiments were set up at seven different building block concentrations: 1.0, 2.0, 3.0, 4.0, 5.0, 6.0 and 7.0 mM. HPLC library samples were diluted with 200% volume DMSO prior to analyses to dissolve any aggregates of the relatively hydrophobic DCL members (see also paragraph 3.3.3). After injecting aliquots of 3 µL, the total peak area of the HPLC-UV chromatograms was determined and plotted against the building block concentrations (Table 3.1). The slope of the linear fit of the data in (Figure 3.9) gave a value for C_2 of 1508 mAU·min·mM^{-1}.

Table 3.1: Total HPLC-UV peak area (mAU·min) of seven DCLs composed of seven different concentrations of building block **2** and 0.25 equivalent (with respect to building block) of template **3.29**.

	Seven DCLs made from building block **2** and 0.25 equivalent of template **3.29**						
Building block concentration (mM)	1.0	2.0	3.0	4.0	5.0	6.0	7.0
Total HPLC-UV peak area (mAU·min)	1117	2391	3825	6038	7263	8306	11927

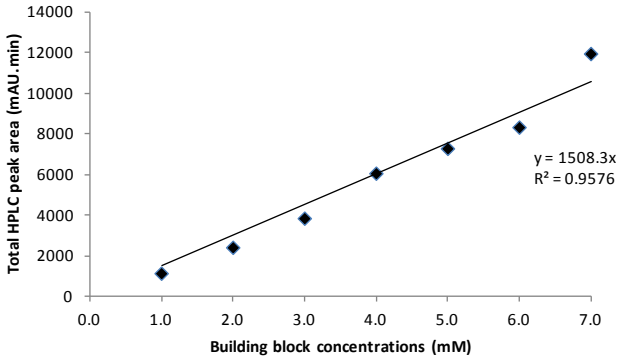

Figure 3.9: Total HPLC peak area as a function of the concentration of building block 2 for DCLs prepared in the presence of 0.25 equivalent (with respect to building block) of template 3.29 (50 mM borate buffer, pH=8.4).

The above procedure was repeated for building block **3** using 0.25 equivalent (with respect to the building block) of template **3.1**. From the slope of the total HPLC peak area, obtained at λ_{abs} = 260 nm and λ_{ref} = 550 nm, plotted against the concentration of **3**, a value for C_3 of 323 mAU·min·mM^{-1} was obtained (Figure 3.10).

Table 3.2: Total HPLC-UV peak area (mAU·min) of seven DCLs composed of seven different concentrations of building block **3** and 0.25 equivalent (with respect to building block) of template **3.1**.

	Seven DCLs made from building block **3** and 0.25 equivalent of template **3.1**						
Building block concentration (mM)	1.0	2.0	3.0	4.0	5.0	6.0	7.0
Total HPLC-UV peak area (mAU·min)	310	634	891	1281	1800	1888	2220

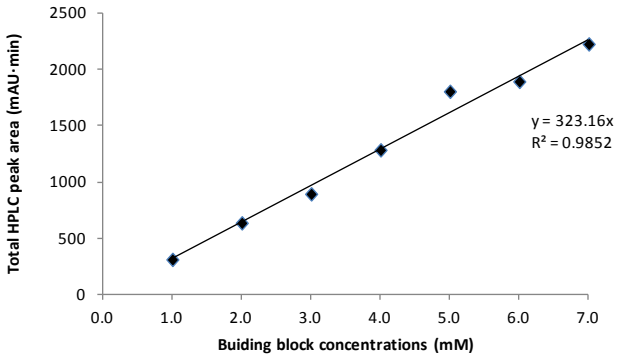

Figure 3.10: Total HPLC peak area as a function of the concentration of building block **3** for DCLs prepared in the presence of 0.25 equivalent (with respect to building block) of template **3.1** (50 mM borate buffer, pH=8.4).

3.3.3 DMSO sample dilution

The relatively hydrophobic DCL members made entirely or even partially from building block **2** and their corresponding complexes with the added templates appeared to aggregate partially under the DCL conditions (Table 3.3).[2d] These aggregates did not disassemble efficiently during HPLC analyses, resulting in material that remains undetectable. To dissolve these aggregates, we diluted the HPLC samples with DMSO prior to analyses. In aim to optimize the added volume of DMSO, two DCLs made from building blocks **2** and **3** were prepared. To the first one we added relatively hydrophobic template **3.30** and to the second we added relatively hydrophilic template **3.3**. After reaching the equilibrium, three samples were taken from each of the two DCLs. The first sample was not diluted the second and the third were diluted with 100% and 200% volume DMSO, respectively, immediately prior to HPLC analyses. HPLC-UV data shows that adding 200% volume DMSO to the samples is able to dissolve the aggregates formed mainly by $(\mathbf{2})_4$ and to a lesser extent by $(\mathbf{2})_3(\mathbf{3})$ without affecting the detection of the relatively hydrophilic macrocycles, made mainly from building block **3** such as $(\mathbf{3})_4$ and $(\mathbf{2})(\mathbf{3})_3$ (Table 3.3).

Table 3.3: HPLC-UV peak areas and normalized areas of the macrocyclic library members formed (a) in a DCL made from equimolar amounts of **2** and **3** (4 mM in total) and 4 mM of template **3.3** and (b) in a DCL made from equimolar amounts of **2** and **3** (5 mM in total) and 2 mM of template **3.30**. For both DCLs, HPLC samples were either not diluted, diluted with 100% volume DMSO or with 200% volume DMSO. For the normalized HPLC-UV peak area values, normalization was relative to the maximum HPLC-UV peak area (=100) for each library member.

a)		Three DCLs made from **2** and **3** (2 mM of each) and 4 mM of template **3.3**.		
Dilution volume of DMSO of HPLC samples prior to analysis(1 µl injection volume)		no dilution	100% dilution	200% dilution
HPLC-UV peak areas	(**3**)$_4$	48	36	44
	(**2**)(**3**)$_3$	205	180	185
	(**2**)$_2$(**3**)$_2$	855	808	861
	(**1**)(**2**)$_3$	613	691	702
	(**2**)$_4$	38	314	430
Normalised HPLC-UV peak areas(x 100)	(**3**)$_4$	100	75	92
	(**2**)(**3**)$_3$	100	88	90
	(**3**)$_2$(**2**)$_2$	99	94	100
	(**1**)(**2**)$_3$	87	98	100
	(**2**)$_4$	9	73	100

b)		Three DCLs made from **2** and **3** (2.5 mM for each) and 2.5 mM of template **3.30**.		
Number of DMSO dilution of HPLC samples prior to analysis(10 µl standard injection volume)		no dilution	100% dilution	200% dilution
HPLC-UV peak areas	(**3**)$_4$	644	645	641
	(**2**)(**3**)$_3$	3678	3525	3516
	(**2**)$_2$(**3**)$_2$	3701	3762	3794
	(**1**)(**2**)$_3$	3602	2859	3864
	(**2**)$_4$	4145	3727	8374
Normalised HPLC-UV peak areas(x 100)	(**3**)$_4$	100	100	99
	(**2**)(**3**)$_3$	100	96	96
	(**2**)$_2$(**3**)$_2$	98	99	100
	(**1**)(**2**)$_3$	93	74	100
	(**2**)$_4$	49	45	100

3.3.4 Equation relating HPLC-UV peak areas of library members to their corresponding concentrations

Using the values of C_2 and C_3 it is possible to convert the HPLC-UV peak area $A_{\mathbf{2}n\mathbf{3}m}$ obtained for an individual library member $\mathbf{2}_n\mathbf{3}_m$ composed of n units of **2** and m units of **3** into its corresponding concentration through equation 3.1:

$$[(\mathbf{2})_n(\mathbf{3})_m] = A_{\mathbf{2}n\mathbf{3}m} / (n\,C_2 + m\,C_3) \qquad (3.1)$$

This equation is valid as long as the values of C_2 and C_3 are independent of the molecular structure in which building blocks **2** and **3** reside. Therefore, the HPLC-UV responses generated by building blocks **2** and **3** should be additive, i.e. the total HPLC-UV peak area values obtained for DCLs made from single building block **2**, single building block **3** and the mixture of building blocks **2** and **3** should be independent of the composition of the corresponding DCL, at constant building block concentrations. In other words, the total HPLC-UV peak area of a DCL should be independent of the nature and the concentration of the added template and should only depend linearly on the total building block concentration. Three control experiments were performed to test the additivity of HPLC-UV peak areas of building blocks **2** and **3**.

3.3.5 Control experiments to test the additivity of the HPLC-UV peak areas of building blocks 2 and 3

3.3.5.1 First control experiment

To test if the HPLC-UV response generated by building blocks **2** is additive, four DCLs were prepared from a solution of 2.0 mM of **2** in 50 mM borate buffer at pH 8.4. The first DCL was left without template, while to the remaining three DCLs N,N,N-trimethyladamantaneammonium iodide **3.29** was added as a template at concentrations of 0.50 mM, 1.0 mM and 5.0 mM, respectively. The four DCLs were analysed by HPLC-UV following the standard protocol (Figure 3.11). While the library compositions of the four samples were markedly different, the total HPLC peak areas obtained upon injecting 10 µL sample were almost identical: 19218 mAU·min; 19094 mAU·min; 19021 mAU·min and 18778 mAU·min, respectively (Table 3.4). The closely similar peak areas demonstrate that building block **2** has constant molar absorptivity irrespective of the library member into which it is incorporated.

3.3.5.2 Second control experiment

A similar experiment was conducted to test if the HPLC-UV response generated by building block **3** is additive by preparing a 2.0 mM DCL made from **3** that was either untemplated, or templated by 0.50 mM, 1.0 mM or 5.0 mM ethylenediamine **3.3** (Figure 3.12). the total HPLC peak areas obtained upon injecting 10 µL sample were almost identical: 5898 mAU·min; 6041 mAU·min; 6189 mAU·min and 5898 mAU·min, respectively, demonstrating that also the molar absorptivity of **3** is independent of the oligomer into which it is incorporated (Table 3.5).

3.3.5.3 Third control experiment

Finally, we tested if the HPLC-UV response generated by a mixed DCL, made from **2** and **3**, is additive. The total HPLC-UV peak area obtained upon injecting 10 µL of a DCL made from 2.5 mM of **2** was determined, as well as the total peak area obtained upon injecting 10 µL of a DCL made from 2.5 mM of **3**. The values were compared with the corresponding peak area obtained from a DCL made from an equimolar mixture of **2** and **3** (5.0 mM total building block concentration). The sum of the peak areas of the DCL made of **2** (23790 mAU) and **3** (6850 mAU·min) matched well with that of the mixed DCL (30743 mAU·min) (Table 3.6).

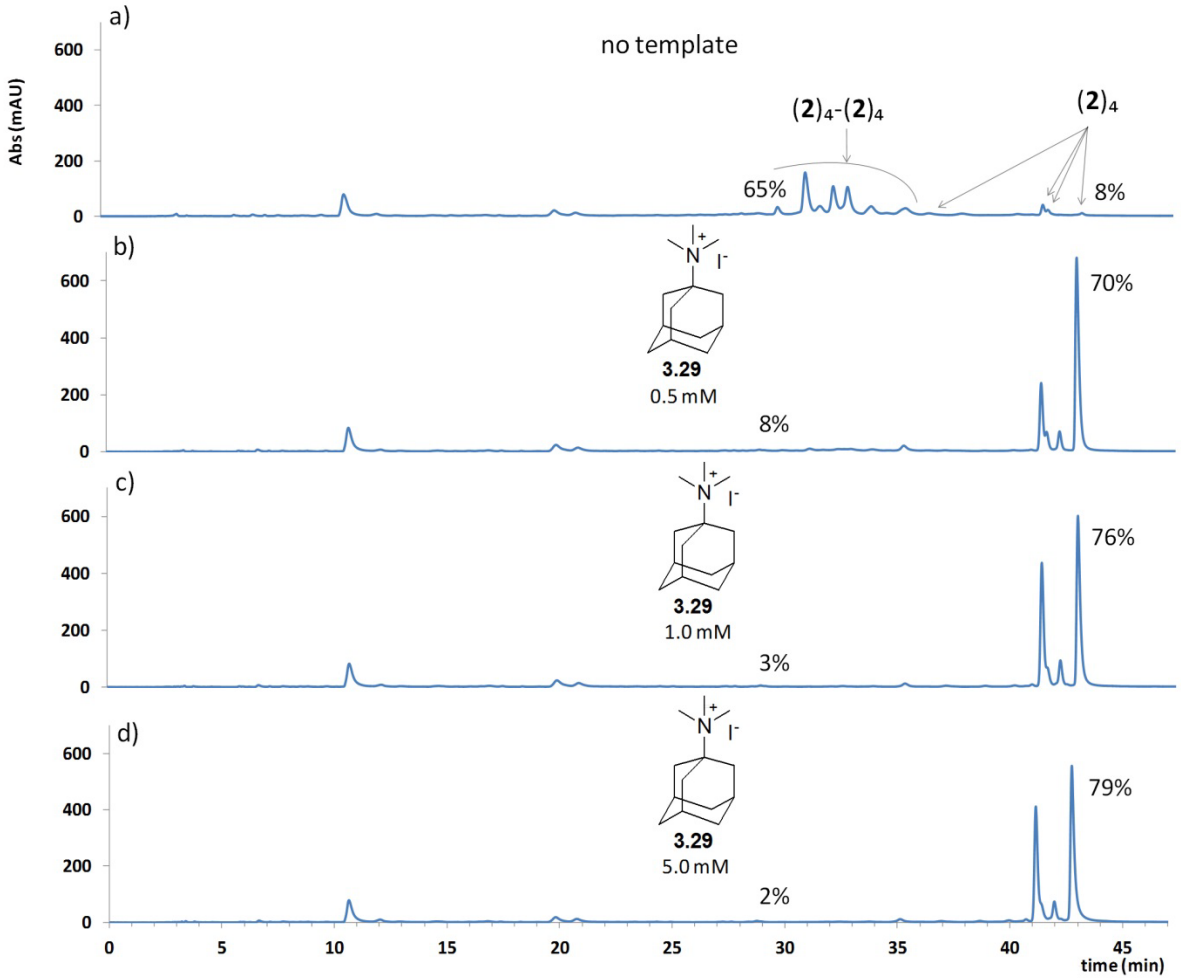

Figure 3.11: HPLC-UV chromatograms (λ_{abs} = 280 nm, λ_{ref} = 550 nm) of DCLs prepared in borate buffer (50 mM, pH 8.4) composed of 2 mM of building block **2** (a) in the absence of template and in the presence of (b) 0.5 mM, (c) 1.0 mM and (d) 5.0 mM of template **3.29**. Volume injected = 10 µL. Samples taken from the DCL solutions were not diluted with DMSO prior to HPLC analyses.

Table 3.4: Total HPLC peak area (mAU·min) and percentage library member composition of a DCL composed of building block 2 (2.0 mM) at different template concentrations.

		Four DCLs made from 2 mM of building block **2**			
Template **3.29** (mM)		0.0	0.5	1.0	5.0
Total HPLC-UV peak area (mAU·min)		19218	19094	19021	18778
DCL percent composition (%)	(**2**)$_4$-(**2**)$_4$	65	8	3	2
	(**2**)$_4$	8	70	76	79

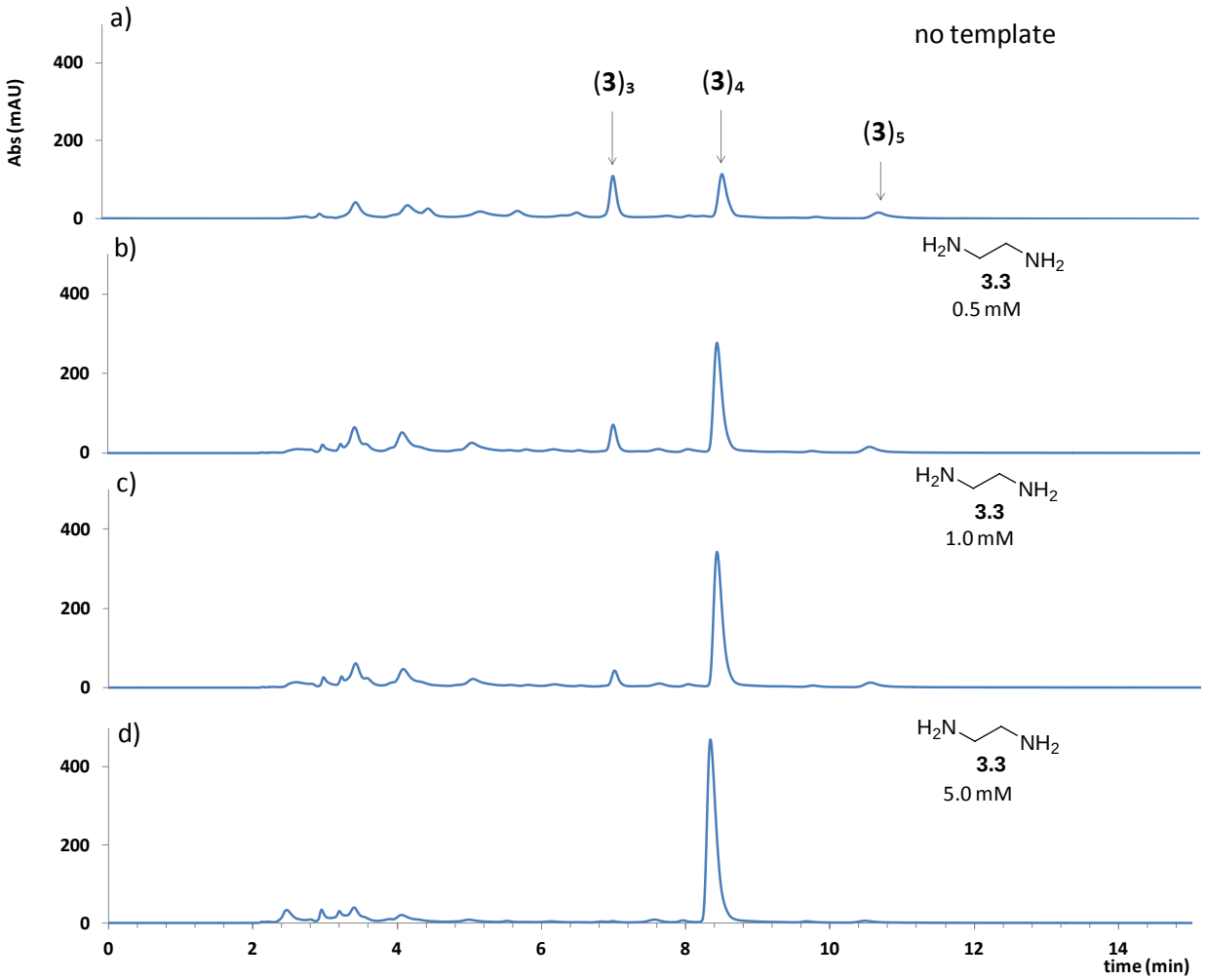

Figure 3.12: HPLC-UV chromatograms (λ_{abs} = 280 nm, λ_{ref} = 550 nm) of DCLs prepared in borate buffer (50 mM, pH 8.4) composed of 2 mM of building block **3** (a) in the absence of template and in the presence of (b) 0.5 mM, (c) 1.0 mM, and (d) 5.0 mM of template **3.3**. Volume injected = 10 µL. Samples taken from the DCL solutions were not diluted with DMSO prior to HPLC analyses.

Table 3.5: Total HPLC-UV peak area (mAU·min) and percentage library member composition of a DCL composed of building block **3** (2.0 mM) at different template concentrations.

		Four DCLs made from 2 mM of building block **3**			
Template **3.3** (mM)		0.0	0.5	1.0	5.0
Total HPLC-UV peak area (mAU·min)		5898	6041	6189	5898
DCL percent composition (%)	$(\mathbf{3})_3$	13	8	4	0
	$(\mathbf{3})_4$	19	41	53	72
	$(\mathbf{3})_5$	5	4	3	1.3

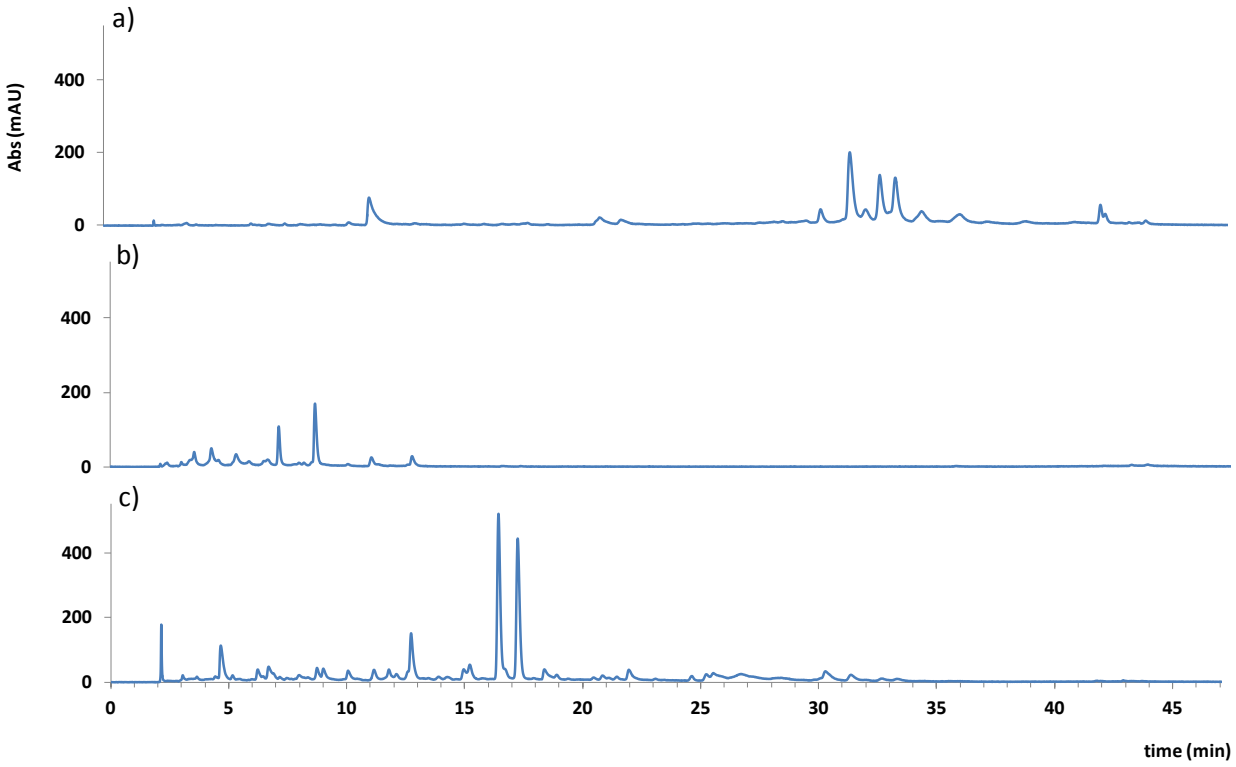

Figure 3.13: HPLC-UV chromatograms (λ_{abs} = 280 nm, λ_{ref} = 550 nm) of DCLs prepared in borate buffer (50 mM, pH 8.4) composed of (a) 2.5 mM of building blocks **2** (b) 2.5 mM of building blocks **3** (c) equimolar amounts building blocks **2** and **3** (5 mM in total). HPLC volume injected = 10 µL and samples taken from the DCL solutions were not diluted with DMSO prior to HPLC analyses.

Table 3.6: Total HPLC-UV peak area (mAU·min) and library member composition of three DCLs composed of building block **2** (2.5 mM), building block **3** (2.5 mM) and equimolar amounts of building block **2** and **3** (2.5 mM for each).

DCL building block(s)	DCL products composition	Total HPLC-UV peak area (mAU·min)
2 (2.5 mM)	$(\mathbf{2})_4$-$(\mathbf{2})_4$ and $(\mathbf{2})_4$	23790
3 (2.5 mM)	$(\mathbf{3})_3$, $(\mathbf{3})_4$ and $(\mathbf{3})_5$	6850
2 and **3** (2.5 mM for each)	$(\mathbf{2})_4$, $(\mathbf{2})_3(\mathbf{3})$, $(\mathbf{2})_2(\mathbf{3})_2$, $(\mathbf{2})(\mathbf{3})_3$, $(\mathbf{3})_4$, $(\mathbf{2})_2(\mathbf{3})_3$, $(\mathbf{2})_4$-$(\mathbf{2})_4$ and $(\mathbf{2})_3(\mathbf{3})$-$(\mathbf{2})_4$	30743

3.3.6 Normalized amplification factors

3.3.6.1 Normalized amplification factors obtained using an excess of template

The AF_n values of the various macrocycles for all templates are shown in Table 3.7. The various isomers of the macrocycles of the same overall building block composition are grouped together and treated as one, as in the vast majority of the cases (90%), the isomers respond similarly to the introduction of templates (Figure 3.8). the data in Table 3.7 were obtained using an excess of template, that is 1:2 template to building block ratio which is translated into 4:1 template to

homotetramer ratio. Values for $AF_n \geq 0.09$ are shown in bold and reveal that all the expected tetrameric receptors are amplified by selected subsets of templates. As the templates increase in size or bulkiness they tend to amplify the larger macrocycles.

Table 3.7: Normalized amplification factors (AF_n) for the six receptors upon addition of a given template (2.5 mM) to a DCL made from **2** and **3** (2.5 mM each). $AF_n > 0.09$ are shown in bold

	template	$(\mathbf{3})_4$	$(\mathbf{2})(\mathbf{3})_3$	$(\mathbf{2})_2(\mathbf{3})_2$	$(\mathbf{2})_3(\mathbf{3})$	$(\mathbf{2})_2(\mathbf{3})_3$	$(\mathbf{2})_4$
3.1	spermine	**0.70**	**0.13**	-0.52	0.01	-0.03	**0.44**
3.2	bis(3-aminopropyl)amine	**0.37**	**0.13**	-0.51	0.01	-0.03	**0.57**
3.3	ethylenediamine	**0.26**	**0.24**	-0.18	0.03	-0.02	0.04
3.4	1,3-diaminopropane	**0.32**	**0.43**	-0.39	0.02	-0.03	**0.39**
3.5	cadaverine	0.04	**0.52**	0.04	0.00	-0.03	**0.31**
3.6	1-amino-3,3-diethoxypropane	**0.09**	**0.39**	-0.06	0.05	-0.02	0.04
3.7	histidinol	0.04	**0.25**	**0.57**	0.00	-0.03	0.03
3.8	1-methylpyrrolidine	0.03	**0.18**	0.03	0.04	-0.02	0.00
3.9	3-aminoquinuclidine	0.03	**0.15**	**0.15**	0.06	-0.02	0.01
3.10	tyramine	0.06	0.02	**0.92**	0.04	-0.03	0.00
3.11	(-)ephedrine	0.03	-0.03	**0.45**	0.05	-0.01	0.00
3.12	nicotine	0.04	-0.01	**0.39**	**0.09**	-0.01	0.00
3.13	hexamethonium chloride	0.03	**0.10**	**0.34**	0.08	-0.03	nd[a]
3.14	carbamoylcholine chloride	0.03	0.00	**0.33**	0.06	-0.02	nd[a]
3.15	salbutamol	0.02	-0.05	**0.31**	0.00	0.00	0.01
3.16	acetylcholine chloride	0.03	0.00	**0.31**	**0.14**	-0.02	0.01
3.17	quinoline	0.04	0.00	**0.28**	0.00	0.00	0.04
3.18	dopamine	0.03	0.06	**0.26**	-0.02	-0.02	0.00
3.19	serotonine	0.00	-0.05	**0.24**	0.00	-0.02	0.06
3.20	succinylcholine chloride	0.04	0.01	**0.24**	**0.10**	0.03	0.00
3.21	dobutamine	0.02	-0.06	**0.28**	**0.38**	-0.02	0.00
3.22	pyridine	0.04	0.02	**0.17**	0.01	-0.02	0.00
3.23	cytisine	0.04	0.07	**0.16**	0.05	-0.01	0.02
3.24	(-)-epinephrine	0.03	0.01	**0.09**	0.01	-0.02	0.00
3.25	trimethylindolenine	0.03	-0.01	0.01	-0.02	0.01	0.00
3.26	pirenzepine	0.00	-0.02	-0.02	0.04	0.02	0.01
3.27	atropine	0.01	-0.02	-0.23	0.07	**0.09**	0.04
3.28	1-adamantylamine	0.02	0.05	-0.31	-0.02	0.00	**0.79**
3.29	ATMA	-0.01	0.00	-0.29	0.00	0.02	**0.64**
3.30	1,9-diaminononane	0.08	**0.16**	-0.40	**0.24**	-0.03	**0.59**

[a] nd = macrocycle not detected

The maximum amplification of the smallest receptor $(\mathbf{3})_4$ is obtained with the polycationic spermine (**3.1**), while cadavarine (**3.5**) is most efficient at amplifying $(\mathbf{2})_1(\mathbf{3})_3$; tyramine (**3.10**) is

best for (**2**)$_2$(**3**)$_2$; dobutamine (**3.20**) is best for (**2**)$_3$(**3**); 1-adamantylamine (**3.28**) is best for (**2**)$_4$ and atropine (**3.27**) induces a modest amplification of pentameric receptor (**2**)$_2$(**3**)$_3$. In most cases amplification appears to be selective for one or two receptors that have similar sizes and charges.

3.3.6.2 Normalized amplification factor values at stoichiometric concentration levels

The data in Table 3.7 shows a few exceptions where a single template amplifies two structurally rather different macrocycles. For instance, polycationic thin templates **3.1**, **3.2**, **3.4** and **3.5** not only amplify the small macrocycles (**3**)$_4$ and (**2**)$_1$(**3**)$_3$ but also the large macrocycle (**2**)$_4$. However, the amplification of (**2**)$_4$ is strongly reduced upon lowering the template to building block ratio to 1:4 (2:1 template to homotetramer ratio) and 1:8 (1:1 template to homotetramer ratio).[32] The amplification of the smaller macrocycles is much less affected (Table 3.8). At stoichiometric levels, templating is more selective for the best binders,[33] suggesting that the small macrocycles are the stronger binders. Furthermore, the amplification of (**2**)$_4$ is facilitated by the fact that much of building block **3** is taken up in the small macrocycles, thus liberating building block **2**. Another exception is 1,9-diaminononane (**3.30**), which amplifies the relatively small oligomer (**2**)(**3**)$_3$ besides the larger oligomers (**2**)$_3$(**3**) and (**2**)$_4$. Upon lowering template to homotetramer ratio to stochiomoetric levels (1:1), the amplifications of (**2**)$_4$ and (**2**)$_1$(**3**)$_3$ are reduced by a factor of 4.2 and 1.8, respectively. The amplification of (**2**)$_1$(**3**)$_3$ (0.09) persists and an increase of the amplification of (**2**)$_2$(**3**)$_2$ by 0.64 amplification factor unit is observed. We speculate that the elongated shape of **3.30** may allow for two receptors to be bound to a single template.

Table 3.8: Normalized amplification factors for macrocycles in a DCL made from 2.5 mM of building block **2** and 2.5 mM of building block **3** upon addition of 2.5 mM, 1.25 mM and 0.625 mM of templates **3.1**, **3.2**, **3.4** and **3.5**. Samples for HPLC analysis where diluted with 200% volume DMSO immediately prior to injection.

template		[template] (mM)	(**3**)$_4$	(**2**)(**3**)$_3$	(**2**)$_2$(**3**)$_2$	(**2**)$_3$(**3**)	(**2**)$_2$(**3**)$_3$	(**2**)$_4$
3.1	spermine	2.5	**0.70**	**0.13**	-0.52	0.01	-0.03	**0.44**
		1.25	**0.60**	**0.27**	-0.47	0.00	-0.03	**0.32**
		0.625	**0.55**	**0.17**	-0.34	0.06	-0.03	**0.14**
3.2	bis(3-aminopropyl)amine	2.5	**0.37**	**0.13**	-0.51	0.01	-0.03	**0.57**
		1.25	**0.31**	**0.30**	-0.44	0.01	-0.03	**0.53**
		0.625	**0.20**	**0.31**	-0.28	0.03	-0.03	**0.26**
3.4	1,3-diaminopropane	2.5	**0.32**	**0.43**	-0.39	0.02	-0.03	**0.39**
		1.25	**0.22**	**0.34**	-0.38	0.03	-0.03	**0.15**
		0.625	**0.27**	**0.36**	-0.26	0.04	-0.02	0.06
3.5	cadaverine	2.5	0.04	**0.52**	0.04	0.00	-0.03	**0.31**
		1.25	-0.01	**0.25**	0.01	-0.01	-0.03	**0.17**
		0.625	0.04	**0.34**	**0.23**	0.00	-0.03	**0.09**
3.30	1,9-diaminononane	2.5	0.08	**0.16**	-0.40	**0.24**	-0.03	**0.59**
		1.25	0.06	**0.13**	0.06	**0.14**	-0.02	**0.45**
		0.625	0.01	**0.09**	**0.24**	0.06	-0.03	**0.14**

3.3.6.3 Normalized amplification factor values for a biased DCL

We performed our template screening using a 1:1 ratio of building blocks **2** and **3**, which puts restraints on the amplifications of library members with building block compositions that do not match this ratio. When the aim is to isolate specific receptors from the DCLs it becomes important to lift such restraints, which is possible by adjusting the building block ratio to match their composition. For example, with template **3.21** we obtained AF_n = 0.38 for (**2**)$_3$(**3**) when using an equimolar amount of building block **2** and **3**, while we obtained AF_n = 0.44 for the same receptor when we used a 3:1 ratio of building block **2** and **3**. More importantly, while the receptor corresponded to 29 % of the total library material in the original DCL, it constituted 61 % of library material in the biased DCL (see Figure 3.14).

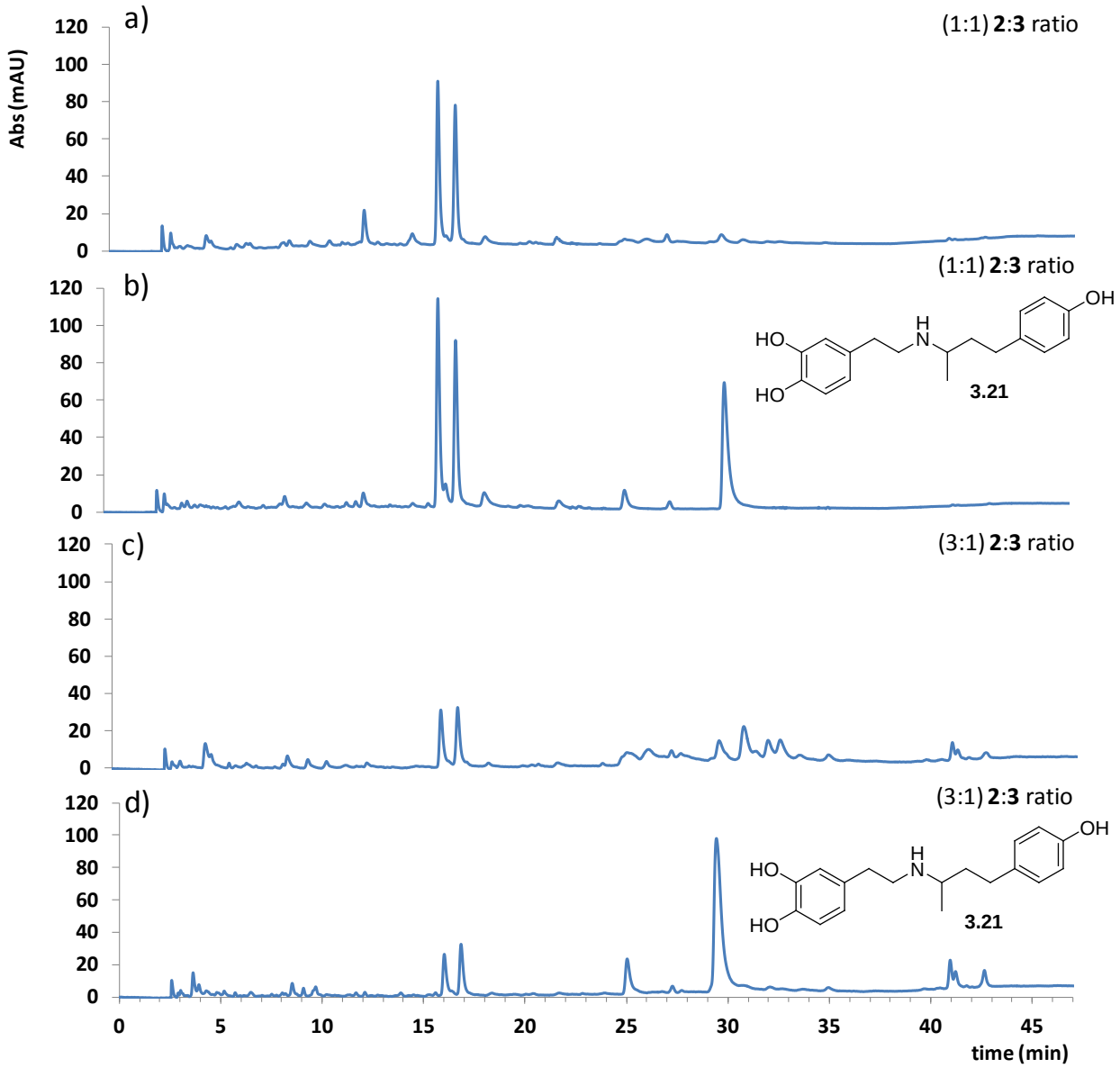

Figure 3.14: HPLC-UV chromatogram (λ_{abs} = 260 nm, λ_{ref} = 550 nm) of a DCL prepared in borate buffer (50 mM, pH 8.4) and composed of (a) equimolar amounts of building blocks **2** and **3** in the absence of template; (b) equimolar amounts of building blocks **2** and **3** and template **3.21**; (c) a 3:1 ratio of building

block **2** (3.75 mM) and building block **3** (1.25 mM) in the absence of template and (d) a 3:1 ratio of **2** (3.75 mM) and **3** (1.25 mM) and 2.5 mM of template **3.21**. Samples taken from the DCL solutions were diluted with 200% volume DMSO immediately prior to HPLC analyses.

Table 3.9: Normalised amplification factors (AF_n) for the six disulfide macrocycles upon addition of template **3.21** (2.5 mM) to a DCL made from two different ratios of building blocks **2** and **3** in 50 mM borate buffer, pH=8.4.

[**2**] (mM)	[**3**] (mM)	$(\mathbf{3})_4$	$(\mathbf{2})(\mathbf{3})_3$	$(\mathbf{2})_2(3)_2$	$(\mathbf{2})_3(\mathbf{3})$	$(\mathbf{2})_2(\mathbf{3})_3$	$(\mathbf{2})_4$
2.5	2.5	0.02	-0.06	0.28	0.38	-0.03	0.00
3.75	1.25	-0.07	-0.02	-0.07	0.44	0.00	0.03

3.4 Conclusion

Our results show that a continuous range of six different receptors of increasing cavity sizes and decreasing anionic charges may be, all, selectively amplified by exposing a DCL made from only two simple building blocks to a large range of different templates at near physiological pH.
Many individual synthetic receptors that have been developed for biologically active amines and ammonium ions have contributed to a better understanding of their molecular recognition properties.[34] Such receptors have been based on crown ethers,[35] calixarenes,[36] porphyrines,[37] cucurbiturils,[38] cyclodextrines[39] and cyclopeptides.[40] In this chapter we have described a DCL made from two simple building blocks from which amines and ammonium ions were able to select several receptors. The designed library showed, consistently, amplification of one or two receptors of similar cavity size and anionic charge after exposing it to almost any of the 30 individual templates. The observed template effects will be further investigated in chapter 4 by studying of a set of homologues α,ω-diamines.
Under conditions of excess of template, the amplification is biased towards those library members which the system can produce in largest quantities.[33] Thus, $(\mathbf{2})_2(\mathbf{3})_2$ will be more readily amplified than $(\mathbf{2})(\mathbf{3})_3$ and $(\mathbf{2})_3(\mathbf{3})$, which are, in turns, more readily amplified than $(\mathbf{2})_4$ and $(\mathbf{3})_4$. Hence, selective amplification of the homotetramers must reflect strong binding affinities. Indeed, templates **3.1** and **3.29**, which strongly amplify $(\mathbf{3})_4$ (AF_n = 0.70) and $(\mathbf{2})_4$ (AF_n = 0.64) respectively, bind receptors $(\mathbf{3})_4$ and $(\mathbf{2})_4$ with a K_a corresponding to 4.6 x 10^7 M^{-1} and 1 x 10^7 M^{-1} respectively.[2d,2f] However when $(\mathbf{2})_2(\mathbf{3})_2$ is strongly amplified it is not necessarily the case that this receptor is also the strongest binder among the ones listed in Table 3.7. This issue will be discussed in more detail in chapter 5

3.5 Experimental part

3.5.1 DCL preparations

Building blocks **2**[2d] and **3**[2f], and template **3.29**[41] were synthesized following literature procedures. All the other templates were obtained from Sigma-Aldrich and used without further purifications.
Stock solutions of individual building blocks **2** and **3** and the used templates (**T**) were freshly prepared at 10 mM concentration by dissolving the appropriate amounts in 50 mM borate buffer at pH 8.4. The pH was readjusted to 8.4 by addition of an appropriate volume of a 1 M solution of KOH.

Table 3.10: Summary of the DCL preparations.

DCL composition at time zero min			Volume added of 10 mM stock solutions			
[**2**] (mM)	[**3**] (mM)	**T**(mM)	(**2**) (µl)	(**3**) (µl)	(**3.1**-**3.30**) (µl)	Borate buffer solution (µl)
2.5	2.5	0	50	50	0	100
2.5	2.5	2.5	50	50	50	50
2.5	2.5	1.25	50	50	25	75
2.5	2.5	0.625	50	50	12.5	87.5
3.75	1.25	0	75	25	0	125
3.75	1.25	2.5	75	25	50	50

The DCL mixtures were allowed to oxidize and equilibrate by stirring for 4 days in closed vials at room temperature. After reaching equilibrium, each of the vials was manually shaken immediately before pipetting 10 µl using an eppendorf pipette. These 10 µl samples were diluted with 200% volume DMSO in HPLC vials immediately prior to HPLC-UV analyses.

3.5.2 HPLC and LC-MS analyseses

HPLC analyses were performed using an Agilent 1100 series HPLC. LC-MS analyses were performed using a HPLC-MS from Thermo Scientific coupled to a LCQ Fleet series mass spectrometer. Acetonitrile was purchased from Biosolve. Formic acid was purchased from Sigma-Aldrich. Analyses were performed using a reversed phase HPLC column (Kromasil C8, 4.6 x 150 mm, 5 µm) by injecting 3 µL of each of the DCL samples that had been diluted with 200% volume DMSO immediately prior to their analyses. A flow rate of 1 ml/min was used. The mobile phase consisted of a mixture of acetonitrile and doubly distilled water (both containing 0.1% formic acid), using the following gradient:

Time (min)	Acetonitrile (%)
0	30
5	40
30	70
35	70
40	95

50	95
55	30

HPLC-UV chromatograms were monitored at λ_{abs} = 260 nm and λ_{ref} = 550 nm.

The use of a splitter (1:5) for the LC-MS brought to the MS a flow of 0.2 mL/min. Negative ion mass spectra were acquired using electrospray ionization and following the LC-MS parameters described below:
Capillary temperature: 350 °C; sheath gas flow: 10 arbitrary units (AU); aux. gas flow rate: 1 AU; sweep gas flow: 1 AU; ionization spray voltage: 3 kV; capillary voltage: -2 V; tube lens: -100.60 V.

3.5.3 Analysis of a DCL made from building block 3

Benzene dithiol building block **3** (Scheme 3.4) was reported previously by R. F. Ludlow in 2006.[2f] It was designed to overcome some of the disadvantages of naphthalene dithiol building block **2** in DCLs, such as formation of aggregates and regioisomers due to its relative hydrophobicity and asymmetric structure.[21] As described by Vial *et*. *al*., a DCL made from building block **3** generates cyclic tetramer (**3**)$_4$ and several other oligomers that were not fully characterized at that time.[2f] To characterize these oligomers, a DCL made from building block **3** (2 mM) in 50 mM borate buffer was prepared following the standard protocol and reexamined using HPLC-MS analyses. The result shows that cyclic trimer (**3**)$_3$, cyclic tetramer (**3**)$_4$ and cyclic pentamer (**3**)$_5$ were the major disulfide products in the absence of a good template (Figure 3.15). Adding polyamine **3**.**1** to a DCL made from **3**, shifts the equilibrium to the quantitative formation of cyclic tetramer (**3**)$_4$.

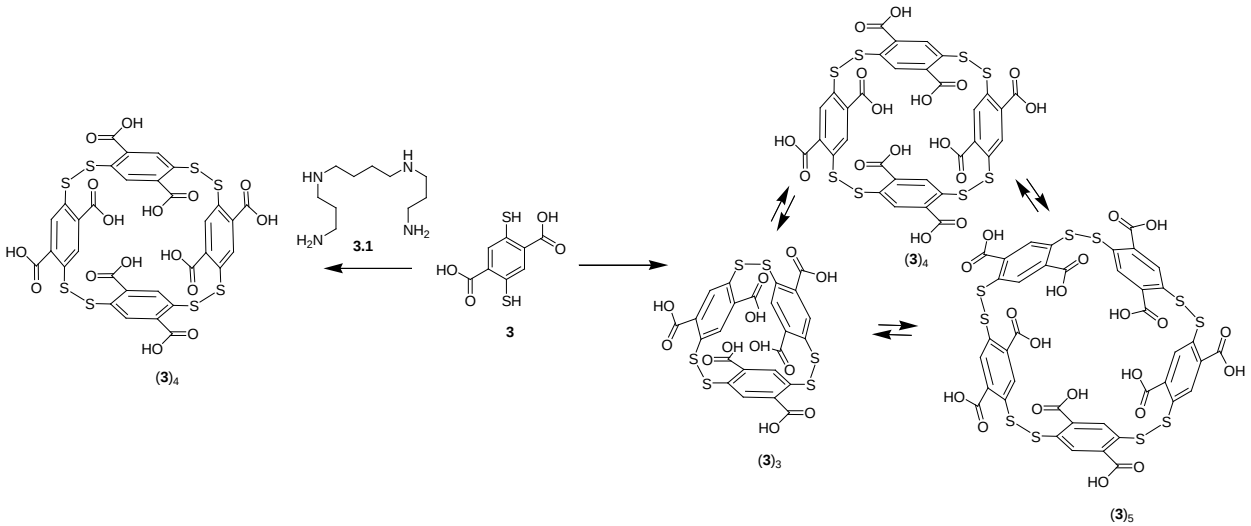

Scheme 3.4: Behavior of a DCL made from building block 3. Without adding a good template, the DCL forms cyclic trimer $(3)_3$, cyclic tetramer $(3)_4$ and cyclic pentamer $(3)_5$ (right), while addition of template 3.1 leads to the quantitative formation of cyclic tetramer $(3)_4$ (left).

In addition to the formed disulfide products (Figure 3.16), a number of peaks were also detected in the HPLC-MS chromatogram. The masses of these species correspond to linear trimer (**3**)$_3$4O, linear tetramer (**3**)$_4$4O and linear pentamer (**3**)$_5$4O with an extra four oxygen atoms, which we assign to compounds in which the terminal thiols have been over-oxidized to sulfinic acids (SO_2H) (Figure 3.17).

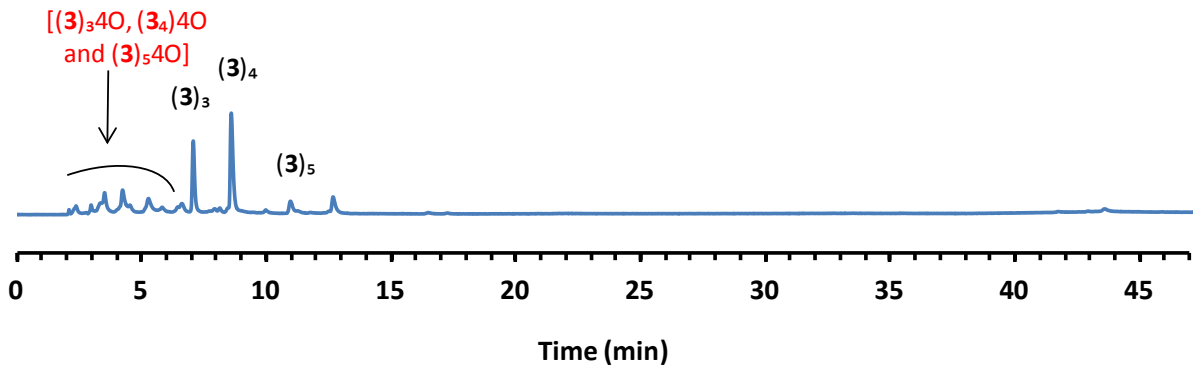

Figure 3.15: HPLC-UV peak assignments showing the cyclic disulfide products $(\mathbf{3})_3$, $(\mathbf{3})_4$ and $(\mathbf{3})_5$ and the the disulfinic acid side products $(\mathbf{3})_3$4O, $(\mathbf{3})_4$4O and $(\mathbf{3})_5$4O in a DCL prepared in borate buffer (50 mM, pH 8.4), composed of 2.5 mM of building block **3** and analyzed after 3 days of equilibration.

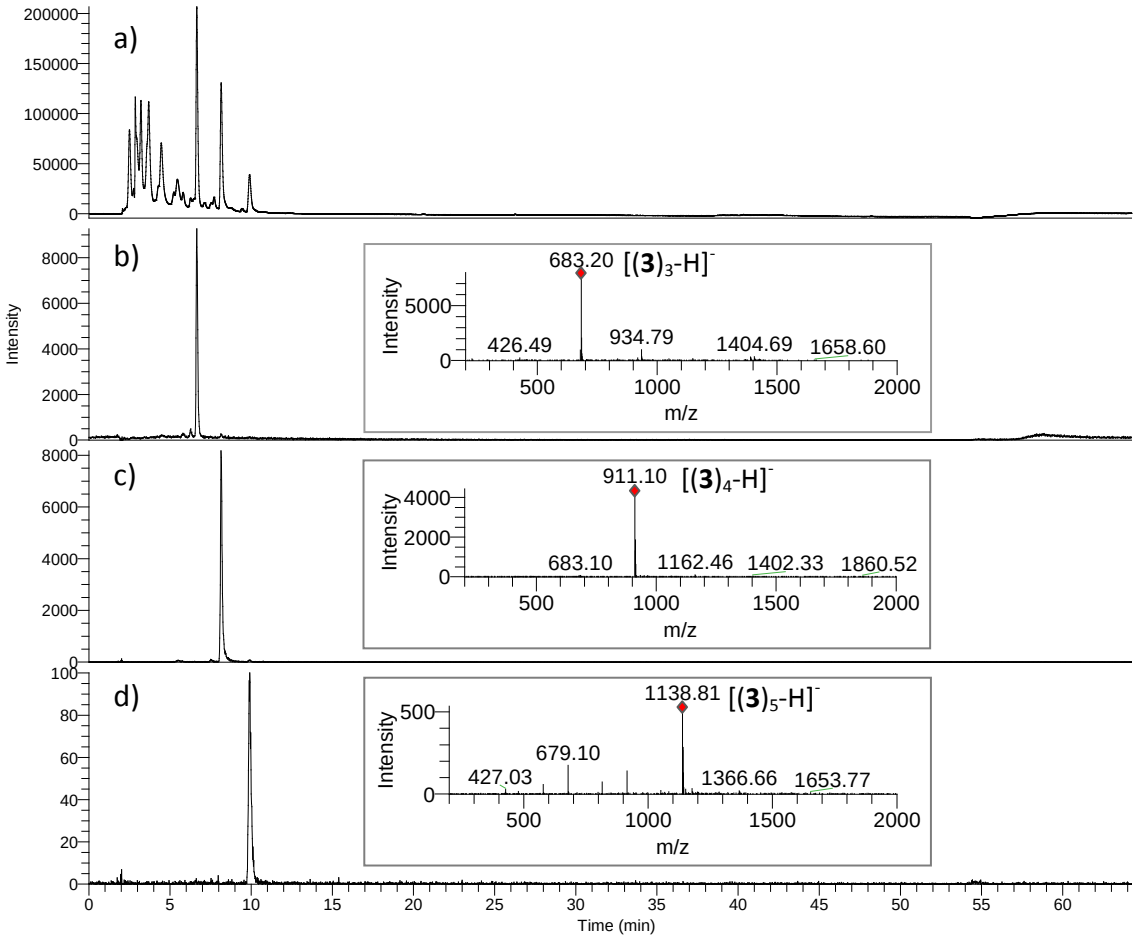

Figure 3.16: Analyses of a DCL prepared in 50 mM borate buffer (pH 8.4) and composed of 2.0 mM of building block **3**: (a) HPLC-UV chromatogram at 280 nm; (b) Extracted ion chromatogram (negative ion mode) corresponding to cyclic homotrimer $(\mathbf{3})_3$ (682.5-683.5) with (insert) ESI-MS spectra [m/z 200-2000] summed over the 6.63-6.69 min retention time window, corresponding to cyclic homotrimer $(\mathbf{3})_3$, showing $[(\mathbf{3})_3\text{-H}]^-$ m/z = 683.20 (expected = 682.85); (c) Extracted ion chromatogram (negative ion mode) corresponding to cyclic homotetramer $(\mathbf{3})_4$ (910.5-911.5) with (insert) ESI-MS spectra [m/z 200-2000]

summed over the 8.06-8.26 min retention time window, corresponding to cyclic homotetramer (**3**)$_4$, showing [(**3**)$_4$-H]$^-$ m/z = 911.10 (expected = 910.81); (d) Extracted ion chromatogram (negative ion mode) corresponding to cyclic homopentamer (**3**)$_5$ (1138.5-1139.5) with (insert) ESI-MS spectra [m/z 200-2000] summed over the 9.80-10.11 min retention time window, corresponding to cyclic homopentamer (**3**)$_5$, showing [(**3**)$_5$-H]$^-$ m/z = 1138.81 (expected = 1138.76).

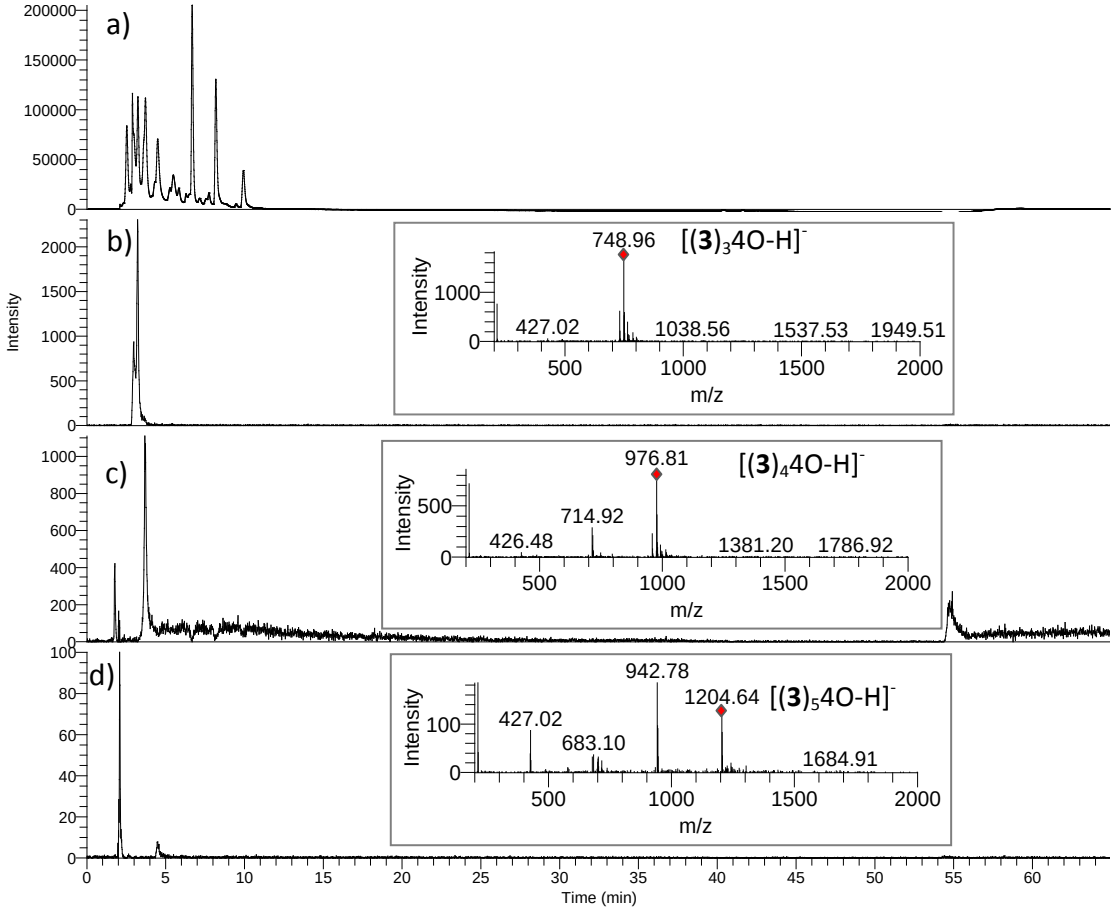

Figure 3.17: Analyses of a DCL prepared in 50 mM borate buffer (pH 8.4) and composed of 2.0 mM of building block **3**: (a) HPLC-UV chromatogram at 280 nm; (b) Extracted ion chromatogram (negative ion mode) corresponding to linear trimer disulfinic acid [(**3**)$_3$4O] (748.5-749.5) with (insert) ESI-MS spectra [m/z 200-2000] summed over the 2.89-3.28 min retention time window, corresponding to linear trimer disulfinic acid [(**3**)$_3$4O], showing [(**3**)$_3$4O-H]$^-$ m/z = 748.96 (expected = 748.86); (c) Extracted ion chromatogram (negative ion mode) corresponding to linear tetramer disulfinic acid [(**3**)$_4$4O] (976.5-977.5) with (insert) ESI-MS spectra [m/z 200-2000] summed over the 3.63-3.75 min retention time window, corresponding to linear tetramer disulfinic acid [(**3**)$_4$4O], showing [(**3**)$_4$4O-H]$^-$ m/z = 976.81 (expected = 976.81); (d) Extracted ion chromatogram (negative ion mode) corresponding to linear pentamer disulfinic acid [(**3**)$_5$4O] (1204.5-1205.5) with (insert) ESI-MS spectra [m/z 200-2000] summed over the 4.41-4.62 min retention time window, corresponding to linear pentamer disulfinic acid [(**3**)$_5$4O], showing [(**3**)$_4$5O-H]$^-$ m/z = 1204.64 (expected = 1204.77).

3.6 References

[1] Beeren, S. R.; Sanders, J. K. M. History and Principles of Dynamic Combinatorial Chemistry. In *Dynamic Combinatorial Chemistry*; Reek, J. N. H.; Otto, S., Wiley-VCH, Weinheim, **2010**; pp 1.

[2] (a) Hamieh, S.; Ludlow, R. F.; Perraud, O.; West, K. R.; Mattia, E.; Otto, S. *Org. Lett.* **2012**, *14*, 5404. (b) Givelet, C.; Sun, J.; Xu, D.; Emge, T. J.; Dhokte, A.; Warmuth, R. *Chem*. *Commun*. **2011**, *47*, 4511. (c) Ludlow, R. F.; Otto, S. *J. Am. Chem. Soc.* **2008**, *130,* 12218. (d) West, K. R.; Ludlow, R. F.; Corbett, P. T.; Besenius, P.; Mansfeld, F. M.; Cormack, P. A. G.; Sherrington, D. C.; Goodman, J. M.; Stuart, M. C. A.; Otto, S. *J. Am. Chem. Soc.* **2008**, *130*, 10834. (e) Besenius, P.; Cormack, P. A. G.; Ludlow, R. F.; Otto, S.; Sherrington, D. C. *Chem*. *Commun*. **2008**, *24*, 2809. (f) Vial, L.; Ludlow, R. F.; Leclaire, J.; Perez-Fernandez, R.; Otto, S. *J. Am. Chem. Soc.* **2006**, *128,* 10253. (g) Corbett, P. T.; Tong, L. H.; Sanders, J. K. M.; Otto, S. *J. Am*. *Chem*. *Soc*. **2005**,*127*, .8902. (h) Otto, S.; Furlan, R. L. E.; Sanders, J. K. M. *Science* **2002**, *297*, 590.

[3] (a) Bru, M.; Alfonso, I.; Bolte, M.; Burguete, M. I.; Luis, S. V. *Chem*. *Commun*. **2011**, *47*, 283. (b) Bru, M.; Alfonso, I.; Burguete, M. I.; Luis, S. V. *Angew*. *Chem*. *Int*. *Ed*. **2006**, *45*, 6155.

[4] (a) Berrocal, J. A.; Cacciapaglia, R.; Di Stefano, S.; Mandolini, L. *New J. Chem*. **2012**, *36*, 40. (b) Klein, J. M.; Saggiomo, V.; Reck, L.; Lüning, U.; Sanders, J. K. M. *Org. Biomol. Chem.* **2012**, *10*, 60. (c) Klein, J. M.; Clegg, J. K.; Saggiomo, V.; Reck, L.; Lüning, U.; Sanders, J. K. M. *Dalton Trans*. **2012**, *41*, 3780. (d) Berrocal, J. A.; Cacciapaglia, R.; Di Stefano, S. *Org. Biomol. Chem.* **2011**, *9*, 8190. (e) Klein, J. M.; Saggiomo, V.; Reck, L.; McPartlin, M.; Pantos, G. D.; Lüning, U.; Sanders, J. K. M. *Chem*. *Commun*. **2011**, *47*,3371

[5] (a) Beeren, S. R.; Sanders, J. K. M. *J. Am*. *Chem*. *Soc*. **2011**, *133*, 3804. (b) Rodriguez-Docampo, Z.; Eugenieva-Ilieva, E.; Reyheller, C.; Belenguer, A. M.; Kubik, S.; Otto, S. *Chem*. *Commun*. **2011**, *47*, 9798. (c) Otto, S.; Kubik, S. *J. Am*. *Chem*. *Soc*. **2003**, *125*, 7804.

[6] Leclaire, J.; Husson, G.; Devaux, N.; Delorme, V.; Charles, L.; Ziarelli, F.; Desbois, P.; Chaumonnot, A.; Jacquin, M.; Fotiadu, F.; Buono, G. *J. Am*. *Chem*. *Soc*. **2010**, *132*, 3582.

[7] (a) Severin, K. Analytical Applications of Dynamic Combinatorial Chemistry. In *Dynamic Combinatorial Chemistry*; Reek, J. N. H.; Otto, S., Wiley-VCH, Weinheim, **2010**; pp 169. (b) Severin, K. *Curr.Opin*. *Chem*. *Biol*. **2010**, *14*, 737. (c) Rochat, S.; Severin, K. *J. Comb*. *Chem*. **2010**, *12*, 595. (d) Muller-Graff, P. K.; Szelke, H.; Severin K.; Kramer, R. *Org*. *Biomol*. *Chem*. **2010**, *8*, 2327. (e) Zaubitzer, F.; Riis-Johannessen, T. ; Severin, K. *Org*. *Biomol*. *Chem*. **2009**, *7*, 4598.

[8] (a) Breuil, P-R. R.; Reek, J. N. H. Dynamic Combinatorial Chemistry for Catalytic Aplications. In . *Dynamic Combinatorial Chemistry* ; Reek, J. N. H.; Otto, S., Wiley-VCH, Weinheim, **2010**; pp 91. (b) Matsumoto, M.; Estes, D.; Nicholas, K. M. *Eur. J. Inorg. Chem.* **2010**, 1847. (c) Gasparini, G.; Molin, M. D.; Prins, L. J. *Eur. J. Org. Chem.* **2010**, 2429. (d) Vial, L.; Sanders, J. K. M.; Otto, S. *New J. Chem.* **2005**, *29*, 1001. (e) Brisig, B.; Sanders, J. K. M.; Otto, S. *Angew. Chem. Int. Ed.* **2003**, *42*, 1270.

[9] (a) Cougnon, F. B. L.; Jenkins, N. A; Pantos, G. D.; Sanders, J. K. M. *Angew*. *Chem*. *Int*. *Ed*. **2012**, *51*, 1443. (b) Lam, T. S. R.; Belenguer, A.; Roberts, S. L.; Naumann, C.; Jarrosson, T.; Otto, S.; Sanders, J. K. M. *Science* **2005**, *308*, 667.

[10] (a) Stefankiewicz, A. R.; Sambrook, M. R.; Sanders, J. K. M. *Chem. Sci.* **2012**, *3*, 2326. (b) Takahagi, H.; Fujibe, S.; Iwasawa, N. *Chem. Eur. J.* **2009**, *15* ,13327.

[11] (a) Riddell, I. A.; Smulders, M. M. J.; Clegg, J. K.; Hristova, Y. R.; Breiner, B.; Thoburn, J. D.; Nitschke, J. R. *Nat. Chem.* **2012**, *4*, 751. (b) Dreos, R.; Randaccio, L.; Siega, P.; Tavagnacco, C.; Zangrando, E. *Inorg. Chim. Acta* **2010**, *363*, 2113. (c) Ajami, D.; Rebek, J. *Angew. Chem. Int. Ed.* **2007**, *46*, 9283. (d) Kerckhoffs, J. M. C. A.; Mateos-Timoneda, M. A.; Reinhoudt, D. N.; Crego-Calama, M. *Chem. Eur. J.* **2007**, *13*, 2377.

[12] Roy, L.; Case, M. A. *J. Phys. Chem. B* **2011**, *115*, 2454.

[13] (a) Greaney, M. F.; Bhat, V. T. Protein-Directed Dynamic Combinatorial Chemistry. In *Dynamic Combinatorial Chemistry: In Drug Discovery, Bioorganic Chemistry, and Materials Science*; Miller, B. L., Wiley, Hoboken, NJ, **2012**; pp 43. (b) Ingerman, L. A.; Cuellar, M. E.; Waters, M. L. *Chem. Commun.* **2010**, *46*, 1839. (c) Bhat, V. T.; Caniard, A. M.; Luksch, T.; Brenk, R.; Campopiano, D. J.; Greaney, M. F. *Nat. Chem.* **2010**, *2*, 490. (d) Shi, B. L.; Stevenson, R.; Campopiano, D. J.; Greaney, M. F. *J. Am. Chem. Soc.* **2006**, *128*, 8459.

[14] (a) Gareiss, P. C.; Miller, B. L. Nucleic Acid-targeted Dynamic Combinatorial Chemistry. In *Dynamic Combinatorial Chemistry: In Drug Discovery, Bioorganic Chemistry, and Materials Science*; Miller, B. L.,

Wiley, Hoboken, NJ, **2012**; pp 83. (b) Bugaut, A.; Jantos, K.; Wietor, J. L.; Rodriguez, R.; Sanders, J. K. M.; Balasubramanian, S. *Angew. Chem. Int. Ed.* **2008**, *47*, 2677. (c) Ladame, S.; Whitney, A.; Balasubramanian, S. *Angew. Chem. Int. Ed.* **2005**, *44*, 5736. (d) Whitney, A. M.; Ladame, S.; Balasubramanian, S. *Angew*. *Chem*. **2004**; *43*,1143.

[15] (a) Ofori, L. O.; Hoskins, J.; Nakamori, M; Thornton, C. A.; Miller, B. L. *Nucl. Acids Res.* **2012**, *40*, 6380. (b) Gareiss, P. C.; Sobczak, K.; McNaughton, B. R.; Palde, P. B.; Thornton, C. A.; Miller, B. L. *J. Am. Chem. Soc.* **2008**, *130*, 16254.

[16] Chung, M.-K.; White, P. S.; Lee, S. J.; Gagne, M. R. *Angew. Chem. Int. Ed.* **2009**, *48*, 8683.

[17] Saggiomo, V.; Hristova, Y. R.; Ludlow, R. F.; Otto, S. *J*. *Syst*. *Chem*. **2013**, *4*, 2.

[18] Riddell, I. A.; Smulders, M. M. J.; Clegg, J. K.; Hristova, Y.R.; Breiner, B.; Thoburn, J. D.; Nitschke, J. R. *Nat. Chem.* **2012**, *4*, 751.

[19] Oae, S.; Takata, T.; Kim, Y. H. *Tetrahedron Lett.* **1981**, *37*, 37

[20] West, K. R. Molecular networks: Molecular Encapsulation through Disulfide Dynamic Combinatorial Chemistry. PhD thesis, University of Cambridge, England, **2006**.

[21] Ludlow, R. F. Molecular networks: From dynamic combinatorial libraries to complex systems. PhD thesis, University of Cambridge, England, **2008**.

[22] Except of $(\mathbf{3})_4$ and $(\mathbf{2})_2(\mathbf{3})_3$ which acquire the same number of anionic charges under near physiological conditions.

[23] (a) Xiu, X.; Puskar, N. L.; Jai, A. P.; Shanata, J. A. P.; Lester, H. A.; Dougherty, D. A. *Nature* **2009**, *458*, 534. (b) Hubbard, B. K.; Walsh, C. T. *Angew. Chem. Int. Ed.* **2003**, *42*, 730. (c) Hill, S. J.; Ganellin, C. R.; Timmerman, H.; Schwartz, J. C.; Shankley, N. P.; Young, J. M.; Schunack, W.; Levi, R.; Haas, H. L. *Pharmacol*. *Rev*. **1997**, *49*, 253

[24] Eaton, J. B.; Peng, J-H.; Schroeder, K. M.; George, A. A.; Fryer, J. D.; Krishnan, C.; Buhlman, L.; Kuo, Y-P.; Steinlein, O.; Lukas, R. J. *Mol*. *Pharmacol*. **2003**, 64, 1283.

[25] De Ponti, F. *Gut*. **2004**; *53*:1520.

[26] (a) Patil, P. N.; Lapidus, G. B.; Campbell, D.; Tye, A. *J*. *P*. *E*. *T*. **1967**, *155*, 13. (b) Weissman, N. J.; Levangie, M. W.; Newell, J. B.;J.; Guerrero, J. L.; Weyman, A. E.; Picard, M. H. *Am*. *Heart J*. **1995**, *130*, 248.

[27] Bruning, T. A.; Hendriks, M. G.; Chang, P. C.; Kuypers, E. A.; van Zwieten, P. A. *J*. *A*. *H*. *A*. **1994**, *74*, 911.

[28] Takao, K.; Rickhag, M.; Hegardt, C.; Oredsson, S.; Persson, L. *Int*. *J*. *Biochem. Cell Biol*. **2006**, *38*, 621.

[29] Silva, T. M.; Andersson, S.; Sukumaran, S. K.; Marques, M. P.; Persson, L.; Oredsson, S. *PLoS One* **2013**, 8, e55651

[30] Warrington, R. C.; Wratten, N. *J. Virol.* **1975**, *16*, 1503.

[31] Sawyer, R. C.; Stolfi, R. L.; Martin, D. S. *Cancer Res*. **1988**, *48*, 6664.

[32] The overoxidation of dithiol building blocks **2** and **3** results in a decrease in the concentrations of the dithiolate monomers generated from these building blocks and therefore a decrease in concentrations of all the generated macrocyclic oligomers. However, this doesn't affect the individually added template concentrations. Therefore the actual template to building block ratio is higher than the theoretical one which is based on total building block concentration equals to 5 mM.

[33] (a) Grote, Z.; Scopelliti, R.; Severin, K. *Angew. Chem. Int. Ed.* **2003**, *42*, 3821. (b) Severin, K. *Chem. Eur. J.* **2004**, *10*, 2565. (c) Saur, I.; Severin, K. *Chem. Commun.* **2005**, 1471. (d) Corbett, P. T.; Otto, S.; Sanders, J. K. M. *Chem. Eur. J.* **2004**, *10*, 3139. (e) Corbett, P. T.; Sanders, J. K. M.; Otto, S. *J. Am. Chem. Soc.* **2005**, *127*, 9390.

[34] Späth, A.; König, B. *Beilstein J. Org. Chem.* ***2010****, 6*, 32.

[35] Rüdiger, V.; Schneider, H.-J.; Solovev, V. P.; Kazachenko, V. P.; Raevsky, O. A. *Eur*. *J*. *Org*. *Chem*. **1999**, 1847.

[36] Koh, K. N.; Araki, K.; Ikeda, A.; Otsuka, H.; Shinkai, S. *J*. *Am*. *Chem*. *Soc*. **1996**, *118*, 755.

[37] Vogel, E. *Pure Appl*. *Chem*. **1996**, *68*, 1355.

[38] Jon, S. Y.; Selvapalam, N.; Oh, D. H.; Kang, J.-K.; Kim, S.-Y.; Jeon, Y. J.; Lee, J. W.; Kim, K. *J*. *Am*. *Chem*. *Soc*. **2003**, *125*, 10186.

[39] Wenz, G. *Angew*. *Chem*. *Int*. *Ed*. **1994**, *33*, 803.

[40] Kubik, S. Cyclopeptides as macrocyclic host molecules for charged guest. In *Highlights in Bioorganic Chemistry – Methods and Applications*; Schmuck, C.; Wennemers, H., Eds.; Wiley-VCH: Weinheim, Germany, **2004**; pp 124.

[41] Kondo, Y.; Uematsu, R.; Nakamura, Y.; Kusabayashi, S. *J. Chem. Soc. Faraday Trans. 1*, **1988**, *84*, 111.

Chapter 4: Towards selective synthetic receptors for aliphatic α,ω-diamines using dynamic combinatorial chemistry

Aliphatic α,ω-diamines play diverse biological roles in essential cellular processes, yet their precise physiological functions and mechanism of actions in vivo are not well understood. Moreover, their structures lack a fluorophore or chromophore moiety promoting their detection. Therefore, many authors reported the synthesis of synthetic receptors which are able to recognize selectively these diamines depending on their varying chain lengths. Some of the reported receptors showed selectivity and good affinity in binding α,ω-diamines of complementary lengths to their cavity sizes, yet their binding to the remaining diamines was often of modest affinity. Moreover, these receptors work in organic solvents and therefore their utilities are restricted in physiological medium. The reported receptors that work in near physiological conditions are few and show, predominantly, modest affinity towards α,ω-diamines.

*Herein, we report selective amplification of several macrocyclic hosts of differents sizes upon exposing the previously reported DCL made from building blocks **2** and **3** to individual α,ω-diamines as templates in near physiological conditions. The amplification depends clearly on the complementarity between the chain lengths of the diamines and the cavity sizes of the hosts. The fact that the DCL generates a pool of receptors, rather than only one receptor, suitable for selectively binding α,ω-diamines of different chain lengths, may overcome the lack in binding efficiency of α,ω-diamines observed with particular (α,ω-diamine) receptors. Moreover, a relationship between the host amplifications and the lengths of the templates was observed. Where the more the length of the diamine template is equivalent to the size of any of the host cavities, the more is its induced amplification for this host. Such a pronounced relationship has not been reported yet in DCC and reflects, in addition to the selectivity in host-guest binding, the ability of the DCL to show distinct properties of the templates. A comparison of AF for 1,5-pentanediamine versus 1,6-hexanediamine reveals an remarkable > 3 fold enhancement in amplification, which is the largest increment per CH_2 ever observed in DCC.*

*The introduction of this chapter reviews the relevant biological roles of aliphatic α,ω-diamines and the reported selective synthetic receptors for these diamines that work in organic and aqueous media. This is followed by evaluation of binding quality (affinity, selectivity and efficiency) of the reported receptors to the α,ω-diamines. Then, the binding features of macrocycle (**3**)$_4$ to spermine, previously reported by our group, are reviewed. The incentives that prompted to use a DCL made from building blocks **2** and **3** to generate several potentially selective receptors for α,ω-diamines are discussed at the end of the introduction. In the second part of this chapter we discuss the effects of the diamines on DCLs made from the individual and the combined building blocks (**2** and **3**).*

4.1 Introduction

4.1.1 Biological importance of aliphatic α,ω-diamines of low molecular weight

Aliphatic α,ω-diamines of general structure $NH_2(CH_2)_nNH_2$ contain two natural polyamines, putrescine **4.3** (n = 4) and cadaverine **4.4** (n = 5) (Scheme 4.1).[1,2] The first is found in all organisms[3] and is the precursor of two other natural polyamines, spermine and spermidine.[4] The second is biosynthesized in mammalian cells under natural polyamine deficient conditions,[5] and is found usually in bacteria.[6] This polyamine is the precursor of the endogenous neuromodulator piperidine.[7] Natural polyamines are derived from amino acids and are protonated under physiological conditions.[8] They have been implicated to play a role in diverse essential cellular processes (replication, transcription, translation, ion channel gating and membrane stability),[9] forming strong interactions with negatively charged molecules such as DNA, RNA, proteins and phospholipids.[10] This family of molecules stabilizes polynucleic acids structures and protects them against denaturation[11] and shearing.[12] They regulate cellular proliferation and apoptosis,[13] and have been investigated as a target for cancer chemotherapy.[14]
The rest of the aliphatic α,ω-diamines are synthetic. These have also been used as bioactive compounds; e.g. trimethylenediamine[15] **4.2** (n = 3) and hexamethylenediamine[16] **4.5** (n = 6) have been used as inhibitors for spermidine synthesis.[15,16] Nonamethylenediamine **4.8** (n = 9)[17] and guanyl derivatives of heptamethylenediamine **4.6** (n = 7) and octamethylenediamine **4.7** (n = 8)[18,19] showed antiproliferative activities towards tumorigenic cell lines.

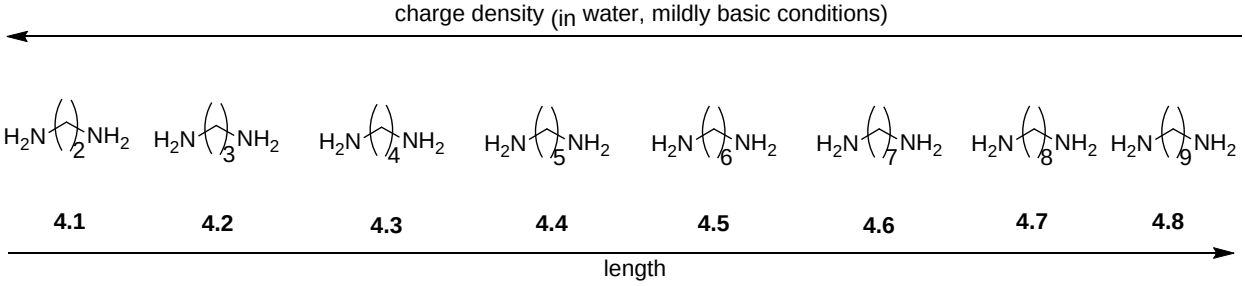

Scheme 4.1: Aliphatic α,ω-diamines with n = 2-9: ethylenediamine **4.1** (n = 2), tritmethylenediamine **4.2** (n = 3), tetramethylenediamine **4.3** (n = 4), pentamethylenediamine **4.4** (n = 5), hexamethylenediamine **4.5** (n = 6), heptamethylenediamine **4.6** (n = 7), octamethylenediamine **4.7** (n = 8) and nanomethylenediamine **4.8** (n = 9). Due to their pK_a values (> 9.9)[20] aliphatic α,ω-diamines are fully protonated in water even under mildly basic conditions, and therefore their charge densities decrease while their lengths increase.

4.1.2 Ditopic synthetic receptors for selective recognition of α,ω-diamines in organic solvents

The diverse biological activities of aliphatic α,ω-diamines of low molecular weight,[1-19] their lack of a fluorophore or chromophore moiety promoting their detection, and their unexplored precise physiological functions and mechanism of actions in vivo[13] have together created an incentive to develop synthetic receptors able to differentially recognize these diamines depending on their chain lengths.
These receptors are based on properties, such as shape, size and functional groups, complementary to those of particular α,ω-diamines. The selective binding is achieved mainly by

using polymacrocyclic ditopic receptors consisting of two cyclic binding sites for the terminal neutral or protonated amino groups and a linker between the macrocycles for binding the methylene chaines (Table 4.1).[21-28] Binding tends to be selective for α,ω-diamine guests of complementary lengths to the distance between the cyclic binding sites of the receptors.
Among the reported receptors, Fuji *et al.*[21,22] described receptors **4.9** and **4.10** (Figure 4.1) which are based on a meso-ternaphthalene backbone and two crown ether rings. These receptors bound α,ω-diammonium ions of n = 6-16, with K_a values varying in a range from 10^3 M^{-1} to 10^7 M^{-1} in chloroform with a preference for the alkyl chain length of n = 10. The group reported also receptor **4.11**[23] based on a *phenolphthalein* skeleton and two crown ethers for use as a synthetic sensor for colorimetric recognition of linear diamines and triamines (Figure 4.2). On amine binding, the phenolic hydroxyl groups are deprotonated, which leads to lactone ring opening and formation of a colored conjugated carboxylate structure. The receptor showed visible difference in degree of coloration after binding α,ω-diammonium ions of n = 6-10, with K_a values varying from 910 to 2020 M^{-1} in methanol and with a preference for the alkyl chain length of n = 9.
Voyer *et al.*[24] reported ditopic receptor **4.12** (Figure 4.3) based on crown ether amino acid (CEAA) which was incorporated twice into an oligo Ala peptide chain. The receptor bound α,ω-diammonium ions of n = 2-9 with K_a values varying from 10^8 M^{-1} to 10^{10} M^{-1} in chloroform with a preference for the alkyl chain length of n = 9.
Kim *et al.*[25] reported two bis(azocrown)anthracene derivatives **4.13** and **4.14** as ditopic fluororeceptors for detecting α,ω-diammonium ions of n = 3-6. Upon binding, hydrogen bonds are formed by both nitrogen atoms to the bis-ammonium ion guests; Hence, the photoinduced electron transfer (PET) is inhibited and the system showed clear difference in fluorescence. The reported K_a values vary from 35 M^{-1} to 4412 M^{-1} in ethanol with a preference for the alkyl chain length of n = 3.
Fages *et al.*[26] reported a macrotricyclic bisanthracenyl receptor **4.15** (Figure 4.5) of cylindrical shape consisting of an anthracene ring and two face-to-face N_2O_4 macrocycles. This ditopic fluorescent receptor bound α,ω-diammonium ions of n = 6-10 and 12 with K_a values varying between 10^4 and 10^7 M^{-1} in chloroform-methanol mixture, thus producing a fluorescence signal with an intensity that depends on the chain lengths of the guests. The binding affinity and intensity of the fluorescence are both maximum for the alkyl chain length of n = 7.
Hayashi *et al.*[27] reported receptor **4.16** (Figure 4.6) based on a zinc porphyrin dimer linked with chiral binaphthyl derivative that is able to bind α,ω-diamines via a zinc–nitrogen coordinated ditopic interaction. This receptor bound α,ω-diamines of n = 2, 6, 8, 10 and 12 with K_a values varying from 10^3 to 10^6 M^{-1} in chloroform with a preference for the diamine of n = 8. The formed α,ω-diamines-**4.16** complexes (except with diamine of n = 2) gave characteristic CD spectra with an intensity that depends on the lengths of the guests and is maximal for the diamine of n = 8. Similarly, Crossley *et al.*[28] reported a bis-zinc(II)-bisporphyrin Tröger's base analogue **4.17** (Figure 4.7) as a ditopic receptor for α,ω-diamines of n = 2-6 with K_a values varying in a range from 10^7 to 10^8 M^{-1} in toluene with a certain preference for n = 2–4.
Mock *et al.*[29] studied the binding affinity of cucurbit[6]uril **4.18** (Figure 4.8) towards α,ω-diammonium ions of n = 3-10 in 50% (v/v) aqueous formic acid, where the determined values vary from 10^2 to 10^6 M^{-1} with a preference for the alkyl chain length of n = 6.

The general trends of K_a values and intensities of signals derived from the interactions between the above mentioned receptors (**4.9-4.18**) and the diamine guests, along with a summary of the effects of the mentioned receptors are reported in Table 4.1.

Table 4.1: Summary of the effects of ditopic receptors **4.9**-**4.18** described for selective recognition of α,ω-diamines or diammonium ions in organic solvents. The table describes for each reported receptor: the range of chain lengths of the diamine guests (n), the range of host-guest K_a values (M^{-1}), the nature of the signal derived from the host-guest interactions, the nature of organic solvent in which the mentioned

receptor works and the trend of K_a values and intensities of signals derived from the interactions with the guests (n =).

Receptor	Range of guests (n =)	Range of K_a values (M^{-1})	Signal derived from the interactions	Organic solvent	Trend of K_a values and intensities of interaction signals with guests (n=)
4.9 and **4.10**	n = 6-16[a]	10^3-10^7	n. r.[c]	chloroform	6 < 8 < 9 < 10 > 11 > 12 > 14
4.11	n = 7-10[a]	910-2020	Colorimetric	methanol	7 < 8 < 9 > 10
4.12	n = 2-9[a]	10^8-10^{10}	n. r.[c]	chloroform	2 < 5 < 6 < 7 < 8 < 9
4.13 and **4.14**	n = 3-6[a]	35-4412	fluorescence	ethanol	3 > 4 > 5 > 6
4.15	n = 6-10, 12[a]	10^4-10^7	fluorescence	chloroform-methano	6 < 7 > 8 > 9 > 10 > 12
4.16	n = 6-12[b]	10^5-10^6	CD absorption	chlorofom	2 < 6 < 8 > 10 > 12
4.17	n = 2-6[b]	10^7-10^8	n. r.[c]	toluene	2-4 > 5 > 6
4.18	n = 2-9[a]	10^2-10^6	n. r.[c]	Acetic acid-water	3 < 4 < 5 < 6 > 7 > 8 > 9 > 10.

[a] = α,ω-diammonium ion guests. [b] = α,ω-diamineguests. [c] = not reported.

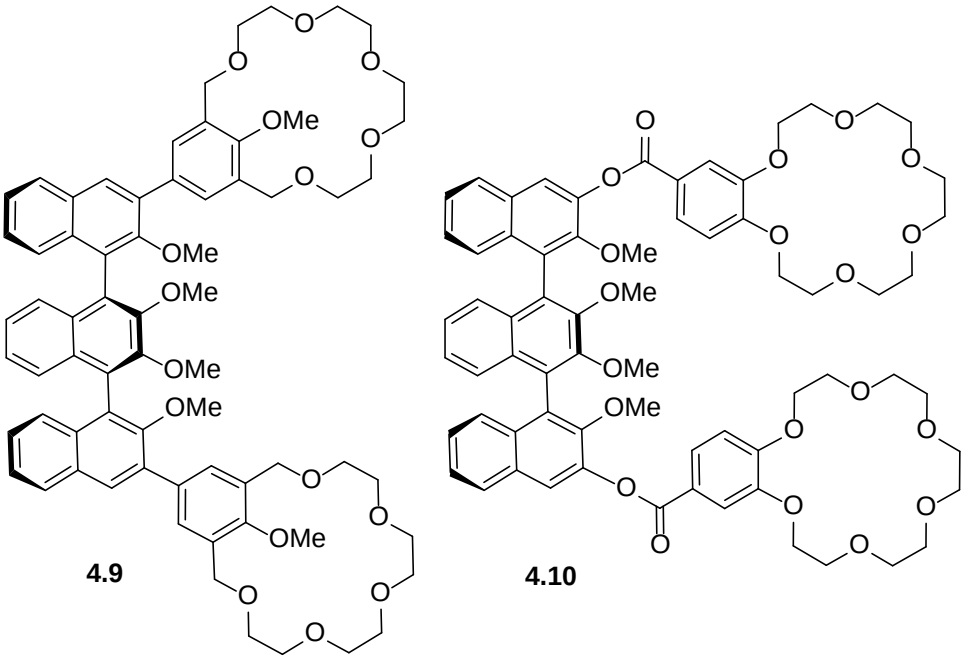

4.9 **4.10**

Figure 4.1: Chiral bis-crown receptors **4.9** and **4.10** with a ternaphthalene backbone, reported by Fuji *et al.*

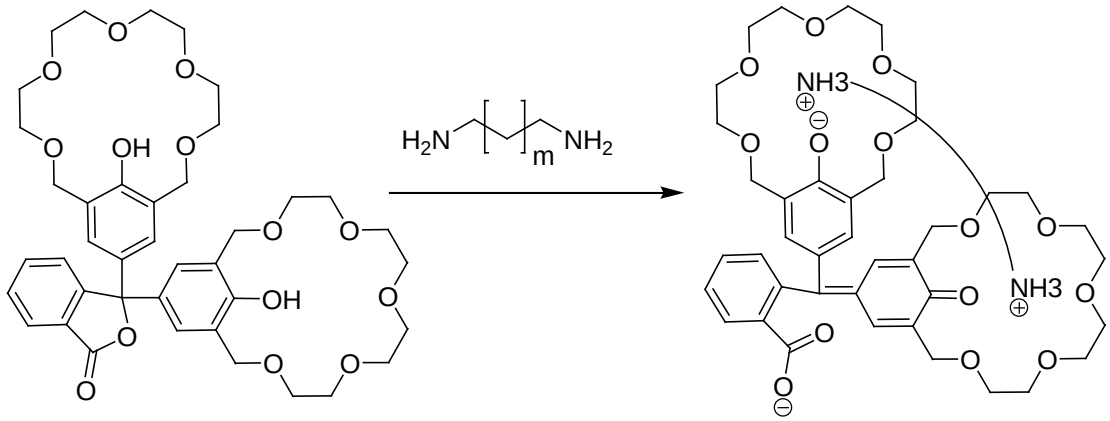

4.11

Figure 4.2: Chromogenic bis-crown receptor **4.11** with a phenolphthalein skeleton.

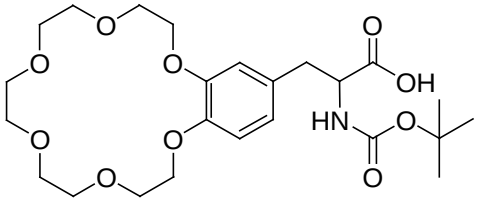

CEAA

Boc-Ala-Ala-CEAA-$(Ala)_{1-3}$-CEAA-Ala-Ala-Pr

4.12

Figure 4.3: Ditopic receptor **4.12** reported by Voyer *et al.*

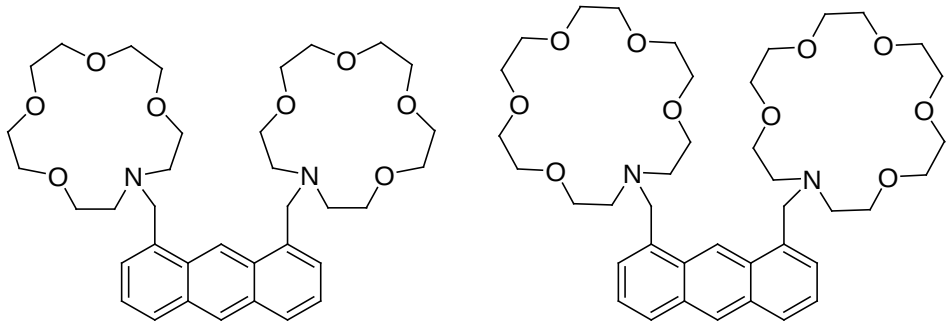

4.13 **4.14**

Figure 4.4: Bis-azocrown Fluorescent receptors **4.13** and **4.14** reported by Kim *et al.* based on an anthracene skeleton.

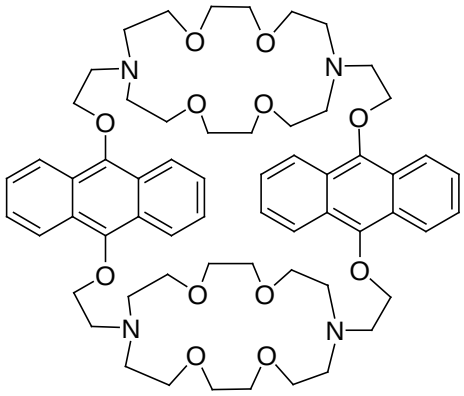

4.15

Figure 4.5: Macrotricyclic ditopic bisanthracenyl receptor reported by Fages *et al.*

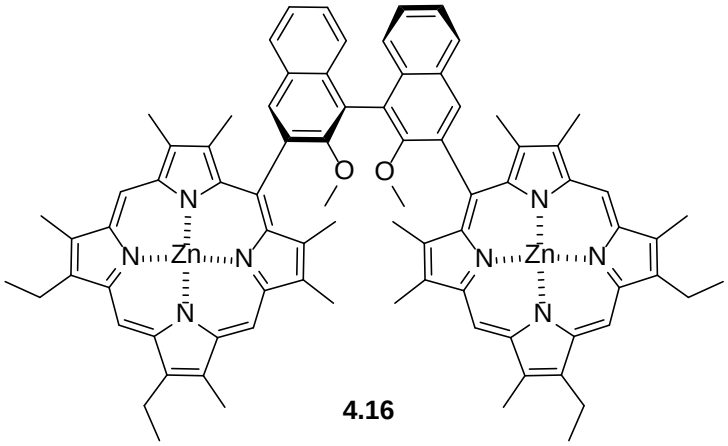

4.16

Figure 4.6: Receptor **4.16** based on a porphyrin dimer linked with a chiral binaphthyl derivative, reported by Hayashi *et al*.

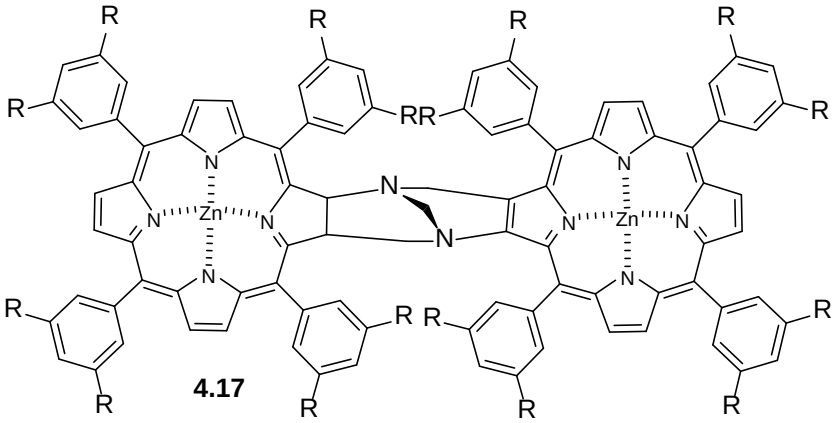

4.17

Figure 4.7: A bis-zinc(II)-bisporphyrin Tröger's base analogue **4.17** reported by Crossley *et al.*

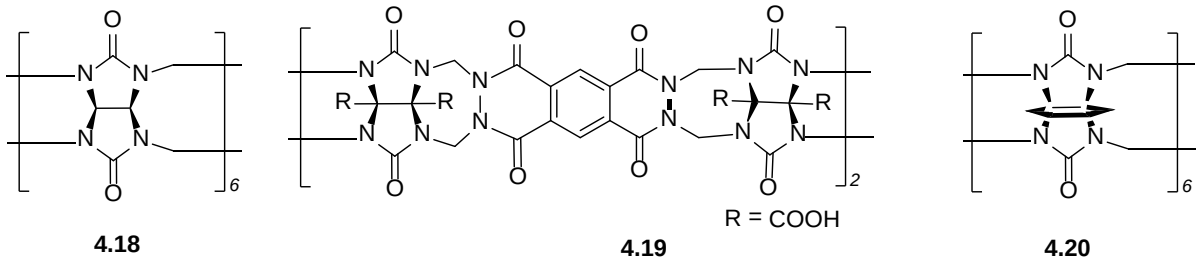

4.18 **4.19** **4.20**

Figure 4.8: Structures of cucurbituril [6] **4.18**, cucurbituril-phthalhydrazide analogue **4.19** reported by Issacs *et al.* and cyclohexanocucurbit[6]uril **4.20** reported by Kim *et al.*

4.1.3 Synthetic receptors for selective recognition of α,ω-diamines in aqueous medium

Since the solubility of CB[6] in aqueous solutions containing alkali or alkaline earth metal ions was discovered during the 1990s,[30] such aqueous solutions have often been employed for studies on complexation properties of CB[6]. For instance, Kim *et al*.[31] studied the binding affinity of CB[6] (**4.18**) towards α,ω-diammonium ions of n = 2 to 10 in 50 mM NaCl solution. The determined K_a values vary from 2 x 10^2 M^{-1} to 2.9 x 10^8 M^{-1} with a preference for the alkyl chain of n = 5. These affinities are 2–3 orders of magnitude higher than those of CB[6] in 50% formic acid reported by Mock *et al.*[29] (See paragraph 4.1.2). Issacs and co-workers[32] described the incorporation of a fluorescent (bis)-phthalhydrazide in CB[6], which made the system accessible to monitoring by fluorescence spectroscopy. This CB[6] analogue (**4.19**) (Figure 4.8) binds α,ω-diammonium ions of n = 6-12 in aqueous buffer at pH 4.7 with K_a values varying from 2.4 x 10^2 M^{-1} to 2.0 x 10^4 M^{-1}. The association constants increase as the length of the alkane (n) is increased.

More relevant to biological systems, Kim *et al.*[33] reported later a water soluble cucurbituril (CB) derivative, cyclohexanocucurbit[6]uril **4.20** (Figure 4.8), by introducing cyclohexane groups at the equator of CB[6]. This latter was able to bind selectively to aliphatic α,ω-diammonium ions of n = 4-8 in water at pH = 6.5–7.2 with K_a values varying from 8.5 x 10^7 M^{-1} to 6.6 x 10^{10} M^{-1}, with a preference for the alkyl chain of n = 5. The selectivity of **4.20** towards the diamine guests matches with the one observed with **4.18** since the cavity dimension is essentially the same as in CB[6] (**4.18**). However, the binding affinity of **4.20** with α,ω-diammonium ion molecules in water is 3–5 orders of magnitude higher than those of **4.18** in 50 % aqueous formic acid due to the larger enthalpic gains upon complex formation in the absence of interfering ions, such as protons (from acetic acid) and Na^+ (from NaCl).

Lehn *et al.*[34] described the synthesis of a hexacarboxylate 27-crown-9 derivative (**4.21**) (Figure 4.9) as a selective receptor for aliphatic α,ω-diammonium ions of n = 2-4 in water at pH = 7. With increasing the length of the guest from n = 2 to n = 4 its K_a toward receptor **4.21** decreases from 2 x 10^5 M^{-1} to 7.2 x 10^3 M^{-1}. The group later reported a tetracarboxylate 18-crown-6 derivative **4.22**[35] (Figure 4.9) as a selective receptor for aliphatic α,ω-diammonium ions of n = 2-8 (except of n = 5 and 7) in water at pH = 7. Like with receptor **4.21**, increasing the length of the guest decreases its K_a toward receptor **4.22** from 4 x 10^4 M^{-1} for n = 2 to less than 9 x 10^2 M^{-1} for n = 8. Also, a tetracarboxylate coproporphyrin derivative **4.23** (Figure 4.10) reported by Fores-Villalobos *et al.*[36] showed selective binding of α,ω-diammonium ions of n = 2-8 in water at pH = 8. Contrary to receptors **4.21** and **4.22**, increasing the length of the guest increases its K_a toward receptor **4.23** from 21 M^{-1} for n = 2 to 4 x 10^2 M^{-1} for n = 8. The general trends of K_a values and intensities of signals derived from the interactions between the above mentioned receptors (**4.18-4.23**) and the diamine guests, along with a summary of the effects of the mentioned receptors are reported in Table 4.2.

Table 4.2: Summary of the effects of receptors **4.18**-**4.23** described for selective recognition of α,ω-diammonium ions in water. The table describes for each reported receptor: the range of chain lengths of α,ω-diammonium ion guests (n), the range of host-guests K_a values (M^{-1}), the nature of the signals derived from the host-guest interactions, the conditions under which the receptor works and the trend of K_a values and intensities of interaction signals with guests.

Receptor	Range (n =) of α,ω-diammonium ion guests	Range of K_a values (M^{-1})	Signal derived from the interactions	Aqueous medium	Trend of K_a values and intensities of interaction signals with guests (n=)
4.18	n = 2-10	10^2-10^8	n. r.[a]	Water, 0.05 M NaCl	2 < 3 < 4 < 5 > 6 > 7 > 8 > 10
4.19	n = 6-10	10^2-10^4	fluorescence	Buffer[b] pH = 4.7	6 < 7 < 8 < 9 <10
4.20	n = 4-8	10^7-10^{10}	n. r.[a]	Water, pH = 6.5-7.2	4 < 5 > 6 < 7 > 8
4.21	n = 2-4	10^3-10^5	n. r.[a]	Buffer[c] pH = 7	2 < 3 < 4
4.22	n = 2-8	10^3-10^4	n. r.[a]	Buffer[d] pH = 7	2 < 3 < 4 < 6 < 8
4.23	n = 2-8	21-10^2	fluorescence	Water pH = 8	2 > 3 > 4 > 5 > 6 > 7 > 8

[a] = not reported. [b] = aqueous sodium acetate. [c] = tris-(2-hydroxyethyl) ammonium hydrochloride. [d] = tetramethylammonium phosphate.

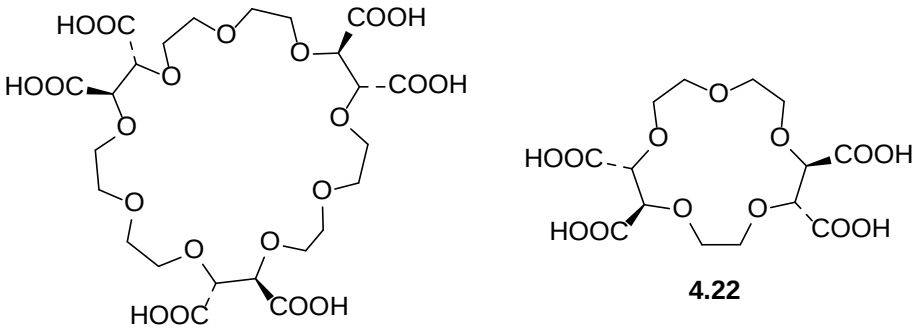

Figure 4.9: receptors **4.21** and **4.22** reported by Lehn *et al*.

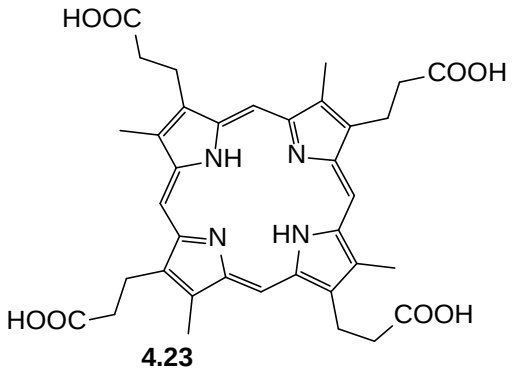

Figure 4.10: receptor **4.23** reported by Fores-Villalobos *et al.*

4.1.4 Evaluation of the binding quality between the reported receptors and α,ω-diamines

For all the reported receptors (**4.9**-**4.23**), both K_a value and intensity of signal derived from their interactions with alkanediamines depend on the length of the diamine chain. These two variables reached a maximum once the diamine chain reached the optimal length equivalent to the distance within the host. This is due to the optimization of both hydrogen bonding and ion-dipole interactions between the ammonium groups of the guests and the receptor binding sites, in addition to hydrophobic interactions between the alkyl chain and the hydrophobic inner part of the receptors (for **4.18-4.23**).

Although the majority of the reported ditopic receptors showed good affinity ($K_a \geq 10^6$ M^{-1}) towards the diamines of the optimal lengths, these, except **4.12** and **4.17**, showed modest affinities towards diamines of lengths much shorter or much longer than their corresponding optimal ones and therefore less efficiency in binding these diamines (Table 4.1). This may be due to a lack of flexibility in their molecular frameworks as in **4.9**-**4.10** or their inabilities to accommodate diamines of lengths much longer than their corresponding optimal ones such as is the case in **4.15**-**4.16**, respectively (Table 4.1).[21,22] It is noteworthy that the affinity constants of the reported ditopic receptors towards α,ω-diammonium ions are derived from picrate salt extraction from water into organic solvents. These affinity constants may have large errors[37] and therefore cannot be compared to other systems investigated in homogeneous solutions. Moreover, the fact that the reported ditopic receptors work only in organic solvents restricts their utilities in physiological medium. Similarly, the poor solubility of CB[6] **4.18** in water ($< 10^{-5}$ M)[33] makes it difficult to study the host–guest chemistry of CB[6] in physiological medium and therefore to reveal its utilities in such medium. Receptor **4.19** showed modest affinities towards the diammonium ion guests (Table 4.2).

On the other hand, with the exception of receptor **4.20**, the affinities of reported receptors working in near physiological conditions towards α,ω diamonium ions are lower by several orders of magnitude than those of biomolecules (Table 4.2).[38] However, cyclohexanocucurbit[6]uril **4.20** revealed remarkably high affinity, size, shape, and functional group selectivity for the diammonium ion guests in near physiological medium. This receptor showed the highest binding constants of all presented receptor families towards alkanediammonium ions in aqueous media (up to 10^{10} M^{-1}) and succeeded in rivaling the efficiency of biomolecule receptors.[38] This strength in binding is the result of coordination between the ammonium groups of the guests and the carbonyl receptor groups by electrostatic ion–dipole interactions assisted by hydrogen bonding, and the hydrophobic interactions between oligomethylene chains and the inner wall of the receptor.[33]

4.1.5 Features of binding of macrocycle $(3)_4$ to α,ω-alkanediammonium ions of n = 4

Vial *et al*.[39] have reported that exposing a DCL made from benzene dithiol building block **3** to linear aliphatic polyamine **3.1** as a template, amplifies macrocycle $(\mathbf{3})_4$ (Figure 4.11). Proton NMR studies of $(\mathbf{3})_4$-**3.1** complex showed that the four central methylene units of **3.1** are located within the aromatic cavity of $(\mathbf{3})_4$. Also, computer modeling studies of the complex suggested hydrogen bonding and electrostatic interactions between the central protonated amines of **3.1** and the carboxylate groups of $(\mathbf{3})_4$. These interactions, in addition to hydrophobic interactions between the hydrocarbon chain of **3.1** and the hydrophobic cavity of $(\mathbf{3})_4$, resulted in a K_a $(\mathbf{3})_4$-**3.1** in the nanomolar range under near physiological conditions, as determined by ITC. Both NMR and computer modeling suggested that **3.1** is threaded through the macrocyclic host and bound mainly from its inner cavity, resulting in a pseudorotaxane complex (Figure 4.11).

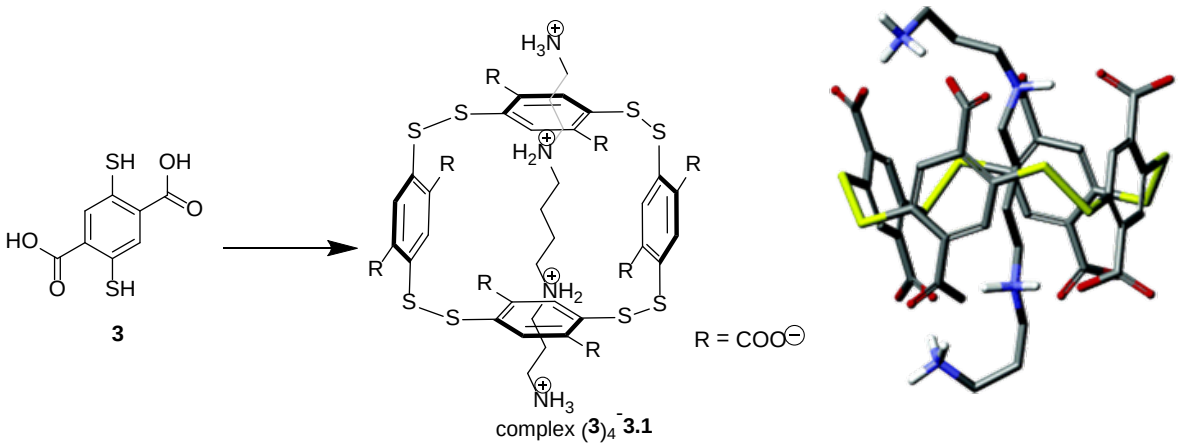

Figure 4.11: (To the left) schematic representation of (**3**)$_4$-**3.1** complex showing that the outer methylene units and the terminal protonated amines of **3.1** are located outside the cavity of receptor (**3**)$_4$. (To the right) side view of the energy minimized complex obtained by computer modeling and reported by Vial *et al.*[39] showing the pseudorotaxane form of complex (**3**)$_4$-**3.1**.

As a result, the three outer methylene units and the terminal protonated amines of **3.1** are much less affected by the interactions. This suggests that α,ω-diamine of n = 4 (**4.3**) is of complementary length to the size of the cavity located between the carboxylate functions of (**3**)$_4$, which are engaged in binding the central amines of **3.1**. On this basis, guest **4.3** may bind receptor (**3**)$_4$ with nanomolar K_a like **3.1**.

4.1.6 Aim of the research reported in this chapter

As reported in chapter 3, adding the naphthalene dithiol building block **2** to building block **3** in water under mildly basic conditions is able to generate macrocycle (**3**)$_4$ among a series of macrocycles of molecular frameworks featuring, predominantly, a continuous increment of one benzene ring. The series includes (**3**)$_4$, (**2**)(**3**)$_3$, (**2**)$_2$(**3**)$_2$, (**2**)$_3$(**3**), (**2**)$_2$(**3**)$_3$ and (**2**)$_4$ in addition to the two [2]-catenanes, (**2**)$_3$(**3**)-(**2**)$_4$ and (**2**)$_4$-(**2**)$_4$ (Scheme 4.2). The outcome of the DCL made from building blocks **2** and **3** in addition to the binding features of macrocyle (**3**)$_4$ to 1,4-butane diammonium ions reported in Paragraph 4.1.5, prompted us to examine the ability of this DCL to selectively amplify different macrocyclic receptors upon exposure to a range of individual α,ω-diaminetemplates, depending on the complementarity between the chain lengths of the α,ω-diamines and the cavity sizes of the macrocycles.

The generated macrocyles are of different cavity sizes, carry different numbers of carboxylate groups and work in near physiological conditions. Therefore, they may lead to selective binding of α,ω-diamines presumed to be protonated under the DCL conditions (pK_A > 9.9).[20] Moreover, the fact that the DCL generates several receptors, in principle, each with a particular preference, may lead to efficiency in binding a range of diamine guest. This aspect is rarely observed with the individually reported receptors (see 4.1.4). The generated receptors feature carboxylate groups which are suitable for hydrogen bonding and electrostatic interactions with the terminal protonated amino groups of α,ω-diamines. While purely electrostatic recognition of diammonium cations by a given receptor is rather non-specific, increasing the total charge of the interacting receptor (*i.e.* from (**2**)$_4$ to (**3**)$_4$) should increase its affinity towards the diammonium ion guests.[40] The hydrophobic cavities of the receptors are of different sizes and therefore are suitable for hydrophobic interactions with the hydrocarbon chains of α,ω-diamines. Such a combination of electrostatic and hydrophobic interactions has been reported for the binding of steroidal polyamines to DNA.[41]

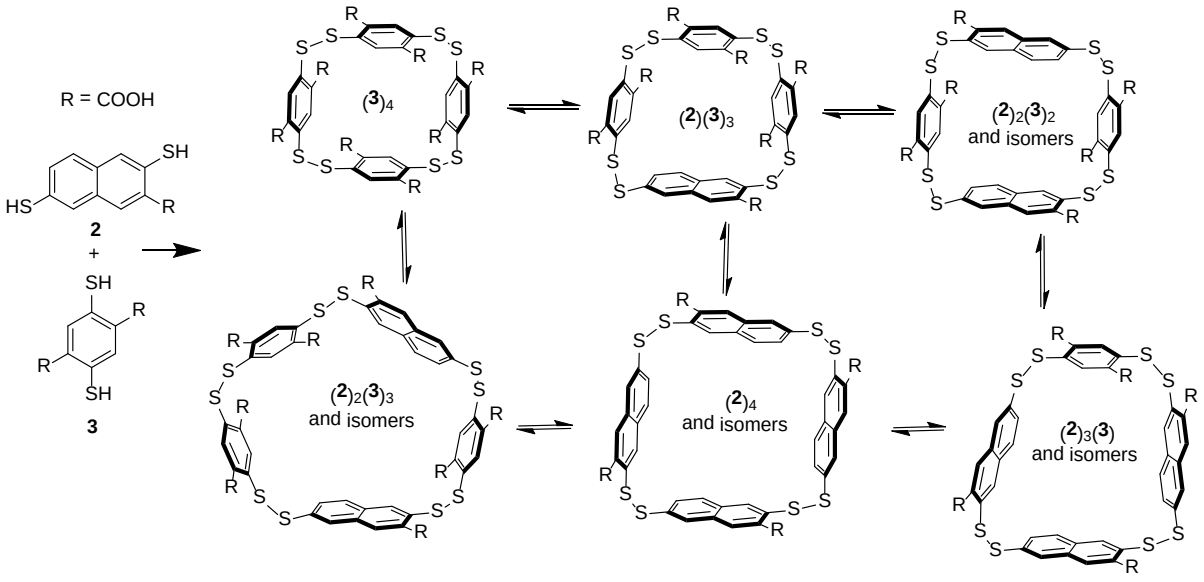

Scheme 4.2: Macrocycles $(\mathbf{3})_4$, $(\mathbf{2})(\mathbf{3})_3$, $(\mathbf{2})_2(\mathbf{3})_2$, $(\mathbf{2})_3(\mathbf{3})$, $(\mathbf{2})_4$ and $(\mathbf{2})_2(\mathbf{3})_3$ generated in a DCL made from building blocks **2** and **3** and listed in order of increasing size.

Finally, DCC has proved to generate receptors with affinities of up to 10^7 M^{-1} for many biomolecules in near physiological conditions.[42] This prompted us to use DCC as a tool to obtain receptors of potentially high affinity for α,ω-diamines in near physiological conditions.

4.2 DCL studies

In the third chapter of this dissertation, we have reported that exposing simple DCLs made from only building block **2** or only building block **3** to diverse amine and ammonium ion templates has resulted in the amplification of receptors $(\mathbf{2})_4$ and $(\mathbf{3})_4$, respectively. If these two DCLs amplify, again, these receptors upon exposure to individual α,ω-diamine templates, the resulting pattern of variation of AFs of $(\mathbf{2})_4$ and $(\mathbf{3})_4$ may reflect features of the interactions between the α,ω-diamines and receptors $(\mathbf{2})_4$ and $(\mathbf{3})_4$. Consequently, this may also help to interpret the effects of α,ω-diamine templates on a DCL made by mixing building blocks **2** and **3** which generates macrocyles $(\mathbf{2})(\mathbf{3})_3$, $(\mathbf{2})_2(\mathbf{3})_2$, $(\mathbf{2})_3(\mathbf{3})$, $(\mathbf{2})_2(\mathbf{3})_3$, in addition to $(\mathbf{2})_4$ and $(\mathbf{3})_4$.
Thus, before studying the effects of α,ω-diamine templates of n = 2-9 on a DCL made from combination of building blocks **2** and **3**, we first studied the effects of this series of templates on DCLs made from only building block **2** or **3**.

4.2.1 Methodology of data analysis

All the studied DCLs were prepared in 50 mM borate buffer at pH = 8-8.5 following standard protocols (see experimental section, paragraph 4.4.1), and analyzed after reaching equilibrium (after three to four days) using an HPLC-UV system. HPLC-UV peak areas of library members in each of the prepared DCLs were converted into regular amplification factors (AF). This allows us to compare the effects of a particular α,ω-diaminetemplate on the various DCL members. In the current work the template concentrations were adjusted to stoichiometric levels. The ratio template to building block in DCLs made from one building block is 1:4 *i.e*. 1:1 template to tetramer ratio, and the ratio template to building blocks in DCLs made from the two building blocks is adjusted to 1:8 *i.e.* 1:1 template to homotetramer ratio.

Ideally, templating the DCLs at stoichiometric level instead of substoichiometric level should not alter the correlation between host-guest binding affinities and host AFs.[43] However due to overoxidation of dithiol building blocks **2** and **3** in solution, the amounts of these building blocks are reduced while the amounts of templates are, ideally, constant. This affects the ratio of template to building blocks in favor of the template and therefore under such conditions the best binder is not necessarily the most amplified among the library members[44] (this notion is discussed in more details in the introduction of chapter 5).
The ratio of template to building block in a DCL showing more than one amplified library member was calculated after taking into account the amounts of overoxidized building block(s) (**2** and/or **3**). Then, the amplifications of the library members are assessed to determine if these are the result of potential affinity to the added template, or liberation of building block that does not mainly constitute the strong binder(s). In order to achieve this, the DCL is prepared at different ratios of template to building block, and the library member with the less reduced amplification upon lowering the ratio of template to building block to a stoichiometric level is counted as the potentially best binder. Moreover, the individual amounts of building blocks **2** and **3** taken up in the different library members were calculated as this may help to identify the liberated building block (this notion is discussed in more details in Paragraph 4.2.4).

4.2.2 Effect of α,ω-diamine templates on a DCL made from building block 3

We proceeded to prepare a series of DCLs made from 2.0 mM of building block **3** in the absence of a template and presence of 0.50 mM of individual α,ω-diamine templates of n = 2-9. HPLC-UV analyses showed that exposing the DCL to the templates amplified exclusively receptor $(\mathbf{3})_4$, while the rest of the library members i.e. $(\mathbf{3})_3$ and $(\mathbf{3})_5$ acted as monomer reservoirs (Figure 4.12). Specifically, exposing the DCL to template **4.3** of n = 4 results in a more pronounced amplification of $(\mathbf{3})_4$ (AF = 6.6) as compared to its amplifications upon exposing the DCL to the remaining templates (AF = 3-6.2) (Table 4.3). A relationship between the AF of $(\mathbf{3})_4$ and the lengths of the templates was observed, where the further n differs from 4 the smaller is the AF of $(\mathbf{3})_4$.
The data obtained supports our thoughts in Paraghraph 4.1.5 that template **4.3** of n = 4 is of complementary length to the cavity of receptor $(\mathbf{3})_4$ located between the carboxylate groups engaged in binding the central protonated amines of **3.1**. Although the hydrophobic contribution in the binding between α,ω-diamines and receptors $(\mathbf{3})_4$ is potentially higher for the diamines of lengths n ≥ 4 compared to the diamines of lengths shorter than n = 4, the decrease in AF of $(\mathbf{3})_4$ is less pronounced in case of the latter as compared to the former (Figure 4.14). Therefore, we speculate that receptor $(\mathbf{3})_4$ has a relative flexible structure allowing diamines of lengths shorter than n = 4 to be accommodated inside the cavity of $(\mathbf{3})_4$. However, it appears that diamines of lengths longer than n = 4 are not readily accommodated inside the cavity of the receptor, presumably due to geometrical constraints.

Table 4.3: Summary of the results of exposing a DCL made from 2.0 mM of building block **3** in 50 mM borate buffer to individual α,ω-diamine templates (0.50 mM) of n = 2-9. The table describes for each library member: the range of added guests, the range of AF values, the AF values as a function of the added templates and the relationship, if it exists, between the lengths of the templates and the AFs of the hosts.

Receptor	Range of guests (n =)	Range of AF values	AFs for different guests with values for n between brackets	Relationship between AF and n

$(\mathbf{3})_4$	n = 2-9	3-6.6	5.9 (2), 6.2 (3) and 6.6 (4)	if n ↗ AF ↗ (for n < 4)
			6.6 (4), 6.1 (5), 4.8 (6), 4.3 (7), 4 (8) and 3 (9)	if n ↗ AF ↘ (for n > 4)
$(\mathbf{3})_3$	n = 2-9	0.1-0.3	n. a.[a]	n. a.[a]
$(\mathbf{3})_5$	n = 2-9	0-1	n. a.[a]	n. a.[a]

[a] = no amplification (AF ≤ 1)

4.2.3 Effect of aliphatic α,ω-diamine templates on a DCL made from 2

A series of DCLs made from 2.0 mM of building block **2** were prepared in the absence of a template and presence of 0.50 mM of individual α,ω-diamine templates of n = 2-9. Similarly to the case of a DCL made from **3**, HPLC-UV analyses showed that exposing the DCL to the templates induced the amplification of only one receptor, in this case $(\mathbf{2})_4$, while the [2]-catenane acted as a monomer reservoir, as expected (Figure 4.13). Exposing the DCL to the longest template of n = 9 leads to the maximum amplification of $(\mathbf{2})_4$ (AF = 8.3) compared to all other templates (Table 4.4). A relationship between the AF of $(\mathbf{2})_4$ and the lengths of the templates was observed, where the shorter the length of the template is, the smaller is the induced AF of $(\mathbf{2})_4$ (Figure 4.14). Adding templates of lengths n < 6 amplified almost equally and slightly receptor $(\mathbf{2})_4$ (AF ≈ 1.2), while adding templates of lengths longer than n = 9 caused precipitation in the DCL. While the precipitation prevented the identification of the diamine guest of potential complementarity with receptor $(\mathbf{2})_4$, the data obtained suggests that a template of n = 9 is better complementary to the binding preferences of $(\mathbf{2})_4$ than the rest of the studied templates. We speculate that α,ω-diamines of n > 6 are of lengths allowing simultaneous coordination of the two ammonium groups to two carboxylate groups located at the molecular framework of receptor $(\mathbf{2})_4$ and thereby are potentially threaded through the hydophobic cavity of $(\mathbf{2})_4$. This aspect appears not to occur with the relatively short α,ω-diamines of n < 6. The dramatic jump in amplification of $(\mathbf{2})_4$ between alkanediammonium ion templates of n = 5 and n = 6 leads us to a conclusion that at least six methylene units are needed for an alkanediammonium ion guest to allow simultaneous coordination of the two ammonium ions with two carboxylate at the opposite ends of $(\mathbf{2})_4$. The amplification is enhanced by 3.1 times by simply adding a single methylene to pentanediammonium ions.

Table 4.4: Summary of the results of exposing a DCL made from 2.0 mM of building block **2** in 50 mM borate buffer to individual α,ω-diamine templates (0.50 mM) of n = 2-9. The table describes for each library member: the range of added guests, the range of AF values, the AF values as a function of the added templates and the relationship, if it exists, between the lengths of the template and the AF of the host.

Library member	Range of guests (n =)	Range of AF values	AFs for different guests with values for n between brackets	Relationship between AF and n
$(\mathbf{2})_4$	n = 2-9	1.2-8.3	1.2 (2), 1.2 (3), 1.2 (4), 1.3 (5), 4 (6), 5.2 (7), 6.2 (8) and 8.3 (9)	if n ↗ AF ↗ (for n > 4)
$(\mathbf{2})_4$-$(\mathbf{2})_4$	n = 2-9	0.2-1	n. a.[a]	n. a.[a]

[a] = no amplification (AF ≤ 1)

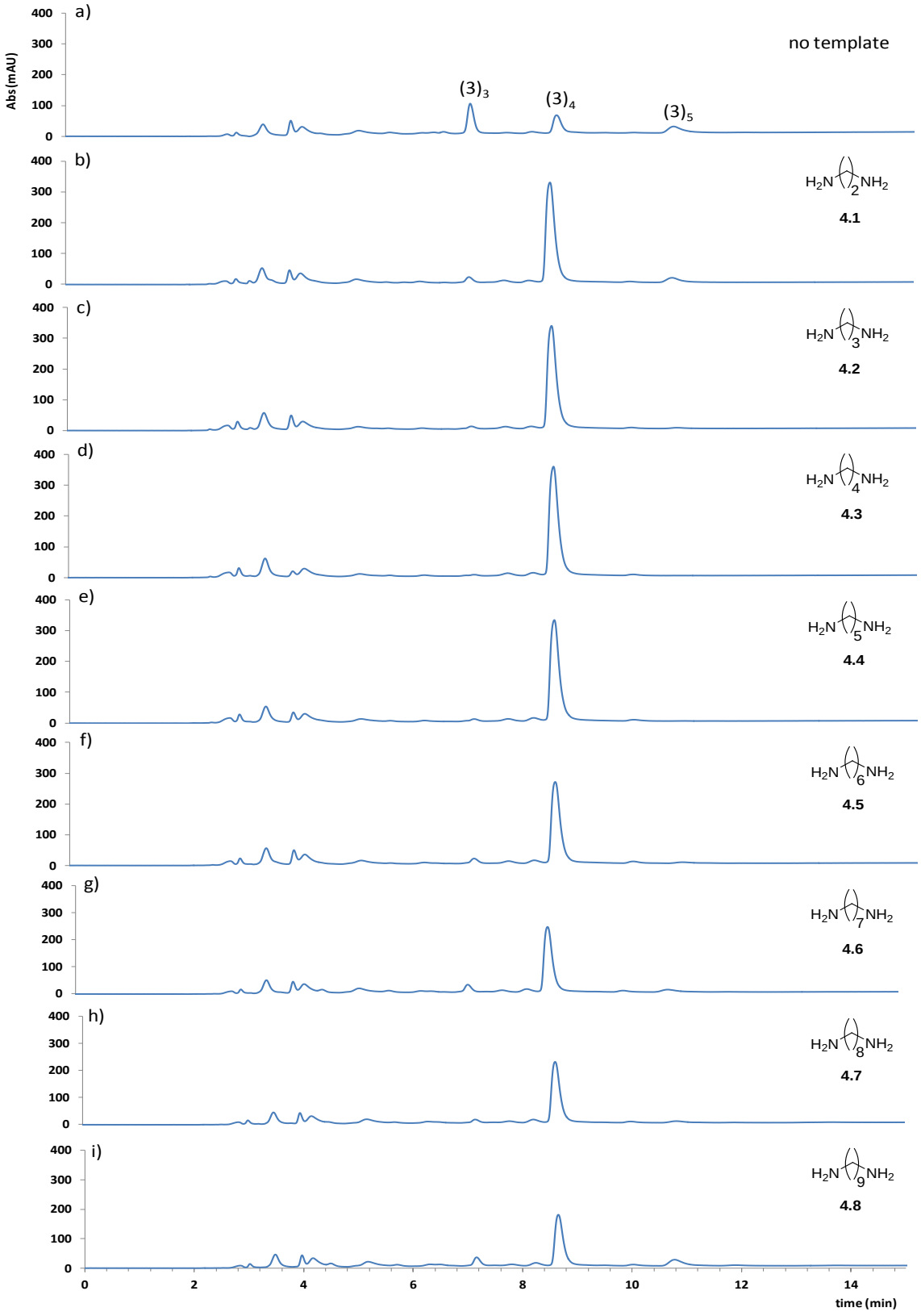

Figure 4.12: HPLC-UV chromatograms (λ_{abs} = 280 nm, λ_{ref} = 550 nm) of DCLs prepared in borate buffer (50 mM, pH 8-8.5) and composed of 2.0 mM of building blocks **3** (a) in the absence of a template and in

the presence of 0.50 mM of individual α,ω-diaminetemplates: (b) **4.1** (n = 2), (c) **4.2** (n = 3), (d) **4.3** (n = 4), (e) **4.4** (n = 5), (f) **4.5** (n = 6), (g) **4.6** (n = 7), (h) **4.7** (n = 8) and (i) **4.8** (n = 9).

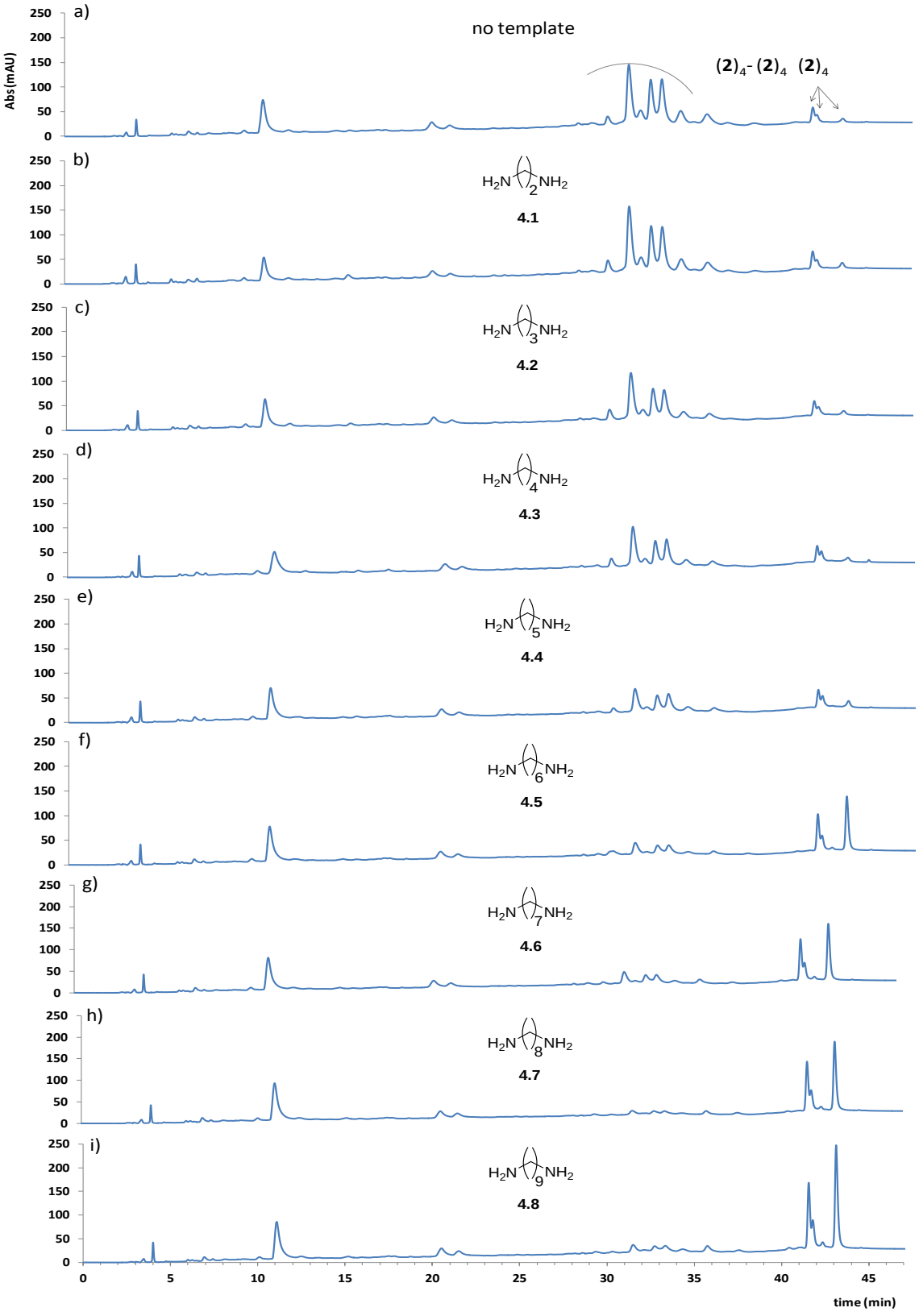

Figure 4.13: HPLC-UV chromatograms (λ_{abs} = 280 nm, λ_{ref} = 550 nm) of DCLs prepared in borate buffer (50 mM, pH 8-8.5) and composed of 2.0 mM of building blocks **2** (a) in the absence of a template and in the presence of 0.50 mM of individual α,ω-diaminetemplates: (b) **4.1** (n = 2), (c) **4.2** (n = 3), (d) **4.3** (n = 4), (e) **4.4** (n = 5), (f) **4.5** (n = 6), (g) **4.6** (n = 7), (h) **4.7** (n = 8) and (i) **4.8** (n = 9).

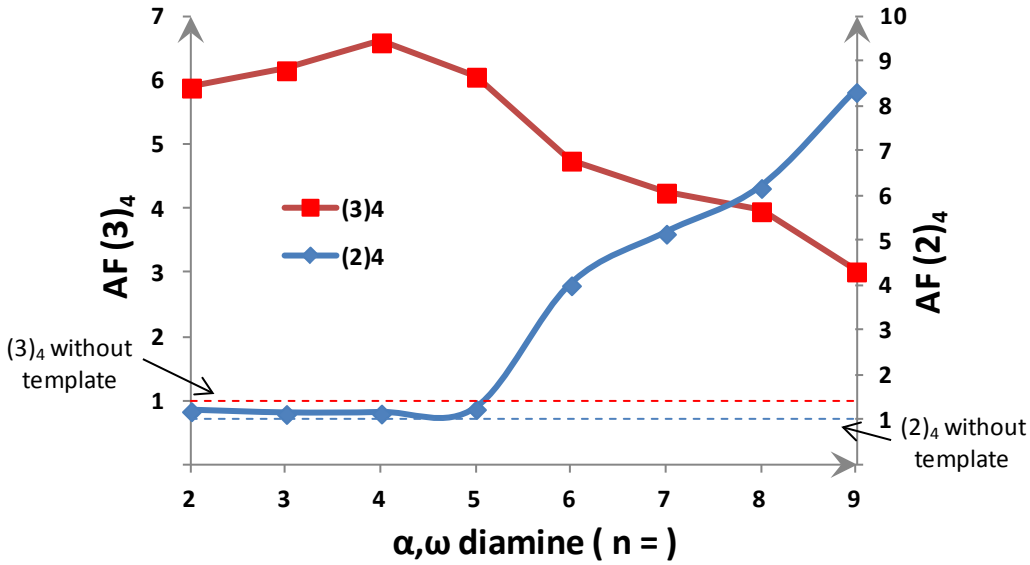

Figure 4.14: Variation of the AFs of $(\mathbf{2})_4$ and $(\mathbf{3})_4$ for different α,ω-diamine templates of n = 2-9 (0.50 mM for each) in DCLs made from building blocks **2** (2.0 mM) or **3** (2.0 mM), respectively. The DCLs were prepared in 50 mM borate buffer at pH = 8-8.5.

4.2.4 Effect of aliphatic α,ω-diamine templates on a DCL made from 2 and 3

A series of DCLs made from equimolar amounts of building blocks **2** and **3** (5.0 mM in total) were prepared in the absence of a template and in the presence of 0.625 mM of individual α,ω-diamine templates of n = 2-9. HPLC-UV analyses showed that exposing the DCL to the templates results in the amplification of more than one library member (Figure 4.15). Thus, we first compared the effects of particular α,ω-diamine templates on the various DCL members to reveal which of these library members is most amplified by a particular α,ω diamine. Afterwards, we compared the effects of the α,ω-diamine templates on particular DCL members to reveal the template preferences of the individual library member.

4.2.4.1 Effects of particular α,ω-diamine templates on the various DCL members

Templates of n = 2-4

Upon exposing the DCL to α,ω-diamine templates of n = 2, 3 and 4 (Table 4.5), 49 %, 76.4 % and 84.4 % of building block **3**, respectively, was taken up in small macrocycles ($(\mathbf{3})_4$ and $(\mathbf{2})(\mathbf{3})_3$) (Table **4.11**) whilst macrocyle $(\mathbf{2})_2(\mathbf{3})_2$ showed a gradual decrease in AF from 0.9 (n = 2) to 0.4 (n = 4) (Table 4.5). This liberated building block **2** and therefore facilitated the amplification of $(\mathbf{2})_4$ and, more interestingly, the amplification of $(\mathbf{2})_4$-$(\mathbf{2})_4$, which is rarely observed thus far (Table 4.7). This amplification further supports the notion that the amplification of $(\mathbf{2})_4$ is not necessarily driven by its affinity for the diamine templates of n = 2-4.

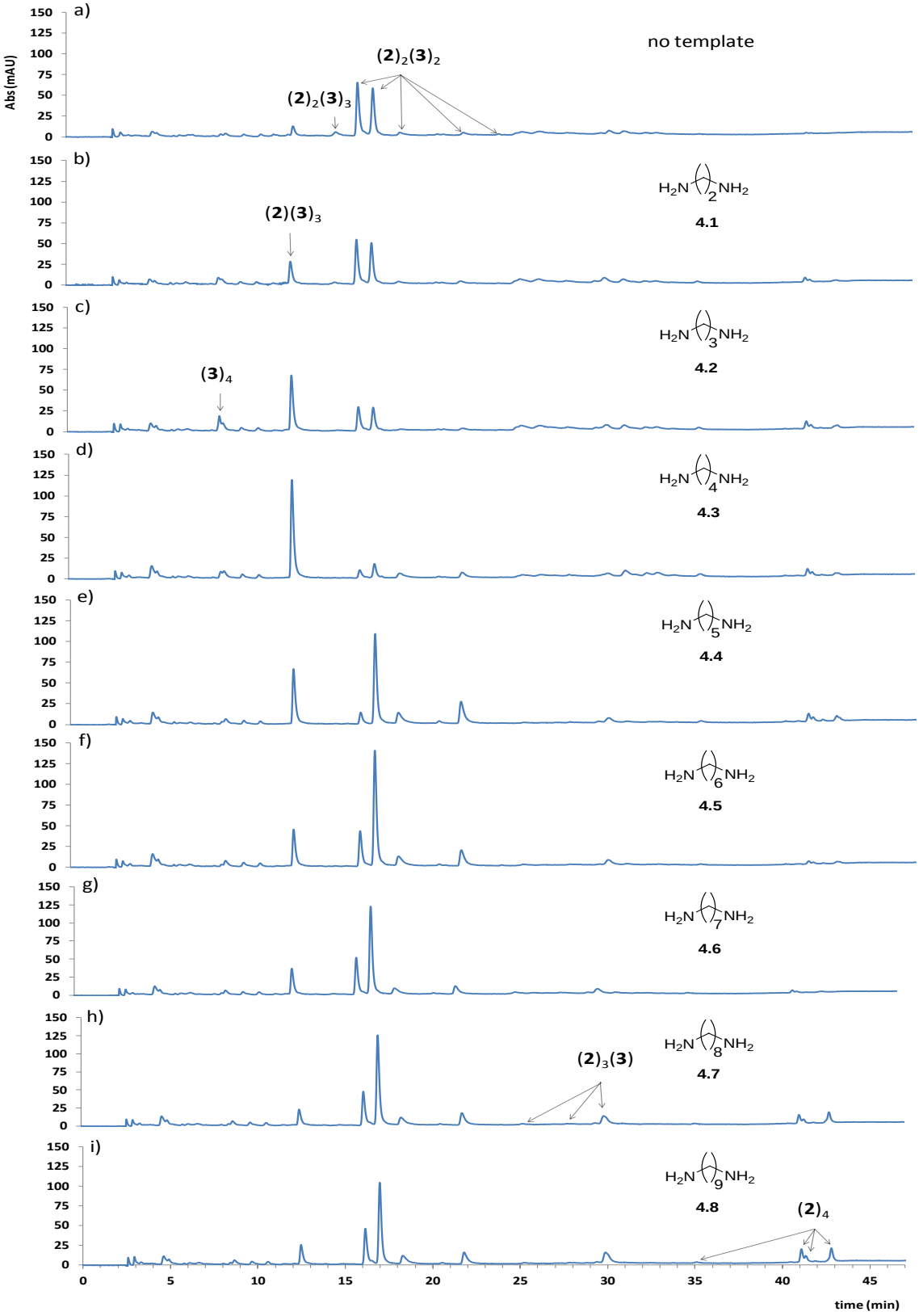

Figure 4.15: HPLC-UV chromatogram (λ_{abs} = 260 nm, λ_{ref} = 550 nm) of a DCL prepared in borate buffer (50 mM, pH 8-8.5) and composed of (a) equimolar amounts of building blocks **2** and **3** (5 mM in total) in the absence of a template and in the presence of 0.625 mM of individual α,ω-diaminetemplates: (b) **4.1** (n

= 2), (c) **4.2** (n = 3), (d) **4.3** (n = 4), (e) **4.4** (n = 5), (f) **4.5** (n = 6), (g) **4.6** (n = 7), (h) **4.7** (n = 8) and (i) **4.8** (n = 9). Samples taken from the DCL solutions were diluted with 200% volume DMSO immediately prior to HPLC analyses.

The driving force for catenation is avoiding unfavorable exposure of the hydrophobic interior of $(\mathbf{2})_4$ to water that happens in the absence of a good template for $(\mathbf{2})_4$.[43d] Note that increasing the template to homotetramer ratio from 1:1 to 2:1 did not decrease the amplification of the catenanes (Table 4.8), and therefore this also supports the notion that the amplification of $(\mathbf{2})_4$ is not driven by its affinity for the diamine templates of n = 2-4. Moreover, upon lowering the template to homotetramer ratio from 2:1 to 1:1 in DCLs templated with the diamines of n = 3 and 4, the amplification of $(\mathbf{2})_4$ is reduced by a factor of 2.4 and 2.7 respectively, however the amplification of $(\mathbf{2})(\mathbf{3})_3$ stayed almost the same (Table 4.8). In the case of a DCL templated with diamine of n = 2, lowering the above-mentioned ratio to 1:1 equally reduced the amplifications of $(\mathbf{2})_4$ and $(\mathbf{2})(\mathbf{3})_3$ by a factor of 1.6. As a result, the data obtained suggest that macrocyle $(\mathbf{2})(\mathbf{3})_3$ is the stronger binder of the diamine templates of n = 2-4.

Template of n =5

Upon addition of the template with n = 5 to the DCL, 49.9 % of building block **3** is taken up in the small macrocycles (Table **4.11**). This liberates building block **2** and facilitates the amplification of $(\mathbf{2})_4$ (Table 4.5). Moreover, upon lowering the template to homotetramer ratio from 2:1 to 1:1, the amplification of $(\mathbf{2})_4$ is reduced by a factor of 3.1, however the amplification of $(\mathbf{2})(\mathbf{3})_3$ is reduced by a factor of 1.4 only (Table 4.8). This suggests that the template with n = 5 has a higher affinity for $(\mathbf{2})(\mathbf{3})_3$ than for $(\mathbf{2})_4$.

Table 4.5: Amplification factors (AF) of the tetrameric macrocycles upon addition of 0.625 mM of individual α,ω-diamine templates to a DCL made from equimolar amounts of **2** and **3** (5.0 mM in total). DCLs were prepared in 50 mM borate buffer at pH=8.4.

Host size →

Guest size ↓

Template	$(\mathbf{3})_4$	$(\mathbf{2})(\mathbf{3})_3$	$(\mathbf{2})_2(\mathbf{3})_2$	$(\mathbf{2})_3(\mathbf{3})$	$(\mathbf{2})_4$
(no template)	1.0	1.0	1.0	1.0	1.0
4.1 (n = 2)	2.0	**2.3**	0.9	2.0	**3.9**
4.2 (n = 3)	3.6	**5.8**	0.5	1.8	**6.1**
4.3 (n = 4)	2.3	**9.9**	0.4	1.1	**6.4**
4.4 (n = 5)	1.3	**5.6**	1.4	1.0	**9.2**
4.5 (n = 6)	1.4	**3.9**	1.8	1.2	**4.0**
4.6 (n = 7)	1.3	**3.2**	1.6	1.6	**3.0**
4.7 (n = 8)	1.2	**2.0**	1.7	2.0	**10.8**
4.8 (n = 9)	1.1	**2.2**	1.5	2.1	**13.5**

Templates of n =6-7

Exposing the DCL to the diamine templates of n = 6 and 7 has amplified, almost equally, $(\mathbf{2})(\mathbf{3})_3$ and $(\mathbf{2})_4$. Upon lowering the template to homotetramer ratio from 2:1 to 1:1, the amplification of $(\mathbf{2})_4$ is reduced by a factor of 2.7 and 2.5, respectively. However the amplification of $(\mathbf{2})(\mathbf{3})_3$ is increased by a factor of 1.3 and 1.5, respectively. This suggests that $(\mathbf{2})(\mathbf{3})_3$ is the best binder of the diamine templates of n = 6-7.

Templates of n =8-9

The amplification data for templates of n = 7 and n = 8 point towards $(\mathbf{2})_4$ as their best binder.

In conclusion, exposing the DCL to α,ω-diamine templates has predominantly led to the amplification of macrocyclic hosts (**2**)(**3**)$_3$ and (**2**)$_4$ (see the values in bold in Table 4.5). The amplification is selective and probably depends on the complementarity between the chain lengths of the diamines and the cavity sizes of the hosts. Where the shorter α,ω-diamines of n = 2-7 induced the amplification of the relatively small macrocycle (**2**)(**3**)$_3$, the longest α,ω-diamines of n = 8-9 induced the amplification of the relatively bigger macrocycles (**2**)$_4$. The relationship between α,ω-diaminelengths and the order of amplifications of the hosts is discussed in 4.2.4.2.

4.2.4.2 Effects of the α,ω-diamine templates on particular DCL members

We also envisaged comparing the effects of the diamine templates on particular DCL members as this reflects, from another perspective, the complementarity between the chain lengths of the templates and the cavity sizes of the receptors. Results show that exposing the mixed DCL to templates of n = 3, n = 4, n = 6 and n = 9 gives more pronounced amplification of (**3**)$_4$, (**2**)(**3**)$_3$, (**2**)$_2$(**3**)$_2$, (**2**)$_3$(**3**) and (**2**)$_4$, respectively, in comparison to their amplifications upon exposing the DCL to the remaining templates (see the underlined values of Table 4.5). A relationship was observed between AFs of (**3**)$_4$ and (**2**)(**3**)$_3$, and the lengths of the templates. Where the further the n values differ from 3 and 4 the smaller are the AFs of (**3**)$_4$ and (**2**)(**3**)$_3$, respectively (Figure 4.16).

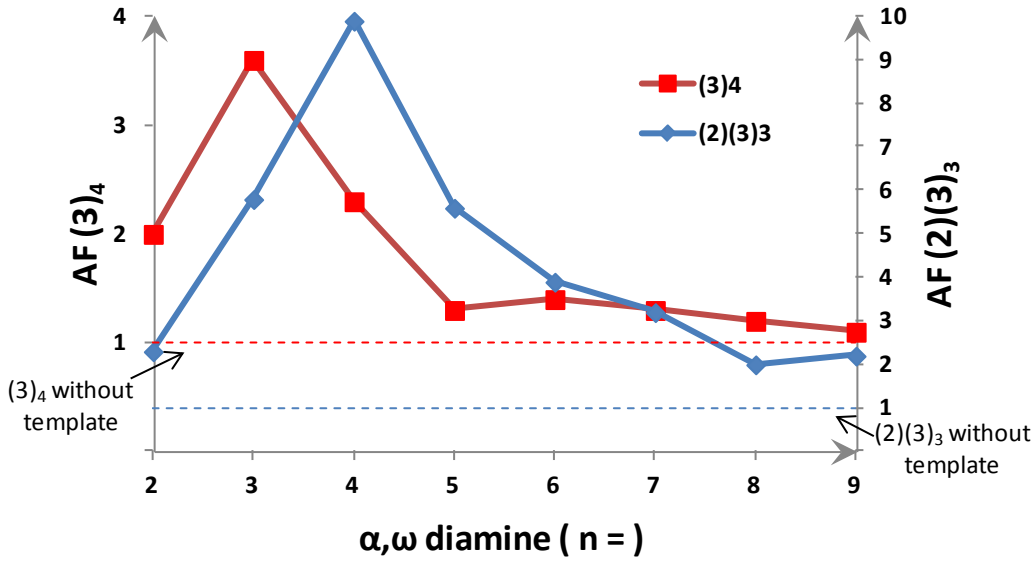

Figure 4.16: Variation of the AFs of (**3**)$_4$ and (**2**)(**3**)$_3$ as a function of addition of α,ω-diamine templates of n = 2-9 (0.625 mM for each) to DCLs made from equimolar amounts of building blocks **2** and **3** (5.0 mM in total). The DCLs were prepared in 50 mM borate buffer at pH = 8.4.

In contrast to receptors (**3**)$_4$ and (**2**)(**3**)$_3$ mainly made from building block **3**, a more complex relationship was observed between the AFs of receptors mainly made from building block **2** *i.e.* (**2**)$_2$(**3**)$_2$, (**2**)$_3$(**3**) and (**2**)$_4$ and the lengths of the templates (Figure 4.17-Figure 4.18).

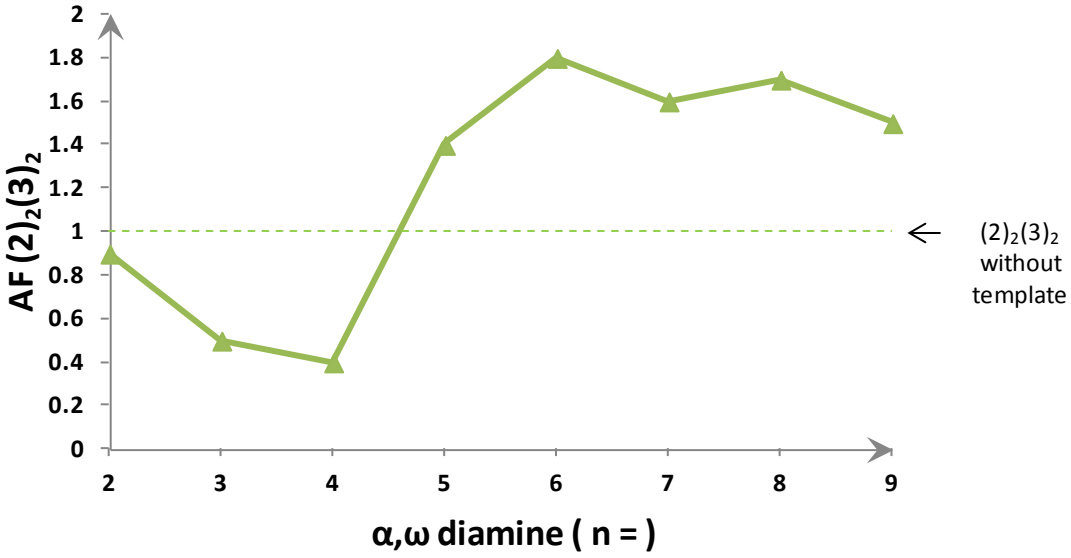

Figure 4.17: Variation of the AFs of $(\mathbf{2})_2(\mathbf{3})_2$ as a function of addition of individual α,ω-diamine templates of n = 2-9 (0.625 mM for each) to DCLs made from equimolar amounts of building blocks **2** and **3** (5.0 mM in total). The DCLs were prepared in 50 mM borate buffer at pH = 8.4.

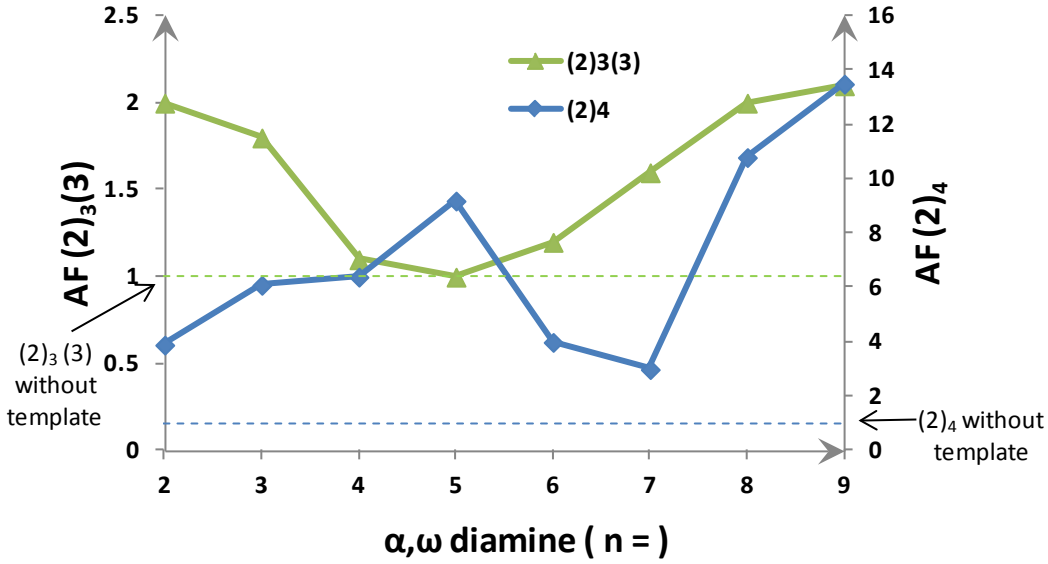

Figure 4.18: Variation of the AFs of $(\mathbf{2})_3(\mathbf{3})$ and $(\mathbf{2})_4$ as a function of addition of α,ω-diamine templates of n = 2-9 (0.625 mM for each) to DCLs made from equimolar amounts of building blocks **2** and **3** (5.0 mM in total). The DCLs are prepared in 50 mM borate buffer at pH = 8.4.

This is due to the fact that upon exposing the DCLs to templates of n = 2-5, large proportions of building block **3** (49 % - 84.4 %) were taken up in small macrocycles ($(\mathbf{3})_4$ and $(\mathbf{2})(\mathbf{3})_3$), and therefore the apparent amplifications of $(\mathbf{2})_3(\mathbf{3})$ and $(\mathbf{2})_4$ were most likely driven by the liberation of building block **2** rather than intrinsic affinities towards these templates (see paragraph 4.2.4.1). The consumption of building block **3** in DCLs with templates of n = 2-5 also affected the amplification of $(\mathbf{2})_2(\mathbf{3})_2$.

In summary, using DCC we were able to generate five macrocyclic hosts of different sizes suitable to bind with some selectively, under near physiological conditions, α,ω-diamines of

different chain lengths, depending on the complementarity between the chain lengths of the diamines and the cavity sizes of the receptors.

4.3 Conclusion

To the best of our knowledge, only one DCL system similar to the one described here was reported by Klein *et al.*,[45,46] where exposing a hydrazone DCL to divalent metal ions of different sizes as templates, has resulted in the selective amplification of different library members depending on the complementarity between the template sizes and the amplified host sizes.

4.4 Experimental section

4.4.1 Methods of preparation of DCLs

Templates **4.1**, **4.2**, **4.3**, **4.4**, **4.5**, **4.6**, **4.7** and **4.8** were purchased from Sigma-Aldrich. Stock solutions of individual building blocks **2** and **3** and the used templates were freshly prepared at 10 mM concentration by dissolving the appropriate amounts of **2**, **3** and the individual templates in 50 mM borate buffer at pH 8-8.5. The pH was readjusted to 8-8.5 by addition of an appropriate volume of a 1 M solution of KOH.
For the untemplated libraries made from 2.0 mM of individual building blocks **2** or **3**, 40 µl of the stock solutions of building blocks **2** or **3** were combined with 160 µl of a borate buffer solution (50 mM borate buffer at pH 8-8.5) in HPLC vials.
For the templated libraries made from 2.0 mM of individual building blocks **2** or **3** and 0.50 mM of individual diamine templates, 40 µl of the stock solutions of building blocks **2** or **3** and 10 µl of the appropriate stock solution of the templates were combined with 150 µl of a borate buffer solution (50 mM, pH 8-8.5) in HPLC vials.
For the untemplated library made from equimolar amounts of building blocks **2** and **3** at 5.0 mM overall building block concentration, 50 µl of each of the stock solutions of the two building blocks were combined with 100 µl of a borate buffer solution (50 mM borate buffer at pH 8-8.5) in an HPLC vial.
For the templated libraries made from equimolar amounts of building blocks **2** and **3** at 5.0 mM overall building block concentration and 0.625 mM of each of the diamine templates, 50 µl of each of the stock solutions of the two building blocks and 12.5 µl of the stock solutions of each of the templates were combined with 87.5 µl of a borate buffer solution (50 mM, pH 8-8.5) in HPLC vials.
The DCL mixtures were allowed to oxidize and equilibrate by stirring for 4 days in closed vials at room temperature. For DCLs that were diluted with DMSO, each of the vials was manually shaken immediately before taking 10 µl samples using an Eppendorf pipette. These 10 µl solutions were diluted with 200% volume DMSO in HPLC vials immediately prior to HPLC-UV analyses.

4.4.2 HPLC analysis conditions

Acetonitrile was purchased from Biosolve. Formic acid was purchased from Sigma-Aldrich. Analyses were performed using a reversed phase HPLC column (Kromasil C8, 4.6 x 150 mm, 5 µm), a flow rate of 1 mL/min of acetonitrile in doubly distilled water (both containing 0.1% formic acid) and following the HPLC gradient shown below. In case of DMSO diluted samples, a volume of 3 µL was injected. In case of the undiluted samples, a volume of 10 µL was injected.

Time (min)	Acetonitrile (%)
0	30
5	40
30	70
35	70
40	95
50	95
55	30

HPLC-UV chromatograms of the diluted samples were monitored at λ_{abs} = 260 nm (λ_{ref} = 550 nm) while the HPLC-UV chromatograms of the undiluted samples were monitored at λ_{abs} = 280 nm (λ_{ref} = 550 nm).

4.4.3 HPLC-UV peak areas (mAU·min) and AFs of the DCL members formed from the combination of building blocks 2 and 3

Table 4.6: HPLC-UV peak areas of library members in DCLs made from equimolar amounts of building blocks **2** and **3** (5.0 mM in total) in borate buffer (50 mM, pH 8-8.5) (a) in the absence of a template and in the presence of 0.625 mM of individual α,ω-diamines of n equals to (b) 2, (c) 3, (d) 4, (e) 5, (f) 6, (g) 7, (h) 8 and (i) 9. Samples taken from the DCL solutions were diluted with 200% volume DMSO immediately prior to HPLC analyses

DCL	Template	(**3**)$_4$	(**2**)(**3**)$_3$	(**2**)$_2$(**3**)$_2$	(**2**)$_3$(**3**)	(**2**)$_4$	(**2**)$_2$(**3**)$_3$	(**2**)$_3$(**3**)-(**2**)$_4$	(**2**)$_4$-(**2**)$_4$
(a)	(no template)	78	143	1593	202	42	101	378	152
(b)	**4.1** (n = 2)	156	325	1377	401	164	55	410	198
(c)	**4.2** (n = 3)	278	828	811	364	258	30	372	268
(d)	**4.3** (n = 4)	179	1417	644	227	270	0	221	449
(e)	**4.4** (n = 5)	104	796	2279	204	385	0	37	81
(f)	**4.5** (n = 6)	113	557	2816	249	166	0	37	84
(g)	**4.6** (n = 7)	100	460	2487	324	128	0	96	95
(h)	**4.7** (n = 8)	96	285	2632	410	454	0	0	50
(i)	**4.8** (n = 9)	84	313	2322	415	565	0	0	0

Table 4.7: Amplification factors (AFs) of library members in DCLs made from equimolar amounts of building blocks **2** and **3** (5.0 mM in total) in borate buffer (50 mM, pH 8-8.5) (a) in the absence of a template and in the presence of 0.625 mM of individual α,ω-diamines of n equals to (b) 2, (c) 3, (d) 4, (e) 5, (f) 6, (g) 7, (h) 8 and (i) 9. Samples taken from the DCL solutions were diluted with 200% volume DMSO immediately prior to HPLC analyses

DCL	Template	(**3**)$_4$	(**2**)(**3**)$_3$	(**2**)$_2$(**3**)$_2$	(**2**)$_3$(**3**)	(**2**)$_4$	(**2**)$_2$(**3**)$_3$	(**2**)$_3$(**3**)-(**2**)$_4$	(**2**)$_4$-(**2**)$_4$
(a)	(no template)	1	1	1	1	1	1	1	1
(b)	**4.1** (n = 2)	2.0	2.3	0.9	2.0	3.9	0.5	1.1	1.3
(c)	**4.2** (n = 3)	3.6	5.8	0.5	1.8	6.1	0.3	1.0	1.8
(d)	**4.3** (n = 4)	2.3	9.9	0.4	1.1	6.4	0.0	0.6	3.0
(e)	**4.4** (n = 5)	1.3	5.6	1.4	1.0	9.2	0.0	0.1	0.5
(f)	**4.5** (n = 6)	1.4	3.9	1.8	1.2	4.0	0.0	0.1	0.6
(g)	**4.6** (n = 7)	1.3	3.2	1.6	1.6	3.0	0.0	0.3	0.6
(h)	**4.7** (n = 8)	1.2	2.0	1.7	2.0	10.8	0.0	0.0	0.3
(i)	**4.8** (n = 9)	1.1	2.2	1.5	2.1	13.5	0.0	0.0	0.0

Table 4.8: Amplification factors (AFs) of library members in DCLs made from equimolar amounts of building blocks **2** and **3** (5.0 mM in total) in borate buffer (50 mM, pH 8-8.5) (a) in the absence of a template and in the presence of 1.25 mM of individual α,ω-diamines of n equals to (b) 2, (c) 3, (d) 4, (e) 5, (f) 6, (g) 7, (h) 8 and (i) 9. Samples taken from the DCL solutions were diluted with 200% volume DMSO immediately prior to HPLC analyses

DCL	Template	(**3**)$_4$	(**2**)(**3**)$_3$	(**2**)$_2$(**3**)$_2$	(**2**)$_3$(**3**)	(**2**)$_4$	(**2**)$_2$(**3**)$_3$	(**2**)$_3$(**3**)-(**2**)$_4$	(**2**)$_4$-(**2**)$_4$
(a)	(no template)	1.0	1.0	1.0	1.0	1.0	1.0	1.0	1.0
(b)	**4.1** (n = 2)	3.1	3.5	0.9	2.0	6.3	0.6	1.5	1.7
(c)	**4.2** (n = 3)	3.1	5.6	0.3	1.5	14.5	0.0	1.2	1.8
(d)	**4.3** (n = 4)	2.1	9.4	0.4	0.9	17.1	0.0	0.5	2.2
(e)	**4.4** (n = 5)	0.9	4.4	1.0	0.8	16.3	0.0	0.0	0.0
(f)	**4.5** (n = 6)	1.2	3.1	1.8	2.4	10.7	0.1	0.0	0.0
(g)	**4.6** (n = 7)	1.5	2.2	2.0	2.2	7.5	0.1	0.0	0.0
(h)	**4.7** (n = 8)	1.4	2.9	1.3	2.6	27.5	0.2	0.0	0.0
(i)	**4.8** (n = 9)	1.6	2.7	1.1	3.7	41.0	0.2	0.0	0.0

Table 4.9: Maximum amplification factors (max AFs) that a library member can have in DCLs made from equimolar amounts of building blocks **2** and **3** (5.0 mM in total) in borate buffer (50 mM, pH 8-8.5) in the presence of individual α,ω-diamines of n equals to (a) 2, (b) 3, (c) 4, (d) 5, (e) 6, (f) 7, (g) 8 and (h) 9. Samples taken from the DCL solutions were diluted with 200% volume DMSO immediately prior to HPLC analyses.

DCL	Template	(**3**)$_4$	(**2**)(**3**)$_3$	(**2**)$_2$(**3**)$_2$	(**2**)$_3$(**3**)	(**2**)$_4$	(**2**)$_2$(**3**)$_3$	(**2**)$_3$(**3**)-(**2**)$_4$	(**2**)$_4$-(**2**)$_4$
(a)	**4.1** (n = 2)	10.4	14.4	2.3	20.0	89.8	32.9	8.6	24.8
(b)	**4.2** (n = 3)	10.4	14.4	2.3	20.0	89.8	32.9	8.6	24.8
(c)	**4.3** (n = 4)	10.4	14.4	2.3	20.0	89.8	32.9	8.6	24.8
(d)	**4.4** (n = 5)	10.4	14.4	2.3	20.0	89.8	32.9	8.6	24.8
(e)	**4.5** (n = 6)	10.4	14.4	2.3	20.0	89.8	32.9	8.6	24.8
(f)	**4.6** (n = 7)	10.4	14.4	2.3	20.0	89.8	32.9	8.6	24.8
(g)	**4.7** (n = 8)	10.4	14.4	2.3	20.0	89.8	32.9	8.6	24.8
(h)	**4.8** (n = 9)	10.4	14.4	2.3	20.0	89.8	32.9	8.6	24.8

4.4.4 Concentrations (mM) of the DCL members formed from the combination of building blocks 2 and 3

To convert the HPLC-UV peaks areas (mAU·min) of the DCL members to their corresponding concentrations (mM), we followed the methodology reported in Paragraph 3.3.2 (Chapter 3). The prepared DCLs were analyzed following the same conditions as used in the experiments

performed to determine the constants relating HPLC-UV peak areas of **2** and **3** to their corresponding concentrations, C_2 and C_3 respectively. Thus, 3 µL aliquots of the 200% DMSO diluted solutions were injected into the HPLC. Also, HPLC-UV chromatograms were recorded at λ_{abs} = 260 nm and λ_{ref} = 550 nm. This allowed us to use the following constants C_2 = 1508 mAU·min·mM^{-1} and C_3 = 323 mAU·min·mM^{-1}.

Table 4.10: Concentrations (mM) of library members and total concentration in library members (mM) made from individual building blocks **2** and **3** in DCLs prepared in borate buffer (50 mM, pH 8.4) and composed of equimolar amounts of building blocks **2** and **3** (5.0 mM in total) (a) in the absence of a template and in the presence of 0.625 mM of individual templates of n equals to (b) 2, (c) 3, (d) 4, (e) 5, (f) 6, (g) 7, (h) 8 and (i) 9. Samples taken from the DCL solutions were diluted with 200% volume DMSO immediately prior to HPLC analyses.

DCL	Template	(**3**)$_4$	(**2**)(**3**)$_3$	(**2**)$_2$(**3**)$_2$	(**2**)$_3$(**3**)	(**2**)$_4$	(**2**)$_2$(**3**)$_3$	(**2**)$_3$(**3**)-(**2**)$_4$	(**2**)$_4$-(**2**)$_4$	[**2**]	[**3**]
(a)	no template	0.06	0.06	0.44	0.04	0.01	0.03	0.04	0.01	1.47	1.44
(b)	**4.1** (n = 2)	0.12	0.13	0.38	0.08	0.03	0.01	0.04	0.02	1.66	1.79
(c)	**4.2** (n = 3)	0.22	0.41	0.22	0.08	0.04	0.01	0.04	0.02	1.61	2.44
(d)	**4.3** (n = 4)	0.14	0.57	0.18	0.05	0.04	0.00	0.02	0.04	1.68	2.69
(e)	**4.4** (n = 5)	0.08	0.32	0.62	0.04	0.06	0.00	0.00	0.01	2.02	2.58
(f)	**4.5** (n = 6)	0.09	0.23	0.77	0.05	0.03	0.00	0.00	0.01	2.11	2.62
(g)	**4.6** (n = 7)	0.08	0.19	0.68	0.07	0.02	0.00	0.01	0.01	1.95	2.3
(h)	**4.7** (n = 8)	0.07	0.12	0.72	0.08	0.08	0.00	0.00	0.00	2.14	2.16
(i)	**4.8** (n = 9)	0.07	0.13	0.63	0.09	0.09	0.00	0.00	0.00	2.03	1.99

Table 4.11: Percentage of building block **3** contained in different library members in DCLs prepared in borate buffer (50 mM, pH 8.4) and composed of equimolar amounts of building blocks **2** and **3** (5.0 mM in total) (a) in the absence of a template and in the presence of 0.625 mM of individual templates of n equals to (b) 2, (c) 3, (d) 4, (e) 5, (f) 6, (g) 7, (h) 8 and (i) 9. Samples taken from the DCL solutions were diluted with 200% volume DMSO immediately prior to HPLC analyses.

DCL	Template	(**3**)$_4$	(**2**)(**3**)$_3$	(**2**)$_2$(**3**)$_2$	(**2**)$_3$(**3**)	(**2**)$_4$	(**2**)$_2$(**3**)$_3$	(**2**)$_3$(**3**)-(**2**)$_4$	(**2**)$_4$-(**2**)$_4$	[**3**]
(a)	no template	16.8	12.1	60.5	2.9	0.0	5.3	2.4	0.0	100.0
(b)	**4.1** (n = 2)	27.0	22.0	42.0	4.6	0.0	2.3	2.1	0.0	100.0
(c)	**4.2** (n = 3)	35.3	41.1	18.2	3.1	0.0	0.9	1.4	0.0	100.0
(d)	**4.3** (n = 4)	20.6	63.8	13.1	1.7	0.0	0.0	0.8	0.0	100.0
(e)	**4.4** (n = 5)	12.5	37.4	48.3	1.6	0.0	0.0	0.1	0.0	100.0
(f)	**4.5** (n = 6)	13.4	25.8	58.8	2.0	0.0	0.0	0.1	0.0	100.0
(g)	**4.6** (n = 7)	13.5	24.2	59.0	2.9	0.0	0.0	0.4	0.0	100.0
(h)	**4.7** (n = 8)	13.7	15.9	66.4	3.9	0.0	0.0	0.0	0.0	100.0
(i)	**4.8** (n = 9)	13.0	19.0	63.6	4.3	0.0	0.0	0.0	0.0	100.0

Table 4.12: Percentage of building block **2** contained in different library members in DCLs prepared in borate buffer (50 mM, pH 8.4) and composed of equimolar amounts of building blocks **2** and **3** (5.0 mM in

total) (a) in the absence of a template and in the presence of 0.625 mM of individual templates of n equals to (b) 2, (c) 3, (d) 4, (e) 5, (f) 6, (g) 7, (h) 8 and (i) 9. Samples taken from the DCL solutions were diluted with 200% volume DMSO immediately prior to HPLC analyses.

DCL	Template	(**3**)$_4$	(**2**)(**3**)$_3$	(**2**)$_2$(**3**)$_2$	(**2**)$_3$(**3**)	(**2**)$_4$	(**2**)$_2$(**3**)$_3$	(**2**)$_3$(**3**)-(**2**)$_4$	(**2**)$_4$-(**2**)$_4$	[**2**]
(a)	no template	0.0	3.9	59.0	8.5	1.9	3.4	16.5	6.8	100.0
(b)	**4.1** (n = 2)	0.0	7.9	45.2	14.9	6.5	1.7	15.9	7.9	100.0
(c)	**4.2** (n = 3)	0.0	20.8	27.6	14.0	10.7	0.9	14.9	11.1	100.0
(d)	**4.3** (n = 4)	0.0	34.0	20.9	8.3	10.6	0.0	8.4	17.7	100.0
(e)	**4.4** (n = 5)	0.0	15.9	61.5	6.2	12.6	0.0	1.2	2.7	100.0
(f)	**4.5** (n = 6)	0.0	10.7	73.0	7.3	5.2	0.0	1.1	2.6	100.0
(g)	**4.6** (n = 7)	0.0	9.5	69.5	10.3	4.3	0.0	3.2	3.2	100.0
(h)	**4.7** (n = 8)	0.0	5.4	67.2	11.9	14.1	0.0	0.0	1.5	100.0
(i)	**4.8** (n = 9)	0.0	6.2	62.6	12.7	18.5	0.0	0.0	0.0	100.0

Table 4.13: Ratios of template to individual building blocks and template to library members calculated after taking into account the amounts of overoxidized building blocks **2** and **3**, in DCLs prepared in borate buffer (50 mM, pH 8.4) and composed of equimolar amounts of building blocks **2** and **3** (5.0 mM in total): in the presence of 0.625 mM of individual templates of n equals to (a) 2, (b) 3, (c) 4, (d) 5, (e) 6, (f) 7, (g) 8 and (h) 9. Samples taken from the DCL solutions were diluted with 200% volume DMSO immediately prior to HPLC analyses.

DCL	Template	(**3**)$_4$	(**2**)(**3**)$_3$	(**2**)$_2$(**3**)$_2$	(**2**)$_3$(**3**)	(**2**)$_4$	(**2**)$_2$(**3**)$_3$	(**2**)$_3$(**3**)-(**2**).	(**2**)$_4$-(**2**)$_4$	[**2**]	[**3**]
(a)	**4.1** (n = 2)	7:5	1:1	3:4	9:8	3:2	1:1	21:8	3:1	3:8	1:3
(b)	**4.2** (n = 3)	1:1	3:4	7:9	7:6	14:9	3:4	19:7	28:9	2:5	1:4
(c)	**4.3** (n = 4)	1:1	2:3	3:4	10:9	3:2	2:3	13:5	3:1	3:8	1:4
(d)	**4.4** (n = 5)	1:1	5:7	5:8	1:1	5:4	5:7	13:6	5:2	1:3	1:4
(e)	**4.5** (n = 6)	1:1	5:7	3:5	8:9	6:5	5:7	2:1	19:8	2:7	1:4
(f)	**4.6** (n = 7)	1:1	4:5	2:3	1:1	9:7	4:5	9:4	18:7	1:3	1:4
(g)	**4.7** (n = 8)	7:6	7:8	3:5	7:8	7:6	7:8	2:1	7:3	2:7	2:7
(h)	**4.8** (n = 9)	5:4	1:1	5:8	1:1	5:4	1:1	13:6	5:2	1:3	1:3

4.5 References

[1] Shah, P.; Swiatlo, E. *Mol. Microbiol.* **2008**, *68*, 4.
[2] Blagbrouh, I. S.; Carrington, S.; Geall, A. *J. Pharm. Pharmacol. Commun*. **1997**, *3*, 223.
[3] Gerner, E. W.; Meyskens, F. L. *Nat. Rev. Cancer* **2004**, *4*, 781.
[4] Thomas, T.; Thomas, T. *J. Cell. Mol. Life Sci.* **2001**, *58*, 244.
[5] Hölttä, E.; Pohjanpelto, P. *Biochem. J.* **1983**, *210*, 945.
[6] Hawel, L.; Tjandrawinata, R. R.; Fukumoto, G. H.; Byus, C. V. *J. Biol. Chem.* **1994**, 269, 7412.
[7] Horton, R. C.; Logan, S. D.; Wolstencroft, J. H. *Br. J. Pharmacol.* **1985**, *85*, 37.
[8] Alhonen-Hongisto, L.; Seppänen, P.; Hölttä, E.; Jänne, J. *Biochem. Biophys. Res. Commun.* **1982**, *106*, 291.
[9] Tabor, C. W.; Tabor, H. *Annu. Rev. Biochem*. **1984**, *53*, 749.
[10] Igarashi, K.; Kashiwagi, K. *Int. J. Biochem. Cell Biol.* **2010**, *42*, 39.
[11] Garriga, P.; Garcia-Quintana, D.; Sagi, J.; Manyosa, *J*. *Biochem.* **1993**, *32*, 1067.
[12] Tabor, C. W.; Tabor, H. *Annu. Rev. Biochem.* **1976**, *45*, 285.
[13] Mandal, S.; Mandal, A.; Johansson, H. E.; Orjalo, A. V.; Park, M. H. *Proc*. *Natl*. *Acad*. *Sci*. **2013**, *110*, 2169.
[14] Farriol, M.; Segovia-Silvestre, T.; Castellanos, J. M.; Venereo, Y.; Orta. X. *Nutrition* **2001**, *17*, 934.
[15] Pegg, A. E.; Conover, C.; Wrona, A. *Biochem. J.* **1978**,*170*, 651.
[16] Houdebine, L. M.; Devinoy, E.; Delouis, C. *Biochimie* **1978**, 60, 735.
[17] Hochreiter, R.; Weiger, T. M.; Colombatto, S.; Langer, T.; Thomas, T. J.; Cabella, C.; Heidegger, W.; Grillo, M. A.; Hermann, A. *Naunyn Schmiedebergs Arch. Pharmacol.* **2002**, *361*,235.
[18] Park, M. H.; Wolff, E. C.; Lee, Y. B.; Folk, J. E. *J. Biol. Chem*. **1994**, *269*, 27827.
[19] Lee, Y.; Kim, H-K.; Park, H-E.; Park, M. H.; Joe, Y. A. *Mol. Cell. Biochem*. **2002**, *237*, 69.
[20] Bryantsev, V. S.; Diallo, M. S.; Goddard, W. A. *J. Phys. Chem. A* **2007**, *111*, 4422.
[21] Tsubaki, K.; Tanaka, H.; Furuta, T.; Kinoshita, T.; Fuji, K. *Tetrahedron Lett.* **2000**, 41, 6089.
[22] Tsubaki, K.; Tanaka, H.; Furuta, T.; Tanaka, K.; Kinoshita, T.; Fuji, K. *Tetrahedron* **2002**, *58*, 5611.
[23] Kaoru, F.; Kazunori, T.; Kiyoshi, T.; Noriyuki, H.; Tadamune, O.; Takayoshi, K. *J. Am. Chem. Soc.* **1999**, *121*, 3807.
[24] Voyer, V.; Deschenes, D.; Bernier, J.; Roby. J. *J. Chem. Soc., Chem. Commun*. **1992**, 664-664.
[25] Kim, S. K.; Bang, M. Y.; Lee, S-H.; Nakamura, K.; Cho, S-W.; Yoon, J. *J. Inclusion Phenom. Macrocyclic Chem.* **2002**, *43*, 71.
[26] Fages, F.; Desvergne, J. P.; Kampke, K.; Bouas-Laurent, H.; Lehn, J. M.; Meyer, M.; Albrecht-Gary, A. M. *J. Am. Chem. Soc*. **1993**,*115*, 3658.
[27] Hayashi, T.; Nonoguchi, M.; Aya, T.; Ogoshi.; H. *Tetrahedron Lett.* **1997**, *38*,1603.
[28] Crossley, M. J.; Hambley, T. W.; Mackay, L. G.; Try, A. C.; Walton, R. *J. Chem. Soc., Chem. Commun*. **1995**, *10*, 1077.
[29] Mock, W. L.; Shih, N. Y. *J. Org. Chem.* **1986**, *51*, 4440.
[30] (a) Whang, D.; Heo, J.; Park, J. H.; Kim, K. *Angew. Chem. Int. Ed.* **1998**, *37*, 78. (b) Jeon, Y.-M.; Kim, J.; Whang, D.; Kim, K. *J. Am. Chem. Soc.* **1996**, *118*, 9790.
[31] Rekharsky, M. V.; Ko, Y. H.; Selvapalam, N.; Kim, K.; Inoue, Y. *Supramol. Chem.* **2007**, *19*, 39.
[32] Lagona, J.; Wagner, B. D.; Isaacs, L. *J. Org. Chem.* **2006**, *71*, 1181.
[33] Kim, Y.; Kim, H.; Ko, Y. H.; Selvapalam, N.; Rekharsky, M. V; Inoue, Y.; Kim, K. *Chemistry* **2009**, *15*, 6143.
[34] Lehn, J. M.; Vierling, P.; Hayward, R. C. *J. Chem. Soc. Chem. Commun.* **1979**, 296.
[35] Behr, J.-P.; Lehn, J.-M.; Vierling, P. *Helv. Chim. Acta* **1982**, *65*, 1853.
[36] Fores-Villalobos, A.; Morales-Rojas, H.; Escalante-Tovar, S.; Yatsimirsky, A. K. *J. Phys. Org. Chem.* **2002**, *15*, 83.
[37] (a) Späth, A.; König, B. *Beilstein J. Org. Chem.* **2010**, *6*, 32. (b) Schneider, H.-J.; Yatsimirsky, A. Principles and Methods in Supramolecular Chemistry; John Wiley & Sons Ltd.: Chichester, U. K., 2000.
[38] Houk, K. N.; Leach, A. G.; Kim, S. P.; Zhang, X. Y. *Angew. Chem., Int. Ed*. **2003**, 42, 4872.
[39] Vial, L.; Ludlow, R. F.; Leclaire, J.; Pérez-Fernandez, R.; Otto, S. *J. Am. Chem. Soc.* **2006**, *128*, 10253.
[40] De Robertis, A.; De Stefano, C.; Gianguzza, A.; Sammartano, S. *Talanta* **1998**, *46*, 1085.
[41] Muller, J. G.; Ng, M. M.; Burrows, C. J. *J. Mol. Recogn.* **1996**, *9*, 143.

[42] (a) Otto, S.; Furlan, R. L. E.; Sanders, J. K. M. *Science* **2002**, *297*, 590. (b) Corbett, P. T.; Tong, L. H.; Sanders, J. K. M.; Otto, S. *J. Am. Chem. Soc.* **2005**, *127*, 8902. (c) Vial, L.; Ludlow, R. F.; Leclaire, J.; Pérez-Fernandez, R.; Otto, S. *J. Am. Chem. Soc.* **2006**, *128*, 10253. (d) Ludlow, R. F.; Otto, S. *J. Am. Chem. Soc.* **2008**, *130*, 12218. (d) West, K. R.; Ludlow, R. F.; Corbett, P. T.; Besenius, P.; Mansfeld, F. M.; Cormack, P. A. G.; Sherrington, D. C.; Goodman, J. M.; Stuart, M. C. A.; Otto, S. *J. Am. Chem. Soc.* **2008**, *130*, 10834. (e) Rodriguez-Docampo, Z.; Eugenieva-Ilieva, E.; Reyheller, C.; Belenguer, A. M.; Kubik, S.; Otto, S. *Chem. Commun.* **2011**, *47*, 9798.
[43] (a) Corbett, P. T.; Sanders, J. K. M.; Otto, S. *J. Am. Chem. Soc.* **2005**, *127*, 9390. (b) Corbett, P. T.; Otto, S.; Sanders, J. K. M. *Chem. Eur. J.* **2004**, *10*, 3139.
[44] Corbett, P. T.; Sanders, J. K. M.; Otto, S. *Chem. Eur. J.* **2008**, *14*, 2153.
[45] Klein, J. M.; Saggiomo, V.; Reck, L.; Lüning, U.; Sanders, J. K. M. *Org. Biomol. Chem.* **2012**, *10*, 60.
[46] Klein, J. M.; Saggiomo, V.; Reck, L.; McPartlin, M.; Pantoş, G. D.; Lüning, U.; Sanders, J. K. M. *Chem. Commun.* **2011**, *47*, 3371.

Chapter 5: Estimation of host-guest binding constants from the product distributions of dynamic combinatorial libraries

DCLFit is a numerical fitting program able to generate estimates of equilibrium constants for binding of DCL members to an added template. The inputs of the program are based on concentrations of the library members, usually obtained from their corresponding HPLC-UV peak areas, in DCLs prepared at different template concentrations. The program has proved to cope with simple experimental DCLs composed of three components, and with more complex simulated DCLs generated using DCLSim, using specified binding constants as inputs for the latter. Herein we report that DCLFit copes with a quite complex experimental DCL made from two dithiol monomers and composed mainly of eight cyclic disulfide oligomers, some of which consist of multiple isomers in addition to many overoxidized linear components. The program was able to estimate, reliably, the equilibrium constants for binding of oligomers to four individual templates that amplified these oligomers. This is reflected in good correlations between fitted and experimental concentrations of these oligomers at different template concentrations. Moreover, reliably fitted binding constants agree with experimental ones obtained using ITC, within a factor of 2.2. Comparing the host-guest binding and the host amplification for the DCLs after adding four individual templates confirmed our previous computational finding that the amplification factors (AFs) of hosts correlate with host-guest binding affinities at a low ratio of template to total building block concentration.

In the first part of the chapter, we introduce the DCL system on which we have applied DCLFit, we discuss the incentives that prompted to use a numerical fitting program for the estimation of binding strengths for the library members and we overview the manner in which this program works. In the second part, we describe the preparation of the DCLs at a selected range of template concentrations and the model used to fit the binding constants. In the third part, we present the fitting results. This is followed by evaluations of the fitting qualities by comparing the fitted library distributions to the observed ones obtained from the HPLC-UV data. After that, we validate some of the binding affinities obtained using DCLFit against the ones obtained using ITC. In the last part of this chapter we compare regular amplification factors (AFs) with the normalized ones (AF_n) introduced in chapter 3, and discuss how they relate to the binding strengths of the oligomers. We then evaluate to which limit DCLFit can cope with a DCL made from dithiol building blocks and we discuss how we may improve the quality of the fitting generated by DCLFit.

Parts of this chapter have been published:

Hamieh, S.; Saggiomo, V.; Nowak, P.; Mattia, E.; Ludlow, R. F.; Otto, S. *Angew. Chem. Int. Ed.* **2013**.

5.1 Introduction

In chapter 3 we have reported that mixing dithiol monomers **2** and **3** under near physiological conditions leads to a DCL composed mainly of six macrocyclic disulfide oligomers of various sizes, two [2]-catenanes and several side products (Scheme 5.1). When exposing this library to a range of individual templates, some of which with biological activities, each time the concentrations of one or two macrocycles that apparently matched with some of the added templates were amplified. In our research group, discovering molecular receptors that bind efficiently to biologically active guests under near physiological conditions is among our research objectives. Hence, we wanted to extend the study of this library toward identifying which of the generated oligomers are more efficient at molecular recognition of the selected templates. This is commonly done by isolation of the hosts for independent host-guest binding studies. Hence, we commenced our investigation by considering the amplified macrocycles as these are likely to have affinities for the templates that induce their amplifications.

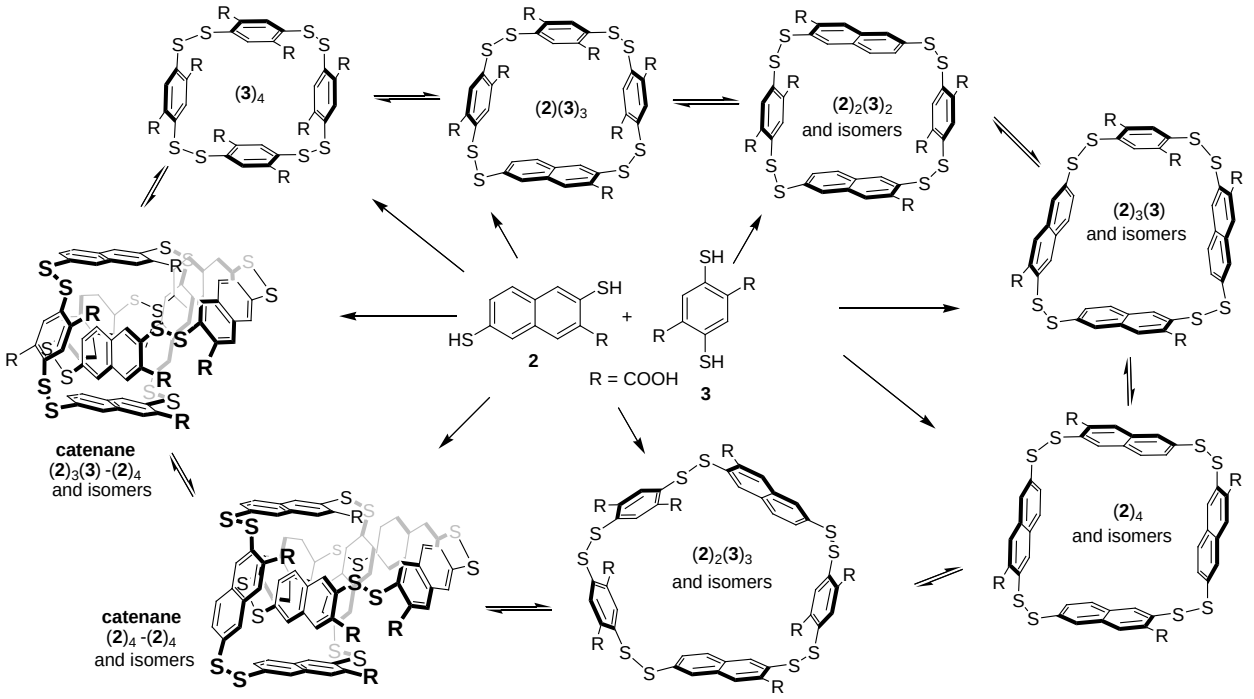

Scheme 5.1: A DCL made from building blocks **2** and **3** and composed of several macrocycles including $(\mathbf{2})_4$, $(\mathbf{2})_3(\mathbf{3})$, $(\mathbf{2})_2(\mathbf{3})_2$, $(\mathbf{2})(\mathbf{3})_3$, $(\mathbf{3})_4$, $(\mathbf{2})_2(\mathbf{3})_3$ and two octameric [2]-catenanes $(\mathbf{2})_4$-$(\mathbf{2})_4$ and $(\mathbf{2})_3(\mathbf{3})$-$(\mathbf{2})_4$.

However, identifying these as the best binders among all the library members, to templates that induce the their amplifications is possible only under special library conditions.[1,2] Among these conditions[1] is the ratio of template to building block concentration, which needs to be reduced to 1 to 10.[3] However, in chapter 3 we have templated the DCLs with an excess of template in order to increase the magnitude of the template effects. Specifically, the ratios of template to total building block concentration that were used were 1:2, 1:4 and 1:8. In these cases, the amplification is biased toward the library members that the system can produce in largest quantities rather than the best hosts in the DCL.[1,3] Hetero oligomers $(\mathbf{2})_2(\mathbf{3})_2$ followed by $(\mathbf{2})(\mathbf{3})_3$ and $(\mathbf{2})_3(\mathbf{3})$ tend to have an advantage in amplification over homo oligomers $(\mathbf{2})_4$ and $(\mathbf{3})_4$ after adding a template.[4] As a result, comparing the amplification factors of the various library members under the mentioned conditions may not lead to the identification of the library member of greatest binding strength, except in case of selective amplification of $(\mathbf{2})_4$ and $(\mathbf{3})_4$

which would reflect a strong binding affinity relative to the other library members. Indeed from our previous work we know that templates **3.1** and **3.29** amplify selectively and bind strongly to $(\mathbf{3})_4$[5] and $(\mathbf{2})_4$,[6] respectively (Table 5.1).

Table 5.1: Amplification factors for the six receptors upon addition of 2.5 mM of templates **3.1** or **3.29** to a DCL made from equimolar amounts (2.5 mM each) of building blocks **2** and **3** compared to equilibrium constants for binding of $(\mathbf{3})_4$ to **3.1** and $(\mathbf{2})_4$ to **3.29**, determined using ITC. The highest amplifications are shown in bold. Both amplifications and affinity constants are measured in 50 mM borate buffer solution at pH 8.4.

	Template		$(\mathbf{3})_4$	$(\mathbf{2})(\mathbf{3})_3$	$(\mathbf{2})_2(\mathbf{3})_2$	$(\mathbf{2})_3(\mathbf{3})$	$(\mathbf{2})_2(\mathbf{3})_3$	$(\mathbf{2})_4$
a	**3.1**	AF_n	**0.70**	0.13	-0.03	-0.52	0.01	0.44
		AF	7.55	2.79	0.00	0.02	1.27	**40.19**
b		Affinity constants	(4.5×10^7 M^{-1})	n.m.[a]	n.m.[a]	n.m.[a]	n.m.[a]	n.m.[a]
c	**3.29**	AF_n	-0.01	0.00	-0.29	0.00	0.02	**0.64**
		AF	0.95	1.06	1.59	0.46	0.92	**58.05**
d		Affinity constants	n.m.[a]	n.m.[a]	n.m.[a]	n.m.[a]	n.m.[a]	(1×10^7 M^{-1})

[a] n.m. = not measured.

As an alternative to the qualitative analysis of amplification factors, one may consider to perform experimental quantifications of the binding strengths of all the individual macrocycles. This requires switching off the disulfide exchange by decreasing the pH, isolation of the macrocyles using preparative HPLC after developing an appropriate preparative HPLC method, checking the purity of the isolated compounds using analytical HPLC and subsequently measuring their binding affinities toward the templates using host-guest titrations by NMR, ITC, UV or other experimental tools. Obviously this is a time consuming multi-step process especially when it comes to determining the binding affinities of the macrocyclic components $(\mathbf{3})_4$, $(\mathbf{2})(\mathbf{3})_3$, $(\mathbf{2})_2(\mathbf{3})_3$, $(\mathbf{2})_2(\mathbf{3})_2$, $(\mathbf{2})_3(\mathbf{3})$, $(\mathbf{2})_4$, $(\mathbf{2})_3(\mathbf{3})$-$(\mathbf{2})_4$ and $(\mathbf{2})_4$-$(\mathbf{2})_4$ toward templates **3.1** to **3.30**. Another factor that can complicate this experimental process is the extensive aggregation of macrocyclic oligomers made mainly from monomer **2**, along with their corresponding complexes under the DCL conditions.[6a] In an attempt to find an alternative to this painstaking process, our group has previously published details of a numerical fitting program named DCLFit.[7] This program is capable of generating estimates of the equilibrium constant for host-guest binding from concentrations of library members in DCLs prepared at different guest concentrations. It enables the binding strengths of the constituent library members to be assessed without the need for their time-consuming isolation and independent studies. DCLFit has proved to cope well with experimental systems composed of three library members[7,8] and with more complex simulated DCLs[7,9] generated using DCLSim, based on known binding constants as inputs. In both cases, the binding strengths for the amplified library members were in good agreement with the values obtained using experimental tools such as host-guest titration by UV[8] and ITC[7] and with the binding constants used as input data for DCLSim software.[7,9]

Motivation of the work

Adding 3-aminoquinuclidine (**3.9**), tyramine (**3.10**), ephedrine (**3.11**) or nicotine (**3.12**) (Figure 5.1) to the DCL induced the amplification of the statistically more favored oligomer $(\mathbf{2})_2(\mathbf{3})_2$ at a high template to total building block concentration ratio (Table 5.2). As mentioned in the introduction, this amplification may not reflect the binding strengths of the amplified oligomers. Therefore in this chapter we report the use of DCLFit to estimate the binding affinities of the

macrocyclic oligomers (**3**)$_4$, (**2**)(**3**)$_3$, (**2**)$_2$(**3**)$_3$, (**2**)$_2$(**3**)$_2$, (**2**)$_3$(**3**), (**2**)$_4$ and the other library components toward templates **3.9**-**3.12**.

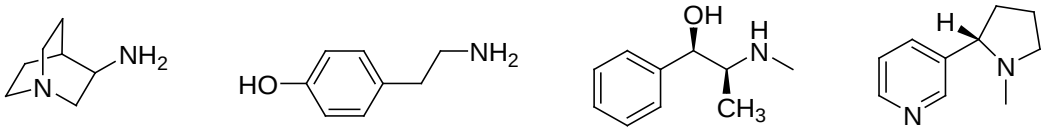

3.9 **3.10** **3.11** **3.12**

Figure 5.1: Structures of the four investigated templates: 3-aminoquinuclidine **3.9**, tyramine **3.10**, (-) ephedrine **3.11** and (-) nicotine **3.12**.

Table 5.2: Normalized amplification factors (AF_n) for the six receptors upon addition of a given template (2.5 mM) to a DCL made from **2** and **3** (2.5 mM each). AF_n > 0.09 are shown in bold. Regular amplification factors (AFs) are shown in 5.8.5.

	Template	(**3**)$_4$	(**2**)(**3**)$_3$	(**2**)$_2$(**3**)$_2$	(**2**)$_3$(**3**)	(**2**)$_2$(**3**)$_3$	(**2**)$_4$
3.9	3-aminoquinuclidine	0.03	**0.15**	**0.15**	0.06	-0.02	0.01
3.10	tyramine	0.06	0.02	**0.92**	0.04	-0.03	0.00
3.11	(-) ephedrine	0.03	-0.03	**0.45**	0.05	-0.01	0.00
3.12	(-) nicotine	0.04	-0.01	**0.39**	**0.09**	-0.01	0.00

5.1.1 How DCLFit works: a general overview

As detailed information along with a user manual of DCLFit program are already published,[7,10] herein we report only a general overview of how DCLFit works. First, a series of DCLs is prepared in the absence of a template and in the presence of increasing concentrations of individual templates of interests (paragraph 5.2). Then we define a model containing the library members, the equilibrium constants defining the equilibrium between the free oligomers and the building blocks (formed before adding a template) and represented by constants of formation of the oligomers ($K_{f\ nmer}$), and the equilibrium constants defining the equilibrium between the oligomers and the added template ($K_{a\ nmer\text{-}template}$) (Figure 5.2). The concentrations of the library members at different template concentrations can be obtained from their corresponding HPLC-UV peak areas after analyzing the templated DCLs (paragraph 5.3). In addition, relative values of $K_{f\ nmer}$ can be obtained after analyzing the untemplated DCL as these constants may be approximated by the concentrations of the corresponding oligomers.[11] After determining the concentrations of complexed and free oligomers and the relative formation constants of the free oligomers, it remains to fit the $K_{a\ nmers\text{-}template}$ by DCLFit. A first guess of the corresponding $K_{a\ nmers\text{-}template}$ is made and DCLFit then simulates the library distribution that corresponds to these values for the range of experimentally used guest concentrations. These simulated distributions are then compared with the experimental distributions obtained from HPLC-UV peak areas and an error (ε) is calculated that quantifies the difference between fitted and experimental data.[12] After the error has been calculated, the affinity constants ($K_{a\ nmers\text{-}template}$) are adjusted in an iterative process[13] that minimizes the error value using the Nelder-Mead Simplex algorithm.[14] A Monte-Carlo procedure repeats the fitting multiple times starting from randomly generated guesses of $K_{a\ nmers\text{-}template}$, each time from different starting points, to ensure that the global minimum of the error value is obtained. As a result, DCLFit generates several sets of fitted binding constants (fitted $K_{a\ nmers\text{-}template}$) where it shows for each set the predicted

concentrations of the oligomers for the range of experimentally used guest concentrations, the error ε that quantifies the difference between predicted and experimental concentrations and the number of times DCLFit could reproduce this set of values. The set of fitted $K_{a\ nmers\text{-}template}$ is then selected which corresponds to the most closely reproduced concentrations (which usually corresponds, simultaneously, to the lowest error ε and the highest number of times the results were reproduced).

5.2 DCL studies and choice of the fitting model

5.2.1 DCL studies

Four sets of DCLs made from equimolar amounts (2.0 mM each) of building blocks **2** and **3** were prepared in the absence of a template and in the presence of increasing concentrations of templates **3.9**-**3.12**. The selected range of template concentrations should allow to oligomer-template binding curves[15] to take, ideally, hyperbolic shapes defined by a sufficient number of data points (this notion is discussed in more detail in paragraph 5.6) (Figure 5.9-Figure 5.12). For the DCLFit experiments presented in this chapter, the selected range of template concentrations is: 0.0, 0.20, 0.40, 0.50, 0.60, 0.80, 1.0, 1.5, 2.0, 3.0 and 4.0 mM in 50 mM borate buffer at pH 8.4. The DCLs were stirred for 3-4 days and analyzed after reaching the equilibrium using the HPLC-UV method described in the experimental section. Next, the HPLC-UV peak areas of the macrocyclic disulfide oligomers $(\mathbf{3})_4$, $(\mathbf{2})(\mathbf{3})_3$, $(\mathbf{2})_2(\mathbf{3})_3$, $(\mathbf{2})_2(\mathbf{3})_2$, $(\mathbf{2})_3(\mathbf{3})$, $(\mathbf{2})_4$, $(\mathbf{2})_3(\mathbf{3})$-$(\mathbf{2})_4$ and $(\mathbf{2})_4$-$(\mathbf{2})_4$ and the disulfinic acids side products $(\mathbf{3})_2$4O, $(\mathbf{3})_3$4O, $(\mathbf{2})(\mathbf{3})$4O and $(\mathbf{2})(\mathbf{3})_2$4O were integrated using Chemstation software from Agilent. The concentrations of the disulfide macrocycles were calculated using the following equation (Table 5.3-Table 5.6):

$$[(\mathbf{2})_n(\mathbf{3})_m] = A\mathbf{2}_n\mathbf{3}_m / (n \times C_2 + m \times C_3)$$ [16]

$A\mathbf{2}_n\mathbf{3}_m$ corresponds to the HPLC-UV peak area of oligomer $(\mathbf{2})_n(\mathbf{3})_m$ (where n and m vary from 0 to 4) obtained at λ_{abs} = 260 nm, λ_{ref} = 550 nm and using an HPLC injection volume of 3 µl of a sample diluted with 200% volume DMSO. C_2 and C_3 are the constants relating areas of building blocks **2** and **3** to their corresponding concentrations under the same experimental conditions (λ_{abs}, λ_{ref}, and $V_{injected}$) as those used used to measure $A\mathbf{2}_n\mathbf{3}_m$. C_2 and C_3 were already calculated in chapter 3 (Paragraph 3.3.2) and their valus are 1508 mAU·min·mM^{-1} and 323 mAU·min·mM^{-1}, respectively. As the extinction coefficients of monomers **2** and **3** are additive only for the cyclic disulfide oligomers, the total concentration of disulfinic acid products were estimated by subtracting the total concentration of building blocks **2** and **3** consumed by the disulfide oligomers from the total concentration of building blocks **2** and **3** (2.0 mM for each) (Table 5.15-Table 5.16).

5.2.2 Model used to fit K_a $(2)_n(3)_m$-template

The model used to fit K_a $(\mathbf{2})_n(\mathbf{3})_m$-template (or $K_{a\ nmers\text{-}template}$) was described previously in paragraph 5.1.1. All of the library members able to be quantified by HPLC-UV analysis were considered in the fitting model, except for the [2]-catenanes $(\mathbf{2})_3(\mathbf{3})$-$(\mathbf{2})_4$ and $(\mathbf{2})_4$-$(\mathbf{2})_4$ and the overoxidized products $(\mathbf{3})_2$4O, $(\mathbf{3})_3$4O, $(\mathbf{2})(\mathbf{3})$4O and $(\mathbf{2})(\mathbf{3})_2$4O. Concerning the [2]-catenanes, results show that adding any of the templates **3.1**-**3.30** to the DCL gradually reduces their concentrations to undetectable values (Table 5.3-Table 5.6). Therefore, these species were considered to have no affinity for any of the templates. They were not included in the model used for data fitting. Similarly, increasing the concentrations of any of the templates reduces the linear disulfinic acid side products to tiny amounts (Table 5.15-Table 5.18). These linear side products were considered to have no affinities for any of the templates and therefore also

excluded from the model. The amounts of building blocks **2** and **3** taken up by the two [2]-catenanes and the side products were subtracted and excluded, respectively, from the total concentration of building blocks **2** and **3** used during the fitting process.[17] As a result, disulfide macrocycles (**3**)$_4$, (**2**)(**3**)$_3$, (**2**)$_2$(**3**)$_3$, (**2**)$_2$(**3**)$_2$, (**2**)$_3$(**3**) and (**2**)$_4$ were the only library members that were explicitly considered in the model (Figure 5.2).

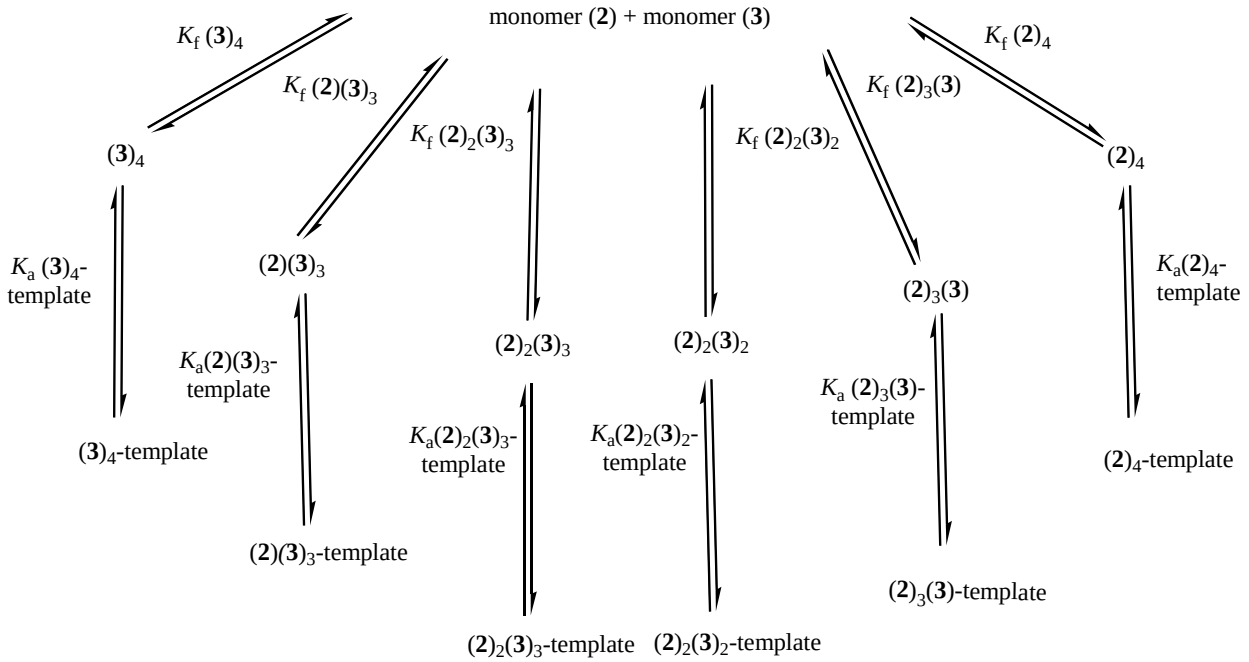

Figure 5.2: Fitting model used to describe the DCL made from building blocks **2** and **3**.

5.3 Fitting results for guests 3.9-3.12

5.3.1 Simplification of the model

In order to reduce the influence of the experimental error on the fitting, we applied the following procedure. First, for each experimental data value (observed concentration of an oligmer obtained from its HPLC-UV peak area), there is a weight which defaults to 1 and reflects the quality of the measured data. When the error ε is calculated for each data point, it is multiplied by this weight. Thus, data points where quantification is less reliable may be given a reduced weight. For the fitting procedures reported in this chapter we assigned for concentrations below 1 x 10^{-5} M a weight of 0.1. Second, for any of the oligomers used in the model, the lowest observable concentration counted as reliable was set as 3% of the concentration of the most abundant oligomer formed in any of the ten (or eleven) prepared DCLs. Any values below this were treated as unreliable and therefore their fittings were ignored. Third, any oligomer for which more than half of its observable concentrations are undetectable, was excluded from the fitting model. Therefore, the amounts of building blocks taken up by this oligomer were substracted from the total building block concentrations.

5.3.2 Fitting results for guest 3.9

First, relative formation constants of oligomers (relative $K_{f\ nmer}$) (**3**)$_4$, (**2**)(**3**)$_3$, (**2**)$_2$(**3**)$_3$, (**2**)$_2$(**3**)$_2$, (**2**)$_3$(**3**) and (**2**)$_4$ were determined from the untemplated library made from building blocks **2** and **3**, as mentioned in 5.1.1. For the purpose of the fitting procedure these constants can be

approximated as the concentrations of their corresponding untemplated oligomers at thermodynamic equilibrium which correspond to 0.43 x 10^{-4} M^{-3}, 0.71 x 10^{-4} M^{-3}, 0.26 x 10^{-4} M^{-3}, 4.03 x 10^{-4} M^{-3}, 0.43 x 10^{-3} M^{-2} and 0.14 x 10^{-4} M^{-3} respectively (Table 5.3). The relative formation constants of the oligomers included in the model, the observable concentrations of these oligomers at various guest **3.9** concentrations and the total concentration in building blocks **2** and **3** consumed by these oligomers for the range of used guest concentrations[17] constitute the input data for DCLFit. The affinity constants of the oligomers toward template **3.9** (K_a $(\mathbf{2})_n(\mathbf{3})_m$-**3.9**) were fitted 30 times using Monte-Carlo fitting starting from randomly guessed affinities varying from 0 to 10^7 M^{-1}. The set of fitted K_a $(\mathbf{2})_n(\mathbf{3})_m$-**3.9** obtained 14 times with an error ε = 0.15 was selected, as it most closely reproduced the observed concentrations of the oligomers. The values selected for fitted K_a $(\mathbf{2})_n(\mathbf{3})_m$-**3.9** are shown in Table 5.7. Note that the majority of the observed concentrations of $(\mathbf{2})_2(\mathbf{3})_3$ are below the applied threshold and therefore $(\mathbf{2})_2(\mathbf{3})_3$ fitting did not yield reliable data.

Table 5.3: Calculated concentrations (mM) of the DCL members in DCLs made from equimolar amounts (2.0 mM each) of building blocks **2** and **3** at different template **3.9** concentrations. DCLs were prepared in 50 mM borate buffer solutions at pH = 8.4. The concentrations of the library members for data fitting imput were converted to molar units.

DCL	[**3.9**] mM	[$(\mathbf{3})_4$] mM	[$(\mathbf{2})(\mathbf{3})_3$] mM	[$(\mathbf{2})_2(\mathbf{3})_3$] mM	[$(\mathbf{2})_2(\mathbf{3})_2$] mM	[$(\mathbf{2})_3(\mathbf{3})$] mM	[$(\mathbf{2})_4$] mM	[$(\mathbf{2})_3(\mathbf{3})$-$(\mathbf{2})_4$] mM	[$(\mathbf{2})_4$-$(\mathbf{2})_4$] mM	[**2**] mM	[**3**] mM
1	0	0.043	0.071	0.026	0.403	0.043	0.014	0.014	0.004	1.113	1.313
2	0.2	0.039	0.110	0.018	0.475	0.047	0.014	0.014	0.002	1.292	1.535
3	0.4	0.046	0.130	0.016	0.473	0.053	0.022	0.012	0.001	1.353	1.622
4	0.5	0.051	0.133	0.015	0.478	0.054	0.023	0.009	0.002	1.373	1.660
5	0.6	0.046	0.152	0.015	0.481	0.048	0.021	0.009	0.001	1.371	1.696
6	0.8	0.051	0.149	0.017	0.500	0.062	0.026	0.008	0.001	1.471	1.765
7	1.0	0.052	0.166	0.012	0.504	0.065	0.026	0	0	1.497	1.815
8	2.0	0.042	0.160	0.012	0.520	0.081	0.031	0	0	1.593	1.805
9	3.0	0.036	0.153	0.010	0.513	0.083	0.029	0	0	1.561	1.742
10	4.0	0.038	0.168	0.011	0.507	0.091	0.038	0	0	1.627	1.793

5.3.3 Fitting results for guest 3.10

The same procedure performed in 5.3.2 was repeated, and the relative formation constants of oligomers (relative $K_{f\ nmer}$) $(\mathbf{3})_4$, $(\mathbf{2})(\mathbf{3})_3$, $(\mathbf{2})_2(\mathbf{3})_3$, $(\mathbf{2})_2(\mathbf{3})_2$, $(\mathbf{2})_3(\mathbf{3})$ and $(\mathbf{2})_4$ correspond to 0.37 x 10^{-4} M^{-3}, 0.53 x 10^{-4} M^{-3}, 0.18 x 10^{-4} M^{-3}, 4.27 x 10^{-3} M^{-1}, 0.31 x 10^{-4} M^{-3} and 0.03 x 10^{-4} M^{-3} respectively (Table 5.4). Then, K_a $(\mathbf{2})_n(\mathbf{3})_m$-**3.10** were fitted 50 times using a Monte-Carlo fitting starting from randomly guessed affinities varying from 0 to 10^7 M^{-1}. The set of fitted affinity constants (fitted K_a $(\mathbf{2})_n(\mathbf{3})_m$-**10**) obtained 20 times with an error ε = 1.36 was selected as it most closely reproduced the observed concentrations of the oligomers. The values selected for fitted K_a $(\mathbf{2})_n(\mathbf{3})_m$-**3.10** are shown in Table 5.7. The majority of the observed concentrations values of $(\mathbf{2})_2(\mathbf{3})_3$ are below the applied threshold and therefore $(\mathbf{2})_2(\mathbf{3})_3$ fitting did not yield reliable data. Moreover, more than 50% of the observable concentration values of $(\mathbf{2})_4$ are equal to zero (undetectable) and therefore $(\mathbf{2})_4$ oligomer was considered to have no affinity for **3.10** and was

removed from the fitting model of the DCL after subtracting the concentrations of building blocks **2** and **3** consumed by this oligomer in all the DCLs where it exists.

Table 5.4: Calculated concentrations (mM) of the DCL members in DCLs made from equimolar amounts (2.0 mM each) of building blocks **2** and **3** at different template **3.10** concentrations. DCLs were prepared in 50 mM borate buffer solutions at pH = 8.4. The concentrations of the library members for data fitting imput were converted to molar units.

DCL	[**3.10**] mM	[(**3**)$_4$] mM	[(**2**)(**3**)$_3$] mM	[(**2**)$_2$(**3**)$_3$] mM	[(**2**)$_2$(**3**)$_2$] mM	[(**2**)$_3$(**3**)] mM	[(**2**)$_4$] mM	[(**2**)$_3$(**3**)-(**2**)$_4$] mM	[(**2**)$_4$-(**2**)$_4$] mM	[**2**] mM	[**3**] mM
1	0	0.037	0.053	0.018	0.427	0.031	0.003	0.014	0.003	1.045	1.245
2	0.2	0.050	0.069	0.016	0.659	0.028	0.003	0.012	0.002	1.515	1.799
3	0.4	0.044	0.050	0.008	0.634	0.025	0.002	0.003	0.0	1.418	1.645
4	0.5	0.042	0.056	0.005	0.717	0.019	0.0	0.0	0.0	1.557	1.803
5	0.6	0.048	0.048	0.003	0.785	0.028	0.0	0.0	0.0	1.707	1.942
6	0.8	0.050	0.046	0.003	0.835	0.037	0.0	0.0	0.0	1.834	2.055
7	1	0.047	0.051	0.005	0.830	0.033	0.0	0.0	0.0	1.820	2.051
8	1.5	0.049	0.049	0.004	0.843	0.037	0.002	0.0	0.0	1.864	2.078
9	2	0.043	0.043	0.003	0.756	0.046	0.002	0.0	0.0	1.708	1.869
10	3	0.042	0.040	0.003	0.812	0.046	0.0	0.0	0.0	1.810	1.969
11	4	0.043	0.040	0.007	0.799	0.048	0.0	0.0	0.0	1.797	1.957

5.3.4 Fitting results for guest 3.11

Relative formation constants of oligomers (**3**)$_4$, (**2**)(**3**)$_3$, (**2**)$_2$(**3**)$_3$, (**2**)$_2$(**3**)$_2$, (**2**)$_3$(**3**) and (**2**)$_4$ correspond to 0.39 x 10^{-4} M^{-3}, 0.56 x 10^{-3} M^{-2}, 0.22 x 10^{-3} M^{-2}, 4.71 x 10^{-4} M^{-3}, 0.34 x 10^{-4} M^{-3} and 0.03 x 10^{-4} M^{-3} respectively (Table 5.5). Then, K_a (**2**)$_n$(**3**)$_m$-**3.11** were fitted 100 times using a Monte-Carlo fitting starting from randomly guessed affinities varying from 0 to 10^7 M^{-1}. The set of fitted K_a (**2**)$_n$(**3**)$_m$-**11** obtained 40 times with an error ε = 0.20 was selected as it closely reproduced the observed concentrations of the oligomers. The values selected for fitted K_a (**2**)$_n$(**3**)$_m$-**3.11** are shown in Table 5.7. The majority of the observed concentration values of (**2**)$_2$(**3**)$_3$ and (**2**)$_4$ are below the applied threshold and therefore fittings of (**2**)$_2$(**3**)$_3$ and (**2**)$_4$ did not yield reliable data.

Table 5.5: Calculated concentrations (mM) of the DCL members in DCLs made from equimolar amounts (2.0 mM each) of building blocks **2** and **3** at different template **3.11** concentrations. DCLs were prepared in 50 mM borate buffer solutions at pH = 8.4. The concentrations of the library members for data fitting imput were converted to molar units.

DCL	[**3.11**] mM	[(**3**)$_4$] mM	[(**2**)(**3**)$_3$] mM	[(**2**)$_2$(**3**)$_3$] mM	[(**2**)$_2$(**3**)$_2$] mM	[(**2**)$_3$(**3**)] mM	[(**2**)$_4$] mM	[(**2**)$_3$(**3**)-(**2**)$_4$] mM	[(**2**)$_4$-(**2**)$_4$] mM	[**2**] mM	[**3**] mM
1	0	0.039	0.056	0.022	0.471	0.034	0.003	0.014	0.002	1.156	1.366
2	0.2	0.040	0.051	0.024	0.531	0.036	0.003	0.012	0.0	1.280	1.485

3	0.4	0.047	0.039	0.021	0.569	0.062	0.004	0.010	0.0	1.420	1.568
4	0.5	0.046	0.044	0.020	0.634	0.055	0.003	0.006	0.0	1.532	1.702
5	0.6	0.035	0.034	0.015	0.548	0.051	0.003	0.0	0.0	1.322	1.431
6	0.8	0.041	0.041	0.017	0.679	0.064	0.003	0.0	0.0	1.636	1.760
7	1	0.040	0.038	0.019	0.607	0.116	0.004	0.0	0.0	1.653	1.661
8	1.5	0.042	0.034	0.016	0.703	0.071	0.002	0.0	0.0	1.696	1.796
9	2	0.045	0.036	0.018	0.747	0.076	0.003	0.0	0.0	1.806	1.910
10	3	0.046	0.036	0.019	0.739	0.076	0.003	0.0	0.0	1.793	1.905
11	4	0.046	0.036	0.017	0.773	0.077	0.005	0.0	0.0	1.865	1.964

5.3.5 Fitting results for guest 3.12

Relative formation constants of oligomers $(\mathbf{3})_4$, $(\mathbf{2})(\mathbf{3})_3$, $(\mathbf{2})_2(\mathbf{3})_3$, $(\mathbf{2})_2(\mathbf{3})_2$, $(\mathbf{2})_3(\mathbf{3})$ and $(\mathbf{2})_4$ correspond to 0.46 x 10^{-4} M^{-3}, 0.69 x 10^{-3} M^{-2}, 0.23 x 10^{-3} M^{-2}, 4.11 x 10^{-4} M^{-3}, 0.42 x 10^{-4} M^{-3} and 0.13 x 10^{-4} M^{-3} respectively. Then, K_a $(\mathbf{2})_n(\mathbf{3})_m$-**3.12** were fitted 25 times using a Monte-Carlo fitting starting from randomly guessed affinities varying from 0 to 10^7 M^{-1}. The set of fitted K_a $(\mathbf{2})_n(\mathbf{3})_m$-**12** obtained 10 times with a error ε = 0.40 was selected as it closely reproduced the observed concentrations of the oligomers. The values selected for fitted K_a $(\mathbf{2})_n(\mathbf{3})_m$-**3.12** are shown in Table 5.7. Half of the observed concentration values of $(\mathbf{2})_2(\mathbf{3})_3$ and the majority of the $(\mathbf{2})_4$ concentrations are below the applied threshold and therefore fittings of $(\mathbf{2})_2(\mathbf{3})_3$ and $(\mathbf{2})_4$ did not yield reliable data.

Table 5.6: Calculated concentrations (mM) of the DCL members in DCLs made from equimolar amounts (2.0 mM each) of building blocks **2** and **3** at different template **3.12** concentrations. DCLs were prepared in 50 mM borate buffer solutions at pH = 8.4. The concentrations of the library members for data fitting imput were converted to molar units.

DCL	[**3.12**] mM	[$(\mathbf{3})_4$] mM	[$(\mathbf{2})(\mathbf{3})_3$] mM	[$(\mathbf{2})_2(\mathbf{3})_3$] mM	[$(\mathbf{2})_2(\mathbf{3})_2$] mM	[$(\mathbf{2})_3(\mathbf{3})$] mM	[$(\mathbf{2})_4$] mM	[$(\mathbf{2})_3(\mathbf{3})$-$(\mathbf{2})_4$] mM	[$(\mathbf{2})_4$-$(\mathbf{2})_4$] mM	[**2**] mM	[**3**] mM
1	0	0.046	0.069	0.023	0.411	0.042	0.013	0.014	0.005	1.113	1.326
2	0.2	0.039	0.066	0.022	0.473	0.033	0.004	0.014	0.0	1.172	1.398
3	0.4	0.048	0.072	0.023	0.587	0.057	0.007	0.012	0.0	1.491	1.708
4	0.5	0.046	0.082	0.028	0.602	0.055	0.017	0.009	0.0	1.578	1.771
5	0.6	0.039	0.056	0.020	0.495	0.047	0.007	0.009	0.0	1.254	1.418
6	0.8	0.052	0.086	0.025	0.637	0.048	0.006	0.008	0.0	1.580	1.861
7	1	0.046	0.076	0.019	0.649	0.066	0.013	0.0	0.0	1.666	1.837
8	1,5	0.049	0.073	0.021	0.597	0.092	0.014	0.0	0.0	1.639	1.763
9	2	0.050	0.088	0.018	0.697	0.066	0.005	0.0	0.0	1.739	1.981
10	3	0.045	0.074	0.013	0.680	0.080	0.006	0.0	0.0	1.724	1.881
11	4	0.046	0.079	0.014	0.678	0.080	0.006	0.0	0.0	1.726	1.898

Table 5.7: Fitted affinity constants (fitted K_a $(\mathbf{2})_n(\mathbf{3})_m$-template) for binding of selected templates to different macrocycles generated in a DCL made from building blocks **2** and **3** in 50 mM borate buffer at pH = 8.4.

Template	$(\mathbf{3})_4$ (M^{-1})	$(\mathbf{2})(\mathbf{3})_3$ (M^{-1})	$(\mathbf{2})_2(\mathbf{3})_2$ (M^{-1})	$(\mathbf{2})_3(\mathbf{3})$ (M^{-1})	$(\mathbf{2})_4$ (M^{-1})
3.9	2.17×10^4	2.85×10^4	7.80×10^3	5.42×10^3	3.15×10^3
3.10	6.17×10^4	4.06×10^4	9.76×10^4	5.79×10^4	n.d.[a]
3.11	4.00×10^3	2.50×10^3	9.87×10^3	1.98×10^4	n.d.[a]
3.12	3.68×10^3	3.16×10^3	3.82×10^3	2.97×10^3	n.d.[a]

[a] = not detected.

5.3.6 Evaluation of the quality of the fit of K_a $(2)_n(3)_m$-3.9, 3.10, 3.11 and 3.12

Ratios of the fitted concentrations of $(\mathbf{2})_n(\mathbf{3})_m$ to the experimental concentrations of $(\mathbf{2})_n(\mathbf{3})_m$, corresponding to its HPLC-UV peak areas, were plotted as a function of the concentrations of templates **3.9**, **3.10**, **3.11** and **3.12** (Figure 5.3-Figure 5.6). The ideal fitting of K_a $(\mathbf{2})_n(\mathbf{3})_m$-template occurs when the fitted concentrations of $(\mathbf{2})_n(\mathbf{3})_m$ are the same as the experimental concentrations. This leads to ratios of fitted to observed concentrations of $(\mathbf{2})_n(\mathbf{3})_m$ equal to 1. Data obtained shows that a good fitting quality of K_a $(\mathbf{2})_n(\mathbf{3})_m$-template occurred when $(\mathbf{2})_n(\mathbf{3})_m$ is a) amplified upon template addition (Table 5.21-Table 5.24) and b) its concentrations exceed the detection limit (1×10^{-5} M), by at least one order of magnitude (Table 5.3-Table 5.6).[18] The fact that an oligomer shows, simultaneously, amplification upon templating in addition to a concentration considerably higher than the detection limit, leads to a relatively high normalized amplification factor (AF_n) for this oligomer compared to the remaining oligomers. This was the case for oligomer $(\mathbf{2})_2(\mathbf{3})_2$ that showed relatively high AF_n after adding different amounts of templates **3.9** (Table 5.8), **3.10** (Table 5.9), **3.11** (Table 5.19) and **3.12** (Table 5.11) to the DCL, and showed therefore ratios of their fitted to observed concentrations as a function of templates **3.9** (Figure 5.3), **3.10** (Figure 5.4), **3.11** (Figure 5.5) and and **3.12** (Figure 5.6) very close to 1, in comparison with the remaining oligomers. This also occurred for $(\mathbf{2})(\mathbf{3})_3$ upon addition of **3.9** (Table 5.8). The fitting of K_a $(\mathbf{2})_n(\mathbf{3})_m$-template was of poorer quality then the one discussed above, when $(\mathbf{2})_n(\mathbf{3})_m$ is of concentrations close to the detection limit albeit this oligomer showed, sometimes, amplification upon templating. This leads to low (normalized) amplification factors (AF_n) and was the case for oligomers $(\mathbf{3})_4$, $(\mathbf{2})(\mathbf{3})_3$, $(\mathbf{2})_3(\mathbf{3})$, $(\mathbf{2})_4$ after adding templates **3.10-3.12**, and for oligomers $(\mathbf{3})_4$, $(\mathbf{2})(\mathbf{3})_3$ and $(\mathbf{2})_4$ after adding template **3.9** to the DCL. As a result, oligomers of low quality data *i.e.* of concentrations close to the detection limit showed low fitting quality and this may be explained by the fact that large changes in the fitted affinity constants of these species have only slight effects on the global library distribution.

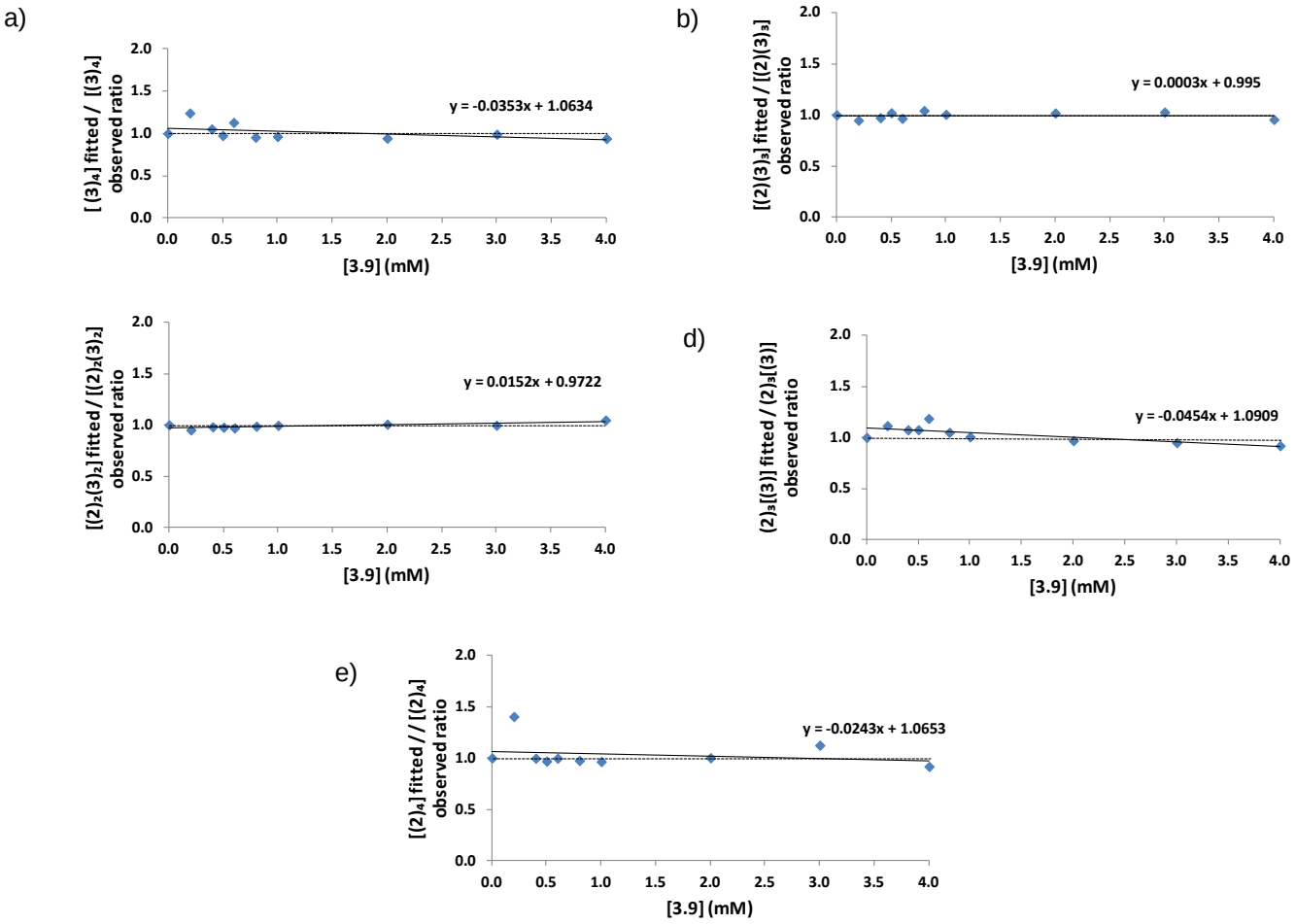

Figure 5.3: Graphs of ratios of the fitted to the observed concentrations of oligomers (a) $(\mathbf{3})_4$, (b) $(\mathbf{2})(\mathbf{3})_3$, (c) $(\mathbf{2})_2(\mathbf{3})_2$, (d) $(\mathbf{2})_3(\mathbf{3})$ and (e) $(\mathbf{2})_4$ as a function of the amount of guest **3.9** added to a library made from equimolar amounts (2.0 mM each) of building blocks **2** and **3** in 50 mM borate buffer solutions at pH = 8.4. The data points were fitted to a linear regression model to describe the trend of variation of the specified ratios of $(\mathbf{2})_n(\mathbf{3})_m$ in function of the template additions.

Table 5.8: AFn of macrocyclic library members $(\mathbf{3})_4$, $(\mathbf{2})(\mathbf{3})_3$, $(\mathbf{2})_2(\mathbf{3})_3$, $(\mathbf{2})_2(\mathbf{3})_2$, $(\mathbf{2})_3(\mathbf{3})$ and $(\mathbf{2})_4$ at different concentrations of template **3.9** in a library made from equimolar amounts (2.0 mM each) of building blocks **2** and **3** in 50 mM borate buffer solutions at pH = 8.4.

DCL	[**3.9**] mM	$[(\mathbf{3})_4]$ mM	$[(\mathbf{2})(\mathbf{3})_3]$ mM	$[(\mathbf{2})_2(\mathbf{3})_3]$ mM	$[(\mathbf{2})_2(\mathbf{3})_2]$ mM	$[(\mathbf{2})_3(\mathbf{3})]$ mM	$[(\mathbf{2})_4]$ mM
2	0.2	-0.01	**0.07**	-0.01	**0.12**	0.01	0.00
3	0.4	0.01	**0.10**	-0.02	**0.12**	0.02	0.02
4	0.5	0.02	**0.10**	-0.02	**0.13**	0.02	0.02
5	0.6	0.01	**0.14**	-0.02	**0.13**	0.01	0.01
6	0.8	0.02	**0.13**	-0.01	**0.16**	0.03	0.02
7	1.0	0.02	**0.16**	-0.02	**0.17**	0.04	0.02

8	2.0	0.00	**0.15**	-0.02	**0.20**	0.06	0.03
9	3.0	-0.02	**0.14**	-0.02	**0.18**	0.06	0.03
10	4.0	-0.01	**0.16**	-0.02	**0.17**	0.08	0.05

a)

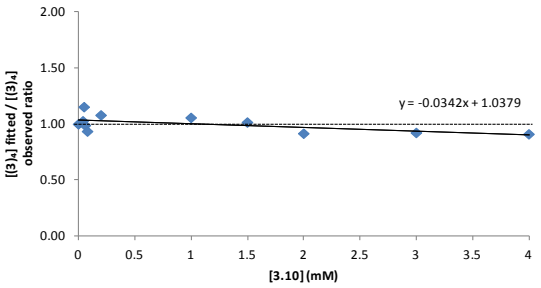

b)

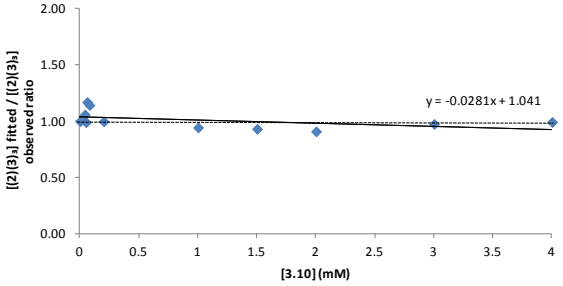

c)

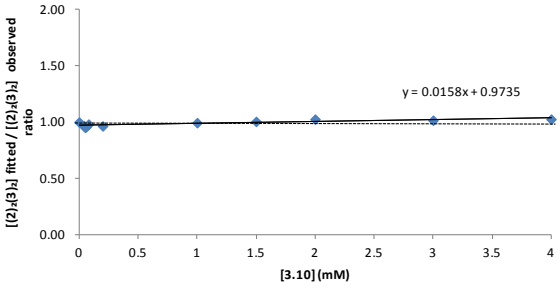

d)

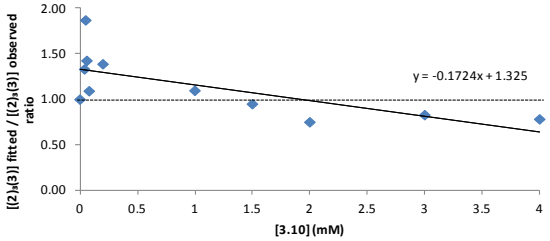

Figure 5.4: Graphs of ratios of the fitted to the observed concentrations of oligomers (a) $(\mathbf{3})_4$, (b) $(\mathbf{2})(\mathbf{3})_3$, (c) $(\mathbf{2})_2(\mathbf{3})_2$ and (d) $(\mathbf{2})_3(\mathbf{3})$ in function of the amount of added guest **3.10**. The data points were fitted to a linear regression model to describe the trend of variation of the specified ratios of $(\mathbf{2})_n(\mathbf{3})_m$ in function of the template additions.

Table 5.9: AF_n of macrocyclic library members $(\mathbf{3})_4$, $(\mathbf{2})(\mathbf{3})_3$, $(\mathbf{2})_2(\mathbf{3})_3$, $(\mathbf{2})_2(\mathbf{3})_2$, $(\mathbf{2})_3(\mathbf{3})$ and $(\mathbf{2})_4$ at different concentrations of template **3.10** in a library made from equimolar amounts (2.0 mM each) of building blocks **2** and **3** in 50 mM borate buffer solutions at pH = 8.4.

DCL	[**3.10**] mM	$[(\mathbf{3})_4]$ mM	$[(\mathbf{2})(\mathbf{3})_3]$ mM	$[(\mathbf{2})_2(\mathbf{3})_3]$ mM	$[(\mathbf{2})_2(\mathbf{3})_2]$ mM	$[(\mathbf{2})_3(\mathbf{3})]$ mM	$[(\mathbf{2})_4]$ mM
2	0.2	0.03	0.03	0.00	**0.40**	0.00	0.00
3	0.4	0.02	0.00	-0.02	**0.36**	-0.01	0.00
4	0.5	0.01	0.00	-0.02	**0.51**	-0.02	-0.01
5	0.6	0.02	-0.01	-0.02	**0.62**	0.00	-0.01
6	0.8	0.03	-0.01	-0.02	**0.71**	0.01	-0.01
7	1.0	0.02	0.00	-0.02	**0.70**	0.00	-0.01
8	1.5	0.03	-0.01	-0.02	**0.73**	0.01	0.00
9	2.0	0.01	-0.02	-0.02	**0.57**	0.02	0.00
10	3.0	0.01	-0.02	-0.02	**0.67**	0.02	-0.01
11	4.0	0.01	-0.02	-0.02	**0.65**	0.03	-0.01

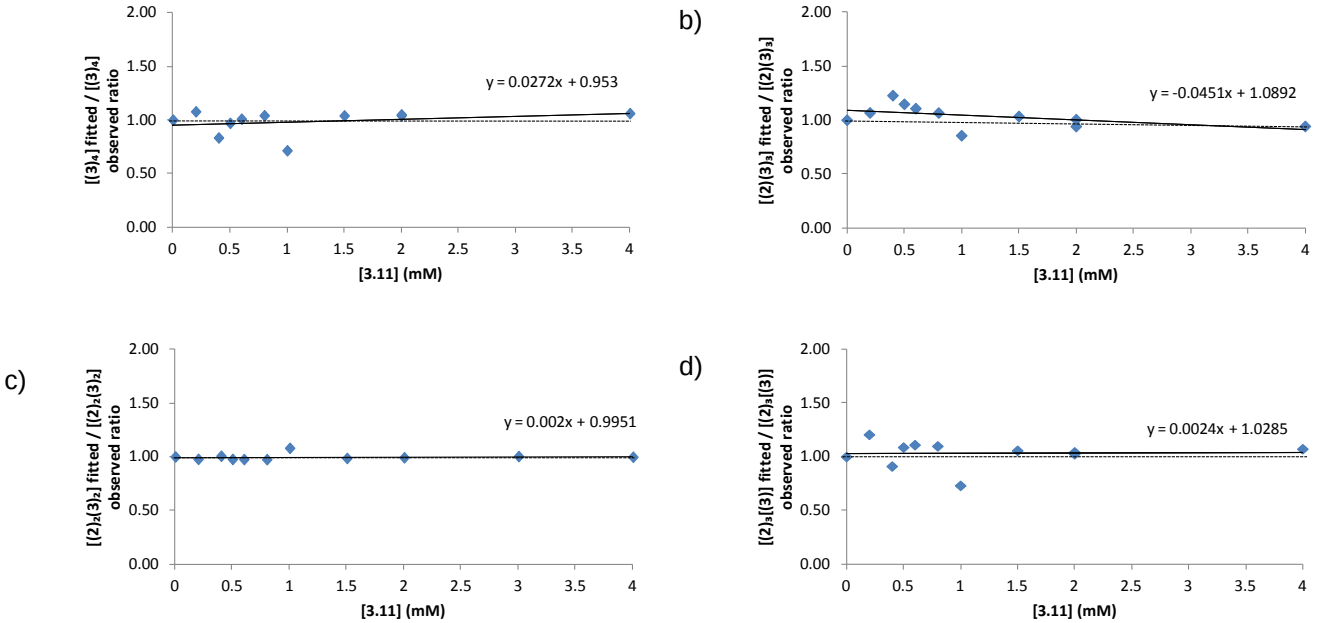

Figure 5.5: Graphs of ratios of the fitted to the observed concentrations of oligomers (a) $(\mathbf{3})_4$, (b) $(\mathbf{2})(\mathbf{3})_3$, (c) $(\mathbf{2})_2(\mathbf{3})_2$ and (d) $(\mathbf{2})_3(\mathbf{3})$ as a function of the amount of added guest **3.11**. The data points were fitted to a linear regression model to describe the trend of variation of the specified ratios of $(\mathbf{2})_n(\mathbf{3})_m$ in function of the template additions.

Table 5.10: AF_n of macrocyclic library members $(\mathbf{3})_4$, $(\mathbf{2})(\mathbf{3})_3$, $(\mathbf{2})_2(\mathbf{3})_3$, $(\mathbf{2})_2(\mathbf{3})_2$, $(\mathbf{2})_3(\mathbf{3})$ and $(\mathbf{2})_4$ at different concentrations of template **3.11** in a library made from equimolar amounts (2.0 mM each) of building blocks **2** and **3** in 50 mM borate buffer solutions at pH = 8.4.

DCL	[**3.11**] mM	$[(\mathbf{3})_4]$ mM	$[(\mathbf{2})(\mathbf{3})_3]$ mM	$[(\mathbf{2})_2(\mathbf{3})_3]$ mM	$[(\mathbf{2})_2(\mathbf{3})_2]$ mM	$[(\mathbf{2})_3(\mathbf{3})]$ mM	$[(\mathbf{2})_4]$ mM
2	0.2	0.00	-0.01	0.00	**0.11**	0.00	0.00
3	0.4	0.02	-0.03	0.00	**0.19**	0.04	0.00
4	0.5	0.02	-0.02	0.00	**0.31**	0.03	0.00
5	0.6	-0.01	-0.04	-0.01	**0.15**	0.03	0.00
6	0.8	0.00	-0.02	-0.01	**0.39**	0.05	0.00
7	1.0	0.00	-0.03	0.00	**0.26**	0.13	0.00
8	1.5	0.01	-0.04	-0.01	**0.44**	0.06	0.00
9	2.0	0.01	-0.03	-0.01	**0.52**	0.07	0.00
10	3.0	0.02	-0.03	0.00	**0.51**	0.07	0.00
11	4.0	0.02	-0.03	-0.01	**0.57**	0.07	0.00

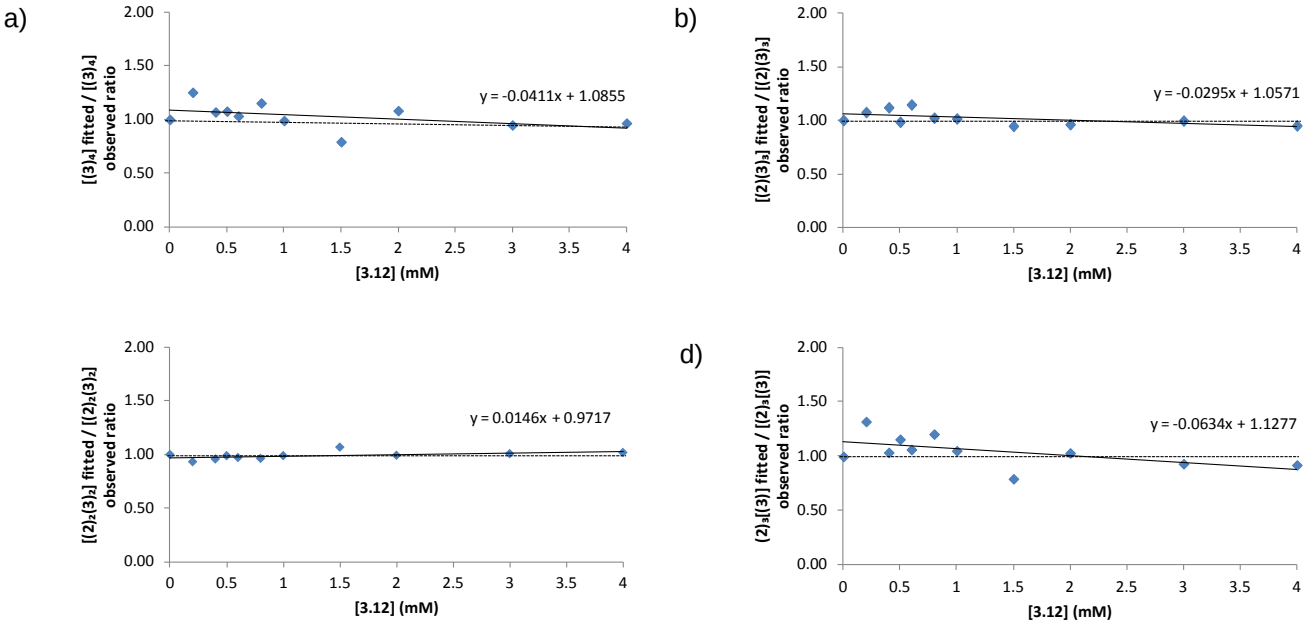

Figure 5.6: Graphs of ratios of the fitted to the observed concentrations of oligomers (a) (**3**)$_4$, (b) (**2**)(**3**)$_3$, (c) (**2**)$_2$(**3**)$_2$ and (d) (**2**)$_3$(**3**) as a function of the amount of added guest **3.12**. The data points were fitted to a linear regression model to describe the trend of variation of the specified ratios of (**2**)$_n$(**3**)$_m$ in function of the template additions.

Table 5.11: AF_n of macrocyclic library members (**3**)$_4$, (**2**)(**3**)$_3$, (**2**)$_2$(**3**)$_3$, (**2**)$_2$(**3**)$_2$, (**2**)$_3$(**3**) and (**2**)$_4$ at different concentrations of template **3.12** in a library made from equimolar amounts (2.0 mM each) of building blocks **2** and **3** in 50 mM borate buffer solutions at pH = 8.4.

DCL	[**3.12**] mM	[(**3**)$_4$] mM	[(**2**)(**3**)$_3$] mM	[(**2**)$_2$(**3**)$_3$] mM	[(**2**)$_2$(**3**)$_2$] mM	[(**2**)$_3$(**3**)] mM	[(**2**)$_4$] mM
2	0.2	-0.02	-0.01	0.00	0.11	-0.01	-0.02
3	0.4	0.00	0.01	0.00	0.30	0.02	-0.01
4	0.5	0.00	0.02	0.01	0.32	0.02	0.01
5	0.6	-0.02	-0.02	0.00	0.14	0.01	-0.01
6	0.8	0.01	0.03	0.00	0.38	0.01	-0.01
7	1.0	0.00	0.01	-0.01	0.40	0.04	0.00
8	1.5	0.01	0.01	0.00	0.32	0.08	0.00
9	2.0	0.01	0.03	-0.01	0.49	0.04	-0.02
10	3.0	0.00	0.01	-0.02	0.46	0.06	-0.01
11	4.0	0.00	0.02	-0.01	0.45	0.06	-0.01

5.4 Validation of some of the fitted affinity constants against their corresponding values obtained using ITC

The binding affinities of oligomers (**2**)$_2$(**3**)$_2$ and (**2**)$_3$(**3**)[19] toward tyramine (**3.10**) and ephedrine (**3.11**) have been already determined experimentally by Dr. R. F. Ludlow, a former member in our research group. These affinities were determined by isothermal titration calorimetry (ITC).[10] The obtained values from the titrations are shown in Table 5.12. This allowed us to validate the fitted binding affinities obtained using DCLFit against the binding affinities obtained using ITC. The results (Table 5.12) show that the data obtained using DCLFit and ITC agree within a range of the up to 2 kJ/mol deviation (a factor 2.2 in binding constant) that may be expected.[7] Afterwards, DCLFit experiments for guests **3.10** and **3.11** were repeated after constraining the binding affinities of (**2**)$_2$(**3**)$_2$ and (**2**)$_3$(**3**) to the ones obtained by ITC. The fitting details are shown in the experimental section (Paragraph 5.8.6). The fitted affinity constants of (**3**)$_4$ and (**2**)(**3**)$_3$ obtained after applying the constraints agree with the ones obtained before applying the constrains, within a range of deviation of up to 2.7 (Table 5.12). Although decreasing the number of binding affinities to fit allowed to reproduce more closely the observed concentrations of (**3**)$_4$ and (**2**)(**3**)$_3$, the error ε increased slightly due to the fact that the constrained affinity constants are slightly different than the fitted constants that correspond to the lowest error (ε).

Table 5.12: Fitted affinity constants, affinity constants obtained using ITC and (in parentheses) fitted affinity constants obtained after constraining the values of the other binding constants to those obtained by ITC (all in M^{-1}) for binding of templates **3.10** and **3.11** to different macrocycles in a DCL made from building blocks **2** and **3** in 50 mM borate buffer. While the fitting experiments were performed at pH = 8.4, ITC experiments were performed at pH = 8.

Template	Method	(**3**)$_4$	(**2**)(**3**)$_3$	(**2**)$_2$(**3**)$_2$	(**2**)$_3$(**3**)	(**2**)$_4$
3.10	DCLFit[b]	6.2×10^4	4.1×10^4	9.8×10^4	5.8×10^4	n.d.[a]
		(4.6×10^4)	(4.0×10^4)	constrained	constrained	n.d.[a]
	ITC	n.m.[a]	n.m.[a]	1.3×10^5	1.0×10^5	n.m.[a]
3.11	DCLFit[b]	4.0×10^3	2.5×10^3	9.9×10^3	2.0×10^4	n.d.[a]
		(1.1×10^4)	(5.8×10^3)	constrained	constrained	n.d.[a]
	ITC	n.m.[a]	n.m.[a]	1.6×10^4	2.5×10^4	n.m.[a]

[a] n.d. = not detected, n.m. = not measured. [b] = values with parentheses were fitted by constraining the values of the other binding constants to those obtained by ITC.

5.5 AF and not AF_n reflects the binding strength of the most amplified library member at substoichiometric template concentration

We then compared the regular amplification factors (AF) and the normalized ones (AF_n) of the hosts with the host-guest binding strengths. The compared amplification data are those obtained at substoichiometric template concentrations (1:10 template to total building block ratio) (Table 5.13). Data obtained show that regular amplification factors (AF) obtained with templates **3.9**, **3.10**, **3.11** and **3.12** point towards (**2**)(**3**)$_3$, (**2**)$_2$(**3**)$_2$, (**2**)$_3$(**3**) and (**2**)$_2$(**3**)$_2$ respectively as strong binders. This turned out to be reflected in the binding constants: templates **3.9**, **3.10**, **3.11** and **3.12** have better affinities for (**2**)(**3**)$_3$, (**2**)$_2$(**3**)$_2$, (**2**)$_3$(**3**) and (**2**)$_2$(**3**)$_2$ respectively, in comparison with their affinities to the rest of the library members. As the most amplified hosts

become a drag on the building block reservoir in each of the templated DCLs, this hampers the amplification of the remaining hosts so that their AF does not correlate any longer with host-guest binding. Note that comparing the amplification data between DCLs templated with different guests is unreliable,[20] as the nature of the added template has a direct impact on the amount of overoxidized products and therefore on the amounts of building blocks available in each of the templated DCLs (Paragraph 5.8.3). The normalized amplification factors (*AFn*) for the generated hosts obtained upon addition of templates **3.9**-**3.12** correlate less well with the host-guest binding constants.

Table 5.13: Comparison between amplification data of the five hosts, obtained at a ratio template to total building block concentration of 1:10, and the host-guest binding affinities (in M^{-1}). The highest amplification factor for each DCL is shown in bold. Amplification data of $(\mathbf{2})_2(\mathbf{3})_3$ are discarded as this oligomer does not respond to templates **3.9**-**3.12**. Templates **3.9**-**3.12** are added at 0.4 mM concentration to a DCL made from equimolar amounts of building blocks **2** and **3** (2.0 mM each) and prepared in 50 mM borate buffer solutions at pH = 8.4. The order of the host-guest binding affinities obtained using both ITC and DCLFit is similar and therefore any of the two data reflect the binding quality.

Template		$(\mathbf{3})_4$	$(\mathbf{2})(\mathbf{3})_3$	$(\mathbf{2})_2(\mathbf{3})_2$	$(\mathbf{2})_3(\mathbf{3})$	$(\mathbf{2})_4$
3.9	AF_n	-0.01	0.07	**0.12**	0.01	0.00
	AF	1.07	**1.83**	1.17	1.23	1.57
	Affinity constants	2.17×10^4	$\mathbf{2.85 \times 10^4}$	7.80×10^3	5.42×10^3	3.15×10^3
3.10	AF_n	0.02	0.00	**0.36**	-0.01	0.00
	AF	1.19	0.94	**1.48**	0.81	0.67
	Affinity constants	6.2×10^4	4.1×10^4	$\mathbf{9.8 \times 10^4}$	5.8×10^4	n.d.[a]
3.11	AF_n	0.02	-0.03	**0.19**	0.04	0.00
	AF	1.21	0.70	1.21	**1.82**	1.33
	Affinity constants	4.0×10^3	2.5×10^3	9.9×10^3	$\mathbf{2.0 \times 10^4}$	4.0×10^3
3.12	AF_n	0.00	0.01	**0.30**	0.02	-0.01
	AF	1.04	1.04	**1.43**	1.36	0.54
	Affinity constants	3.68×10^3	3.16×10^3	$\mathbf{3.82 \times 10^3}$	2.97×10^3	n.d.[a]

[a] n.d. = not detected

5.6 Range of affinity constants that DCLFit can reliably generate

DCLFit is capable to generate estimates of equilibrium constants for binding of DCL members to templates that induce the amplifications of these library members. In principle, the estimated constants can be calculated for an unlimited range of affinity constants. However in practice, the reliability of the fitting results depends on two experimental conditions: a) the detection limit of the analytical tool used to measure the concentrations of the library members which constitute the input data and b) the relevant range of library member concentrations suitable to obtain accurate binding constants. First, the analytical tool used to generate the input data for the DCLFit experiments presented in this chapter is an HPLC-UV system with a detection limit in the order of 10^{-5} M. This restricted the capability of DCLFit to estimate, reliably, the binding strengths of library members with concentrations close to the detection, although these members were amplified after the template addition. This was the case for oligomers (**2**)$_3$(**3**) and (**2**)$_4$ after adding **3.9**, **3.11** and **3.12**, and (**2**)$_3$(**3**) and (**3**)$_4$ after adding **3.10**, where relatively poor correlations between their fitted and experimental concentrations were observed. However better fittings were observed for oligomers with concentrations in the order of 10^{-4} M, where good correlations between their fitted and experimental concentrations were observed. This was the case for (**2**)$_2$(**3**)$_2$ and (**2**)(**3**)$_3$ after adding **3.9** and (**2**)$_2$(**3**)$_2$ after adding **3.10**-**3.12**. As a result, the use of an analytical tool with a better detection limit such as an UPLC-UV system may improve the fitting quality for library members with concentrations lower than 10^{-4} M. Second, the range of equilibrium constant values for host-guest binding that DCLFit can reliably generate should be, ideally, in the same range as the values of the reciprocal host concentrations. This gives quasi host-guest binding curves ideally of hyperbolic shapes where any change of the binding affinity should change the shape of the curve. For the DCL distributions fitted in this chapter, the range of affinity constants for host-guest binding generated using DCLFit varies from 10^3 to 10^4 M^{-1}. This can be counted as reliable as it is within the range of the reciprocal host concentrations (10^{-5} M to 10^{-4} M). However, in case of DCL members with binding affinities to the added template that are considerably higher (several orders of magnitude) than the affinities of the rest of the library members, the concentrations of these library members should be within the range of their reciprocal affinity constants. If not, the fitted affinity values generated by the program are not reliable. In principle decreasing the total building block concentration would decrease the concentrations of the formed oligomers and therefore result in host-guest binding curves that may be reliably fitted. However, lowering the building block concentration affects also the rates of the reversible disulfide reaction used to connect the building blocks. Disulfide exchange is second order in overall building block concentration and thiol oxidation is first-order in building block concentration, and therefore the dependence of each process on the concentration is different. Al low concentration, oxidation is faster than disulfide exchange and therefore the product distribution of the system is often not longer under thermodynamic control.[21]

5.7 Conclusion

Using DCLFit software, we have estimated reliably the affinity constants of some of the receptors generated in a DCL made from building blocks **2** and **3** toward three biologically active compounds **3.10**, **3.11** and **3.12** and compound **3.9** of unknown biological activity. All of the reported affinities were estimated in near physiological conditions i.e. in borate buffer solution at pH = 8.4. The affinity of receptor (**2**)$_2$(**3**)$_2$ toward tyramine (**3.10**) is the highest reported thus far for synthetic receptors for tyramine,[22] and is within the range of affinities of adrenergic receptors for this amine.[23] The affinity of receptor (**2**)$_3$(**3**) toward ephedrine (**3.11**) is the highest reported thus far for synthetic receptors for this compound,[24] and is within the range of affinities of adrenergic receptors for ephedrine.[25] The affinity of receptor (**2**)$_2$(**3**)$_2$ toward nicotine (**3.12**) is

higher than the affinity of our previously reported receptor (**1**)$_2$(**2**)$_2$ toward nicotine (3.82 x 10^{-3} M^{-1} vs 1.81 x 10^{-3} M^{-1}) and is the highest reported thus far for synthetic receptors for this compound.[26] However, this affinity is still separated by a gap of several orders of magnitude from the affinity of nicotinic acetylcholine receptors for nicotine.[27]

5.8 Experimental section

5.8.1 DCL preparations

Building blocks **2** and **3** were synthesized following literature procedures.[6] Templates (**T**) **3.9**, **3.10**, **3.11** and **3.12** were obtained from Sigma-Aldrich and used without further purification.
Stock solutions of building blocks **2** and **3** and the templates were freshly prepared at 10 mM concentration by dissolving the appropriate amounts of building blocks **2** and **3** and of the chosen templates in 50 mM borate buffer at pH 8.4. The pH was readjusted to 8.4 by addition of an appropriate volume of a 1 M solution of KOH.

Table 5.14: Summary of the DCL preparations for the DCLFit experiments

	DCL composition at time zero min			Volume added of 10 mM stock solutions			
DCL number	[**2**] (mM)	[**3**] (mM)	**T**(mM)	(**2**) (µl)	(**3**) (µl)	(**3.9**-**3.12**) (µl)	Borate buffer solution (µl)
1	2.0	2.0	0	40	40	0	120
2	2.0	2.0	0.20	40	40	4	116
3	2.0	2.0	0.40	40	40	8	112
4	2.0	2.0	0.50	40	40	10	110
5	2.0	2.0	0.60	40	40	12	108
6	2.0	2.0	0.80	40	40	16	104
7	2.0	2.0	1.0	40	40	20	100
8	2.0	2.0	1.5	40	40	30	90
9	2.0	2.0	2.0	40	40	40	80
10	2.0	2.0	3.0	40	40	60	60
11	2.0	2.0	4.0	40	40	80	40

The DCL mixtures were allowed to oxidize and equilibrate by stirring for 4 days in closed vials at room temperature. After reaching equilibrium, each of the vials was manually shaken immediately before pipetting 10 µl using an eppendorf pipette. These 10 µl solutions were diluted with 200% volume DMSO in HPLC vials immediately prior to HPLC-UV analyses.

5.8.2 HPLC-UV analysis

HPLC analyses were performed using an Agilent 1100 series. Acetonitrile was purchased from Biosolve. Formic acid was purchased from Sigma-Aldrich. Analyses were performed using a reversed phase HPLC column (Kromasil C8, 4.6 x 150 mm, 5 µm) by injecting 3 µL of each of the DCL samples that were diluted with 200% volume DMSO immediately prior to their analyses. A flow rate of 1 ml/min was used. The mobile phase consisted of a mixture of acetonitrile and doubly distilled water (both containing 0.1% formic acid), using the following gradient:

Time	Acetonitrile

(min)	(%)
0	30
5	40
30	70
35	70
40	95
50	95
55	30

HPLC-UV chromatograms were monitored at λ_{abs} = 260 nm and λ_{ref} = 550 nm.

5.8.3 Quantification of overoxidized species

Table 5.15: Estimation of concentrations and percentages of building blocks **2** and **3** (mM) taken up by the overoxidized species formed in DCLs made from equimolar amounts (2.0 mM each) of building blocks **2** and **3** (to the left) at ten different template **3.9** concentrations and (to the right) at ten different template **3.12** concentrations.

		Concentration and percentage in overoxidized products									
DCL	[**3.9**] mM	[**2**] mM	[**3**] mM	(**2**) %	(**3**) %	DCL	[**3.12**] mM	[**2**] mM	[**3**] mM	(**2**) %	(**3**) %
1	0	0.754	0.673	37.7	33.7	1	0	0.750	0.660	37.5	33.0
2	0.2	0.595	0.452	29.7	22.6	2	0.2	0.733	0.588	36.7	29.4
3	0.4	0.551	0.366	27.5	18.3	3	0.4	0.426	0.280	21.3	14.0
4	0.5	0.547	0.331	27.4	16.5	4	0.5	0.356	0.219	17.8	11.0
5	0.6	0.554	0.295	27.7	14.7	5	0.6	0.680	0.573	34.0	28.7
6	0.8	0.465	0.227	23.3	11.3	6	0.8	0.361	0.131	18.0	6.5
7	1	0.503	0.185	25.2	9.3	7	1	0.334	0.163	16.7	8.1
8	2	0.407	0.195	20.4	9.7	8	1.5	0.361	0.237	22.0	13.5
9	3	0.439	0.258	22.0	12.9	9	2	0.261	0.019	13.1	1.0
10	4	0.373	0.207	18.7	10.4	10	3	0.276	0.119	13.8	5.9
						11	4	0.274	0.102	13.7	5.1

Table 5.16: Estimation of concentrations and percentages of building blocks **2** and **3** (mM) taken up by the overoxidized species formed in DCLs made from equimolar amounts (2.0 mM each) of building blocks **2** and **3** (to the left) at ten different template **3.10** concentrations and (to the right) at ten different template **3.11** concentrations.

	Concentration and percentage in overoxidized products									
DCL	[**3.10**] mM	[**2**] mM	[**3**] mM	(**2**) %	(**3**) %	[**3.11**] mM	[**2**] mM	[**3**] mM	(**2**) %	(**3**) %
1	0	0.833	0.740	41.6	37.0	0	0.728	0.620	36.4	31.0
2	0.2	0.391	0.189	19.6	9.5	0.2	0.633	0.503	31.7	25.1
3	0.4	0.560	0.352	28.0	17.6	0.4	0.510	0.422	25.5	21.1
4	0.5	0.443	0.197	22.2	9.9	0.5	0.424	0.291	21.2	14.6
5	0.6	0.293	0.058	14.6	2.9	0.6	0.678	0.569	33.9	28.5
6	0.8	0.166	0.000	8.3	0.0	0.8	0.364	0.240	18.2	12.0
7	1	0.180	0.000	9.0	0.0	1	0.347	0.339	17.4	17.0
8	1.5	0.136	0.000	6.8	0.0	1.5	0.304	0.204	15.2	10.2
9	2	0.292	0.000	14.6	0.0	2	0.194	0.090	9.7	4.5
10	3	0.190	0.031	9.5	1.6	3	0.207	0.095	10.4	4.8
11	4	0.203	0.043	10.2	2.1	4	0.135	0.036	6.8	1.8

5.8.4 Measured HPLC-UV peak areas

Table 5.17: Measured HPLC-UV peak areas corresponding to the DCL members in DCLs made from equimolar amounts (2.0 mM each) of building blocks **2** and **3** at ten different template **3.9** concentrations. DCLs were prepared in 50 mM borate buffer solutions at pH = 8.4.

		HPLC-UV peak areas (mAU·min)							
DCL	[**3.9**] mM	$(\mathbf{3})_4$	$(\mathbf{2})(\mathbf{3})_3$	$(\mathbf{2})_2(\mathbf{3})_3$	$(\mathbf{2})_2(\mathbf{3})_2$	$(\mathbf{2})_3(\mathbf{3})$	$(\mathbf{2})_4$	$(\mathbf{2})_3(\mathbf{3})$-$(\mathbf{2})_4$	$(\mathbf{2})_4$-$(\mathbf{2})_4$
1	0	56	177	102	1475	208	85	151	54
2	0.2	50	272	70	1740	230	82	147	28
3	0.4	60	321	65	1731	258	130	130	18
4	0.5	66	330	60	1752	262	136	102	22
5	0.6	60	376	59	1762	233	126	102	14
6	0.8	66	370	67	1832	299	154	90	9
7	1	67	410	49	1847	316	154	0	0
8	2	54	397	48	1905	391	190	0	0
9	3	47	378	40	1878	401	172	0	0
10	4	49	415	45	1856	440	227	0	0

Table 5.18: Measured HPLC-UV peak areas corresponding to the DCL members in DCLs made from equimolar amounts (2.0 mM each) of building blocks **2** and **3** at ten different template **3.10** concentrations. DCLs were prepared in 50 mM borate buffer solutions at pH = 8.4.

		HPLC-UV peak areas (mAU·min)							
DCL	[**3.10**] mM	(**3**)$_4$	(**2**)(**3**)$_3$	(**2**)$_2$(**3**)$_3$	(**2**)$_2$(**3**)$_2$	(**2**)$_3$(**3**)	(**2**)$_4$	(**2**)$_3$(**3**)-(**2**)$_4$	(**2**)$_4$-(**2**)$_4$
1	0	48	131	71	1564	148	16	156	33
2	0.2	64	171	62	2415	137	16	126	20
3	0.4	57	125	31	2323	121	13	34	0
4	0.5	54	139	19	2625	93	0	0	0
5	0.6	62	118	13	2873	136	0	0	0
6	0.8	65	113	13	3058	181	0	0	0
7	1	61	127	20	3040	159	0	0	0
8	1.5	63	122	16	3086	181	14	0	0
9	2	56	106	13	2768	222	15	0	0
10	3	54	100	13	2975	223	0	0	0
11	4	55	98	29	2927	233	0	0	0

Table 5.19: Measured HPLC-UV peak areas corresponding to the DCL members in DCLs made from equimolar amounts (2.0 mM each) of building blocks **2** and **3** at eleven different template **3.11** concentrations. DCLs were prepared in 50 mM borate buffer solutions at pH = 8.4.

		HPLC-UV peak areas (mAU·min)							
DCL	[**3.11**] mM	(**3**)$_4$	(**2**)(**3**)$_3$	(**2**)$_2$(**3**)$_3$	(**2**)$_2$(**3**)$_2$	(**2**)$_3$(**3**)	(**2**)$_4$	(**2**)$_3$(**3**)-(**2**)$_4$	(**2**)$_4$-(**2**)$_4$
1	0	51	139	86	1724	164	21	149	30
2	0.2	52	126	97	1945	174	16	135	0
3	0.4	61	97	83	2082	300	25	109	0
4	0.5	60	110	80	2321	269	20	68	0
5	0.6	45	84	58	2006	245	18	0	0
6	0.8	53	101	69	2485	311	16	0	0
7	1	52	93	76	2222	564	22	0	0
8	1.5	54	85	64	2576	344	15	0	0
9	2	58	88	70	2737	370	17	0	0
10	3	60	90	75	2706	367	21	0	0
11	4	59	89	67	2831	372	28	0	0

Table 5.20: Measured HPLC-UV peak areas corresponding to the DCL members in DCLs made from equimolar amounts (2.0 mM each) of building blocks **2** and **3** at eleven different template **3.12** concentrations. DCLs were prepared in 50 mM borate buffer solutions at pH = 8.4.

		HPLC-UV peak areas (mAU·min)							
DCL	[**3.12**] mM	(**3**)$_4$	(**2**)(**3**)$_3$	(**2**)$_2$(**3**)$_3$	(**2**)$_2$(**3**)$_2$	(**2**)$_3$(**3**)	(**2**)$_4$	(**2**)$_3$(**3**)-(**2**)$_4$	(**2**)$_4$-(**2**)$_4$
1	0	60	171	93	1504	203	76	151	60
2	0.2	50	163	89	1733	159	25	147	0
3	0.4	62	178	93	2150	274	43	130	0
4	0.5	59	202	111	2206	269	105	102	0
5	0.6	50	138	78	1812	229	42	102	0
6	0.8	67	212	99	2332	235	39	92	0
7	1	60	189	76	2378	322	81	0	0
8	1.5	63	181	85	2185	444	84	0	0
9	2	65	218	73	2553	320	33	0	0
10	3	58	183	53	2491	387	35	0	0
11	4	59	195	57	2484	386	35	0	0

5.8.5 Amplification factor (AF) data

Table 5.21: Amplification factors of library members in DCLs made from equimolar amounts (2.0 mM each) of building blocks **2** and **3** at ten different template **3.9** concentrations. DCLs were prepared in 50 mM borate buffer solutions at pH = 8.4.

		Amplification factor (AF)							
DCL	[**3.9**] mM	(**3**)$_4$	(**2**)(**3**)$_3$	(**2**)$_2$(**3**)$_3$	(**2**)$_2$(**3**)$_2$	(**2**)$_3$(**3**)	(**2**)$_4$	(**2**)$_3$(**3**)-(**2**)$_4$	(**2**)$_4$-(**2**)$_4$
1	0	1.0	1.0	1.0	1.0	1.0	1.0	1.0	1.0
2	0.2	0.9	**1.5**	0.7	**1.2**	**1.1**	**1.0**	1.0	0.5
3	0.4	1.1	**1.8**	0.6	**1.2**	**1.2**	**1.5**	0.9	0.3
4	0.5	1.2	**1.9**	0.6	**1.2**	**1.3**	**1.6**	0.7	0.4
5	0.6	1.1	**2.1**	0.6	**1.2**	**1.1**	**1.5**	0.7	0.3
6	0.8	1.2	**2.1**	0.7	**1.2**	**1.4**	**1.8**	0.6	0.2
7	1	1.2	**2.3**	0.5	**1.3**	**1.5**	**1.8**	0.0	0.0
8	2	1.0	**2.2**	0.5	**1.3**	**1.9**	**2.2**	0.0	0.0
9	3	0.8	**2.1**	0.4	**1.3**	**1.9**	**2.0**	0.0	0.0
10	4	0.9	**2.3**	0.4	**1.3**	**2.1**	**2.7**	0.0	0.0

Table 5.22: Amplification factors of library members in DCLs made from equimolar amounts (2.0 mM each) of building blocks **2** and **3** at ten different template **3.10** concentrations. DCLs were prepared in 50 mM borate buffer solutions at pH = 8.4.

		Amplification factor (AF)							
DCL	[**3.10**] mM	(**3**)$_4$	(**2**)(**3**)$_3$	(**2**)$_2$(**3**)$_3$	(**2**)$_2$(**3**)$_2$	(**2**)$_3$(**3**)	(**2**)$_4$	(**2**)$_3$(**3**)-(**2**)$_4$	(**2**)$_4$-(**2**)$_4$
1	0	1.0	1.0	1.0	1.0	1.0	1.0	1.0	1.0
2	0.2	**1.3**	1.3	0.9	**1.5**	0.9	1.0	0.8	0.6
3	0.4	**1.2**	1.0	0.4	**1.5**	0.8	0.8	0.2	0.0
4	0.5	**1.1**	1.1	0.3	**1.7**	0.6	0.0	0.0	0.0
5	0.6	**1.3**	0.9	0.2	**1.8**	0.9	0.0	0.0	0.0
6	0.8	**1.4**	0.9	0.2	**2.0**	**1.2**	0.0	0.0	0.0
7	1	**1.3**	1.0	0.3	**1.9**	**1.1**	0.0	0.0	0.0
8	1.5	**1.3**	0.9	0.2	**2.0**	**1.2**	0.9	0.0	0.0
9	2	**1.2**	0.8	0.2	**1.8**	**1.5**	0.9	0.0	0.0
10	3	**1.1**	0.8	0.2	**1.9**	**1.5**	0.0	0.0	0.0
11	4	**1.1**	0.7	0.4	**1.9**	**1.6**	0.0	0.0	0.0

Table 5.23: Amplification factors of library members in DCLs made from equimolar amounts (2.0 mM each) of building blocks **2** and **3** at eleven different template **3.11** concentrations. DCLs were prepared in 50 mM borate buffer solutions at pH = 8.4.

		Amplification factor (AF)							
DCL	[**3.11**] mM	(**3**)$_4$	(**2**)(**3**)$_3$	(**2**)$_2$(**3**)$_3$	(**2**)$_2$(**3**)$_2$	(**2**)$_3$(**3**)	(**2**)$_4$	(**2**)$_3$(**3**)-(**2**)$_4$	(**2**)$_4$-(**2**)$_4$
1	0	1.0	1.0	1.0	**1.0**	**1.0**	1.0	1.0	1.0
2	0.2	1.0	0.9	1.1	**1.1**	**1.1**	0.8	0.9	0.0
3	0.4	1.2	0.7	1.0	**1.2**	**1.8**	1.2	0.7	0.0
4	0.5	1.2	0.8	0.9	**1.3**	**1.6**	1.0	0.5	0.0
5	0.6	0.9	0.6	0.7	**1.2**	**1.5**	0.9	0.0	0.0
6	0.8	1.0	0.7	0.8	**1.4**	**1.9**	0.8	0.0	0.0
7	1	1.0	0.7	0.9	**1.3**	**3.4**	1.0	0.0	0.0
8	1.5	1.1	0.6	0.7	**1.5**	**2.1**	0.7	0.0	0.0
9	2	1.1	0.6	0.8	**1.6**	**2.3**	0.8	0.0	0.0
10	3	1.2	0.6	0.9	**1.6**	**2.2**	1.0	0.0	0.0
11	4	1.2	0.6	0.8	**1.6**	**2.3**	1.3	0.0	0.0

Table 5.24: Amplification factors of library members in DCLs made from equimolar amounts (2.0 mM each) of building blocks **2** and **3** at eleven different template **3.12** concentrations. DCLs were prepared in 50 mM borate buffer solutions at pH = 8.4.

		Amplification factor (AF)							
DCL	[**3.12**] mM	$(\mathbf{3})_4$	$(\mathbf{2})(\mathbf{3})_3$	$(\mathbf{2})_2(\mathbf{3})_3$	$(\mathbf{2})_2(\mathbf{3})_2$	$(\mathbf{2})_3(\mathbf{3})$	$(\mathbf{2})_4$	$(\mathbf{2})_3(\mathbf{3})$-$(\mathbf{2})_4$	$(\mathbf{2})_4$-$(\mathbf{2})_4$
1	0	1.0	**1.0**	1.0	**1.0**	**1.0**	1.0	1.0	1.0
2	0.2	0.8	**1.0**	1.0	**1.2**	**0.8**	0.3	1.0	0.0
3	0.4	1.0	**1.0**	1.0	**1.4**	**1.3**	0.6	0.9	0.0
4	0.5	1.0	**1.2**	1.2	**1.5**	**1.3**	1.4	0.7	0.0
5	0.6	0.8	**0.8**	0.8	**1.2**	**1.1**	0.6	0.7	0.0
6	0.8	1.1	**1.2**	1.1	**1.6**	**1.2**	0.5	0.6	0.0
7	1	1.0	**1.1**	0.8	**1.6**	**1.6**	1.1	0.0	0.0
8	1.5	1.1	**1.1**	0.9	**1.5**	**2.2**	1.1	0.0	0.0
9	2	1.1	**1.3**	0.8	**1.7**	**1.6**	0.4	0.0	0.0
10	3	1.0	**1.1**	0.6	**1.7**	**1.9**	0.5	0.0	0.0
11	4	1.0	1.1	0.6	**1.7**	**1.9**	0.5	0.0	0.0

5.8.6 Fitting details and graphs of the ratio of fitted to observed concentrations of $(3)_4$ and $(2)(3)_3$ in the presence of templates 3.10 and 3.11, after constraining K_a of binding of $(2)_2(3)_2$ and $(2)_3(3)$ to 3.10 and 3.11 to the values obtained using ITC

K_a $(\mathbf{2})_n(\mathbf{3})_m$-**3.10** were fitted 50 times using a Monte-Carlo fitting method starting from randomly guessed affinities over a range of affinities varying from 0 to 10^7 M^{-1}. The set of fitted affinity constants (fitted K_a $(\mathbf{2})_n(\mathbf{3})_m$-**10**) (Table 5.12) obtained 43 times with a error ε = 0.35 was selected as it most closely reproduced the observed concentrations of the oligomers.

a)

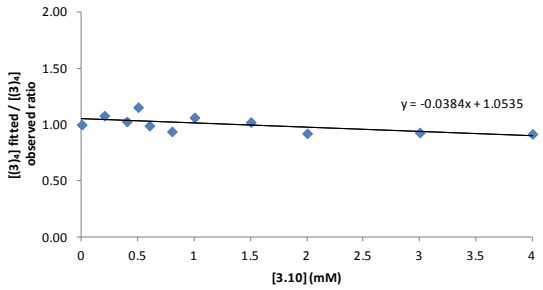

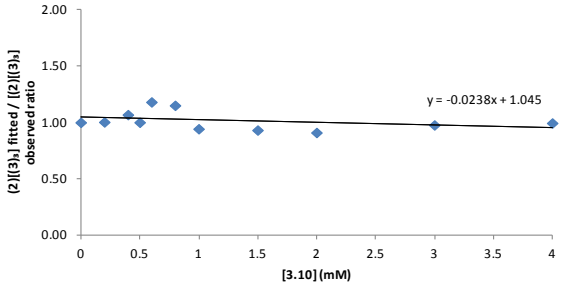

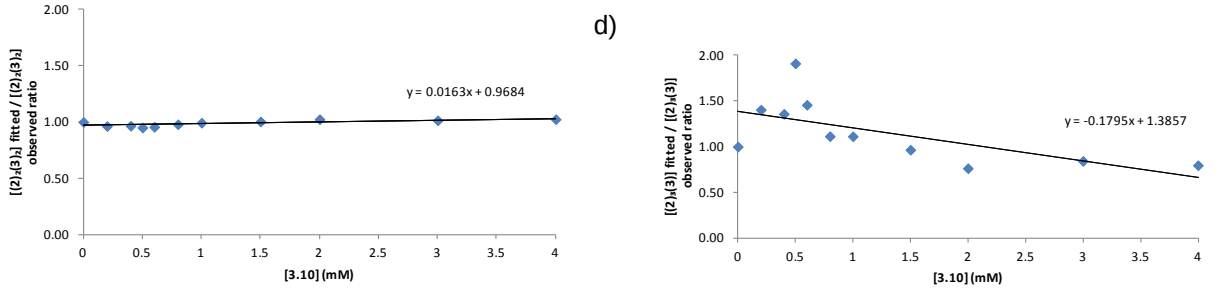

Figure 5.7: Graphs of the ratio of the fitted to the observed concentrations of (a) $(\mathbf{3})_4$, (b) $(\mathbf{2})(\mathbf{3})_3$, (c) $(\mathbf{2})_2(\mathbf{3})_2$ and (d) $(\mathbf{2})_3(\mathbf{3})$ as a function of the amount of added guest **3.10**.

K_a $(\mathbf{2})_n(\mathbf{3})_m$-**3.11** were fitted 100 times using a Monte-Carlo fitting method starting from randomly guessed affinities over a range of affinities varying from 0 to 10^7 M^{-1}. The set of fitted K_a $(\mathbf{2})_n(\mathbf{3})_m$-**11** (Table 5.12) obtained 80 times with a error ε = 0.14 was selected as it closely reproduced the observed concentrations of the oligomers.

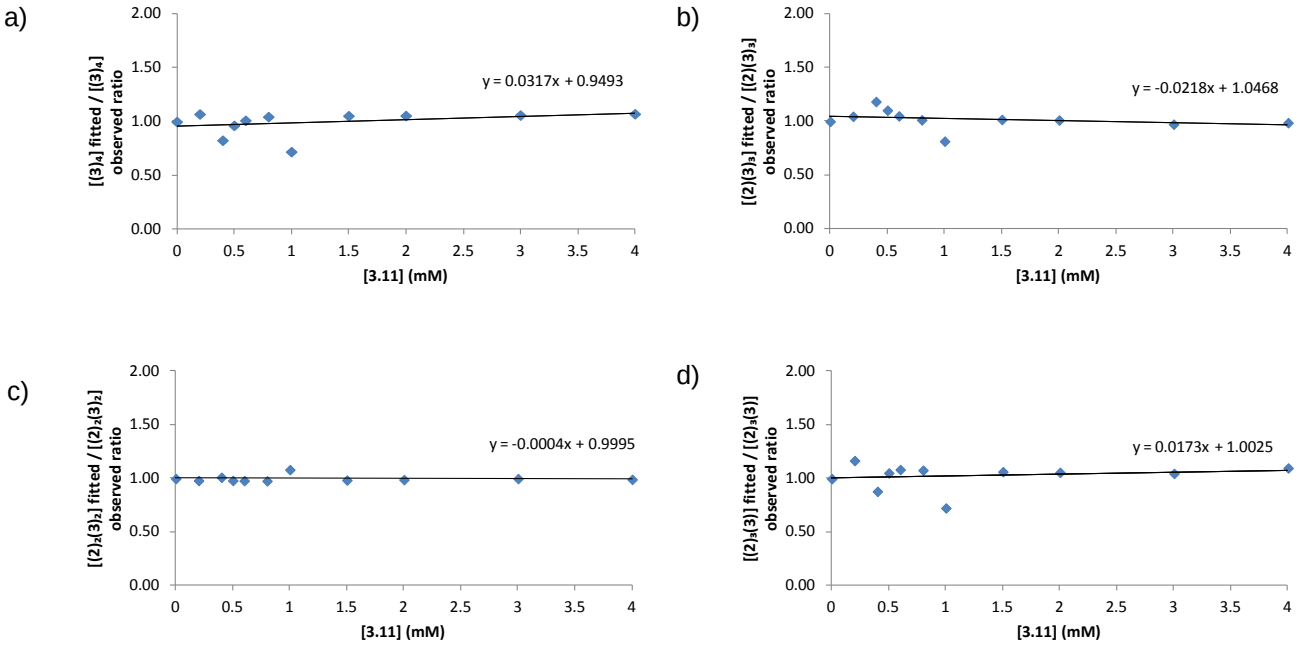

Figure 5.8: Graphs of the ratio of the fitted to the observed concentrations of (a) $(\mathbf{3})_4$, (b) $(\mathbf{2})(\mathbf{3})_3$, (c) $(\mathbf{2})_2(\mathbf{3})_2$ and (d) $(\mathbf{2})_3(\mathbf{3})$ as a function of the amount of added guest **3.11**.

5.8.7 Variation of observed concentrations of the oligomers as a function of concentrations of the individual templates

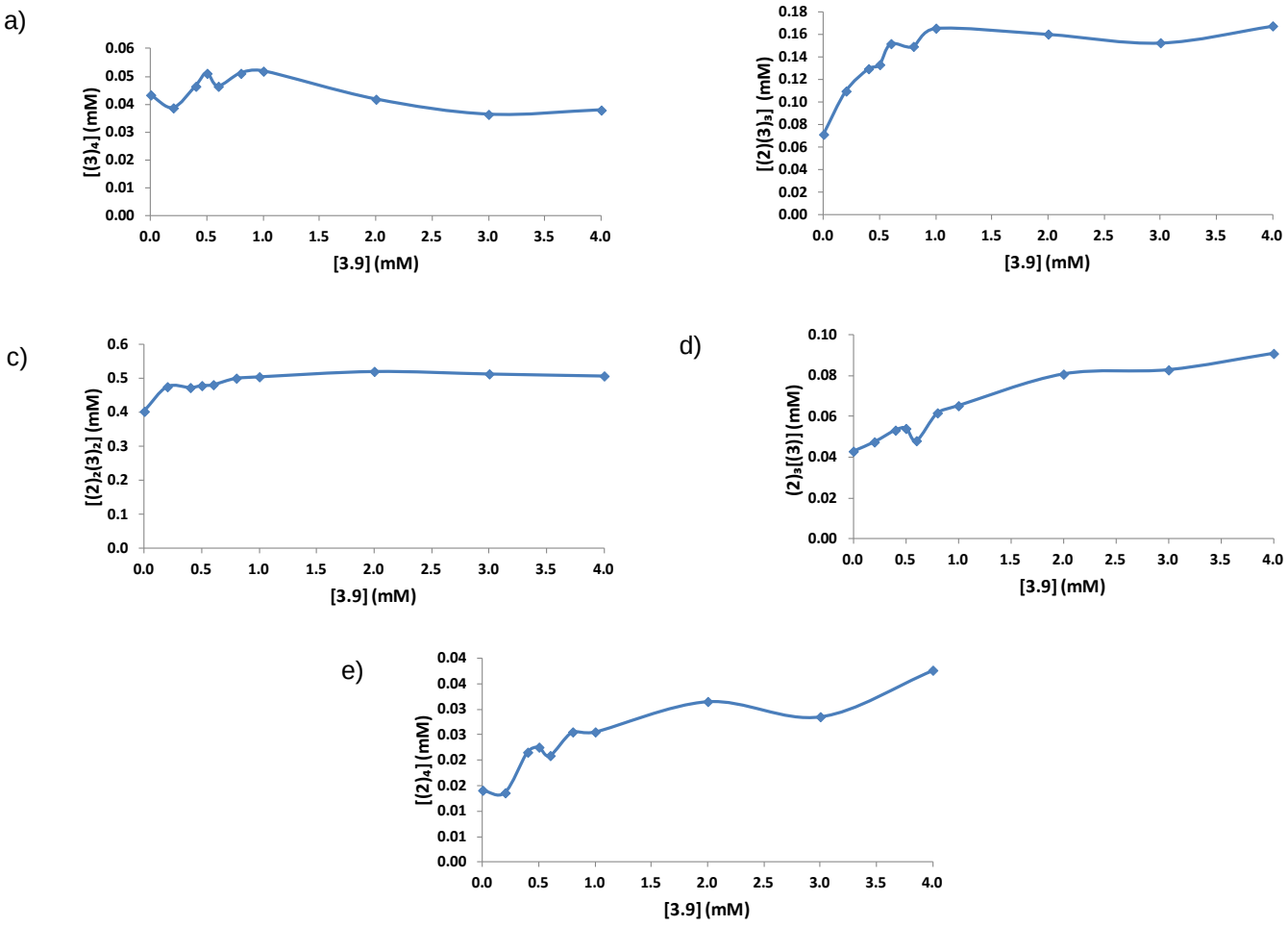

Figure 5.9: Variation of the observed concentrations of oligomers (a) (**3**)$_4$, (b) (**2**)(**3**)$_3$, (c) (**2**)$_2$(**3**)$_2$, (d) (**2**)$_3$(**3**) and (e) (**2**)$_4$ as a function of the concentration of template **3.9**.

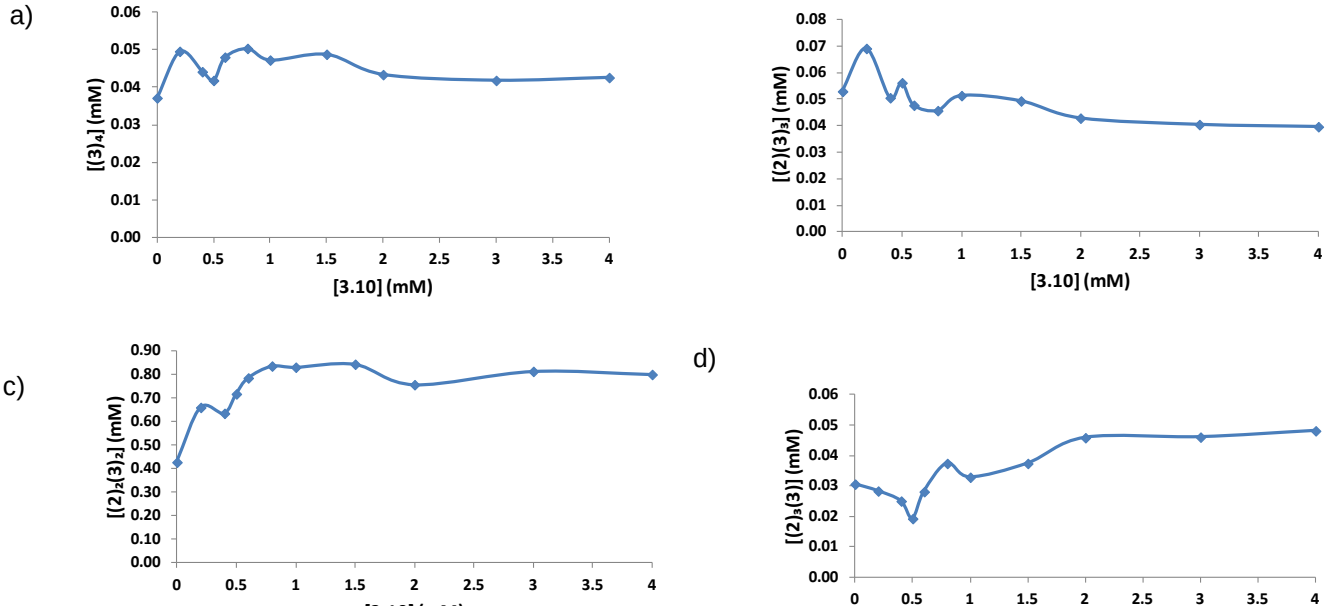

Figure 5.10: Variation of the observed concentrations of oligomers (a) (**3**)$_4$, (b) (**2**)(**3**)$_3$, (c) (**2**)$_2$(**3**)$_2$ and (d) (**2**)$_3$(**3**)as a function of the concentration of template **3.10**.

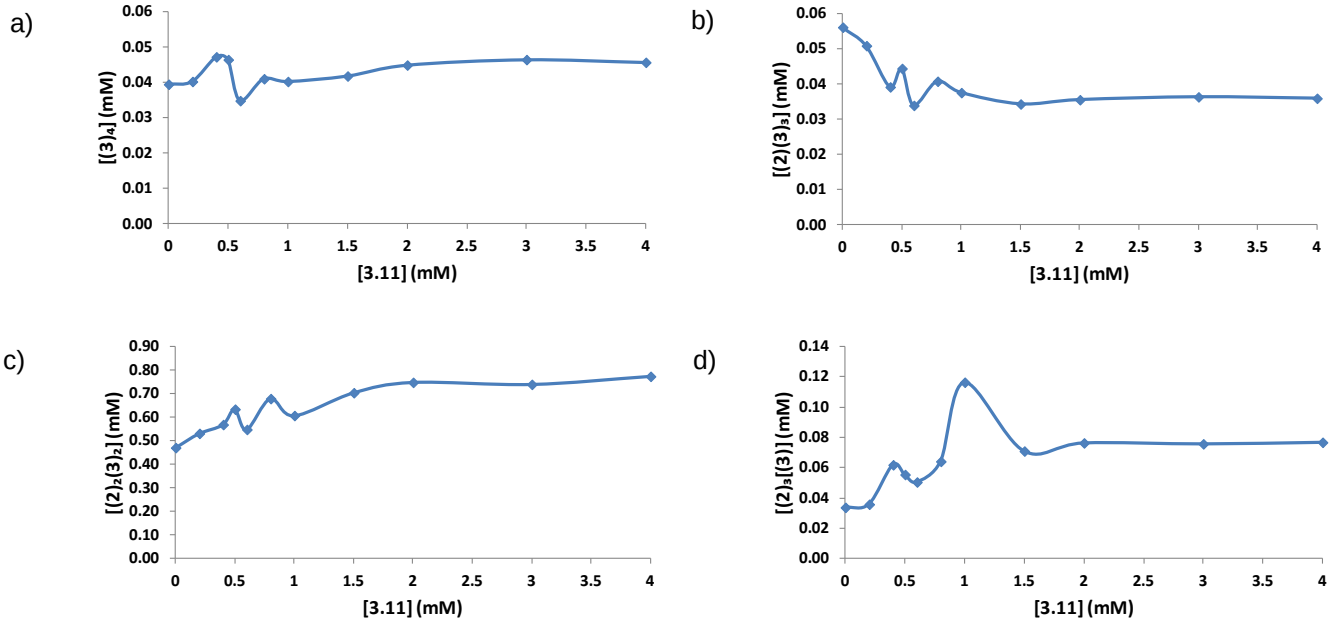

Figure 5.11: Variation of the observed concentrations of oligomers (a) (**3**)$_4$, (b) (**2**)(**3**)$_3$, (c) (**2**)$_2$(**3**)$_2$ and (d) (**2**)$_3$(**3**) as a function of the concentration of template **3.11**.

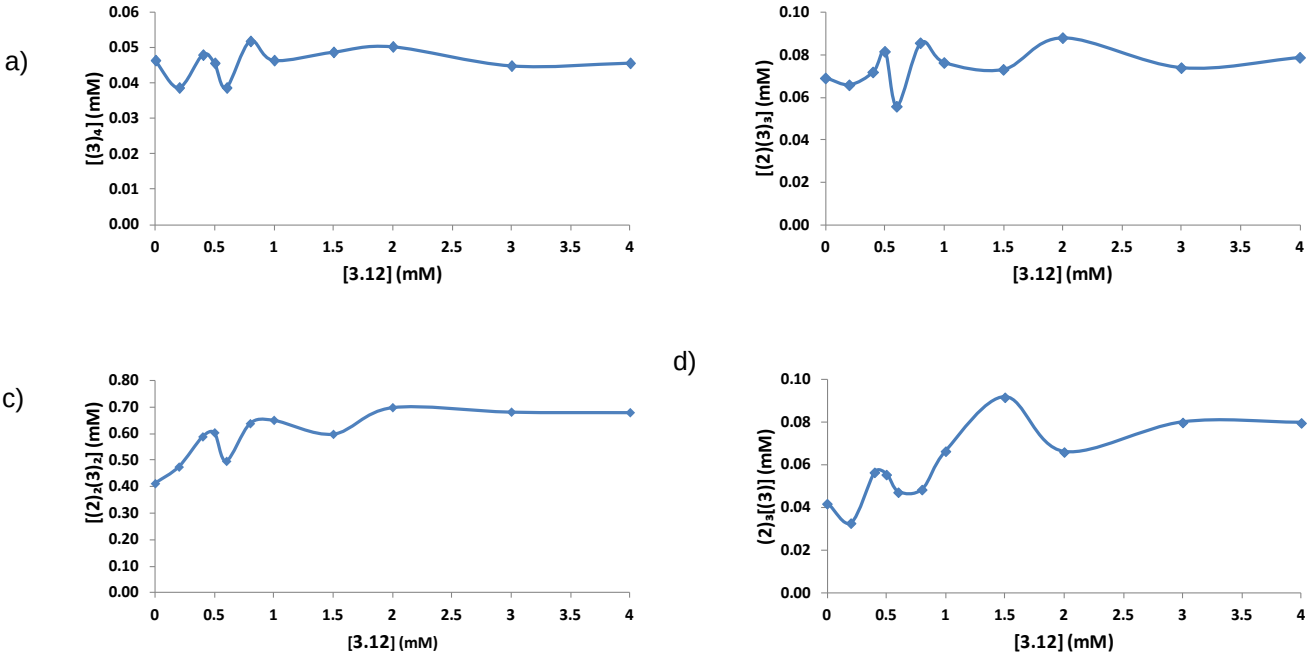

Figure 5.12: Variation of the observed concentrations of oligomers (a) (**3**)$_4$, (b) (**2**)(**3**)$_3$, (c) (**2**)$_2$(**3**)$_2$ and (d) (**2**)$_3$(**3**) as a function of the concentration of template **3.12**.

5.9 References

[1] (a) Grote, Z.; Scopelliti, R.; Severin, K. *Angew. Chem. Int. Ed.* **2003**, *42*, 3821. (b) Severin, K. *Chem. Eur. J.* **2004**, *10*, 2565. (c) Saur, I.; Severin, K. *Chem. Commun.* **2005**, 1471.

[2] Otto, S. The practice of Dynamic Combinatorial Librairies: Analytical Chemistry, Experimental Design, and Data Analysis. In *Dynamic Combinatorial Chemistry*; Reek, J. N. H.; Otto, S., Wiley-VCH, Weinheim, **2010**; pp 23.

[3] (a) Corbett, P. T.; Sanders, J. K. M.; Otto, S. *J. Am. Chem. Soc.* **2005**, *127*, 9390. (b) Corbett, P. T.; Otto, S.; Sanders, J. K. M. *Chem. Eur. J.* **2004**, *10*, 3139.

[4] Corbett, P. T.; Sanders, J. K. M.; Otto, S. *Chem. Eur. J.* **2008**, *14*, 2153.

[5] While the two statistically less favored receptors $(\mathbf{2})_4$ and $(\mathbf{3})_4$ are both amplified upon addition of **3.1**, and without knowing the binding affinity of receptor $(\mathbf{2})_4$ to template **3.1**, it is difficult to conclude which of the two receptors has better affinity for **3.1**. However, upon lowering the template to total building block ratio from 1:2 to 1:8 (0.625 mM template : 5 mM (theoretical) total building block concentration), amplification of $(\mathbf{2})_4$ is reduced by 68.2 % while the amplification of $(\mathbf{3})_4$ is only reduced by 21.4 %. This suggests that the amplification of $(\mathbf{2})_4$ is facilitated by the fact that much of building block **3** is taken up in $(\mathbf{3})_4$ and $(\mathbf{2})(\mathbf{3})_3$ upon addition of **3.1** thus liberating building block **2**, rather than that $(\mathbf{2})_4$ has the highest affinity to **3.1** (see chapter 3 Paragraph 3.3.6.2 for more information).

[6] (a) West, K. R.; Ludlow, R. F.; Corbett, P. T.; Besenius, P.; Mansfeld, F. M.; Cormack, P. A. G.; Sherrington, D. C.; Goodman, J. M.; Stuart, M. C. A.; Otto, S. *J. Am. Chem. Soc.* **2008**, *130*, 10834. (b) Vial, L.; Ludlow, R. F.; Leclaire, J.; Perez-Fernandez, R.; Otto, S. *J. Am. Chem. Soc.* **2006**, *128,* 10253.

[7] Ludlow, R. F.; Liu, J.; Li, H.; Roberts, S. L.; Sanders, J. K. M.; Otto, S. *Angew. Chem. Int. Ed. Engl.* **2007**, *46*, 5762.

[8] Au-Yeung, H. Y.; Pengo, P.; Pantoş, G. D.; Otto, S.; Sanders, J. K. M. *Chem. Commun.* **2009**, 419.

[9] Hunt, R. A. R.; Ludlow, R. F.; Otto, S. *Org. Lett.* **2009**, *11*, 5110.

[10] Ludlow, R. F. Molecular networks: From dynamic combinatorial libraries to complex systems. PhD thesis, University of Cambridge, UK, **2008**.

[11] The absolute values of the constants of formation of the oligomers (Absolute K_f $(\mathbf{2})_n(\mathbf{3})_m$ = $[(\mathbf{2})_n(\mathbf{3})_m]$ / $[\mathbf{2}]^n$ x $[\mathbf{3}]^m$) do not need to be determined. Their relative values (relative K_f $(\mathbf{2})_n(\mathbf{3})_m$ = Absolute K_f $(\mathbf{2})_n(\mathbf{3})_m$ x $[\mathbf{2}]^n$ x $[\mathbf{3}]^m$) can just be set to the untemplated concentrations of the formed oligomers ($[(\mathbf{2})_n(\mathbf{3})_m]$) at thermodynamic equilibrium, since the concentrations of the two monomers **2** and **3** at thermodynamic equilibrium are constant and far below the detectability limit (for disulfide, the oxidation process is irreversible and the concentration of dithiols is almost zero). The relative K_f of oligomer $(\mathbf{2})_n(\mathbf{3})_m$ will reproduce its concentration in the simulation of the untemplated library.

[12] The error ε is defined as the sum of the logs of the ratios of observed and predicted concentration: $\varepsilon = \sum \sum (\log y_{i,j} - \log p_{i,j})^2$. $y_{i,j}$ = observed concentrations, of *i* library members in *j* libraries, calculated from the corresponding HPLC-UV peak areas. $p_{i,j}$ = predicted concentrations, of *i* library members in *j* libraries, calculated from the fitted affinity constant obtained using DCLFit.

[13] For more information about the iterative process and DCLFit see reference 10.

[14] Nelder, J.; Mead, R. *Computer J.*, **1965**, *7*, 308.

[15] The quasi host-guest binding curve is a graph that describes the variation of the observed concentration of an oligomer as a function of the concentration of the added template.

[16] This equation is valid as long as the value of C_2 and C_3 are independent of the molecular structures in which building blocks **2** and **3** reside. This was proven in chapter 3 where the extinction coefficients of monomers **2** and **3** were found to be additive for the cyclic library members.

[17] The total concentrations in building blocks **2** and **3** consumed by the disulfide macrocycles in all the prepared DCLs were not considered as constant. These were calculated following the mass balance equation: $[\mathbf{1} + \mathbf{2}] = \sum[\mathbf{1}]_n[\mathbf{2}]_m$ x n + $\sum[\mathbf{1}]_n[\mathbf{2}]_m$ x m. Note that DCLFit tries to find a set of final fitted concentrations of the oligomers which simultaneously satisfies the guessed equilibrium constants (fitted K_a $(\mathbf{2})_n(\mathbf{3})_m$-template) and the mass balance equations for the building blocks, using GOGS algorithm (see Perrin, D. D.; Sayce, I. G., *Talanta*, **1967**, *14*, 833).

[18] Without template addition, relative formation constants of the oligomers (relative $K_{f\ nmer}$) are able to reproduce their observed concentrations and therefore the ratios fitted/observed concentrations in this case are equal to one.

[19] Oligomers ($(\mathbf{2})_2(\mathbf{3})_2$ and $(\mathbf{2})_3(\mathbf{3})$) were isolated using preparative HPLC as mixtures of isomers.

[20] Regardless of the inconsistent experimental errors related to the manner of DCL preparations and analyses.
[21] Escalante, A. M.; Furlan, R. L. E. Development of Synthetic Receptors using Dynamic Combinatorial Chemistry. In *Dynamic Combinatorial Chemistry*; Reek, J. N. H.; Otto, S., Wiley-VCH, Weinheim, **2010**; pp 49.
[22] (a) Kim, J.; Raman, B.; Ahn, K. H. *J. Org. Chem.* **2006**, *71*, 38. (b) Secor, K. E.; Glass, T. E. *Org. Lett.* **2004**, *6*, 3727. (c) Inoue, M. B.; Velazquez, E. F.; Inoue, M.; Fernando, Q. *J. Chem. Soc. Perkin Trans. 2* **1997**, 2113.
[23] (a) Enan, E. E. *Insect Biochem. Mol. Biol.* **2005**, *35*, 309. (b) Roeder, T. *Annu. Rev. Entomol.* **2005**, *50*, 447. (c) Saudou, F.; Amlaiky, N.; Plassat, J. L.; Borrelli, E.; Hen, R. *EMBO J.* **1990**, *9*, 3611.
[24] (a) Witt, D.; Dziemidowicz, J.; Rachon, J. *Heteroat. Chem.* **2004**, *15*, 155. (b) Schrader, T. *J. Org. Chem.* **1998**, *63*, 264.
[25] (a) Vansal, S. S.; Feller, D. R. Biochem. Pharmacol. 1999, 58, 807. (b) Ma, G.; Bavadekar, S. A.; Davis, Y. M.; Lalchandani, S. G.; Nagmani, R.; Schaneberg, B. T.; Khan, I. A.; Feller, D. R. J. Pharmacol. Exp. Ther. 2007, 322, 214.
[26] (a) Kearney, P. C.; Mizoue, L. S.; Kumpf, R. A.; Forman, J. E.; McCurdy, A.; Dougherty, D. A. *J. Am. Chem. Soc.* **1993**, *115*, 9907. (b) Zhou, Y.; Yu, H.; Zhang, L.; Xu, H.; Wu, L.; Sun, J.; Wang, L. *Microchim. Acta.* **2009**, *164,* 63. (c) Berglund, J.; Cedergren, L.; Andersson, S. B. *Int. J. Pharma.* **1997**, *156,* 195.
[27] Xiu, X.; Puskar, N. L.; Shanata, J. A. P.; lester, H. A.; Dougherty, D. A. *Nature* **2009**, *458,* 534

Chapter 6: Dynamic combinatorial chemistry with amino acid derivatized building blocks: towards new structurally diverse and more responsive dynamic combinatorial libraries

Amino acids are part of the structure of many (non-peptidic) natural macrocycles with diverse biological activities including antiproliferative, antibiotic and ionophoric activities involving molecular recognition phenomena. This fact has inspired many supramolecular chemists to incorporate amino-acid residues into a wide range of synthetic macrocycles. These include crown ethers, cyclodextrins, calixarenes, cyclophanes, cyclams, zinc porphyrins and many other structures that have shown promising applications as catalysts, building blocks of self-assembled nanotubes, antibiotics, selective ion-transporters across a lipid membrane and in stereoselective recognition of biomolecules. In the DCC research field, DCLs of non-peptidic macrocycles containing amino acids, and working in aqueous and organic media, have been widely reported. These macrocycles have also shown applications as receptors for biomolecules, metal ions and electrostatically-complementary guests, as stereoselective receptors for biomolecules, covalent cage-like receptors for polyamines, in the formation of [2] and [3]-catenanes and as building blocks of a molecular trefoil knot. However, the reported DCLs working in near physiological conditions, which are our subjects of interest, are often formed from building blocks functionalized with only cysteine as amino acid. This is to mainly provide access to disulfide exchange and thereby allow monomeric building blocks to inter-connect and form large oligomers. In this chapter we survey DCC systems targeting the development of macrocycles functionalized with diverse amino acids and working in near physiological conditions.

*The first part of the introduction reviews the natural and synthetic amino acid functionalized macrocycles reported in the literature which have shown promising applications. Then, the reported DCLs which are able to generate amino acid derived macrocycles working in aqueous and organic media are reviewed. Afterwards, the importance of intra-molecular interactions potentially occurring in amino acid derived hosts in reinforcing the guest binding is highlighted as part of the motivation of the work presented in this chapter. Finally, the expected advantages from the derivatization of building blocks **2** and **3**, which are reported in the previous chapters, with natural amino acids are highlighted to further motivate the research presented in this chapter.*

*The second part of the chapter describes the synthesis of novel amino acid functionalized building blocks derived from dithiols **2** and **3**. The third part demonstrates how this new set of building blocks can be used to generate new structurally diverse DCLs. The use of these DCLs to select amino acid functionalized receptors for a range of biologically relevant molecules in water at near physiological pH and their abilities to address stereoselective recognition phenomena are also discussed in the third part of the chapter.*

6.1 Introduction

6.1.1 Natural and synthetic amino acid derived macrocycles: structures and applications

Amino acids are the building blocks of many enzymes, hormones, proteins and peptides, and are involved in many biological processes occurring in living cells. This made them a target for selective binding by many synthetic hosts[1-7] as these represent a tool to understand the phenomena governing the molecular recognition in biological environments. These include a wide range of receptors such as crown ether derivatives,[1] antibodies,[2] RNA,[3] pillarene,[4] ferrocene, calixarene, peptides, cucurbit[*n*]urils, sapphyrin-lasalocid conjugates, metalloporphyrins and many others.[5,6,7]

Amino acids are part of the structure of many non-peptidic[8] natural macrocycles of diverse biological activities[9-13] involving molecular recognition phenomena and including anti-cancer,[9,10] antibiotic,[11] ionophoric[12] and many other biological activities.[13] For instance the lithium complex of jasplakinolide (**6.1**) (Figure 6.1), a cyclodepispeptide isolated from the marine sponge *Jaspis johnstoni*, promotes through cation–π interactions the actin polymerization.[9] Cryptophycin-1 (**6.2**), a cytotoxin extracted from *Cyanobacterium*, inhibits the tubulin polymerization as a result of non covalent interactions with tubilin.[10] The biaryl ether K-13 (**6.3**), isolated from a *Micromonospora halophytica* culture, exhibited antibiotic activity by coordinating Zn^{2+} located in the active site of a member of zinc metalloproteinase family resulting in the inhibition of the latter.[11] Frangufoline (**6.4**), an alkaloid isolated from the seeds of *Zizyphus vulgaris*, exhibited Ca^{2+} and Mg^{2+} ionophoric activity (over Na^{+} , K^{+}, Ag^{+} or Ba^{2+}).[12]

The biological activities of the natural macrocycles derived from amino acids have inspired many supramolecular chemists to incorporate amino-acid residues into a wide range of synthetic receptors. These are based on crown ethers (**6.5** and **6.6**)[14], cyclodextrins (**6.7**),[15] calixarenes (**6.8** and **6.9**)[16,17] and calixarene-like macrocycles (**6.10**, **6.11** and **6.12**) (Figure 6.2),[18] in addition to cyclophanes (**6.13** and **6.14**)[19,20], cyclams (**6.15**)[21], zinc porphrins (**6.16** and **6.17**)[22,23] and many other macrocycles such as **6.18**[24] and **6.19**[25] (Figure 6.3). Some of the synthetic macrocycles that have been reported showed promising applications as antibiotics (**6.9**),[17] selective ion-transporters across a lipid membrane (**6.10**, **6.11** and **6.12**),[18] building blocks of self-assembled nanotubes (**6.14**),[20] catalysts (**6.15** and **6.19**)[21,25] and in stereoselective recognition of amino-acid derivatives (**6.18**).[24]

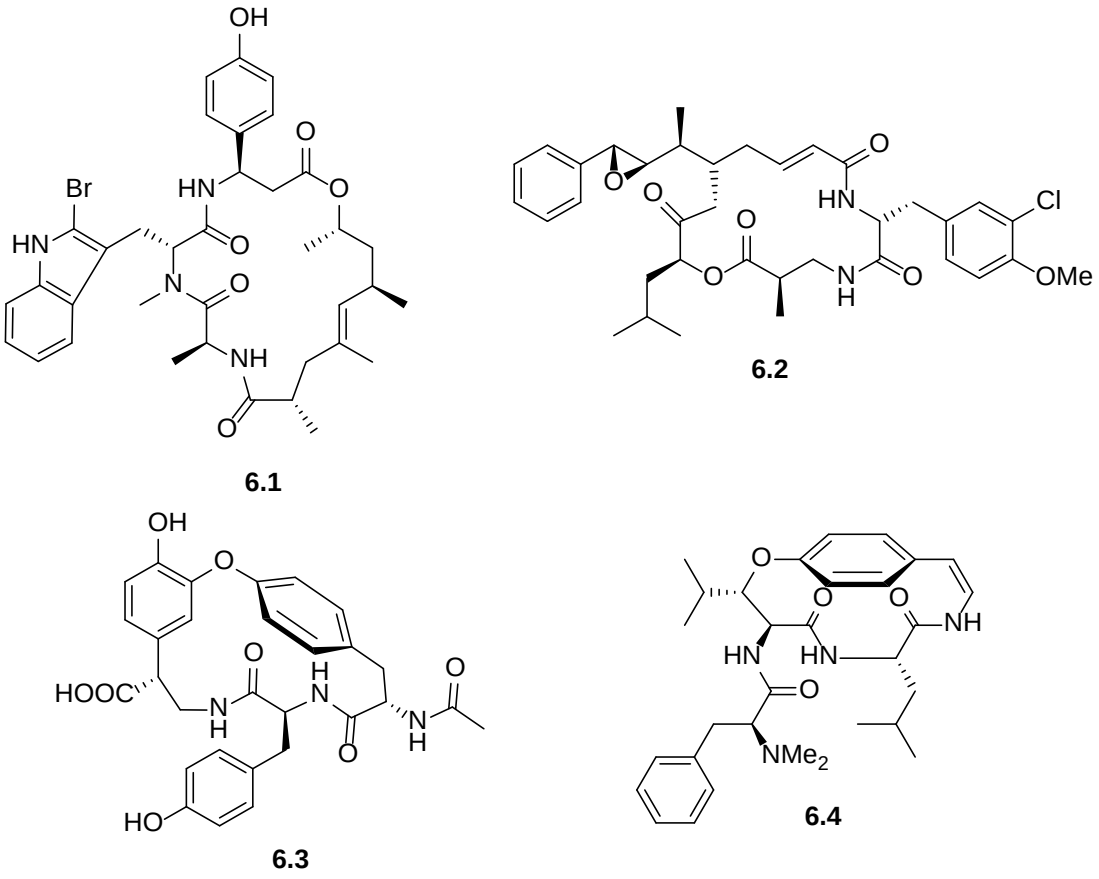

Figure 6.1: Naturally occurring amino acid derived macrocycles: jasplakinolide **6.1**, cryptophycin **6.2**, biaryl ether K-13 **6.3** and frangufoline **6.4**.

Dioxycyclam macrocycle **6.15** forms catalytically active complexes with Ni^{2+} for the conversion of trans-2-methylstyrene into the corresponding epoxide with sodium hypochlorite as terminal oxidant.[21] The Fe^{3+} complex of chiral macrocycle **6.19** was shown to catalyze the conversion of alkenes into corresponding epoxides in the presence of iodosylbenzene as terminal oxidant.[25] The (S)-phenylalanine-derived macrocycle **6.18** binds selectively to the carboxylic acid terminus of *N*-Cbz-β-alanyl-(*S*)-amino acids.[24]

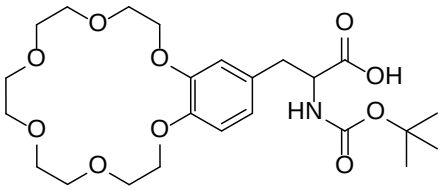

6.5

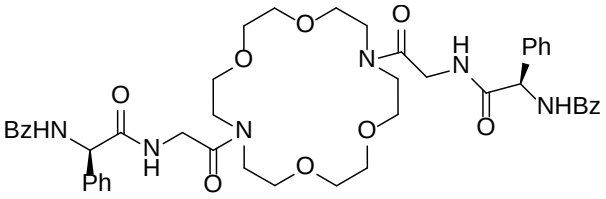

6.6

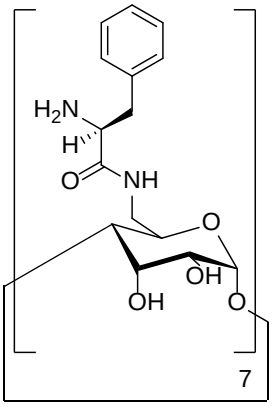

6.7

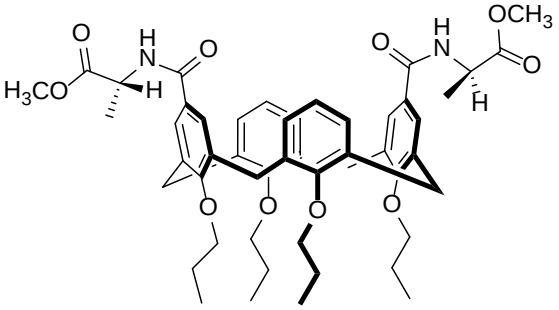

6.8

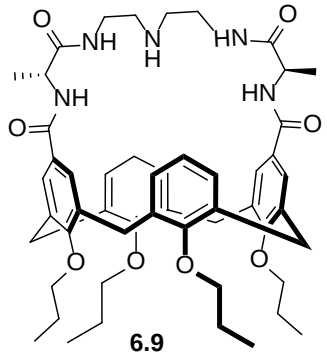

6.9

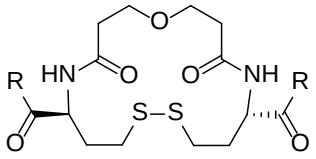

6.10 (R = OMe, LeuOMe, adamantane)

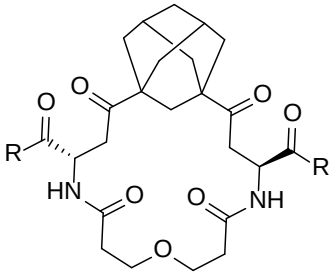

6.11 (R = OMe, LeuOMe, adamantane)

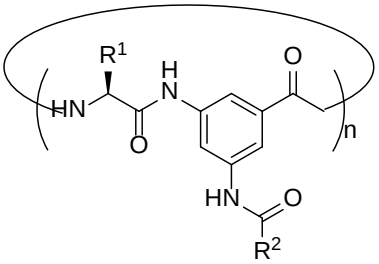

6.12

$R^1 = CH_3$, CH_2COO^-, $(CH_2)_4NH_3^+$

$R^2 = n\text{-}C_9H_{19}$, $n\text{-}C_{15}H_{31}$, $n\text{-}C_{17}H_{35}$

n = 3-5

Figure 6.2: Synthetic macrocycles derived from amino acids based on crown ethers (**6.5** and **6.6**), cyclodextrins (**6.7**), calixarenes (**6.8** and **6.9**) and calixarene-like macrocycles (**6.10**, **6.11** and **6.12**)

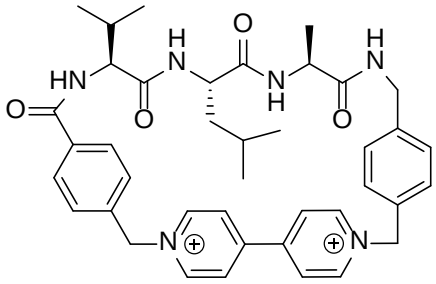

6.13

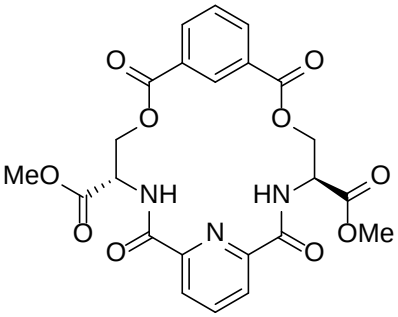

6.14

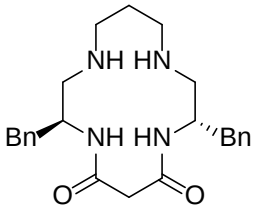

6.15

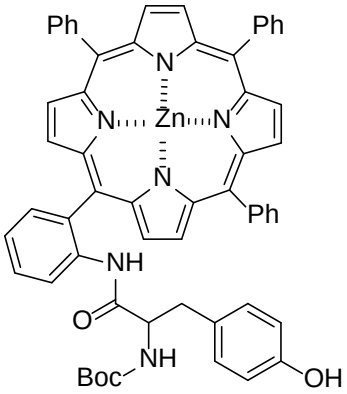

6.16

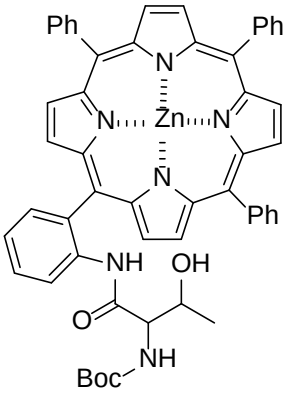

6.17

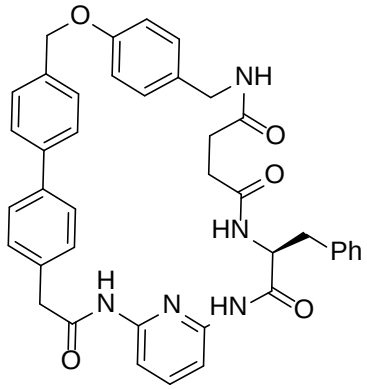

6.18

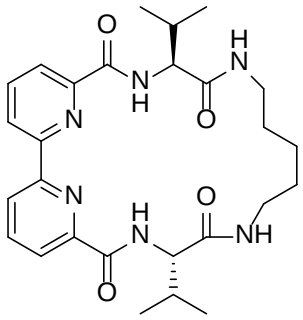

6.19

Figure 6.3: Synthetic macrocycles derived from amino acids based on cyclophanes (**6.13** and **6.14**), cyclams (**6.15**) and zinc porphrins (**6.16** and **6.17**) in addition to amino acid derived macrocycles **6.18** and **6.19**.

6.1.2 DCLs of amino acid functionalized macrocycles: structures and applications

Disulfide DCLs working in water at near physiological pH

DCLs of macrocycles containing amino acids have been widely reported in literature.[26-41] Cysteine is one of the amino acids that is most often introduced into the structures of building blocks forming these DCLs. As any other amino acid, cysteine provides amide and carboxylate functions capable to be engaged in hydrogen-bonding, ion pairing and salt bridge interactions useful in the context of molecular recognition, water solubility and flexibility of the building blocks. Furthermore, cysteine is the only natural amino acid that provides access to disulfide exchange and thereby allows building blocks to connect and form large oligomers in water at mildly basic conditions.[26-34]

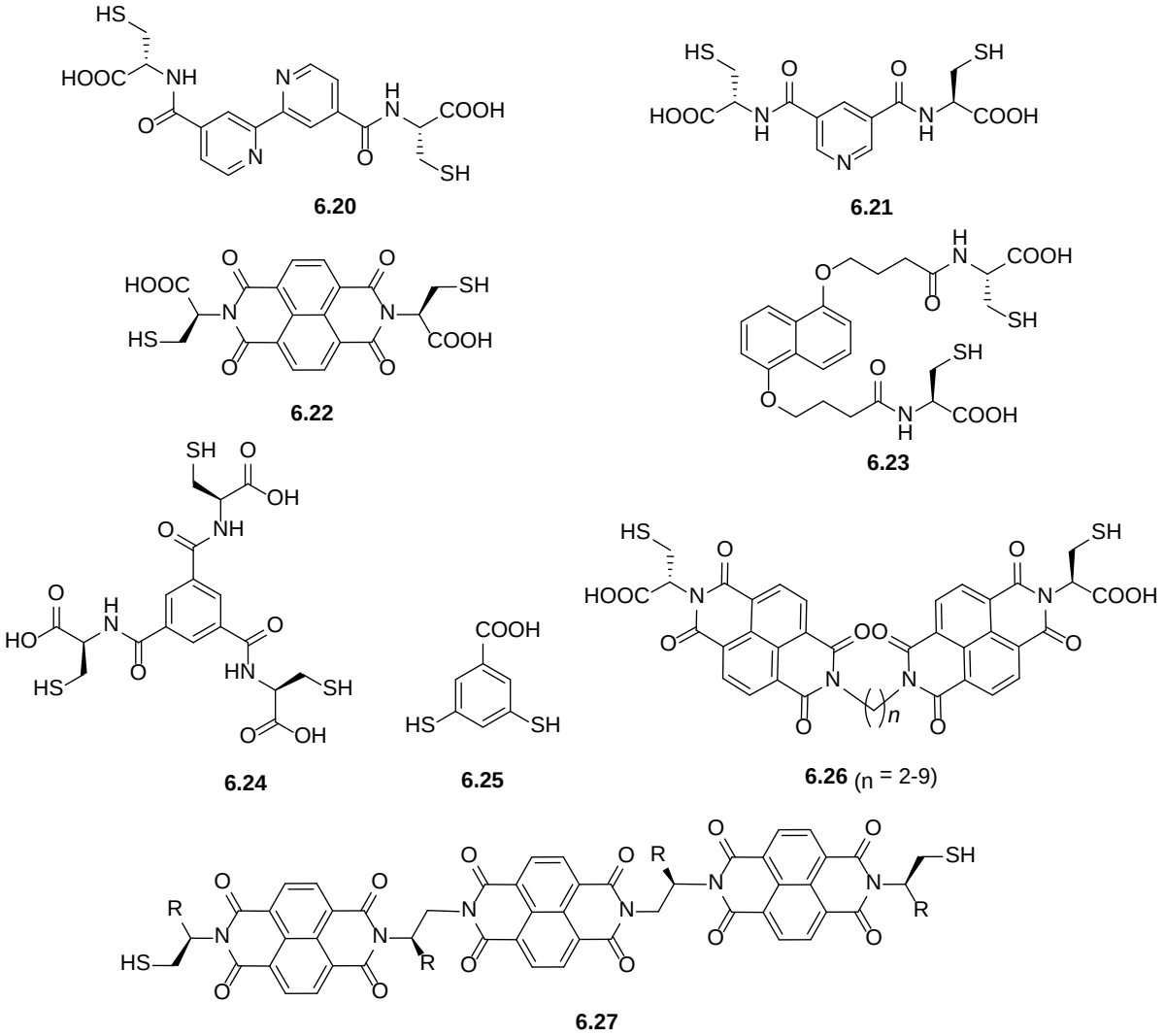

Figure 6.4: Di-cysteine functionalized building blocks **6.20**-**6.23**, and **6.26**-**6.27** in addition to tri-cysteine functionalized building block **6.24** and disulfide building block **6.25**.

Hence, cysteine was incoroporated into many building blocks structures to generate, through DCC, macrocyclic receptors for dopamine[26] and electronically-complementary guests[27,28] in addition to donor-acceptor [2] and [3]-catenanes[29,30,31] and an "all acceptor" [2]-catenane.[29]
Moreover, cysteine functionalized building blocks were used to generate, through DCC, covalent cage-like receptors for many polyamines[32,33] and a molecular trefoil knot.[34]
For instance, a DCL made from the mixture of building blocks **6.20** and **6.21** (Figure 6.4) was able to amplify macrocyclic heterodimer (**6.20**)(**6.21**) and homodimer (**6.21**)$_2$ upon addition of dopamine as a template.[26] A DCL made from the electron-deficient acceptor building block **6.22** and another made from the electron-rich donor building block **6.23** were able to amplify macrocyclic homotetramer (**6.22**)$_4$ and homotrimer (**6.22**)$_3$ and homodimer (**6.23**)$_2$, respectively, upon addition of variously electronically-complementary guests as templates.[27,28]
Mixing building blocks **6.22** and **6.23** led to the donor-acceptor [2]-catenane (**6.22**)(**6.23**)-(**6.22**)(**6.23**).[29,30] Moreover, adding building block **6.23** to the electron-deficient acceptor building block **6.26** of n ≤ 6 (even linker) was able to generate, through DCC, the donor-acceptor [3]-catenane (**6.23**)$_2$-(**6.26**)$_4$-(**6.23**)$_2$, while a DCL made from building block **6.26** of n > 8 was able to generate the "all acceptor" [2]-catenane (**6.26**)$_4$-(**6.26**)$_2$.[29] Furthermore, a DCL made from the mixture of building blocks **6.24** and **6.25** was able to generate covalent cage-like receptors for many polyamines including spermine such as heterononamer (**6.24**)$_2$(**6.25**)$_7$,[32,33] while a DCL made from the electron deficient acceptor building block **6.27** was able to generate the molecular trefoil knot (**6.27**)$_3$.[34]

Hydrazone DCls working in organic solvents, typically chloroform

Moreover, DCLs of dipeptide hydrazone macrocycles which were formed from building blocks equipped with hydrazide and protected aldehyde functionalities of a para (or meta) substituted aromatic linker, L-proline and a variable amino acid component were reported (Figure 6.5).[35-41] The DCLs were prepared in organic solvents, typically in chloroform, in presence of acid catalyst to initiate hydrazone exchange. The dipeptide residue provided a range of non-covalent interactions useful in the context of molecular recognition, and the presence of proline enforced some degrees of curvature that facilitated the formation of macrocycles. The DCLs were used to generate receptors for metal-ions Na^+ and Li^+[35,36,37] and organic biomolecules such as acetylcholine and *N*-methyl quinuclidine.[38,39] The DCLs also showed the ability to address stereoselective molecular recognition phenomena by generating stereoselective receptors for (-) cytidine[40] and (-) adenosine.[41]
For instance, a DCL made from **6.28** was used to generate a macrocyclic trimer that binds alkaline metal cations (Li^+ and Na^+) with micromolar affinity in $CHCl_3$/MeOH (98:2),[35,36,37] and a [2]-catenane made from two interlocked macrocyclic trimers able to bind acetylcholine with nanomolar affinity in $CHCl_3$/DMSO (95:5).[38] The fact that the generated macrocyle was found to undergo substantial conformational rearrangements upon binding the metal ion guest Li^+ reflects a flexibility induced by the dipeptide residues.
Also, the same DCL prepared in $CHCl_3$/MeOH (98:2) was able to exhibit diastereoselective recognition by amplifying a macrocyclic dimer and tetramer after adding, separately, the diastereomeric templates quinine and quinidine, respectively.[42] Substituting the Phe residue in building block **6.28** for Val (**6.29**) changes the library distribution from mostly dimer, trimer and tetramer to mostly tetramer.[43] A DCL made from **6.30** was able to generate a macrocyclic trimer with micromolar affinity for acetylcholine and *N*-methyl quinuclidine in $CHCl_3$/MeOH (98:2).[38,39] A DCL made from the diastereomeric combination of building blocks **6.31** and **6.32** in $CHCl_3$ amplifies a heterohexameric macrocycle as a result of addition of (-) cytidine.[40]

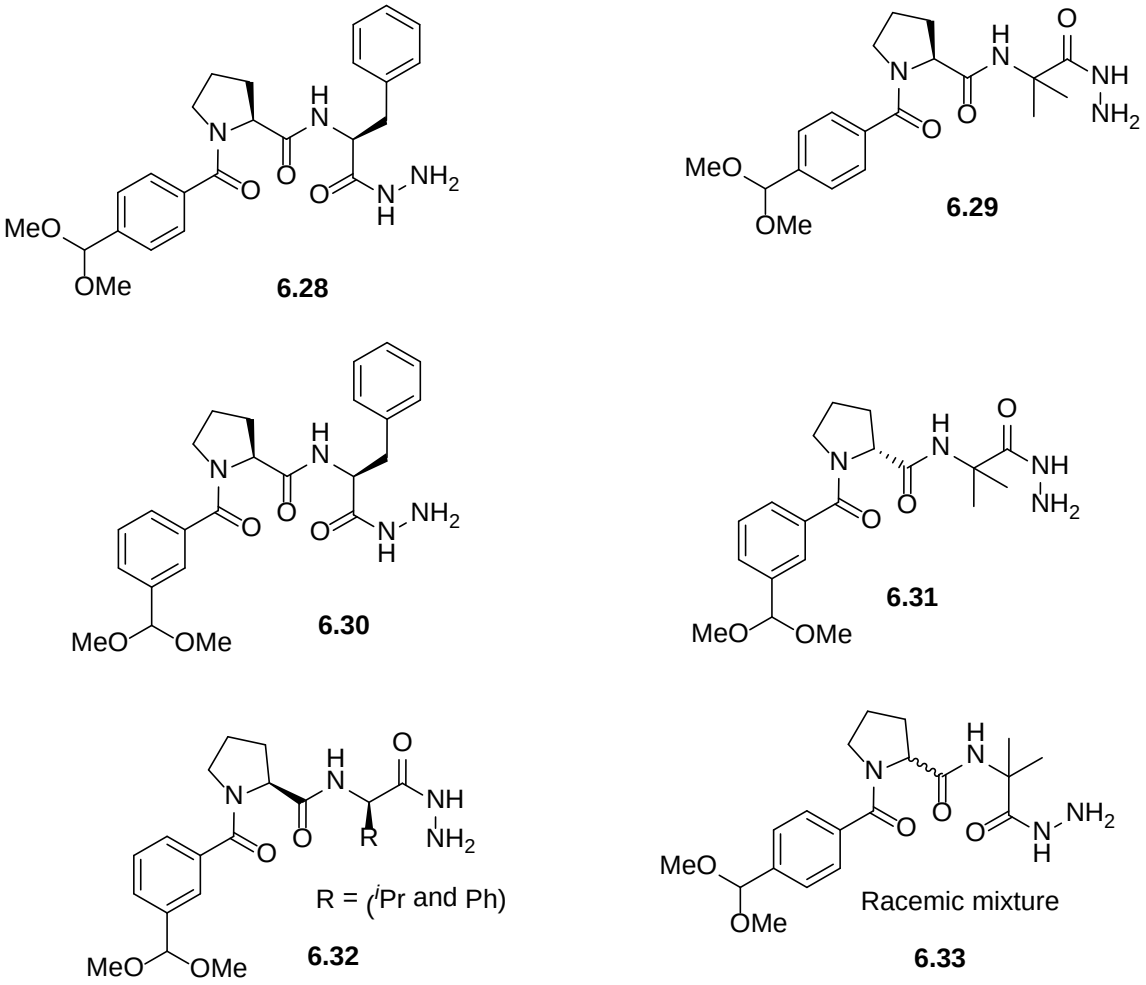

Figure 6.5: Bi-functional building blocks **6.28**-**6.30** able to generate DCLs of dipeptide hydrazone macrocycles in organic solvents, typically chloroform, in presence of a catalytic amount of acid.

A DCL formed from a racemic mixture of building block **6.33** in $CHCl_3$/MeOH (1:3) amplifies the enantioselective (S,S) dimeric macrocycle as a result of addition of (-) adenosine as a template.[41]

6.1.3 Intra-molecular interactions in an amino acid derived host may reinforce guest binding

In general, the approach to designing a synthetic host focuses, exclusively, on the direct host-guest interactions, and what this implies for introducing functional groups into the host composition. These functional groups are selected to be of complementary recognition properties to those of the guest. Nevertheless, synthetic hosts are still predominantly several orders of magnitude less efficient in binding than their biological counterparts.[44] A review of the molecular recognition in proteins suggested that the observed efficiency in ligand binding involve, in addition to the direct protein-ligand interactions, non covalent interactions within the protein.

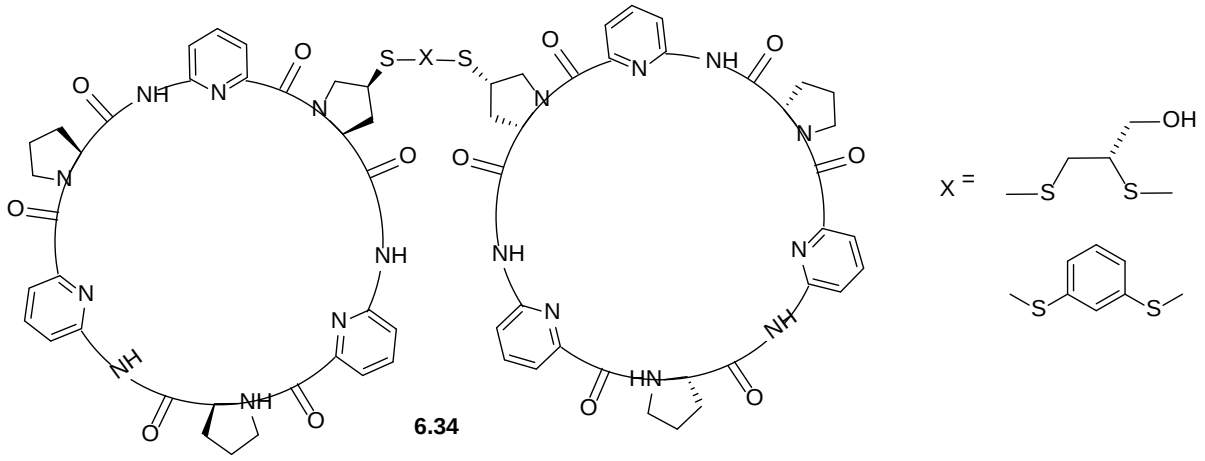

Figure 6.6: Bicyclopeptide **6.34**

This reinforcement in ligand binding occurs when the ligand binding and the intra-molecular interactions require very similar conformational rearrangement of parts of the protein.[45] Binding of natural antibiotic vancomycin to lysyl-R-alanyl-R-alanine peptide residue[46] in bacterial cells exemplifies well the reinforcement of guest binding by intramolecular interactions in biology. Vancomycin has a tendency to dimerise and the dimer was found to bind the peptide ligand more strongly than the monomer. This implies that the interactions between the vancomycin units enhance ligand binding.[47] In synthetic systems, analysis of molecular recognition in a bicyclopeptide (**6.34**) (Figure 6.6) developed by the Kubik group in collaboration with our group has provided quantitative evidence of the reinforcement of guest binding by intramolecular interactions.[48] That is hydrophobic intramolecular interactions between the two covalently linked peptide rings in **6.34**, which do not directly involve the guest, contributed to the complexation of the sulfate anion guest. The authors supported their notion by several pieces of evidence such as a) an X-ray crystal structure of the sulfate complex of **6.34** showing close contacts between hydrophobic surfaces of the two peptide rings of the receptor; b) the binding of iodide by receptor **6.34** was relatively solvent insensitive upon increasing the water fraction in the solvent mixture. This suggests that the increased cost of desolvating the anion was compensated by the increased stabilization of the iodide complex by hydrophobic intra-receptor interactions; and c) the stepwise analysis of binding of the monomer peptide to sulfate in 1:1 methanol-water to form a 2:1 sandwich complex, showed that the second peptide binds 100 times stronger than statistically expected, thus indicating that the intra-receptor interactions reinforce guest binding.
In conclusion, introducing amino acid residues into receptors may become an attractive methodology to bring binding affinities of synthetic receptors closer to the binding affinities of biomolecules.

6.2 Work motivation

*Simple and effective method for functionalizing building blocks **2** and **3***

As a part of our ongoing projects, we needed an easy entry to structurally diversify our existing set of easily obtained and successful dithiol building blocks **2** and **3** (Scheme 6.1), which could be realized by introducing additional groups late in their syntheses. We envisaged functionalizing these building blocks with natural amino acids as the synthesis is

simple and employs well-established peptide coupling methods. Furthermore, given the fundamental role played by thiol and disulfides in biology, disulfide chemistry was assumed to be compatible with the amino acid functional groups. Ultimately, the presence of amino acid residues permits the introduction of new functionalities while conserving the carboxylic acid groups which can be utilized for additional post-synthetic modifications.

Acquired molecular recognition properties

Incorporating amino acid residues to the building block structures potentially present many significant advantages for the molecular recognition. Specifically, the amide bond, introduced with any amino acid residue, potentially provides two hydrogen-bonding binding sites in close proximity to the hydrophobic cores. Moreover, given the large inventory of commercially available amino acids, a large diversity of functional groups can thus be introduced. For instance, negatively charged carboxylates introduced with glutamic acid (pK_a = 4.2)[49] provides potential hydrogen-bonding and electrostatic binding sites. Neutral amide moieties introduced with glutamine provide two additional hydrogen bonding binding sites, and positively charged amino groups introduced with lysine (pK_a = 10.5)[49] provide hydrogen bonding binding sites. Also, phenyalanine provides a sterically bulky residue potentially able to form π- π, cation- π and hydrophobic interactions.

Acquired DCL diversity, solubility, *chirality and flexibility or predefined geometry.*

The nature of the incorporated amino acids may have effects on the macrocyclization process and therefore on the diversity of the resulting DCLs.[43] These may also have effects on the binding behavior and functional properties of the resulting DCL members. Moreover, given that amino acid moieties are charged at mildly basic conditions, this can enhance the water solubility of the building blocks and therefore may prevent the aggregation of hydrophobic macrocycles such as homo-tetramer (**2**)$_4$, known to aggregate under near physiological conditions.[50] Furthermore, natural amino acids represent one of the most important classes of substances in nature which possess a stereogenic center and therefore exemplify a good system to demonstrate the applicability of oligomeric macrocycles formed from building blocks **2** and **3** (*i.e.* (**3**)$_4$, (**2**)(**3**)$_3$, (**2**)$_2$(**3**)$_2$, (**2**)$_3$(**3**), (**2**)$_2$(**3**)$_3$ and (**2**)$_4$) to address stereoselective recognition phenomena, after being functionalized with the amino acids.

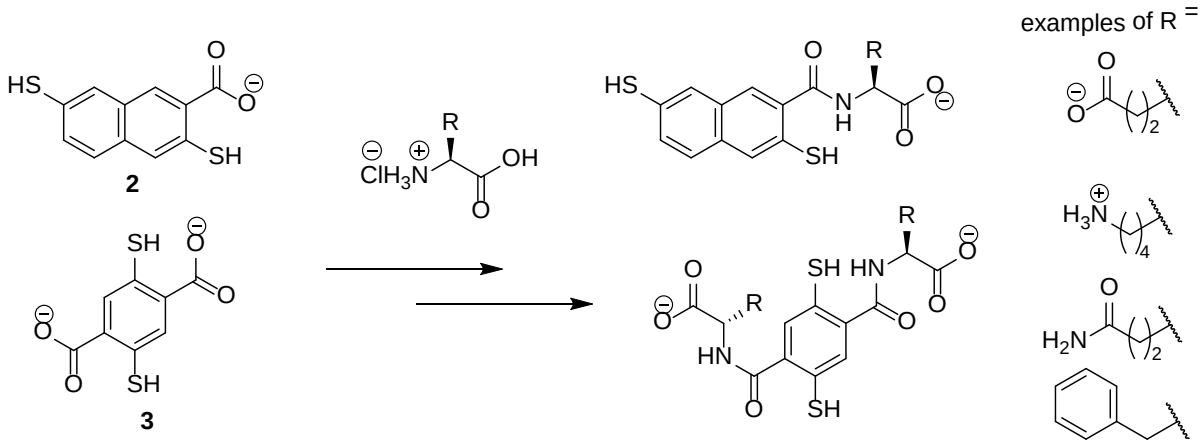

Scheme 6.1: Proposed derivatization of building blocks **2** and **3** with natural amino acid residues.

At the end, a macrocycle generated from building blocks **2** and **3** may provide a predefined cavity for binding, but a lack of flexibility may inhibit its ability to adopt a suitable conformation to best bind a guest. Introducing multiple flexible amino acid residues as appendages to this macrocycle, may enable optimal intermolecular interactions between these flexible groups and the guest. In contrast, intramolecular interactions such as hydrogen bonding and hydrophobic interactions possibly occurring between the incorporated amino acid residues could restrict the conformational freedom of such a macrocycle to give a well defined geometry.[51,52]

6.3 Building block syntheses

6.3.1 Synthesis of valine derived naphthalene dithiol building block

The synthesis of building block **2** was described earlier by Kevin West. It consists of three steps starting from commercial 3,7-dihydroxy-2-naphthoic acid **6.35** by preparing methyl ester **6.36** through acid-catalyzed esterification of the carboxylic acid group with acetylchloride in MeOH. Then, dimethylthiocarbamoyl groups were added to the hydroxyl groups of **6.36** to give **6.37**. Afterwards, the dimethylthiocarbamoyl units were thermally rearranged, using the Newman-Kwart rearrangement, in diphenyl ether at 230 ºC[53, 54] to give the protected naphthalene dithiol **6.38** in quantitative yield. Carbamoylsulfanyl groups were deprotected along with the ester group, under a nitrogen atmosphere to prevent thiol oxidation, with potassium hydroxide solution to give the naphthalene dithiol building block **2** (Scheme 6.2).

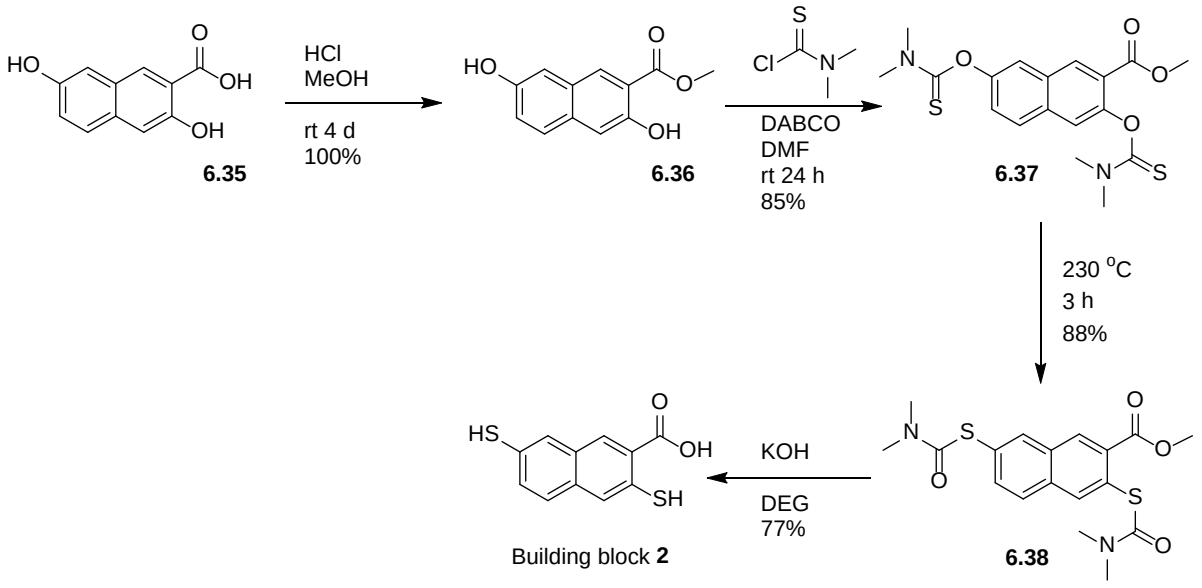

Scheme 6.2: The synthesis of naphthalene dithiol building block **2** as described by Kevin West.

Valine derived naphthalene building block (**4**) was prepared in three steps starting from dithiol building blok **2**. First, the dithiol functions of **2** were protected by trithyl chloride (TrCl) as an acid labile protecting group to give the tritylated protected dithiol building block **6.39** in quantitative yield. Then, commercially available L-valine with its carboxylic acid group

protected as an acid labile tert-butyl ester (**6.40**) was coupled to **6.39** under standard peptide coupling conditions. The coupling reaction gives the protected dithiol valine derived

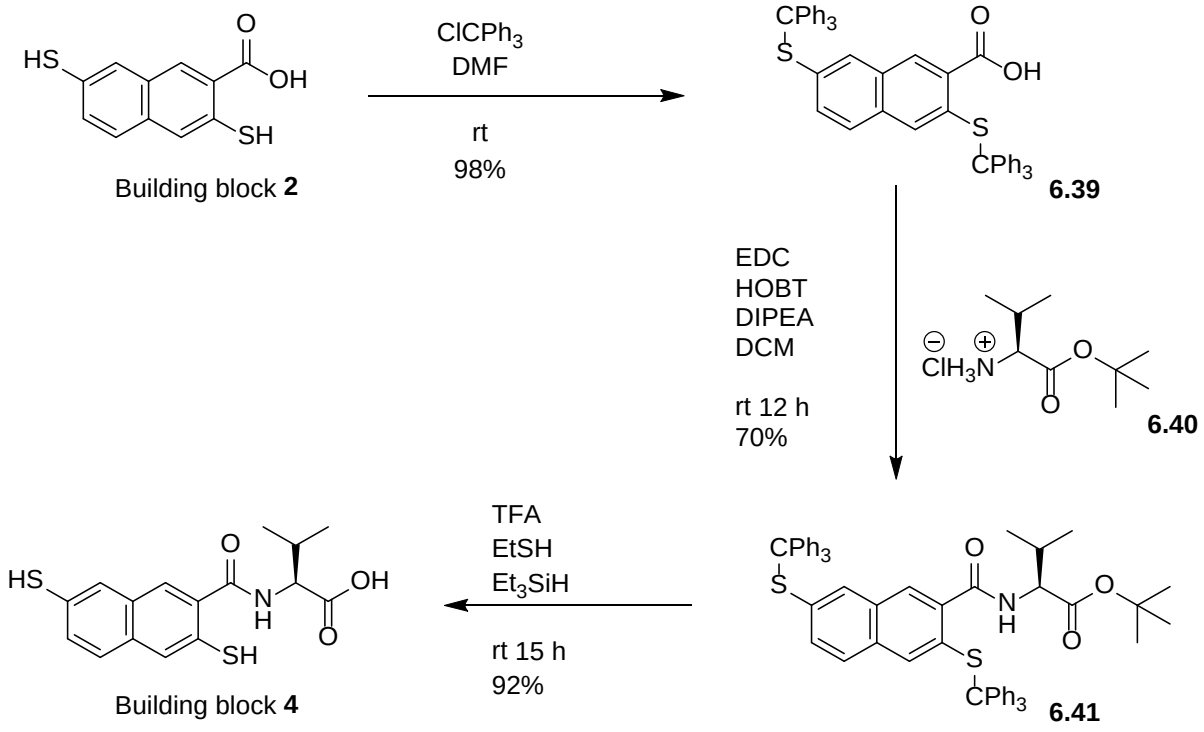

Scheme 6.3: Synthesis of valine derived naphthalene dithiol building block **4**.

building block **6.41** after a purification step through column chromatography. Acid labile protecting groups are expected to be stable under the coupling reaction conditions and could be cleaved in a single step. After, the deprotection of **6.41** was achieved using TFA, Et_3SiH as a scavenger for the tert-butyl cation and ethanethiol as a co-solvent to compete with the thiols (Scheme 6.3).

6.3.2 Synthesis of valine derived benzene dithiol building block

2,5-Dimercapto terephthalic acid **3** was first used in DCC by Fred Ludlow and Laurent Vial in 2008 as a smaller, symmetrical and more hydrophilic version of building block **2.**[55] Its synthesis described earlier by Field *et al.,*[56] consists of three steps starting from commercially available dihydroxyterephthalic acid **6.42**, by adding dimethylthiocarbamoyl groups to the hydroxyl groups of **6.42** to give **6.43** in near-quantitative yield. Compound **6.43** was then heated to 220 ºC for two hours before the dimetylthiocarbamoyl units were thermally rearranged, using the Newman-Kwart rearrangement, in diphenyl ether at 230 ºC to give the protected building block **6.44**. The cleavage step of ester and carbamoylsulfanyl groups was achieved by refluxing **6.44** using KOH in degassed $EtOH/H_2O$ instead of KOH/ethylene glycol to give the benzene dithiol dicarboxylic acid building block **3** in quantitative yield (Scheme 6.4).
Valine derivatized benzene building block **5** was synthesized following the same strategy as used for the synthesis of building block **4** (Scheme 6.5).

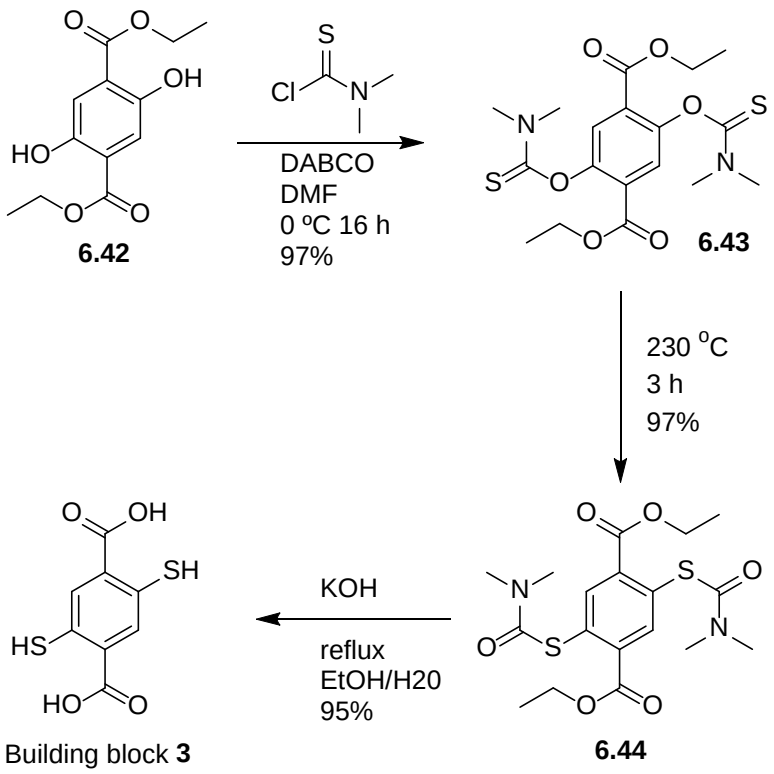

Scheme 6.4: The synthesis of benzene dithiol building block **3** as described by Ludlow *et al.*

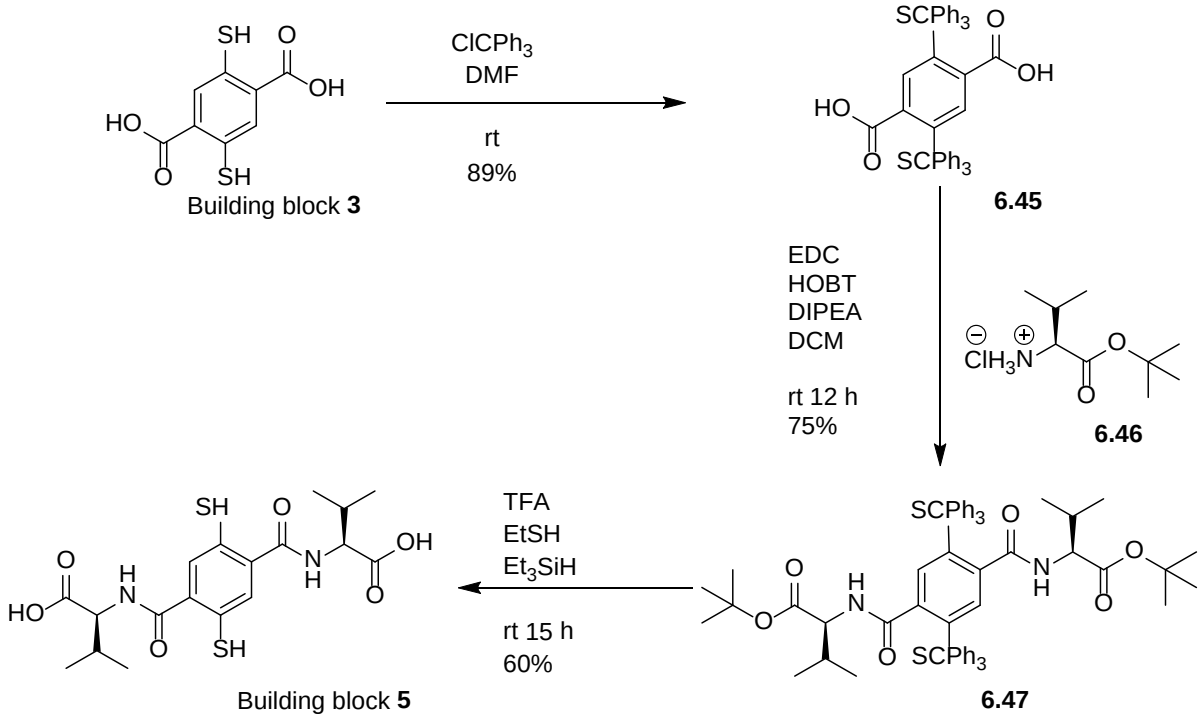

Scheme 6.5: Synthesis of valine derived benzene building block **5**

6.4 DCL studies

6.4.1 DCL made from valine derived naphthalene dithiol building block 4

A DCL made from building block **4** was prepared in 50 mM borate buffer at pH 8.4 and allowed to oxidize and equilibrate for 5-6 days following standard protocols (see experimental part). Subsequently, a sample of the DCL was diluted with 200 volume % DMSO immediately prior to analysis, as a standard protocol used to dissolve aggregates potentially formed from building blocks with naphthalene cores (see chapter 3, paragraph 3.3.3). The composition of the library was first analyzed by HPLC (Figure 6.7). A comparison between HPLC chromatograms of the DCL performed before and after DMSO dilution revealed that the majority of DCL members has aggregated under the DCL conditions.

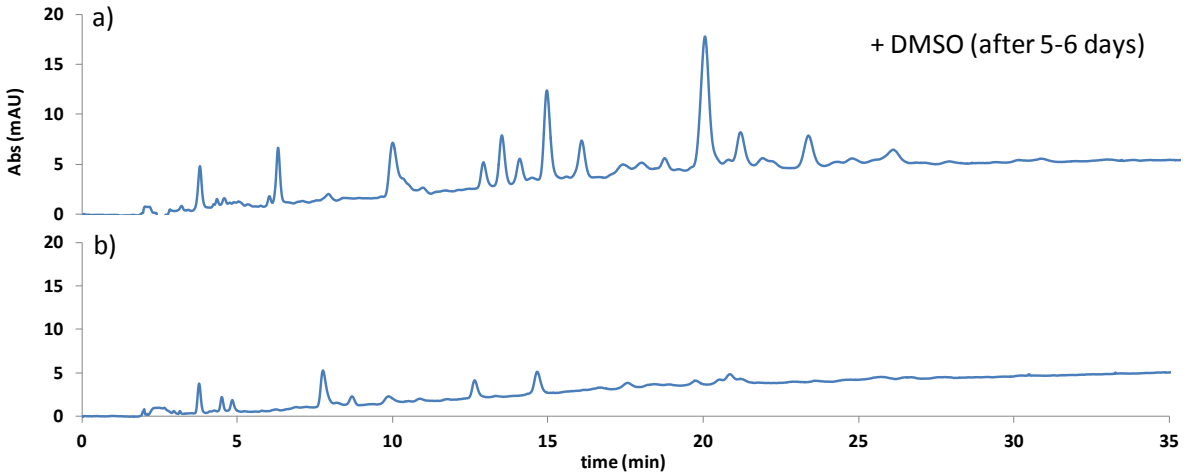

Figure 6.7: HPLC-UV analyses (λ_{abs} = 280 nm, λ_{ref} = 550 nm) of a DCL made from 2.0 mM of building block **4** in 50 mM borate buffer at pH 8.4, (a) after adding 200 volume % DMSO immediately prior to the analysis and (b) without DMSO dilution.

6.4.1.1 Disulfide products

Given that the amino acid residue is attached to the periphery of building block **4**, it was not expected that it would intrinsically interfere with the macrocyclization process of this building block. Thus, the DCL made from building block **4** was expected to mainly produce tetrameric macrocycles, similarly to the DCL made from building block **2** (Table 25). However, this was not observed and HPLC-MS analysis of the DCL showed the formation of two isomers of the relatively small macrocycle trimer $(\mathbf{4})_3$, in addition to three isomers of cyclic tetramer $(\mathbf{4})_4$ (Figure 6.8-Figure 6.9). Besides the cyclic disulfide macrocycles, a number of other peaks are also detected in the HPLC chromatogram of this DCL. The masses of these species correspond to library members that lost two or four mass units such as is the case for linear dimer minus four daltons [$(\mathbf{4})_2$-4Da] and cyclic trimer minus two daltons [$(\mathbf{6.38})_3$-2Da] (Figure 6.10). This subject will be further discussed in paragraph 6.4.1.1.1.

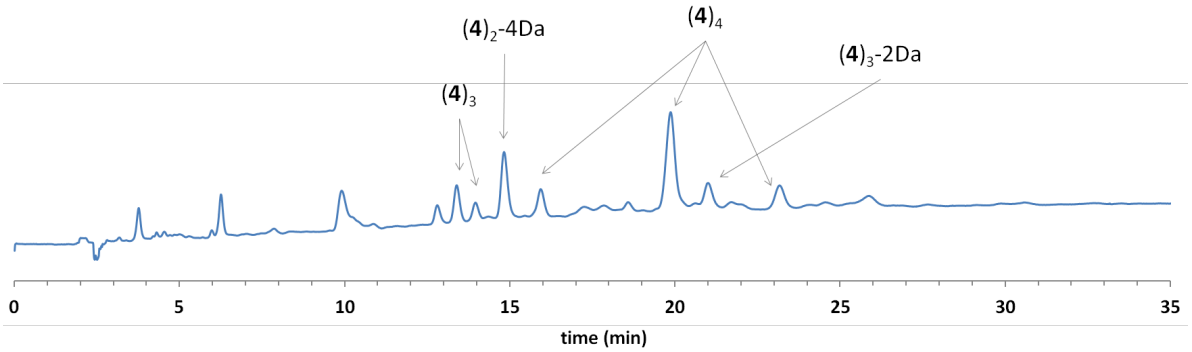

Figure 6.8: HPLC-UV analyses (λ_{abs} = 280 nm, λ_{ref} = 550 nm) of a DCL made from 2.0 mM of building block **4** in 50 mM borate buffer at pH 8.4, after adding 200 volume % DMSO immediately prior to the analysis. The HPLC chromatogram shows cyclic disulfide products (trimer $(\mathbf{4})_3$ and tetramer $(\mathbf{4})_4$) in addition to side products (linear dimer $[(\mathbf{4})_2$-4Da] and cyclic trimer $[(\mathbf{4})_3$-2Da]).

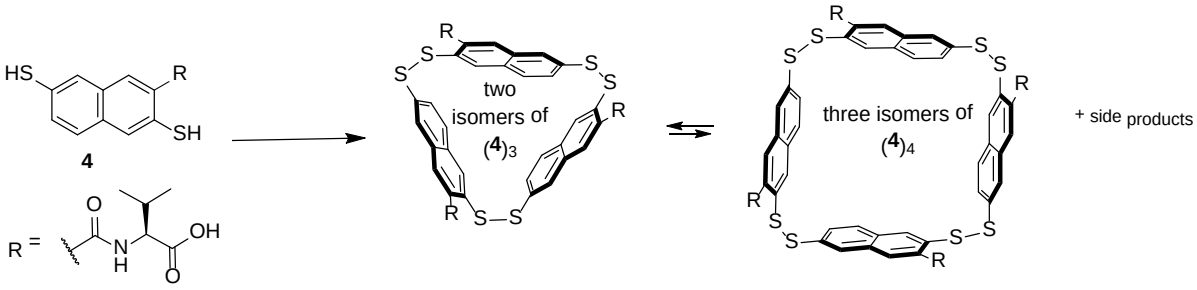

Scheme 6.6: DCL made from building block **4** and composed of macrocycles trimer $(\mathbf{4})_3$ and tetramer $(\mathbf{4})_4$ in addition to the side products: linear dimer $[(\mathbf{4})_2$-2Da] and cyclic trimer $[(\mathbf{4})_3$-2Da].

Based on the carboxylate substituent arrangements, the asymmetric structure of **4** can give rise to four different isomers of $(\mathbf{4})_4$ and two different isomers of $(\mathbf{4})_3$ (Scheme 6.7).

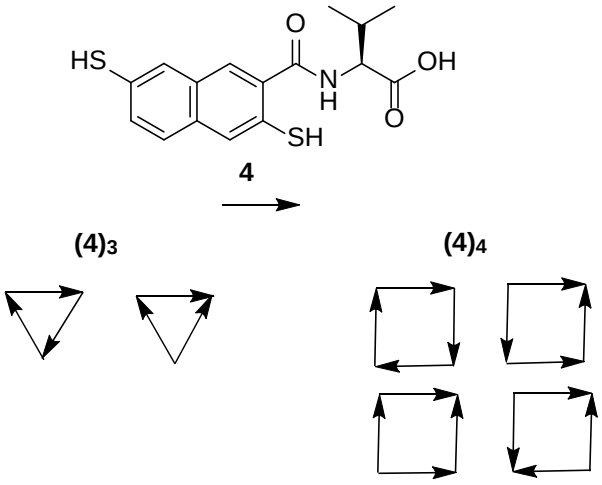

Scheme 6.7: Schematic representation of the two possible isomers of trimeric macrocycle $(\mathbf{4})_3$ and the four possible isomers of tetrameric macrocyle $(\mathbf{4})_4$ formed from a DCL made from building block **4**. Asymmetric building block **4** is represented as an arrow.

6.4.1.1.1 Side products

The loss of two or four mass units from the masses of the formed oligomers could potentially be assigned to a loss of one or more pairs of hydrogen from the oligomer structures. We first considered that this phenomenon might be related to the accessibility of thio-quinone and related resonance forms from compounds containing two thiols para on a benzene ring or in the 2,6- positions of a naphthalene ring,[55,57] even though the actual mechanism is not understood (Scheme 6.8-a). Alternatively, this surprising loss of mass maybe a result of oxidation of one or more amino acid residues carried by the DCL members, through the loss of the hydrogens from the α-amino group and the α- carbon atom of one or more amino acid residues (Scheme 6.8-b). It is also not clear what mechanism is operating in this case. Given that the loss of one or more pairs of hydrogens is not observed in DCLs made from building block **2**, the second speculation is the more likely. Also, the oxidation of amino-acid residues would induce further conjugation. Furthermore, the presence of a monomer acquiring two oxygen atoms and losing two daltons [(**4**)2O-2Da] (see paragraph 6.4.1.2) in the DCL pushes us to speculate that the amino acid oxidation may be to blame and therefore the second speculation is again the most reasonable.

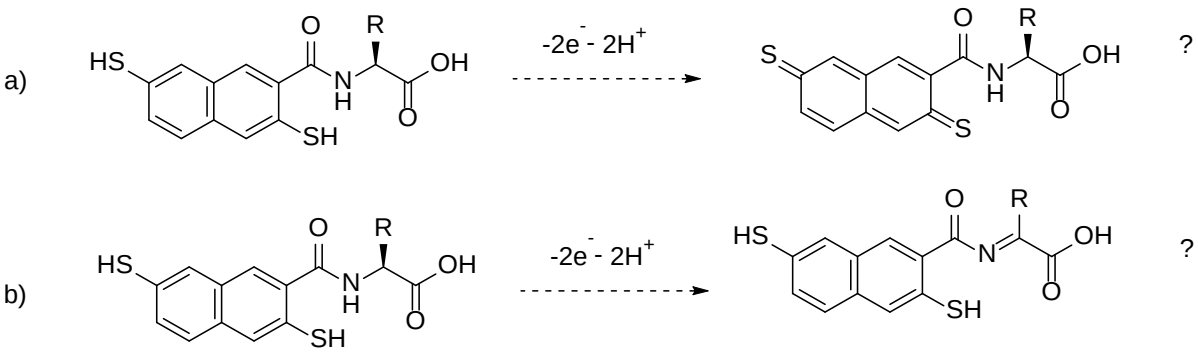

Scheme 6.8: Possible formation of thioquinone from a 2,6-dimercapto naphthalene and speculated oxidation of an amino acid residue connected to a 2,6-dimercapto naphthalene.

6.4.1.2 (Linear) sulfinic acid and sulfonate side products

Similarly, the diversity of over-oxidized products formed in a DCL made from building block **4** is also different from the one observed in a DCL made from building block **2**, where the over-oxidized side products are constituted of (linear) disulfinic acid (**2**)$_2$4O (Table 25).

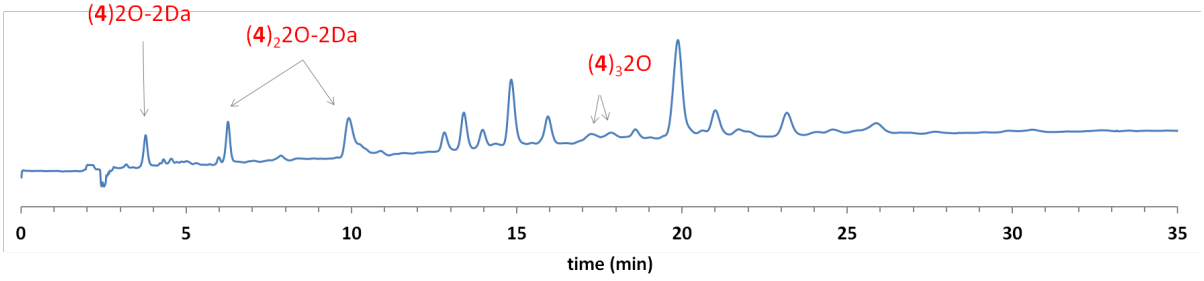

Figure 6.9: HPLC-UV analyses (λ_{abs} = 280 nm, λ_{ref} = 550 nm) of a DCL made from 2.0 mM of building block **4** in 50 mM borate buffer at pH 8.4, after adding 200 volume % DMSO immediately prior to the

analysis. The HPLC-UV chromatogram shows over-oxidized side products: monomer (**4**)2O-2Da, linear dimer $(\mathbf{4})_2$2O-2Da and cyclic trimer $(\mathbf{4})_3$2O.

A cyclic trimer plus 32 daltons [$(\mathbf{4})_3$2O] corresponding to the mass of two oxygen atoms and correlating with a thiosulfonate oxidation state (-SO_2-S-) of a disulfide bond was found (Figure 6.9-Figure 6.10). Similar oxidations have been reported elsewhere,[58] although it is not clear what mechanism is operating in this case (see chapter 3, paragraph 3.2.2.2). Moreover, a monomer and a linear dimer plus 30 daltons each, [(**4**)2O-2Da] and [$(\mathbf{4})_2$2O-2Da] respectively, corresponding to the mass of two oxygen atoms minus two daltons, were also detected. The incorporation of two oxygen atoms may correspond to a thiosulfonate oxidation state of a disulfide bond (-SO_2-S-) in the case of the dimer, while it likely corresponds to a sulfinic acid oxidation state of a terminal thiol (SO_2H) in the case of the monomer.[58] The loss of two mass units from both the monomer and the dimer may correspond to the oxidation of amino acid residues carried by both over-oxidized products (Scheme 6.8) (see paragraph 6.4.1.1).

Table 25: An overview of product distributions of DCLs made from individual building blocks **2** and **4** and prepared in 50 mM borate buffer at pH = 8.4. The products mentioned in the table are all of cyclic forms unless the opposite is indicated.

DCL building block	Disulfide DCL products	Over-oxidized side products	Other side products
2	Catenane [$(\mathbf{2})_4$-$(\mathbf{2})_4$] and $(\mathbf{2})_4$	Linear [$(\mathbf{2})_2$4O]	----
4	$(\mathbf{4})_3$ and $(\mathbf{4})_4$	[$(\mathbf{4})_3$2O]	[$(\mathbf{4})_3$-2Da] and linear [$(\mathbf{4})_2$-4Da]. Linear [(**4**)2O-2Da], linear [$(\mathbf{4})_2$2O-2Da]

6.4.1.3 Effect of derivatization of building block 2 with a valine residue on the diversity of the DCL products

The DCLs made from valine functionalized building block **4** contained isomers of oligomeric macrocycles $(\mathbf{4})_3$ and $(\mathbf{4})_4$. Thus, the functionalization of monomer **2** with valine has affected its macrocyclization process, resulting in the formation of relatively small macrocyclic trimer $(\mathbf{4})_3$, which was not observed in the DCL made from monomer **2**. We speculate that intramolecular interactions that may have occurred between the amino acid residues of trimer $(\mathbf{4})_3$, such as hydrogen bonding and hydrophobic interactions, have led to the stabilization of this species in the DCL and therefore shifted the equilibrium towards its formation. Such interactions, if they exist, could reinforce the binding of a guest provided that guest binding and the intramolecular interactions require very similar conformational rearrangement of part of the host.[48,65] Moreover, given that the driving force for catenation (*i.e.* formation of $(\mathbf{2})_4$-$(\mathbf{2})_4$) is avoiding unfavorable exposure of the hydrophobic interior of a macrocycle to water,[59] we speculate that the absence of catenation in the DCL made from building block **4** could be the result of orientation of the valine residues into the inside of the cavity, at least, of macrocycle $(\mathbf{4})_4$. This notion further supports the possible occurrence of intra-molecular interactions between the valine residues of the formed macrocycles.

6.4.1.4 Effect of derivatization of dithiol 2 with a valine residue on its rate of oxidation

It is noteworthy to mention that the library member with a mass corresponding to linear dimer minus four daltons [(**4**)$_2$-4Da] remains in the DCL after more than a week of equilibration. This observation suggests a slow oxidation rate of valine derivatized dithiol **4** versus the relatively fast oxidation rate observed for dithiol **2** for which no linear species had remained in the DCL for longer than 24 hours. It seems that substituting the electron donating carboxylate group of building block **2** with the electron withdrawing amide group may have reduced the nucleophilicity of the formed dithiol (**4**) resulting in a slow thiol oxidation rate. Moreover, the steric hindrance caused by the bulky amino-acid substituent that is adjacent to one of the sulfur atoms may also have reduced the rate of oxidation of dithiol **4**. The slow oxidation rate may have increased the chance of the DCL products to get over-oxidized forming sulfinic acid and sulfonate derivatives. Alfonso *et al.*[60] have reported that the use of DMSO as aqueous co-solvent in a DCL of pseudopeptide building blocks promotes thiol oxidation and reduces the reaction time for the disulfide formation. However, this approach has not been applied to our systems.

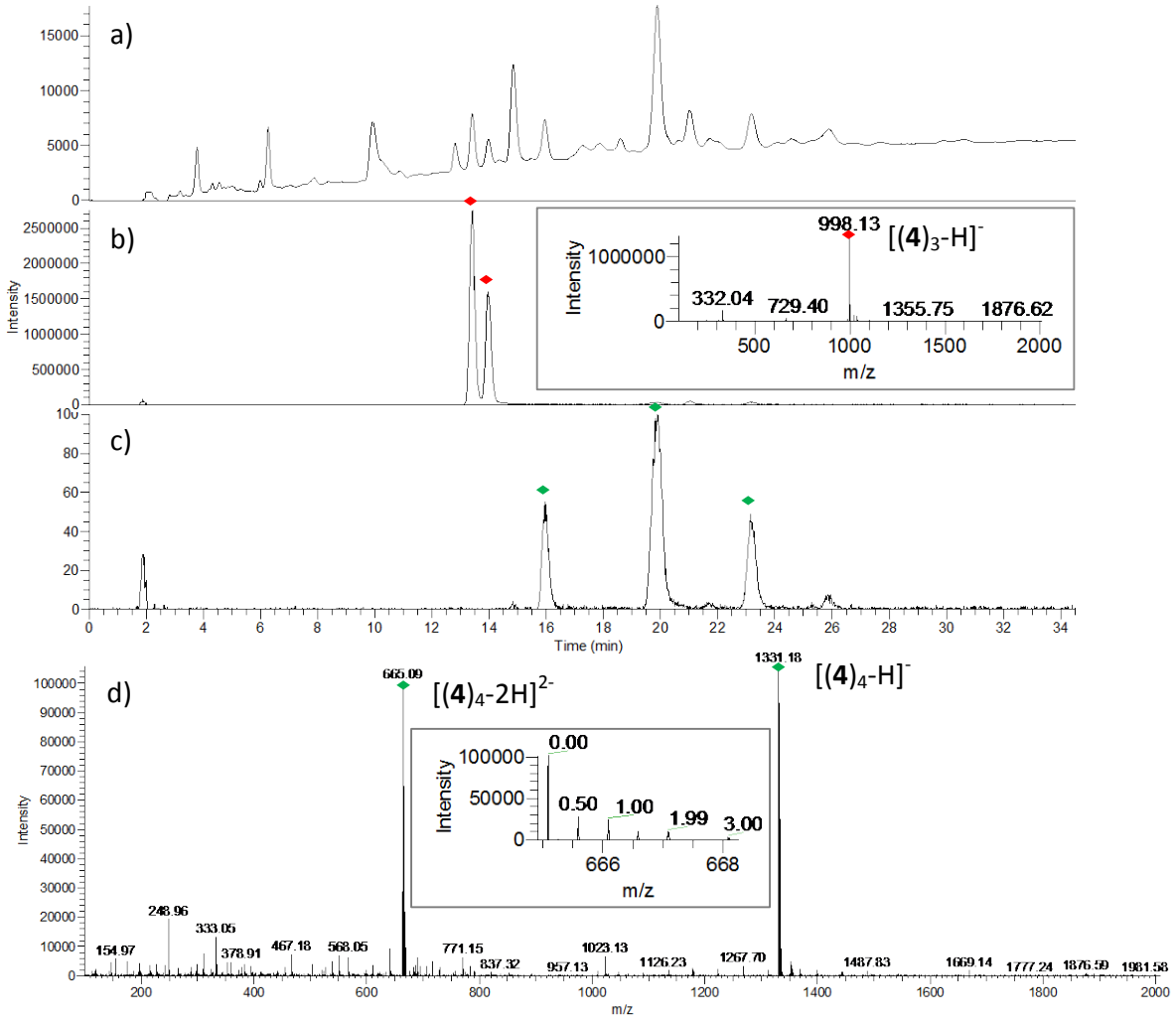

Scheme 6.9: Analyses of a DCL prepared in 50 mM borate buffer (pH 8.4) and composed of 2.0 mM of building block **4**. The DCL was diluted with 200 volume % DMSO immediately prior to analysis. (a) HPLC-UV chromatogram at 280 nm (λ_{ref} = 550 nm); (b) Extracted ion chromatogram (negative ion mode) corresponding to monocharged cyclic trimer $(\mathbf{4})_3$ (997.5-998.5) with (insert) ESI-MS spectra [m/z 200-2000] summed over the 13.2-13.6 and 13.8-14.2 min retention time windows, corresponding to two isomers of cyclic trimer $(\mathbf{4})_3$, showing $[(\mathbf{4})_3\text{-H}]^-$ m/z = 998.13 (expected = 998.15); (c) Extracted ion chromatogram (negative ion mode) corresponding to monocharged cyclic tetramer $(\mathbf{4})_4$ (1330.5-1331.5) and (d) ESI-MS spectra [m/z 200-2000] summed over the 15.7-16.3, 19.5-20.3 and 22.9-23.5 min retention time windows corresponding to the three isomers of cyclic tetramer $(\mathbf{4})_4$, showing $[(\mathbf{4})_4\text{-H}]^-$ m/z = 1331.18 (expected = 1331.20) and $[(\mathbf{4})_4\text{-2H}]^{2-}$ m/z = 665.09 (expected = 665.10). The spacing of 0.5 mass units (insert) demonstrates that the $[(\mathbf{4})_4\text{-2H}]^{2-}$ ions are doubly charged.

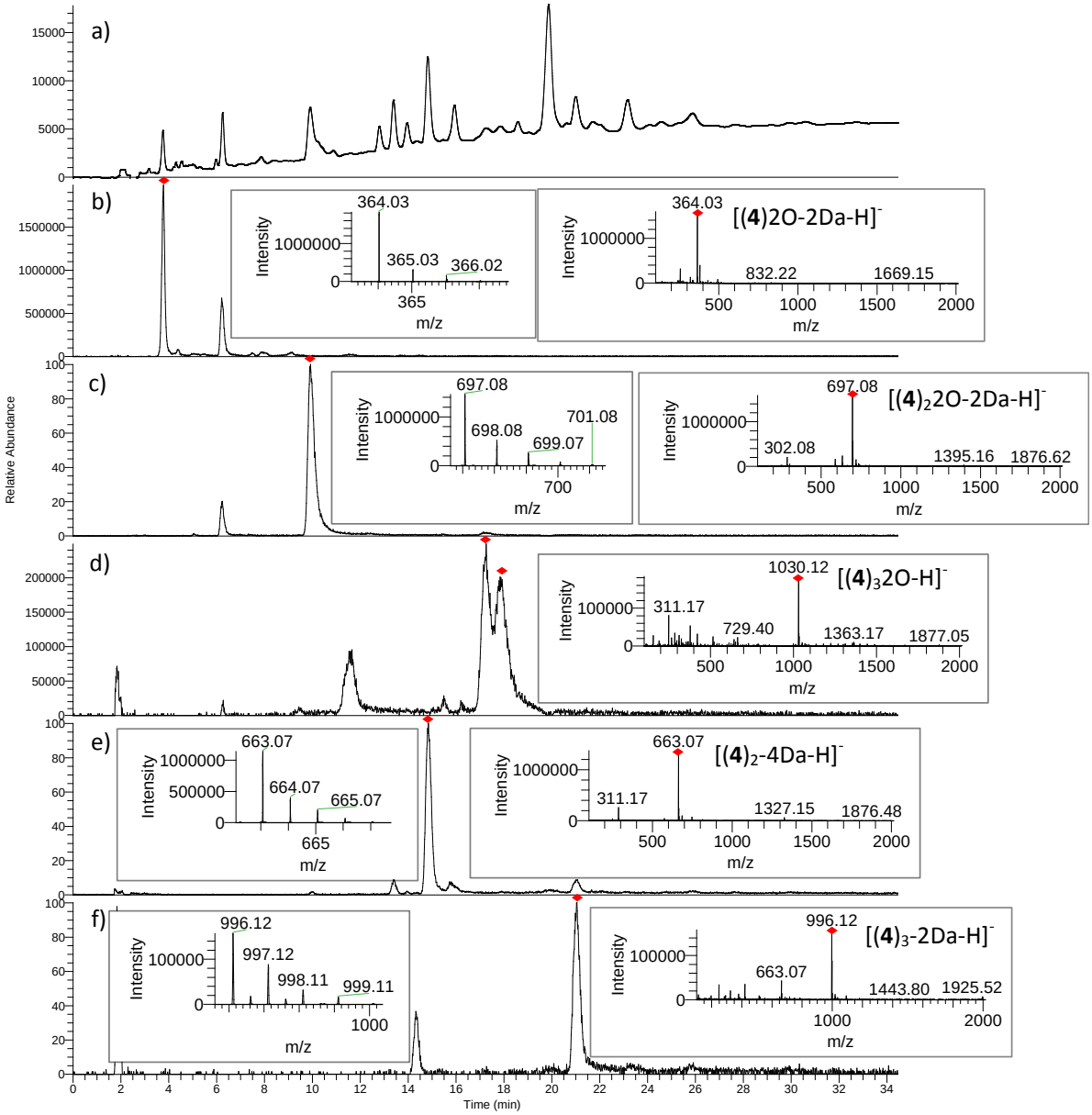

Figure 6.10: Analyses of a DCL prepared in 50 mM borate buffer (pH 8.4) and composed of 2.0 mM of building block **4**. The DCL was diluted with 200 volume % DMSO immediately prior to analysis. (a) HPLC-UV chromatogram at 280 nm (λ_{ref} = 550 nm); (b) Extracted ion chromatogram (negative ion mode) corresponding to monocharged over-oxidized monomer minus two daltons [(**4**)2O-2Da] (363.5-364.5) with (right insert) ESI-MS spectra [m/z 200-2000] summed over the 3.6-3.9 min retention time window, corresponding to [(**4**)2O-2Da], showing [(**4**)2O-2Da-H]$^-$ m/z = 364.03 (expected = 364.04). (left insert) Isotopic distribution of [(**4**)2O-2Da-H]$^-$; (c) Extracted ion chromatogram (negative ion mode) corresponding to monocharged over-oxidized linear dimer minus two daltons [$(\mathbf{4})_2$2O-2Da] (696.5-697.5) with (right insert) ESI-MS spectra [m/z 200-2000] summed over the 9.7-10.3 min retention time window, corresponding to [$(\mathbf{4})_2$2O-2Da], showing [$(\mathbf{4})_2$2O-2Da-H]$^-$ m/z = 697.08 (expected = 697.1). (left insert) Isotopic distribution of [$(\mathbf{4})_2$2O-2Da-H]$^-$; (d) Extracted ion chromatogram (negative ion mode) corresponding to monocharged over-oxidized cyclic trimer

[(**4**)$_3$2O] (1029.50-1030.50) with (insert) ESI-MS spectra [m/z 200-2000] summed over the 11.2-11.8 and 17.0-18.3 min retention time windows, corresponding to over-oxidized cyclic trimer (**4**)$_3$2O, showing [(**4**)$_3$2O-H]$^-$ m/z = 1030.12 (expected = 1030.15); (e) Extracted ion chromatogram (negative ion mode) corresponding to monocharged linear dimer [(**4**)$_2$-4Da] (662.50-663.50) with (right insert) ESI-MS spectra [m/z 200-2000] summed over the 14.7-15 min retention time window, corresponding to linear dimer (**4**)$_2$-4Da, showing [(**4**)$_2$-4Da-H]$^-$ m/z = 663.07 (expected = 663.10). (Left insert) isotopic distribution of [(**4**)$_2$-4Da-H]$^-$; (f) extracted ion chromatogram (negative ion mode) corresponding to monocharged cyclic trimer [(**4**)$_3$-2Da] (995.50-996.50) with (right insert) ESI-MS spectra [m/z 200-2000] summed over the 20.8-21.4 min retention time window, corresponding to cyclic trimer [(**4**)$_3$-2Da], showing cyclic trimer [(**4**)$_3$-2Da-H]$^-$ m/z = 996.12 (expected = 996.15). (Left insert) isotopic distribution of [(**4**)$_3$-2Da-H]$^-$.

6.4.2 DCL made from building blocks 1 and 4

In the second chapter of this dissertation we have seen that mixing building blocks **1** and **2** in borate buffer solution at pH = 8.4 enabled the generation of diverse higher molecular weight species, including oligomeric macrocycles (**1**), (**1**)$_2$, (**1**)(**2**) and (**2**)$_4$ in addition to catenane (**2**)$_4$-(**2**)$_4$.[61] Thus, it was intuitive to study the effect of derivatization of building block **2** with a valine residue (*i.e.* building block **4**) on the composition of a DCL made from mixture of building blocks **1** and **4**. We proceeded to prepare a DCL made from building blocks **1** and **4** in 50 mM borate buffer at pH 8.4 and allowed it to oxidize and exchange following standard protocols (see experimental part). The composition of the resulting DCL was analyzed by HPLC and mass spectrometry (Figure 6.11 and Figure 6.13-Figure 6.16).

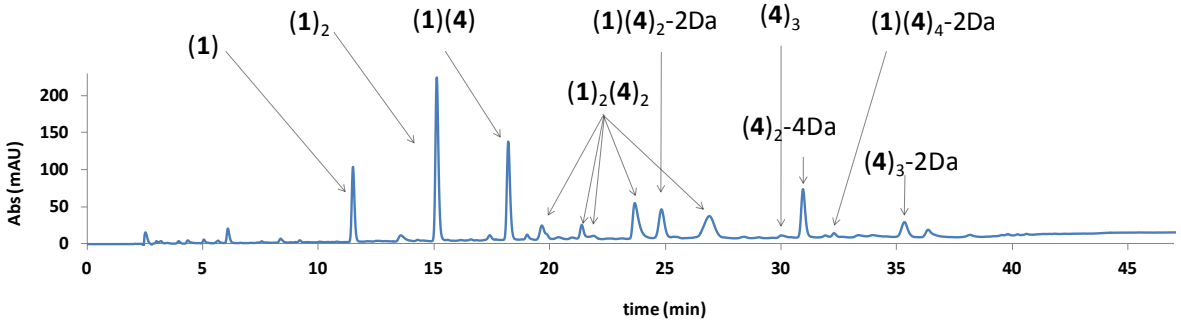

Figure 6.11: HPLC-UV chromatogram (λ_{abs} = 260 nm and λ_{ref} = 360 nm) showing the cyclic disulfide products including (**1**), (**1**)$_2$, (**1**)(**4**), (**1**)$_2$(**4**)$_2$ and (**4**)$_3$, in addition to cyclic side products (**1**)(**4**)$_2$-2Da, (**1**)(**4**)$_4$-2Da and (**4**)$_3$-2Da and linear side product (**4**)$_2$-4Da. The DCL was prepared in borate buffer (50 mM, pH 8.4) and composed of equimolar amounts (2.0 mM for each) of building blocks **1** and **4**, and analyzed after four to five days of equilibration. The DCL was diluted with 200 volume % DMSO immediately prior to analysis.

Monomer (**1**), homodimer (**1**)$_2$, heterodimer (**1**)(**4**), heterotetramer (**1**)$_2$(**4**)$_2$ and homotrimer (**4**)$_3$ were the major disulfide macrocycles formed in the DCL (Scheme 6.10). In addition to these products, a number of peaks with masses corresponding to library members that lost one or more pairs of daltons were also detected in the HPLC chromatogram of this DCL. These include macrocyclic heterotrimer [(**1**)(**4**)$_2$-2Da] and homotrimer [(**4**)$_3$-2Da] in addition to linear homodimer [(**4**)$_2$-4Da]. Moreover, cyclic heteropentamer [(**1**)(**4**)$_4$-2Da] was also detected however in a small quantity according to the HPLC chromatogram. The loss of two daltons from the masses of these DCL members has been discussed in paragraph 6.4.1.1.1. Based on the carboxylate substituent arrangements, the asymmetric structure of **4**

can give rise to five different isomers of $(\mathbf{1})_2(\mathbf{4})_2$ and two different isomers of $(\mathbf{4})_3$ (Figure 6.12).

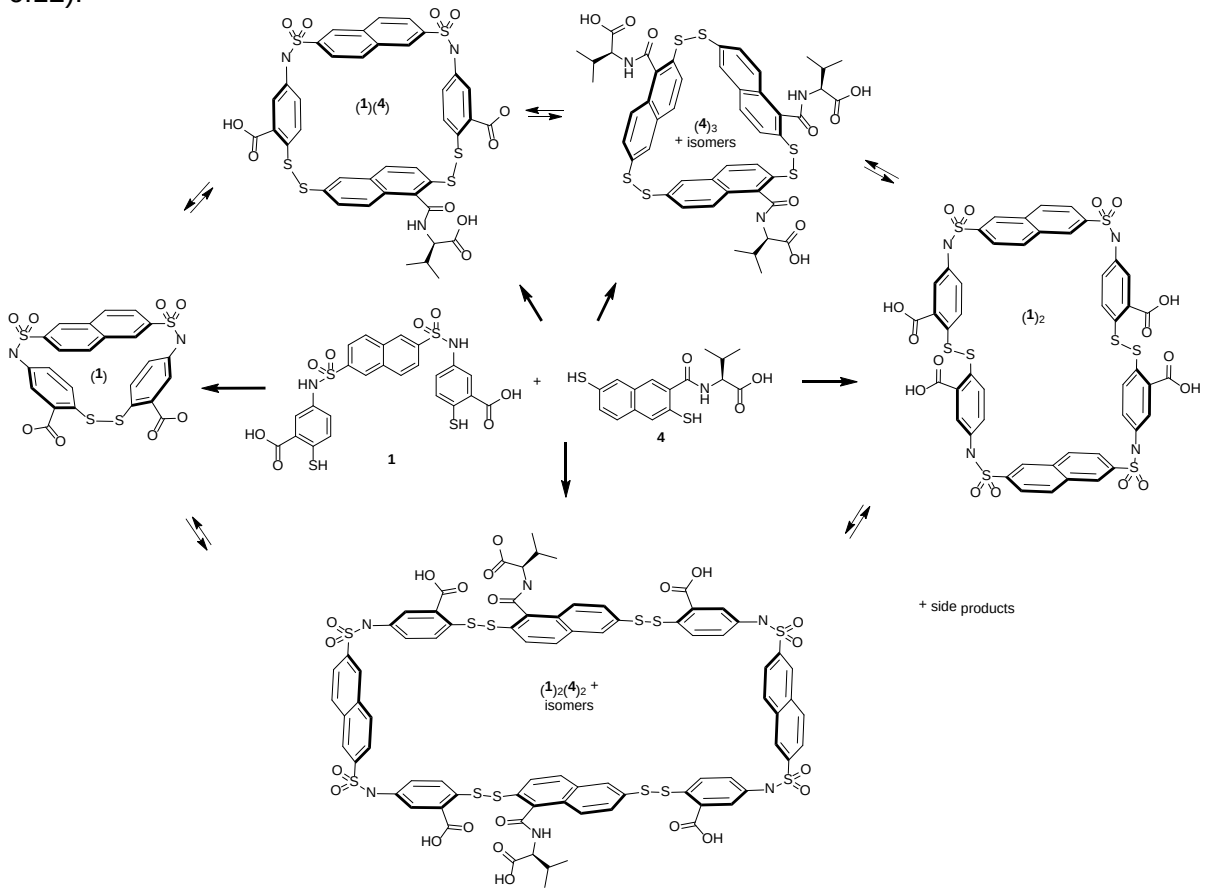

Scheme 6.10: Disulfide library products formed from building blocks **1** and **4** in 50 mM borate buffer at pH = 8.4. The DCL members include the following macrocycles: monomer (**1**), homodimer $(\mathbf{1})_2$, heterodimer (**1**)(**4**), heterotetramer $(\mathbf{1})_2(\mathbf{4})_2$ and homotrimer $(\mathbf{4})_3$. The side products include: macrocyclic heterotrimer (**1**)$(\mathbf{4})_2$-2Da, heteropentamer (**1**)$(\mathbf{4})_4$-2Da and homotrimer $(\mathbf{4})_3$-2Da in addition to linear homodimer $(\mathbf{4})_2$-4Da.

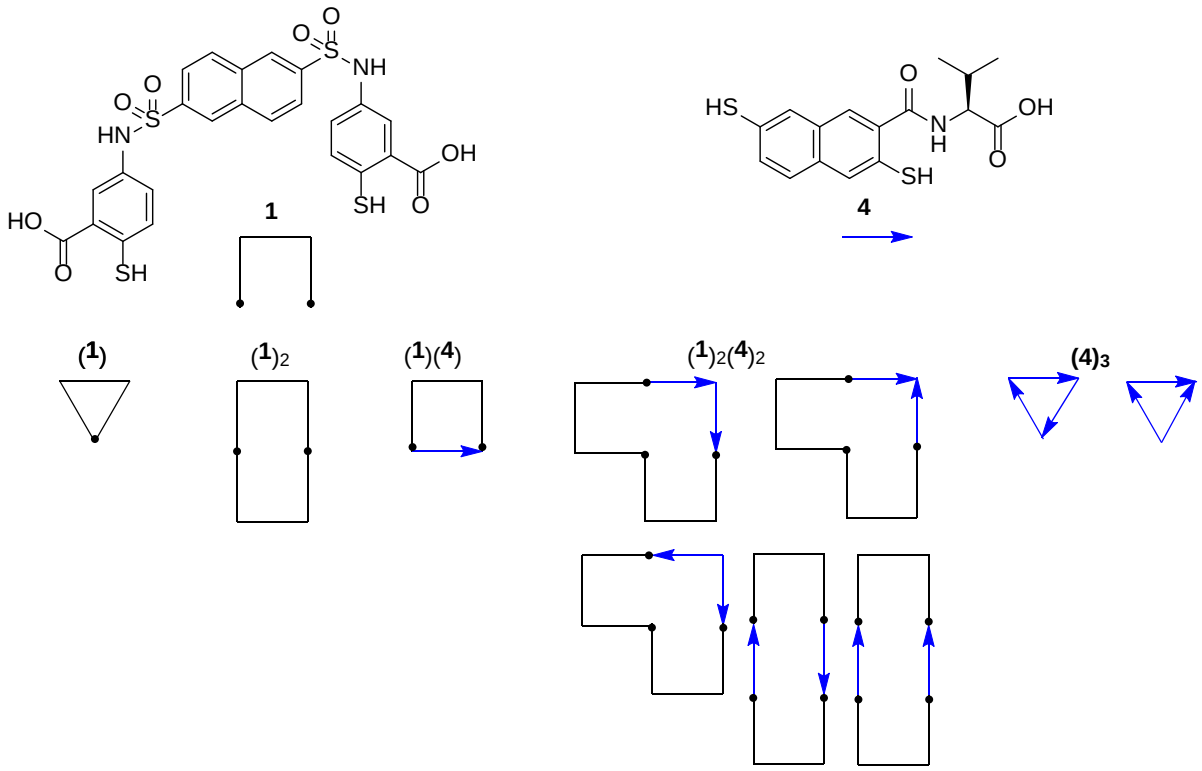

Figure 6.12: Schematic representation of the isomers expected in DCL products formed upon oxidizing a mixture of building blocks **1** and **4** in 50 mM borate buffer at pH 8.4. The possible numbers of isomers of the DCL product are: (from left to right) one isomer for (**1**), (**1**)$_2$ and (**1**)(**4**), five isomers for (**1**)$_2$(**4**)$_2$ and two isomers for (**4**)$_3$.

6.4.2.1 LC-MS data of the DCL products

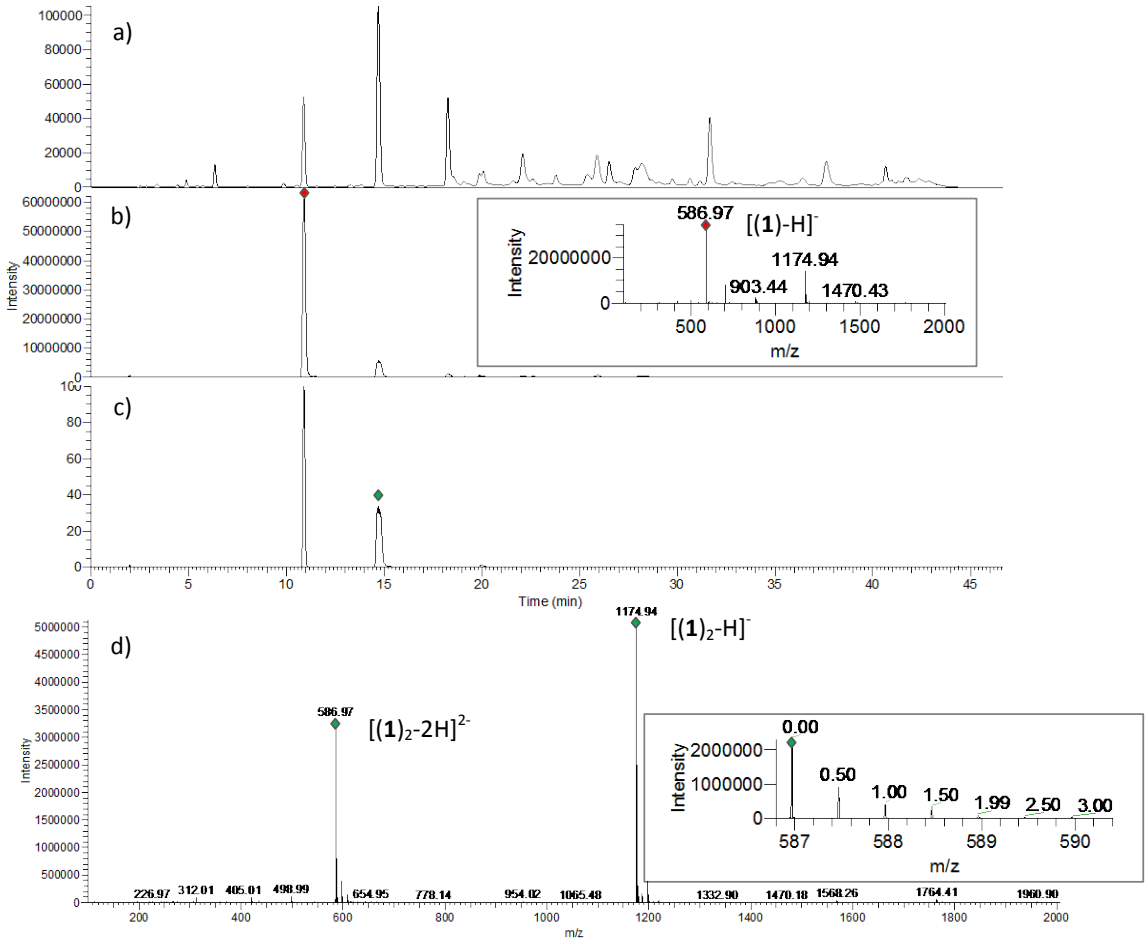

Figure 6.13: HPLC-MS analyses of a DCL prepared in 50.0 mM borate buffer (pH 8.4) and made from equimolar amounts of building blocks **1** and **4** and template **6.49** (2.0 mM for each). The DCL was diluted with 200 volume % DMSO immediately prior to analysis. (a) HPLC-UV chromatogram at λ_{abs} = 280 nm (λ_{ref} = 550 nm); (b) Extracted ion chromatogram (negative ion mode) corresponding to monocharged cyclic monomer (**1**) (586.5-587.5) with (insert) ESI-MS spectra [m/z 200-2000] summed over the 10.80-11.10 min retention time window, corresponding to cyclic monomer (**1**), showing [(**1**)-H]$^-$ m/z = 586.97 (expected = 586.98); (c) Extracted ion chromatogram (negative ion mode) corresponding to monocharged cyclic homodimer (**1**)$_2$ (1174.5-1175.5) and (d) ESI-MS spectra [m/z 200-2000] summed over the 14.50-15.00 min retention time window, corresponding to cyclic homodimer (**1**)$_2$, showing [(**1**)$_2$-H]$^-$ m/z = 1174.94 (expected = 1174.95) and [(**1**)$_2$-2H]$^{2-}$ m/z = 586.97 (expected = 586.98). The spacing of 0.5 mass units (insert) demonstrates that the [(**1**)$_2$-2H]$^{2-}$ ions are doubly charged. It is noteworthy to mention that the MS spectrum of the species eluting at 10.9 min shows a base peak corresponding to monocharged anion [(**1**)-H]$^-$, suggesting that the species is monomer (**1**), which further appears to aggregate in the ion source forming [(**1**)$_2$-H]$^-$, of lower intensity. By contrast, the MS spectrum of the species eluting at 14.8 min shows a base peak corresponding to [(**1**)$_2$-H]$^-$ and a corresponding doubly charged anion [(**1**)$_2$-2H] $^{2-}$. The different relative intensities of the two main peaks in the two spectra and the different charge states of the anions, easily identified from the isotopic peak spacing, help confirm the identity of both.

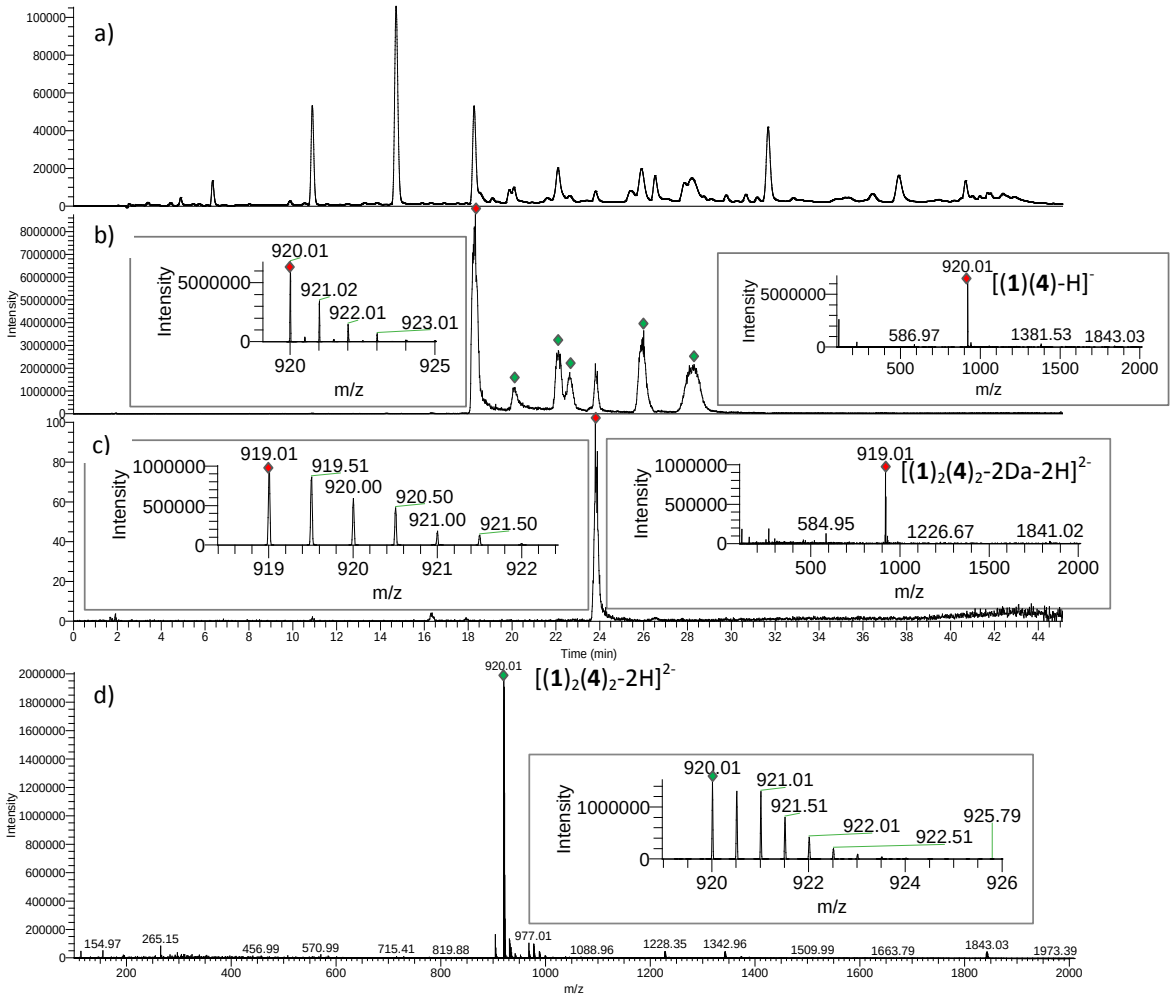

Figure 6.14: HPLC-MS analyses of a DCL prepared in 50.0 mM borate buffer (pH 8.4) and made from equimolar amounts of building blocks **1** and **4** and template **6.49** (2.0 mM for each). The DCL was diluted with 200 volume % DMSO immediately prior to analysis. (a) HPLC-UV chromatogram at 280 nm (λ_{ref} = 550 nm); (b) Extracted ion chromatogram (negative ion mode) corresponding to mono-charged cyclic heterodimer (**1**)(**4**) (919.5-920.5) with (right insert) ESI-MS spectra [m/z 200-2000] summed over the 18.00-18.60 min retention time window, corresponding to cyclic heterodimer (**1**)(**4**), showing [(**1**)(**4**)-H]$^-$ m/z = 920.01 (expected = 920.03). The spacing of 1 mass units (left insert) demonstrates that the [(**1**)(**4**)-H]$^-$ ions are mono-charged; (c) Extracted ion chromatogram (negative ion mode) corresponding to doubly charged cyclic heterotetramer [(**1**)$_2$(**4**)$_2$-2Da] (918.5-919.5) with (right insert) ESI-MS spectra [m/z 200-2000] summed over the 23.6-24.2 min retention time window, corresponding to cyclic heterodimer [(**1**)$_2$(**4**)$_2$-2Da], showing [(**1**)$_2$(**4**)$_2$-2Da-2H]$^{2-}$ m/z = 919.01 (expected = 919.03). The spacing of 0.5 mass units (left insert) demonstrates that the [(**1**)$_2$(**4**)$_2$-2Da-2H]$^{2-}$ ions are doubly charged; (d) ESI-MS spectra [m/z 200-2000] summed over the 20.0-20.4 min, 22.00-22.40 min, 22.40-22.80 min, 25.60-26.40 min and 28.00-29.00 retention time windows, corresponding to the fives isomers of cyclic heterotetramer (**1**)$_2$(**4**)$_2$, showing [(**1**)$_2$(**4**)$_2$-2H]$^{2-}$ m/z = 920.01 (expected = 920.03). The spacing of 0.5 mass units (insert) demonstrates that the [(**1**)$_2$(**4**)$_2$-2H]$^{2-}$ ions are doubly charged.

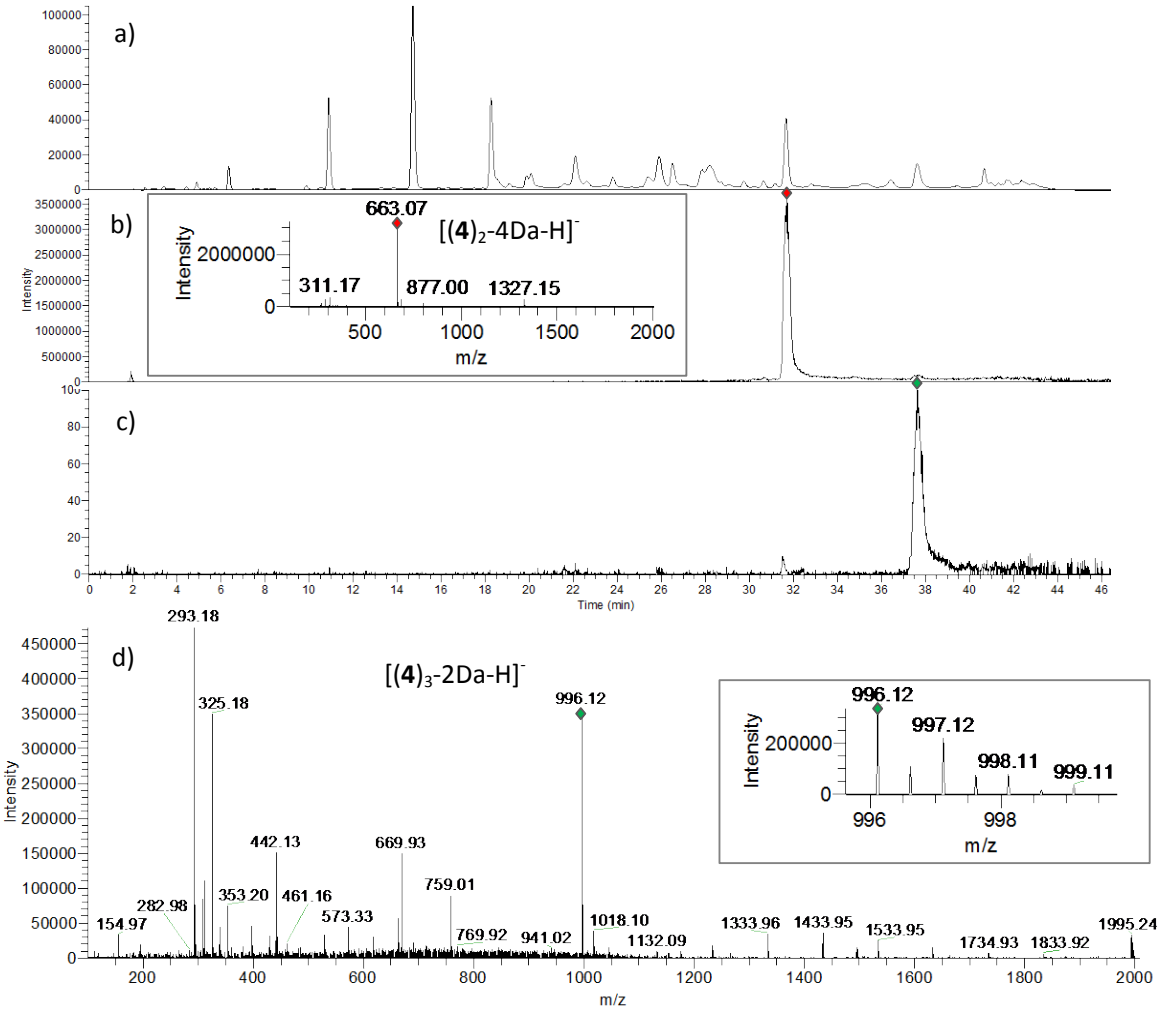

Figure 6.15: HPLC-MS analyses of a DCL prepared in 50 mM borate buffer (pH 8.4) and made from equimolar amounts of building blocks **1** and **4** and template **6.49** (6.0 mM in total). The DCL was diluted with 200 volume % DMSO immediately prior to analysis. (a) HPLC-UV chromatogram at 280 nm (λ_{ref} = 550 nm); (b) Extracted ion chromatogram (negative ion mode) corresponding to monocharged linear homodimer [(**4**)$_2$-4Da] (662.5-663.5) with (insert) ESI-MS spectra [m/z 200-2000] summed over the 31.40-32.0 min retention time window, corresponding to linear dimer [(**4**)$_2$-4Da], showing [(**4**)$_2$-4Da-H]$^-$ m/z = 663.07 (expected = 663.10); (c) Extracted ion chromatogram (negative ion mode) corresponding to monocharged cyclic homotrimer [(**4**)$_3$-2Da] (995.5-996.5); (d) ESI-MS spectra [m/z 200-2000] summed over the 37.30-38.07 min retention time window, corresponding cyclic homotrimer [(**4**)$_3$-2Da], showing [(**4**)$_3$-2Da-H]$^-$ m/z = 996.12 (expected = 996.15). The base peak in the MS spectrum of the species with retention time 37.68 min corresponds to the trimer [(**4**)$_3$-2Da] which also aggregates (as it happened also in Figure 6.14) in the source yielding [((**4**)$_3$-2Da)$_2$], further appearing in the spectrum as the peak envelope with lower intensity and peak spacing of 0.5 m/z units (insert) superimposed with the main peak and its corresponding isotopic peaks .

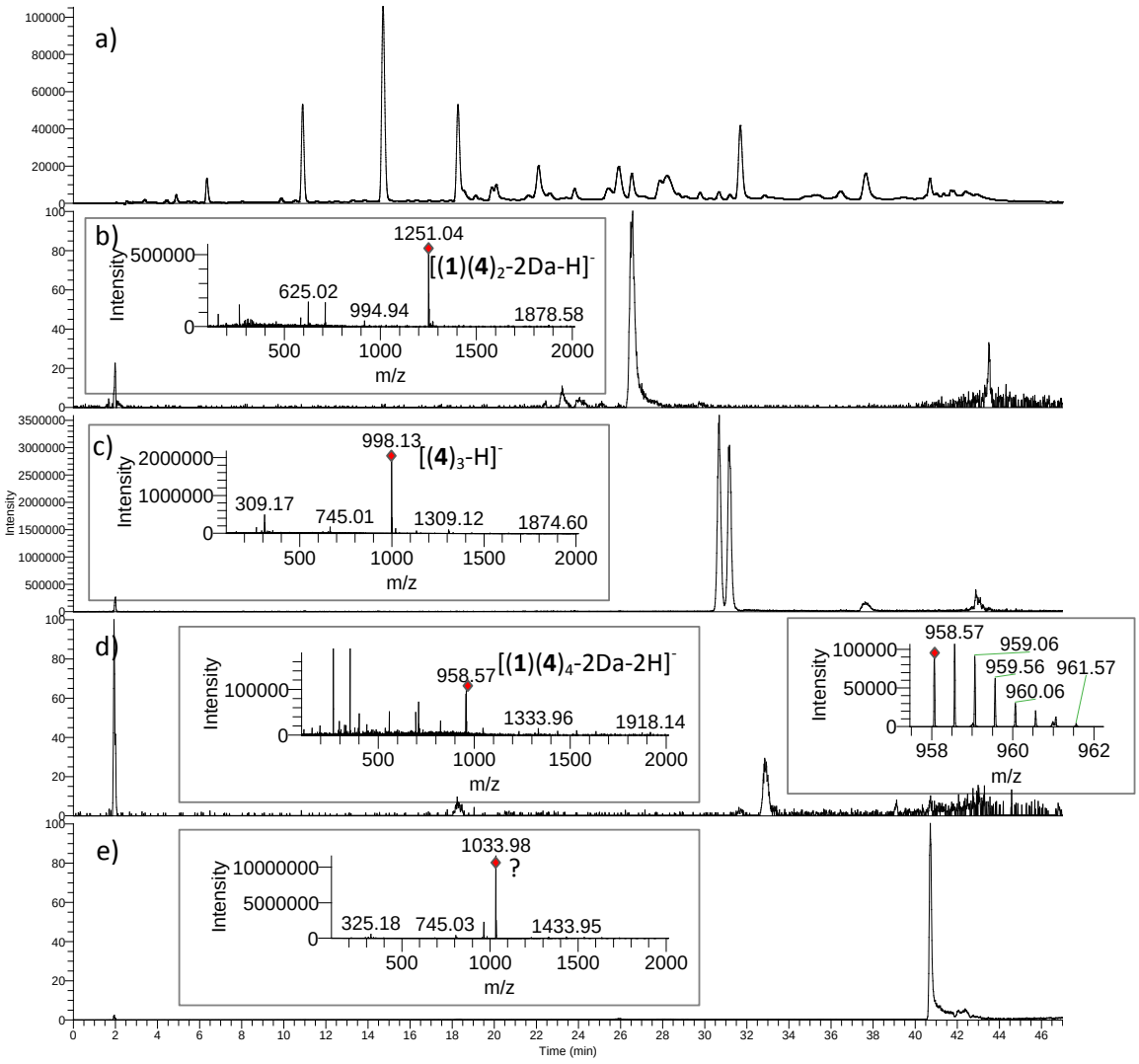

Figure 6.16: HPLC-MS analyses of a DCL prepared in 50 mM borate buffer (pH 8.4) and made from equimolar amounts of building blocks **1** and **4** and template **6.49** (6.0 mM in total). The DCL was diluted with 200 volume % DMSO immediately to analysis. (a) HPLC-UV chromatogram at 280 nm (λ_{ref} = 550 nm); (b) Extracted ion chromatogram (negative ion mode) corresponding to monocharged cyclic heterotrimer [(**1**)(**4**)$_2$-2Da] (1250.5-1251.5) with (insert) ESI-MS spectra [m/z 200-2000] summed over the 26.29-26.85 min retention time window, corresponding to cyclic heterotrimer [(**1**)(**4**)$_2$-2Da], showing [(**1**)(**4**)$_2$-2Da-H]$^-$ m/z = 1251.04 (expected = 1251.08) ; (c) Extracted ion chromatogram (negative ion mode) corresponding to monocharged cyclic homotrimer (**4**)$_3$ (918.5-919.5) with (insert) ESI-MS spectra [m/z 200-2000] summed over the 30.6-31.25 min retention time window, corresponding to two isomers of cyclic homotrimer (**4**)$_3$, showing [(**4**)$_3$-H]$^-$ m/z = 998.13 (expected = 998.15); (d) Extracted ion chromatogram (negative ion mode) corresponding to doubly charged cyclic heteropentamer [(**1**)(**4**)$_4$-2Da] (957.5-958.5) with (left insert) ESI-MS spectra [m/z 200-2000] summed over the 32.63-33.22 min retention time window, corresponding to cyclic heteropentamer [(**1**)(**4**)$_4$-2Da], showing [(**1**)(**4**)$_4$-2Da-2H]$^{2-}$ m/z = 957.06 (expected = 957.09). (right insert) The spacing of 0.5 mass units (insert) demonstrates that the [(**1**)(**4**)$_4$-2Da]$^{2-}$ ions are doubly charged. (e) Undefined singly charged product with m/z = 1033.98.

6.4.2.2 Effect of nicotine on a DCL made from building block 1 and 4

We then proceeded to compare the effects of nicotine (**6.48**) as a template on DCLs made from equimolar amounts of building blocks **1** and **2** and the corresponding DCL made from building blocks **1** and **4**. The effect of nicotine on a DCL made from building blocks **1** and **2** is described in chapter 2. We proceeded to prepare two DCLs made from equimolar amounts (2.0 mM for each) of building blocks **1** and **4** in the presence and absence of template **6.48** (2.0 mM) (Figure 6.17). The DCLs were prepared following standard protocols (see experimental part), allowed to equilibrate for three to four days at room temperature and analyzed using HPLC. When nicotine was introduced into the DCL, the area of the peak corresponding to macrocyclic heterodimer (**1**)(**4**) increased by an amplification factor of 1.6 relative to the untemplated DCL. This amplification factor is modest compared to the one obtained for macrocyclic dimer (**1**)(**2**) (AF = 3.2) in a DCL made from building blocks **1** and **2** after adding nicotine as a template. Moreover, introduction of nicotine drove the conversion of 40% of dithiols **1** and **2** into the formation of receptor (**1**)(**2**), while it drove the conversion of only 17.9 % of dithiols **1** and **4** into the formation of receptor (**1**)(**4**). However, adding the nicotine to the DCL has also increased the areas of the peaks corresponding to macrocyclic homotrimer [(**4**)$_3$-2Da], heteropentamer [(**1**)(**4**)$_4$-2Da] and undefined compound x by amplification factors of 3.8, 5.2 and 4.9 respectively, relative to the untemplated DCL (Figure 6.17). These library members in addition to macrocycle (**1**)(**4**) represent 34.2 % of the DCL materials.

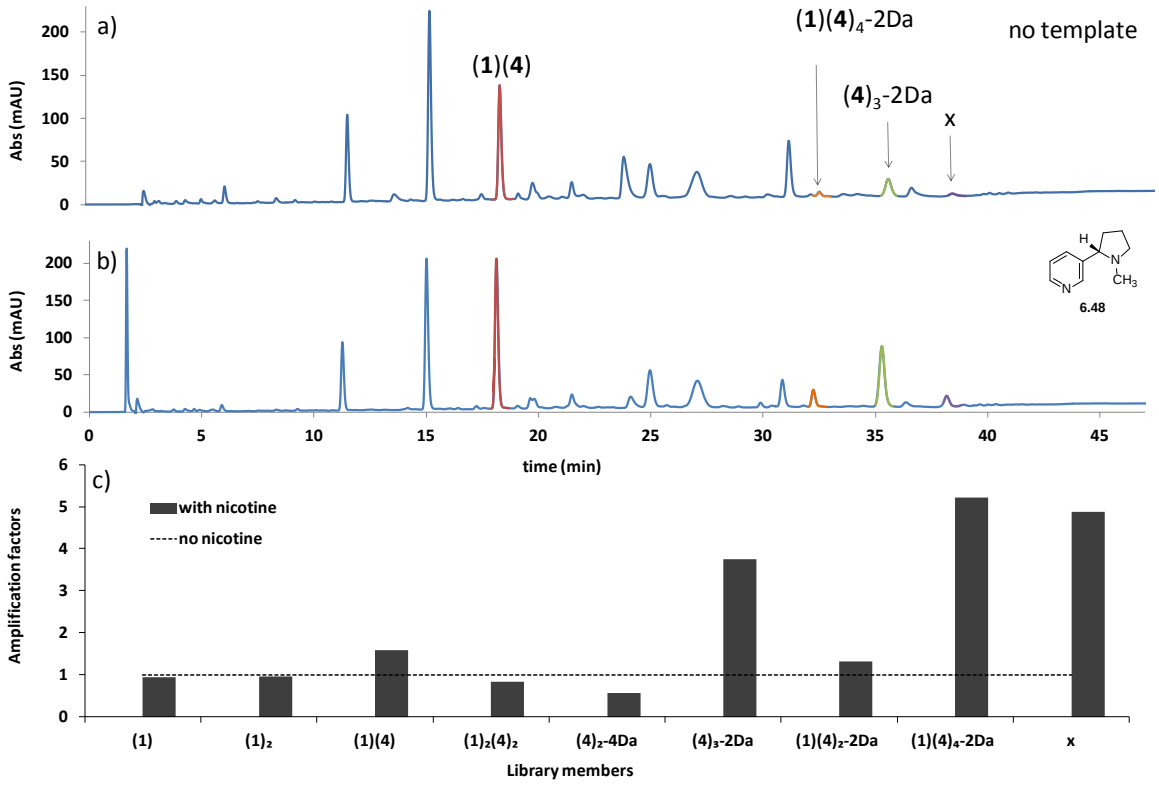

Figure 6.17: HPLC-UV chromatograms (λ_{abs} = 260 nm and λ_{ref} = 360 nm) of DCLs prepared in borate buffer (50 mM, pH 8.4) composed of equimolar amounts (2.0 mM for each) of building blocks **1** and **4**,

(a) in the absence (top) and (b) in presence (bottom) of nicotine **6.48** (2.0 mM). (c) Amplification factors for the main library members. DCLs were diluted with 200 volume % DMSO immediately prior to analyses.

6.4.2.3 Effect of (R,S)-ephedrine and its stereoisomers on a DCL made from building block 1 and 4

We proceeded to study the ability of oligomeric macrocycles formed from building blocks **1** and **4** in an attempt to address stereoselective recognition phenomena. Thus, we templated the DCL with ephedrine (Figure 6.18), as this compound has two chiral centres giving rise to four stereoisomers. Ephedrine also contains moieties convenient for the recognition of the formed macrocycles, such as the hydrophobic benzene ring and the hydrophilic amine which is protonated at physiological pH (pK_a = 9.6).[62] These moieties are capable to be engaged in hydrogen-bonding, ion pairing and salt bridge interactions with the macrocycles in the DCL.

Four DCLs made from equimolar amounts (2.0 mM for each) of the two building blocks in the absence and presence of (R,S)-ephedrine (**6.49**), (S,S)-ephedrine (**6.50**), (R,R)-ephedrine (**6.51**) and (S,R)-ephedrine (**6.52**) as individual templates (2.0 mM for each) were prepared (Figure 6.18). The DCLs were prepared following standard protocols (see experimental part), allowed to equilibrate for five to six days at room temperature and analyzed using HPLC-UV. When template **6.49** was introduced into the DCL, the area of the peak corresponding to macrocyclic heterotrimer [(**4**)$_3$-2Da] increased by an amplification factor of 1.9 relative to the untemplated DCL. Adding template **6.50**, a diastereoisomer of **6.49**, into the DCL induced a very similar increase in the area of the peak corresponding to [(**4**)$_3$-2Da] (AF = 2), in comparison with its AF after adding **6.49**. Adding template **6.51**, another diasterioisomer of **6.49**, increased the area of the peak corresponding to [(**4**)$_3$-2Da] slightly less than **6.49** (AF = 1.6), however adding template **6.51**, the enantiomer of **6.49**, increased the area of [(**4**)$_3$-2Da] 1.5 times more than **6.49**.

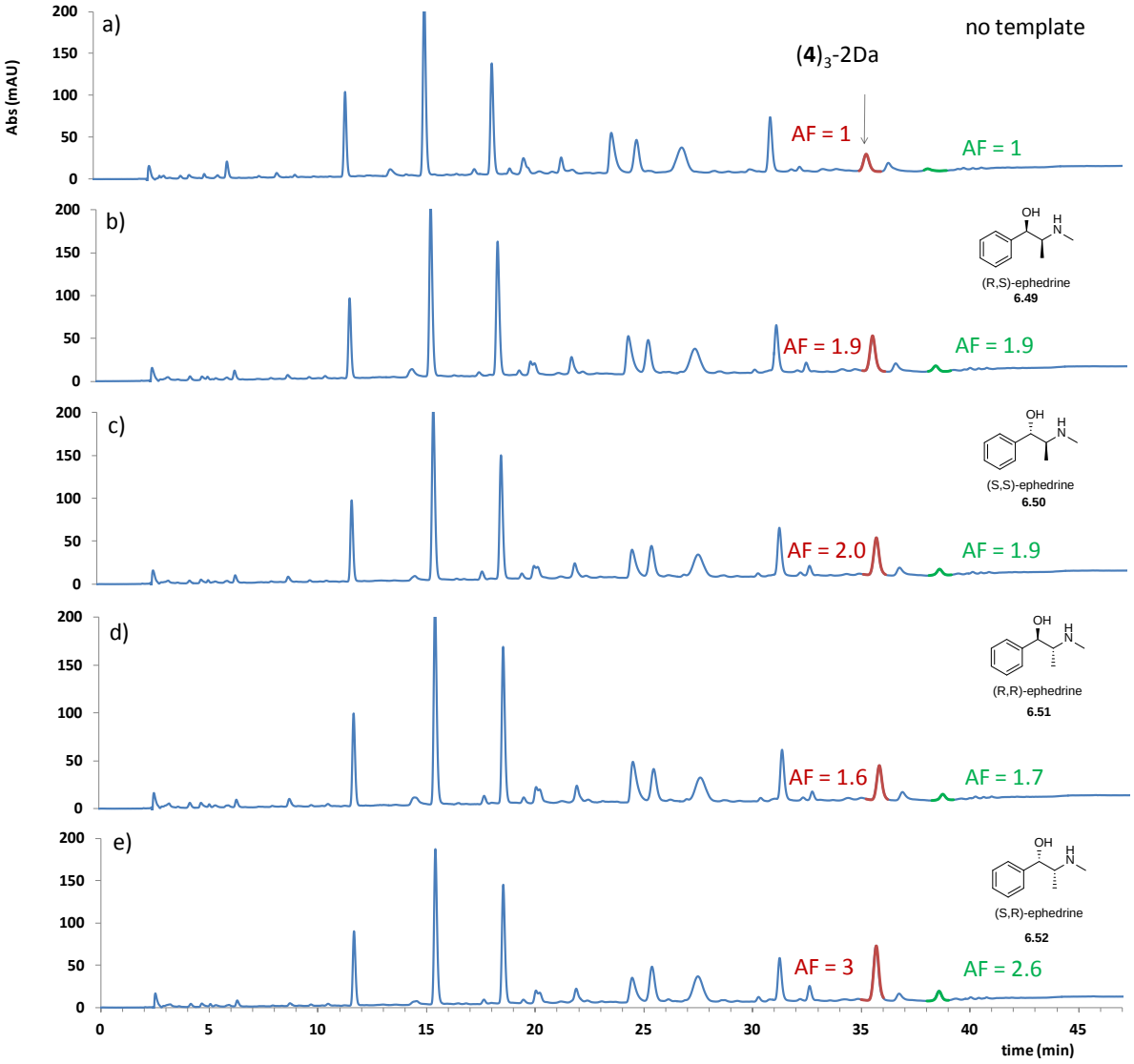

Figure 6.18: HPLC-UV chromatograms (λ_{abs} = 260 nm and λ_{ref} = 360 nm) of DCLs prepared in borate buffer (50 mM, pH 8.4) composed of equimolar amounts (2.0 mM for each) of building blocks **1** and **4**, (a) in the absence of template and (b) presence of (R,S)-ephedrine (**6.49**), (c) (S,S)-ephedrine (**6.50**), (R,R)-ephedrine (**6.51**) and (S,R)-ephedrine (**6.52**) as individual templates (2.0 mM for each). DCLs were diluted with 200 volume % DMSO immediately to analysis.

6.4.2.4 Effect of derivatization of building block 2 with a valine residue on the diversity of a DCL made from building blocks 1 and 4

Mixing building block **1** with valine derivatized building block **4** has generated, through DCC, diverse higher molecular weight species. These include many macrocycles which probably have receptor properties such as heterodimer (**1**)(**4**), homotrimer [(**4**)$_3$-2Da] and heteropentamer [(**1**)(**4**)$_4$-2Da] which exhibited amplification upon addition of template **6.48**. The amplification of these three macrocycles signifies that the DCL is more responsive after the derivatization of **2** with valine, whereas only one library member, (**1**)(**2**), was amplified upon addition of template **6.48** to a DCL made from building blocks **1** and **2** . Moreover, the resulting DCL appeared to be able to exhibit modest enantioselective recognition by amplifying, to different extents, macrocyclic trimer [(**4**)$_3$-2Da] upon addition of the enantiomeric templates **6.49** and **6.52**. Furthermore, although the valine functionalization of building block **2** is at its periphery, it has affected its macrocyclization process, resulting in the formation of the relatively big macrocycle (**1**)$_2$(**4**)$_2$ and a small amount of macrocyclic trimer (**4**)$_3$, which both were not observed in the DCL made from building block **1** and **2** (Table 26). The entropic costs for the synthesis of relatively big macrocycle (**1**)$_2$(**4**)$_2$, (relative to macrocyle (**1**)(**2**)), must be counterbalanced by favorable intramolecular interactions between the amino acids carried by this macrocycle which have shifted the equilibrium towards its formation. The absence of catenantion has been commented on in paragraph 6.4.1.3.
On the other hand, the fact that the cyclic side products homotrimer [(**4**)$_3$-2Da] and heteropentamer [(**1**)(**4**)$_4$-2Da] have exhibited amplifications after exposing the DCL to nicotine, suggests that the products with masses reduced by one or more pairs of daltons are included in the thermodynamic equilibrium of the DCL.

Table 26: An overview of product distributions of binary DCLs made from equimolar amounts of building blocks **1** and **2**, and building blocks **1** and **4.** Both DCLs were prepared in 50 mM borate buffer at pH = 8.4. The products mentioned in the table are all cyclic unless indicated otherwise.

DCL building blocks	Main disulfide DCL products	Side products
1 + **2**	(**1**), (**1**)$_2$, (**1**)(**2**), (**2**)$_4$ and catenane (**2**)$_4$-(**2**)$_4$	----------
1 + **4**	(**1**), (**1**)$_2$, (**1**)(**4**), (**1**)$_2$(**4**)$_2$ and (**4**)$_3$.	(**1**)(**4**)$_2$-2Da, (**1**)(**4**)$_4$-2Da, (**4**)$_3$-2Da and linear (**4**)$_2$-4Da

6.4.3 DCL made from building blocks 3 and 4

For the same reasons that prompted us to study a DCL made from building blocks **1** and **4** in paragraph 6.4.2, we proceeded to prepare a DCL made from building blocks **3** and **4** in 50 mM borate buffer at pH 8.4 and allowed it to oxidize and exchange following standard protocols (see experimental part). The composition of the resulting DCL was analyzed by HPLC and mass spectrometry (Figure 6.19-Figure 6.24).

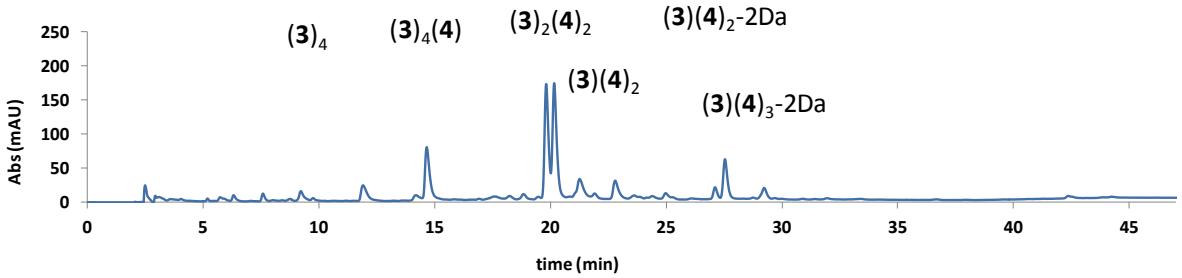

Figure 6.19: HPLC-UV chromatogram (λ_{abs} = 260 nm, λ_{ref} = 360 nm) showing the cyclic disulfide products including (**3**)$_4$, (**3**)$_4$(**4**), (**3**)$_2$(**4**)$_2$ and (**3**)(**4**)$_2$ in addition to cyclic side products (**3**)(**4**)$_2$-2Da and (**3**)(**4**)$_3$-2Da. The DCL was prepared in borate buffer (50 mM, pH 8.4) and composed of equimolar amounts (2.0 mM of each) of building blocks **3** and **4**, and analyzed after four to five days of equilibration. The DCL was diluted with 200 volume % DMSO immediately prior to analysis.

Homotetramer (**3**)$_4$, heterotetramers (**3**)$_4$(**4**), two isomers of heterotetramer (**3**)$_2$(**4**)$_2$ and heterotrimer (**3**)(**4**)$_2$ were the major disulfide macrocycles formed in the DCL. In addition to these products, a number of peaks of masses corresponding to library members that lost one pair of mass units were also detected in the HPLC chromatogram of this DCL. These include macrocyclic heterotrimer [(**3**)(**4**)$_2$-2Da] and heterotetramer [(**3**)(**4**)$_3$-2Da].The loss of two daltons from the masses of valine derivatized DCL members has been commented on in paragraph 6.4.1.1.1. Based on the carboxylate substituent arrangements, the asymmetric structure of **4** can give rise to five different isomers of (**3**)$_2$(**4**)$_2$ and three different isomers of (**3**)(**4**)$_2$ (Figure 6.21).
Moreover a monomer, a linear homodimer and a linear heterodimer, [(**4**)2O-2Da], [(**4**)$_2$2O-2Da] and [(**3**)(**4**)2O-2Da], respectively, each plus 30 daltons corresponding to the mass of two oxygen atoms minus two daltons were detected in the HPLC chromatogram of the DCL (Figure 6.20 and Figure 6.23). The incorporation of two oxygen atoms may correspond to a sulfinic acid oxidation state (SO_2H) of a terminal thiol in the case of the monomer, while it corresponds to a thiosulfonate oxidation state of a disulfide bond (-SO_2-S-) in the case of both dimers.[58] The loss of a pair of daltons from both the monomer and the dimers may correspond to oxidation of amino acid residues carried by the three over-oxidized products (see paragraph 6.4.1.1.1).

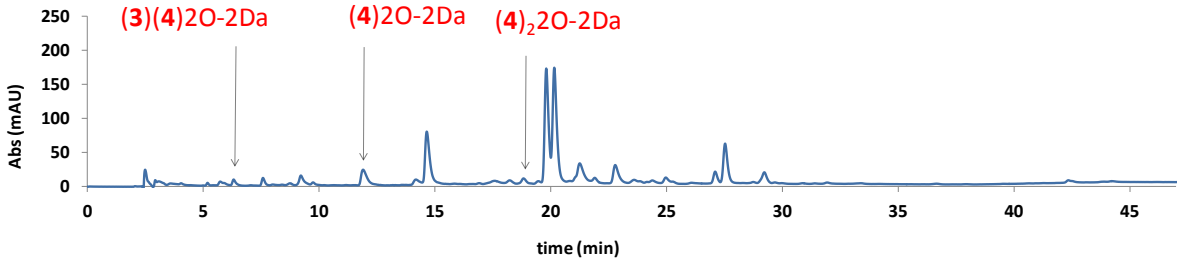

Figure 6.20: HPLC-UV analysis (λ_{abs} = 280 nm, λ_{ref} = 550 nm) of a DCL made from equimolar amounts of building blocks **3** and **4** (2.0 mM of each) in 50 mM borate buffer at pH 8.4, after adding 200 volume % DMSO prior to the analysis. The HPLC-UV chromatogram shows linear over-oxidized side products: (**3**)(**4**)2O-2Da, (**4**)2O-2Da and (**4**)$_2$2O-2Da.

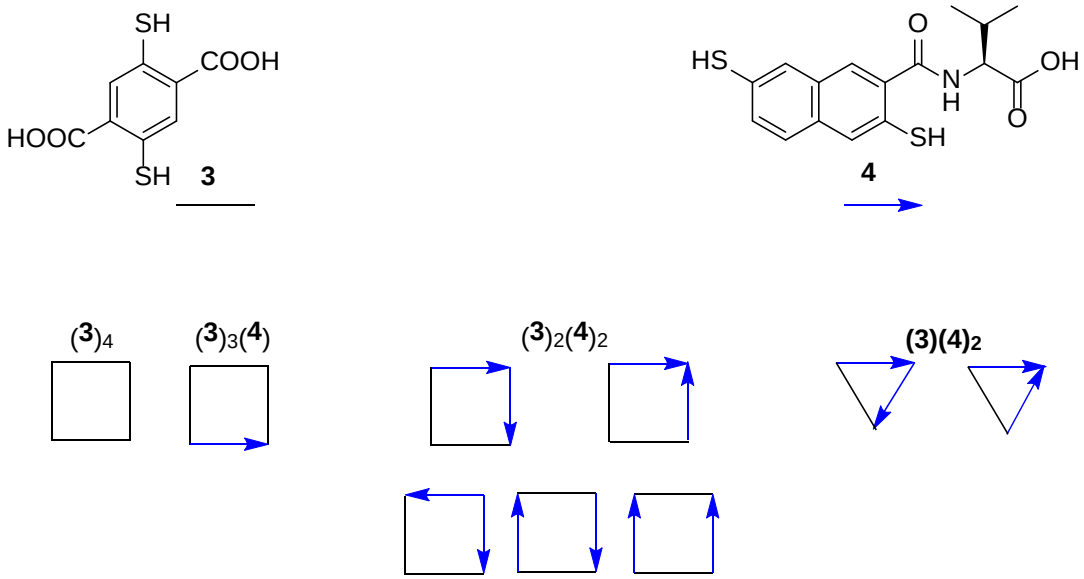

Figure 6.21: Schematic representation of the isomers expected in DCL products formed upon oxidizing a mixture of building blocks **3** and **4** in water at pH 8.4. The possible numbers of isomers of the DCL product are: (from left to right) one isomer for (**3**)$_4$ and (**3**)$_3$(**4**), five isomers for (**3**)$_2$(**4**)$_2$ and two isomers for (**3**)(**4**)$_2$.

6.4.3.1 LC-MS Data of the DCL products

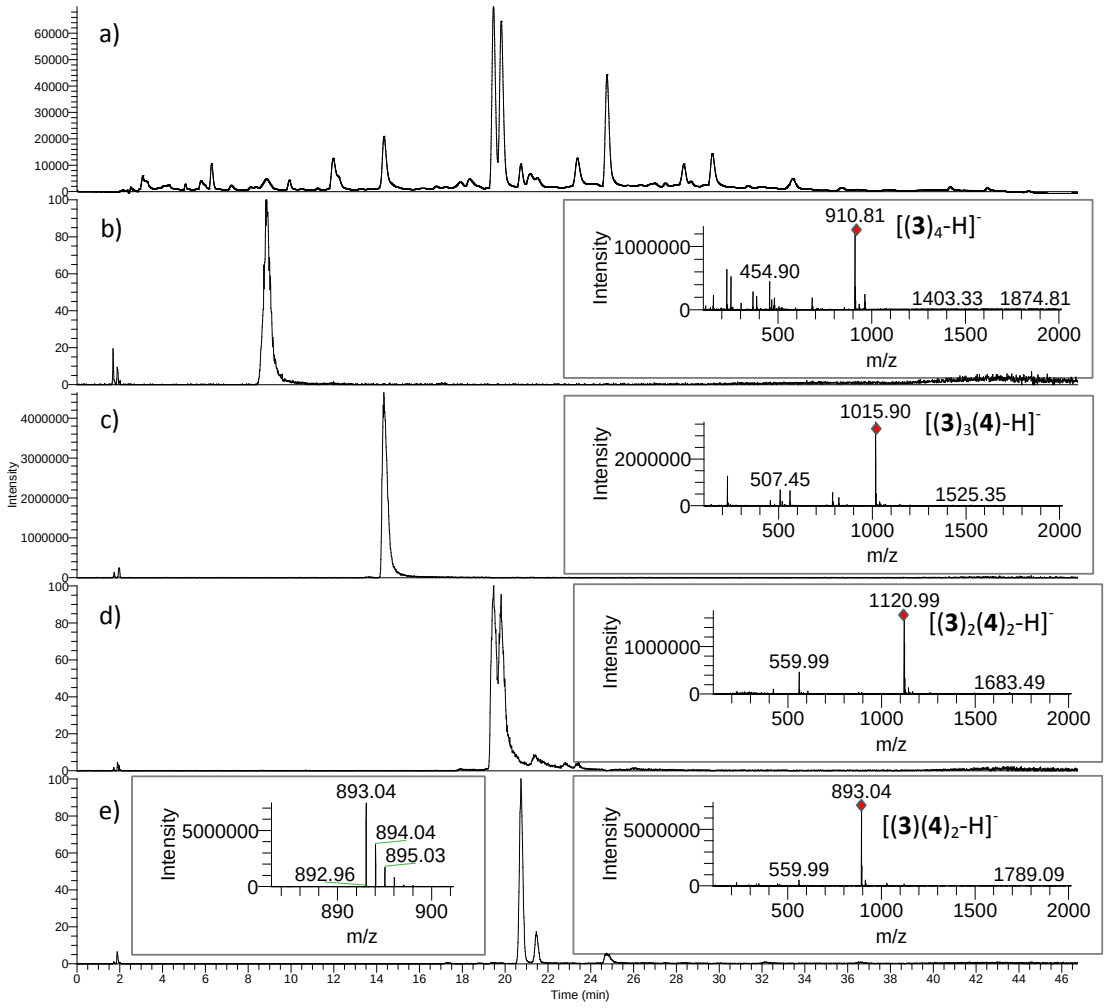

Figure 6.22: Analyses of a DCL prepared in 50 mM borate buffer (pH 8.4) and made from equimolar amounts of building blocks **3** and **4** and template **6.49** (6.0 mM in total). The DCL was diluted with 200 volume % DMSO prior to analysis. (a) HPLC-UV chromatogram at 280 nm (λ_{ref} = 550 nm); (b) Extracted ion chromatogram (negative ion mode) corresponding to monocharged cyclic homotetramer $(\mathbf{3})_4$ (910.5-911.5) with (insert) ESI-MS spectra [m/z 200-2000] summed over the 8.53-9.35 min retention time window, corresponding to cyclic homotetramer $(\mathbf{3})_4$, showing $[(\mathbf{3})_4\text{-H}]^-$ m/z = 910.81 (expected = 910.84); (c) Extracted ion chromatogram (negative ion mode) corresponding to monocharged cyclic heterotetramer $(\mathbf{3})_3(\mathbf{4})$ (1015.5-1016.5) with (insert) ESI-MS spectra [m/z 200-2000] summed over the 14.08-14.76 min retention time window corresponding to cyclic heterotetramer $(\mathbf{3})_3(\mathbf{4})$, showing $[(\mathbf{3})_3(\mathbf{4})\text{-H}]^-$ m/z = 1015.90 (expected = 1015.93);. (d) Extracted ion chromatogram (negative ion mode) corresponding to monocharged cyclic heterotetramer $(\mathbf{3})_2(\mathbf{4})_2$ (1120.5-1121.5) with (insert) ESI-MS spectra [m/z 200-2000] summed over the 19.18-19.32 and 19.32-20.14 min retention time windows, corresponding to isomers of cyclic heterotetramer $(\mathbf{3})_2(\mathbf{4})_2$, showing $[(\mathbf{3})_2(\mathbf{4})_2\text{-H}]^-$ m/z = 1120.99 (expected = 1121.02); (e) Extracted ion chromatogram (negative ion mode) corresponding to monocharged cyclic heterotrimer $(\mathbf{3})(\mathbf{4})_2$ (892.5-893.5) with (insert) ESI-MS spectra [m/z 200-2000] summed over the 20.6-20.9 and 21.43-21.70 min retention time windows, corresponding to cyclic heterotrimer $(\mathbf{3})(\mathbf{4})_2$, showing $[(\mathbf{3})(\mathbf{4})_2\text{-H}]^-$ m/z = 893.04 (expected = 893.06).

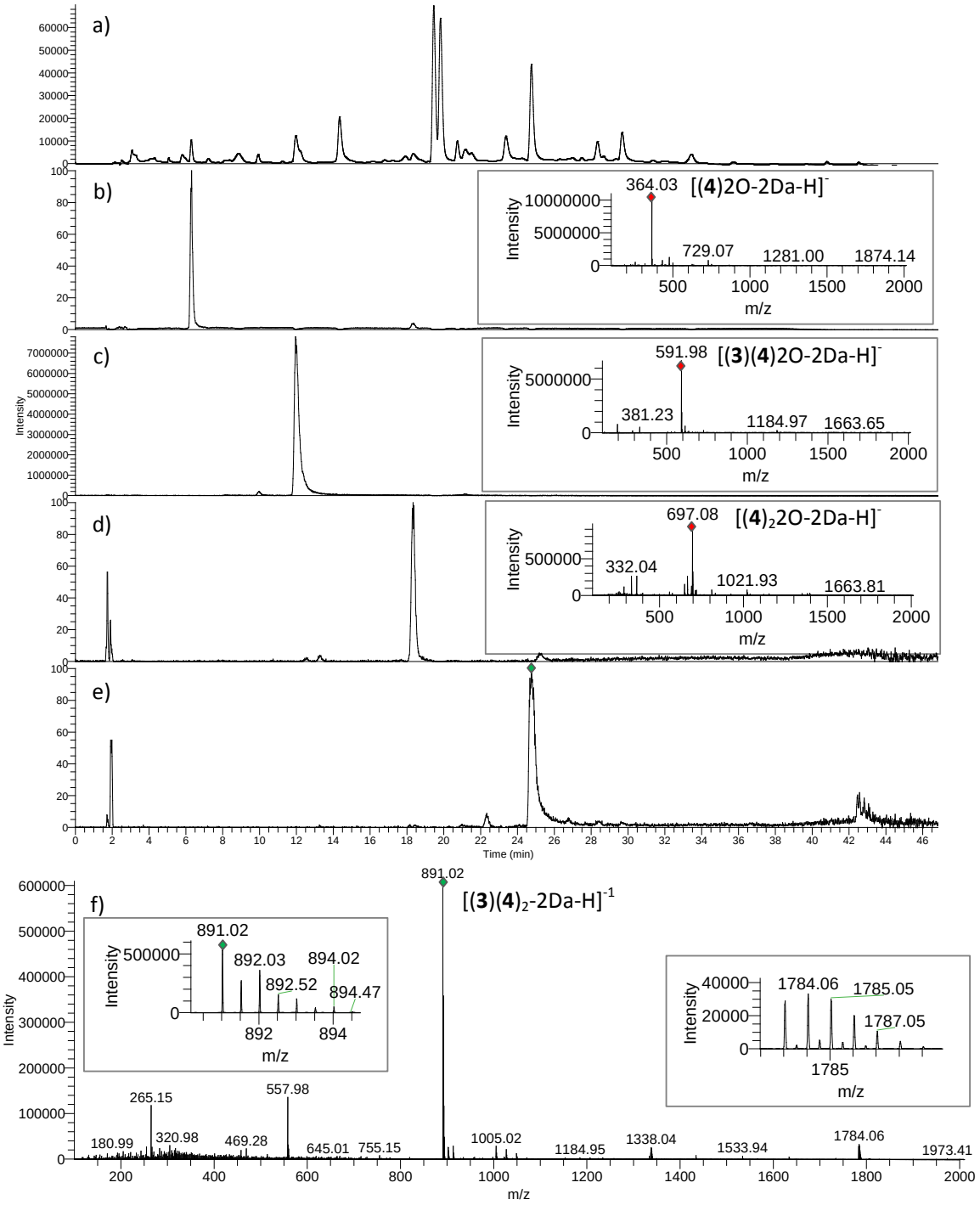

Figure 6.23: Analyses of a DCL prepared in 50 mM borate buffer (pH 8.4) and made from equimolar amounts of building blocks **3** and **4** and template **6.49** (6.0 mM in total). The DCL was diluted with 200 volume % DMSO prior to analysis. (a) HPLC-UV chromatogram at 280 nm (λ_{ref} = 550 nm); (b) Extracted ion chromatogram (negative ion mode) corresponding to monocharged over-oxidized monomer [(**4**)2O-2Da] (363.5-364.5) with (insert) ESI-MS spectra [m/z 200-2000] summed over the 6.08-6.55 min retention time window, corresponding to over-oxidized monomer [(**4**)2O-2Da], showing [(**4**)2O-2Da-H]$^-$ m/z = 364.03 (expected = 364.04); (c) Extracted ion chromatogram (negative ion mode) corresponding to monocharged linear over-oxidized linear dimer [(**3**)(**4**)2O-2Da] (591.5-592.5)

with (insert) ESI-MS spectra [m/z 200-2000] summed over the 11.68-12.44 min retention time window, corresponding over-oxidized linear dimer [(**3**)(**4**)2O-2Da], showing [(**3**)(**4**)2O-2Da-H]$^-$ m/z = 591.98 (expected = 592.01);. (d) Extracted ion chromatogram (negative ion mode) corresponding to monocharged over-oxidized linear dimer [(**4**)$_2$2O-2Da] (696.5-697.5) with (insert) ESI-MS spectra [m/z 200-2000] summed over the 17.8-18.7 min retention time window, corresponding over-oxidized linear dimer [(**4**)$_2$2O-2Da], showing [(**4**)$_2$2O-2Da-H]$^-$ m/z = 697.08 (expected = 697.10); (e) Extracted ion chromatogram (negative ion mode) corresponding to mono-charged cyclic heterotrimer [(**3**)(**4**)$_2$-2Da] (890.5-891.5) and (f) ESI-MS spectra [m/z 200-2000] summed over the 24.5-25.5 min retention time window, corresponding to cyclic heterotrimer [(**3**)(**4**)$_2$-2Da], showing [(**3**)(**4**)$_2$-2Da-H]$^-$ m/z = 891.02 (expected = 891.06). The base peak in the MS spectrum corresponding to [(**3**)(**4**)$_2$-2Da-H]$^-$ also aggregates in the source forming the monocharged hexamer ((**3**)(**4**)$_2$-2Da-H)$_2^-$. The different isotopic distributions between the base peak [(**3**)(**4**)$_2$-2Da-H]$^-$ and the aggregate ((**3**)(**4**)$_2$-2Da-H)$_2^-$ allow us to exclude the possible assignment of the aggregate peak to hexamer [(**3**)$_2$(**4**)$_4$-4Da-H]$^-$, which if doubly charged would display a very similar isotopic distribution as the parent monocharged ion [(**3**)(**4**)$_2$-2Da-H]$^-$.

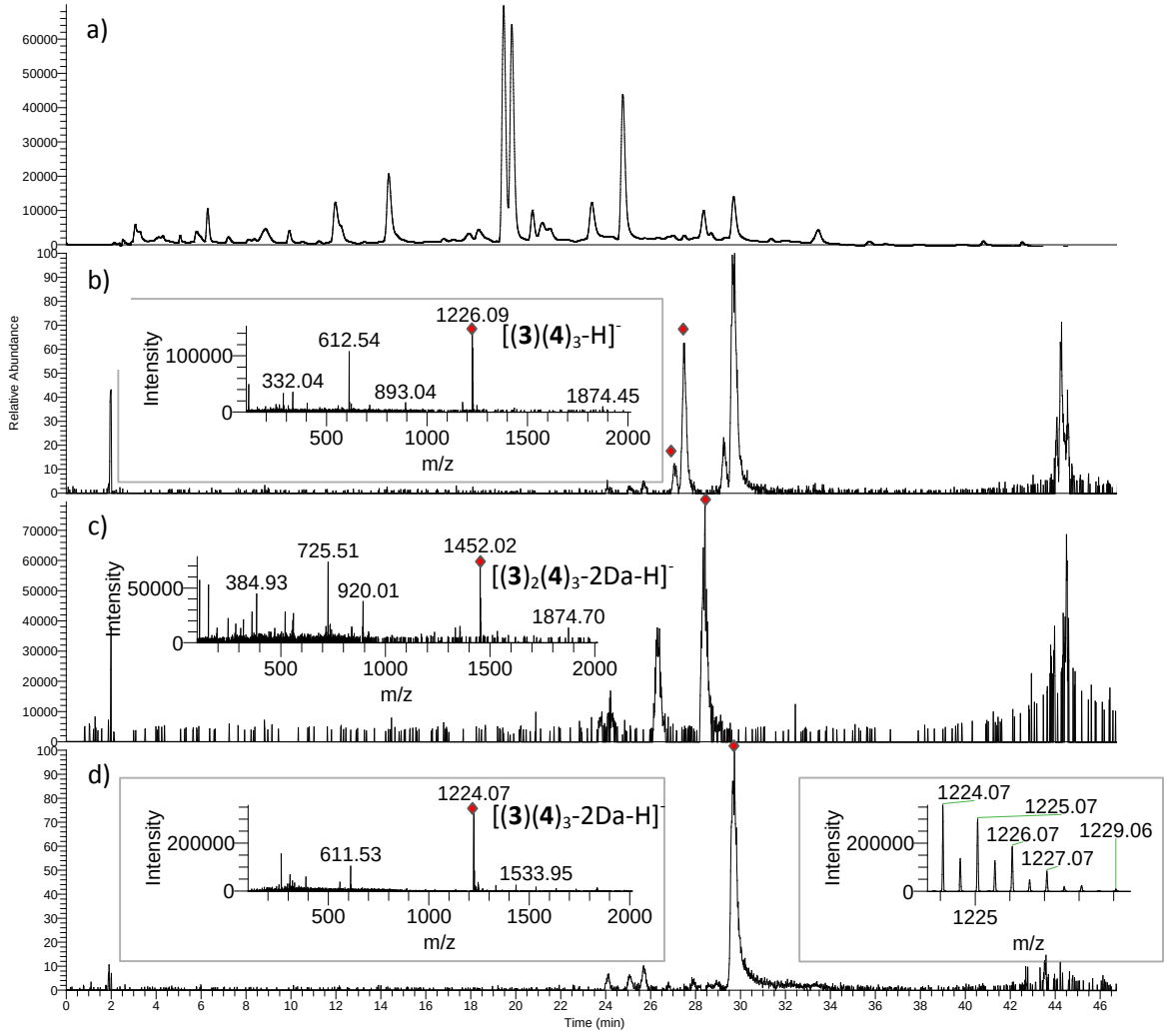

Figure 6.24: Analyses of a DCL prepared in 50 mM borate buffer (pH 8.4) and made from equimolar amounts of building blocks **3** and **4** (4.0 mM in total) and template **6.49** (6.0 mM in total). The DCL was diluted with 200 volume % DMSO prior to analysis. (a) HPLC-UV chromatogram at 280 nm (λ_{ref} = 550 nm); (b) Extracted ion chromatogram (negative ion mode) corresponding to monocharged

heterotetramer (**3**)(**4**)$_3$ (1225.5-1226.5) with (insert) ESI-MS spectra [m/z 200-2000] summed over the 27.06-27.13 and 27.13-27.8 min retention time windows, corresponding to isomers of homotetramer (**3**)(**4**)$_3$, showing [(**3**)(**4**)$_3$-H]$^-$ m/z = 1226.09 (expected = 1226.11); (c) Extracted ion chromatogram (negative ion mode) corresponding to monocharged heteropentamer [(**3**)$_2$(**4**)$_3$-2Da] (1451.5-1452.5) with (insert) ESI-MS spectra [m/z 200-2000] summed over the 28.25-28.73 min retention time window, corresponding heteropentamer [(**3**)$_2$(**4**)$_3$-2Da], showing [(**3**)$_2$(**4**)$_3$-2Da-H]$^-$ m/z = 1452.02 (expected = 1452.07); (d) Extracted ion chromatogram (negative ion mode) corresponding to monocharged heterotetramer [(**3**)(**4**)$_3$-2Da] (1223.5-1224.5) with (insert) ESI-MS spectra [m/z 200-2000] summed over the 29.4-30.20 min retention time window, corresponding to heterotetramer (**3**)(**4**)$_3$-2Da, showing [(**3**)(**4**)$_3$-2Da-H]$^-$ m/z = 1224.07 (expected = 1224.11).

6.4.3.2 Effect of (R,S)-ephedrine on a DCL made from building blocks 3 and 4

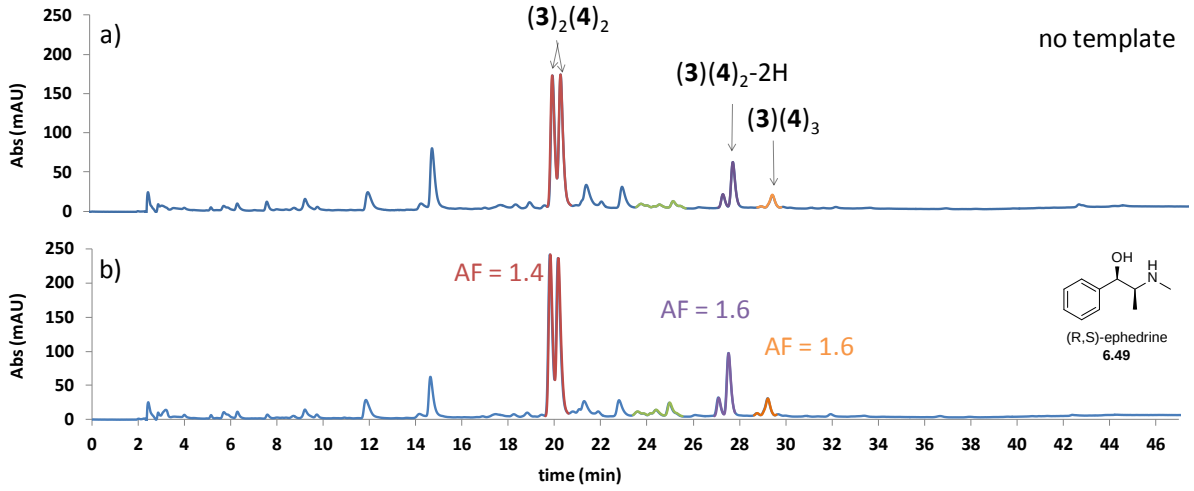

Figure 6.25: HPLC-UV chromatograms (λ_{abs} = 260 nm and λ_{ref} = 360 nm) of DCLs prepared in borate buffer (50 mM, pH 8.4) composed of equimolar amounts (2.0 mM for each) of building blocks **3** and **4**, (a) in the absence and (b) in presence of (R,S)-ephedrine **6.49** (2.0 mM).

Two DCLs made from equimolar amounts of building blocks **3** and **4** (4.0 mM in total) were prepared in the absence and presence of (R,S)-ephedrine (**6.49**) (2.0 mM) as a template. When template **6.49** was introduced into the DCL, the areas of the peaks corresponding to macrocyclic heterodimer (**3**)$_2$(**4**)$_2$, heterotrimer [(**3**)(**4**)$_2$-2Da] and heterotetramer (**3**)(**4**)$_3$ increased by amplification factors of 1.4, 1.6 and 1.6, respectively, relative to the untemplated DCL (Figure 6.25). The comparison between the effects of template **6.49** on a DCL made from building blocks **2** and **3** and a DCL made from building blocks **3** and **4** revealed that the latter is more responsive towards template **6.49** addition. That is the addition of template **6.49** to the first DCL has resulted in the increase of concentrations of (**2**)$_2$(**3**)$_3$ and (**2**)(**3**)$_3$ by AFs corresponding to 1.40 and 1.46, respectively. As a result, functionalizing building block **2** with valine has resulted in a somewhat more responsive DCL.

6.4.3.3 Effect of derivatization of building block 2 with a valine residue on the diversity of a DCL made from building blocks 3 and 4

The formation of the relatively small macrocycle (**3**)(**4**)$_2$ and the absence of catenation has been commented on in paragraph 6.4.1.3.

Table 27: An overview of product distributions of DCLs made from equimolar amounts of building blocks **2** and **3** and equimolar amounts of building blocks **3** and **4.** Both DCLs were prepared in 50 mM borate buffer at pH = 8.4. The products mentioned in the table are all cyclic unless indicated otherwise.

DCL building blocks	Disulfide DCL products	Side products with substracted masses	Linear over-oxidized side products
2 + **3**	(**3**)$_4$, (**2**)(**3**)$_3$, (**2**)$_2$(**3**)$_2$, (**2**)$_3$(**3**), (**2**)$_4$, (**2**)$_2$(**3**)$_3$ and catenanes (**2**)$_4$-(**2**)$_4$ and (**2**)$_3$(**3**)-(**2**)$_4$.	----------	(**3**)$_2$4O, (**3**)$_3$4O, (**2**)(**3**)4O and (**2**)(**3**)$_2$4O
3 + **4**	(**3**)$_4$, (**3**)$_4$(**4**), (**3**)$_2$(**4**)$_2$ and (**3**)(**4**)$_2$	(**3**)(**4**)$_2$-2Da and (**3**)(**4**)$_3$-2Da	(**3**)(**4**)2O-2Da, (**4**)2O-2Da and (**4**)$_2$2O-2Da

6.4.4 DCL made from building blocks 2 and 5

Similarly to the experiments performed on binary DCLs made from the mixture of building blocks **1**, **3** and **4**, we proceeded to prepare a DCL made from equimolar amounts of building blocks **2** and **5** (2.0 mM each) in 50 mM borate buffer at pH 8.4 and allowed it to oxidize and equilibrate following standard protocols (see experimental part). The composition of the resulting DCL was analyzed by HPLC and mass spectrometry (Figure 6.26 and Figure 6.28).

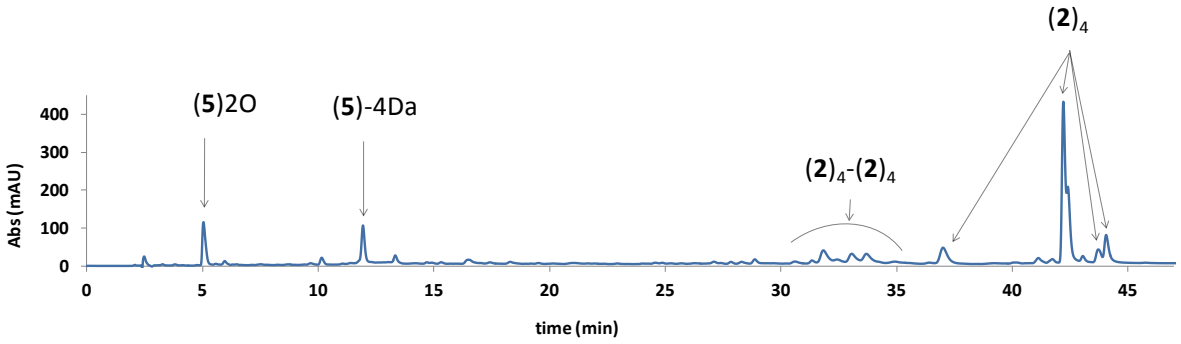

Figure 6.26: HPLC-UV chromatogram (λ_{abs} = 260 nm and λ_{ref} = 360 nm) of a DCL composed of equimolar amounts (2.0 mM for each) of building blocks **2** and **5** and prepared in 50 mM borate buffer at pH 8.4. The DCL was diluted with a 200 volume % DMSO immediately prior to analysis. The HPLC-UV chromatogram shows the disulfide macrocyles (**2**)$_4$ and catenane (**2**)$_4$-(**2**)$_4$ in addition to side products (**5**)2O and (**5**)-4Da.

Homocatenane (**2**)$_4$-(**2**)$_4$ and homotetramer (**2**)$_4$ were the major disulfide macrocycles detected in the HPLC chromatogram of the DCL. Moreover, monomer **5** plus 32 daltons,

(**5**)2O, corresponding to the mass of two oxygen atoms and probably corresponding to the sulfinic acid oxidation state (SO_2H) of dithiol **5**, in addition to monomer **5** minus four mass units were also detected. The behavior of building block **5** in the DCL is in line with our understanding of amino acid functionalized building block **2** reported in paragraph 6.4.1.1.1. Whereas the maximal loss is 2 Da for monomer **4**, it is 4 Da for monomer **5**. This observation is in line with our speculation that the amino acid residues are responsible for the dalton pair loss (see paragraph 6.4.1.1.1). Moreover, substituting the two electron donating carboxylate groups of building block **3** with two electron withdrawing amide groups (building block **5**) has reduced the nucleophilicity of the latter in a more pronounced way than dithiol **4**, which carries only one withdrawing amide group. This has reduced the oxidation rate of dithiol **5** a lot more compared to dithiol **4**. Furthermore, the steric hindrance caused by the two bulky amino acid residues adjacent to the two sulfur atoms may also have reduced the oxidation rate of dithiol **5**. The effect of steric hindrance on the oxidation rate could be more pronounced in case of dithiol **5** than in case of dithiol **4**, which carries only one bulky residue adjacent to sulfur atom. The slow rate of oxidation explains the fact that after 7 days of equilibration the main DCL members were monomer (**5**)-4Da in addition to over-oxidized monomer (**5**)2O. It also explains why monomers **5** did not react with each other or with monomers **2**, while the latter were able to interact with each other forming homo-catenane $(\mathbf{2})_4$-$(\mathbf{2})_4$ and homotetramer $(\mathbf{2})_4$. Furthermore, the ratio homotetramer $(\mathbf{2})_4$/catenane $(\mathbf{2})_4$-$(\mathbf{2})_4$ obtained in the DCL is seven times higher than the one obtained in a DCL made only from building block **2** (see chapter 4, Figure 4.14). While this happened in absence of any external template effect, we speculate that intermolecular interactions potentially occurring between amino acid functionalized monomers (**5**)2O or [(**5**)-4Da] and homotetramer $(\mathbf{2})_4$ have played a role in the amplification of homotetramer $(\mathbf{2})_4$.

6.4.4.1 Effects of (R,S)-ephedrine and (S,S)-ephedrine on a DCL made from building blocks 2 and 5

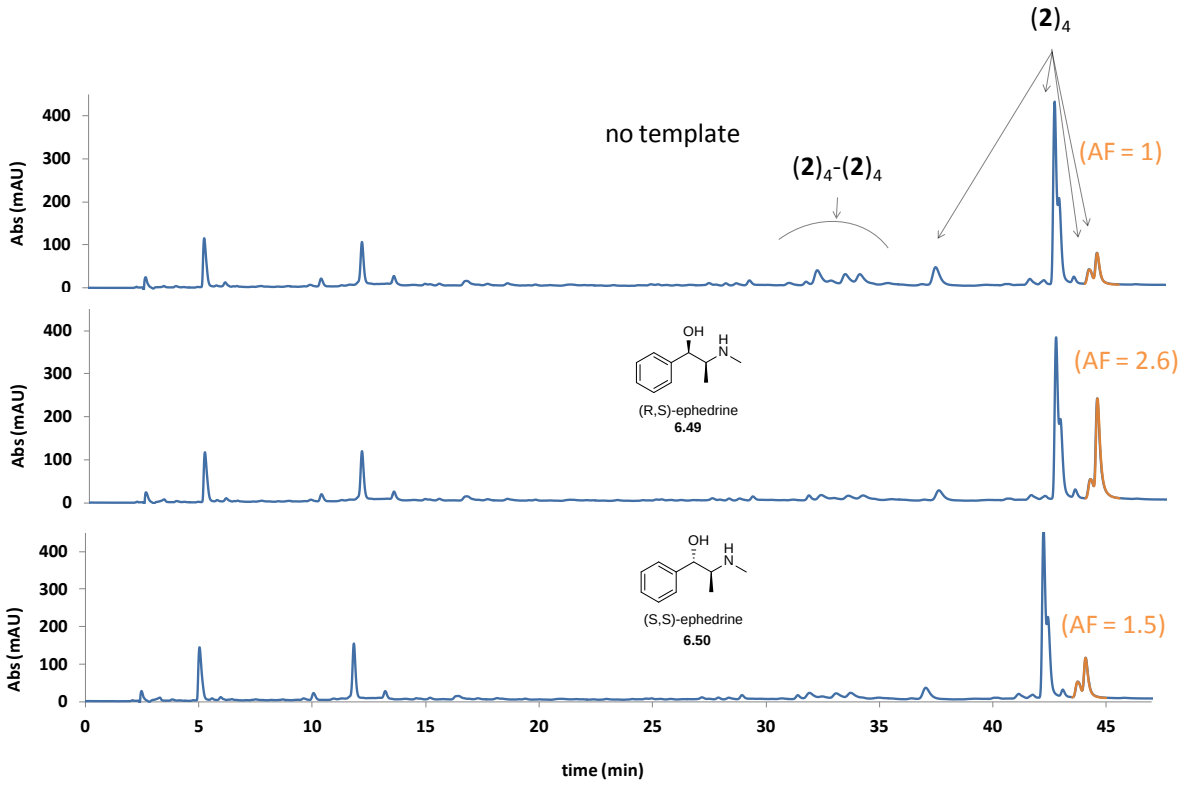

Figure 6.27: HPLC-UV chromatograms (λ_{abs} = 260 nm and λ_{ref} = 360 nm) of DCLs prepared in borate buffer (50 mM, pH 8.4) composed of equimolar amounts (2.0 mM for each) of building blocks **2** and **5**, (a) in the absence of template and (b) presence of (R,S)-ephedrine (**6.49**) and (c) (S,S)-ephedrine (**6.50**) as individual templates (2.0 mM for each). DCLs were diluted with 200 volume % DMSO prior to analysis.

Three DCLs made from equimolar amounts of building blocks **2** and **5** (4.0 mM in total) were prepared in absence and presence of (R,S)-ephedrine (**6.49**) and (S,S)-ephedrine (**6.50**) (2.0 mM for each) as templates. When template (**6.49**) was introduced into the DCL, the area of the peak corresponding to one isomer of the macrocyclic homotetramers $(\mathbf{2})_4$ was amplified 2.6 times while adding the diasterioisomer **6.50** has amplified the same isomer 1.5 time, relative to the untemplated DCL. The presence of these templates did not significantly Affect the behavior of building block **5.**

6.4.4.2 LC-MS Data of the DCL products

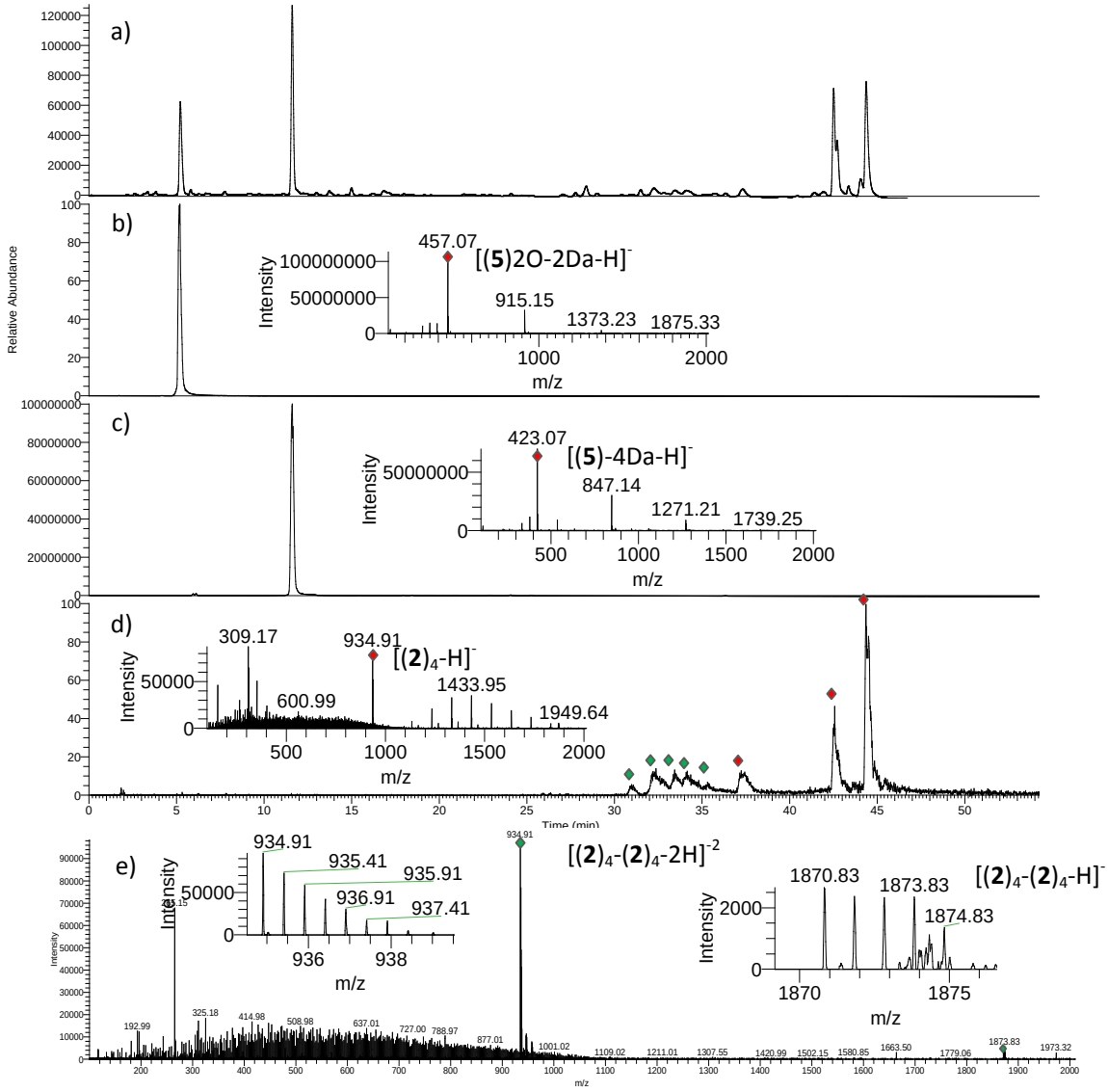

Figure 6.28: HPLC-MS analysis of a DCL prepared in 50.0 mM borate buffer (pH 8.4) and made from equimolar amounts of building blocks **2** and **5** and template **6.49** (6.0 mM in total). (a) HPLC-UV chromatogram at 280 nm (λ_{ref} = 550 nm); (b) Extracted ion chromatogram (negative ion mode) corresponding to monocharged over-oxidized monomer minus two daltons [(**5**)2O-2Da] (456.5-457.5) with (insert) ESI-MS spectra [m/z 200-2000] summed over the 5.02-5.27 min retention time window, corresponding to monomer [(**5**)2O-2Da], showing [((**5**)2O-2Da)-H]$^-$ m/z = 457.07 (expected = 457.09); (c) Extracted ion chromatogram (negative ion mode) corresponding to monocharged monomer minus four daltons [(**5**)-4Da] (422.5-423.5) with (insert) ESI-MS spectra [m/z 200-2000] summed over the 11.35-11.70 min retention time window, corresponding to monomer [(**5**)-4Da], showing [(**5**)-4Da-H]$^-$ m/z = 423.07 (expected = 423.09); (d) Extracted ion chromatogram (negative ion mode) corresponding to monocharged homotetramer $(\mathbf{2})_4$ (934.5-935.5) with (insert) ESI-MS spectra [m/z 200-2000] summed over the 37.06-38.06, 42.24-42.98 and 44.10-44.50 min retention time windows, corresponding to tetramer $(\mathbf{2})_4$, showing [$(\mathbf{2})_4$-H]$^-$ m/z = 934.91 (expected = 934.92); (e) ESI-MS spectra [m/z 200-2000] summed over the 30.98-35.31 min retention time window showing the doubly charged homocatenane [($(\mathbf{2})_4$-$(\mathbf{2})_4$)-2H]$^{-2}$ m/z = 934.91 (expected = 934.92) with (left insert) showing

the 0.5 mass unit isotopic spacing proving that $[((\mathbf{2})_4\text{-}(\mathbf{2})_4)\text{-}2H]^{-2}$ ions are doubly charged and (right insert) showing the monocharged homocatenane $[((\mathbf{2})_4\text{-}(\mathbf{2})_4)\text{-}H]^-$ m/z = 1870.83 (expected = 1870.84).

6.4.5 DCL made from building blocks 4 and 5

We also prepared a DCL made from equimolar amounts of building blocks **4** and **5** (2.0 mM for each) in 50 mM borate buffer at pH 8.4 and allowed it to oxidize and equilibrate following standard protocols (see experimental part). The composition of the resulting DCL was analyzed by HPLC and mass spectrometry after 3 weeks of equilibration to allow the thiols to oxidize.

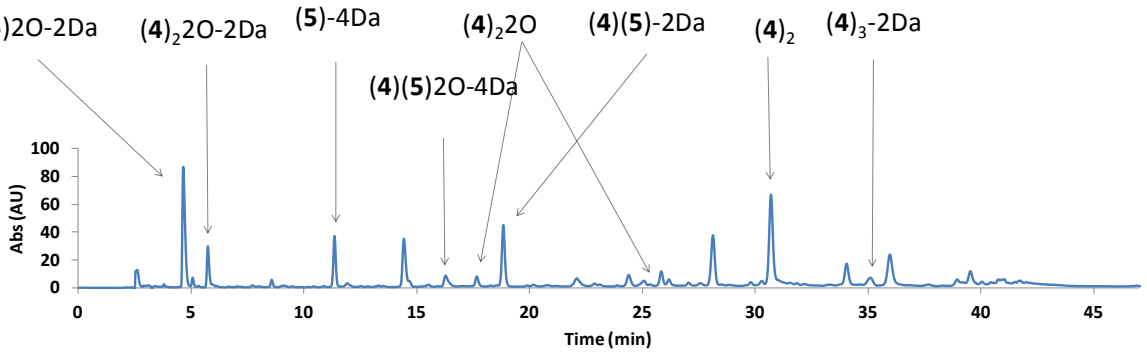

Figure 6.29: HPLC-UV chromatograms (λ_{abs} = 280 nm and λ_{ref} = 550 nm) of a DCL prepared in borate buffer (50 mM, pH 8.4) composed of equimolar amounts (2.0 mM for each) of building blocks **4** and **5**. The DCL was diluted with a 200 % DMSO volume prior to analysis.

Overoxidized monomers (**5**)2O-2Da and (**4**)2O-2Da, monomer (**5**)-4Da, linear overoxidized dimers (**4**)(**5**)2O-4Da and $(\mathbf{4})_2$2O and linear dimers $(\mathbf{4})_2$ and (**4**)(**5**)-2Da were the major formed species in the DCL. The outcome of the DCL further supports the notion of slow oxidation rates of buildings **4** and **5** which prevented the formation of cyclic oligomers or linear oligomers of higher molecular weights than dimers, within the used timescale of the experiment. This suggests that the product distribution of the DCL did not reach thermodynamic control. Moreover, the percentage of overoxidized library members in a DCL made from building blocks **4** and **5** is much higher than that in a DCL made from building blocks **2** and **3** in which the overoxidized DCL members constitute a minority of the total DCL members. This suggests that the slow oxidation rates of building blocks **4** and **5** have allowed the time for the overoxidation (side) reactions to occur. This is also in line with our consideration that the thiol overoxidation (side) reaction is slowed down by the presence of a good template promoting the formation of oligomers and therefore the disulfide formation.[55,57]

DCL building blocks	Disulfide DCL products	Side products with substracted masses	Linear over-oxidized side products
2 + **3**	$(\mathbf{3})_4$, $(\mathbf{2})(\mathbf{3})_3$, $(\mathbf{2})_2(\mathbf{3})_2$, $(\mathbf{2})_3(\mathbf{3})$, $(\mathbf{2})_4$, $(\mathbf{2})_2(\mathbf{3})_3$ and catenanes $(\mathbf{2})_4\text{-}(\mathbf{2})_4$ and $(\mathbf{2})_3(\mathbf{3})\text{-}(\mathbf{2})_4$.	----------	$(\mathbf{3})_2$4O, $(\mathbf{3})_3$4O, (**2**)(**3**)4O and $(\mathbf{2})(\mathbf{3})_2$4O
4 + **5**	Linear $(\mathbf{4})_2$ and $(\mathbf{4})_3$	$(\mathbf{4})_3$-2Da, (**5**)-4Da and (**4**)(**5**)-2Da	(**5**)2O-2Da, (**4**)2O-2Da, (**4**)(**5**)2O-2Da and $(\mathbf{4})_2$2O

6.4.5.1 LC-MS data of the DCL products

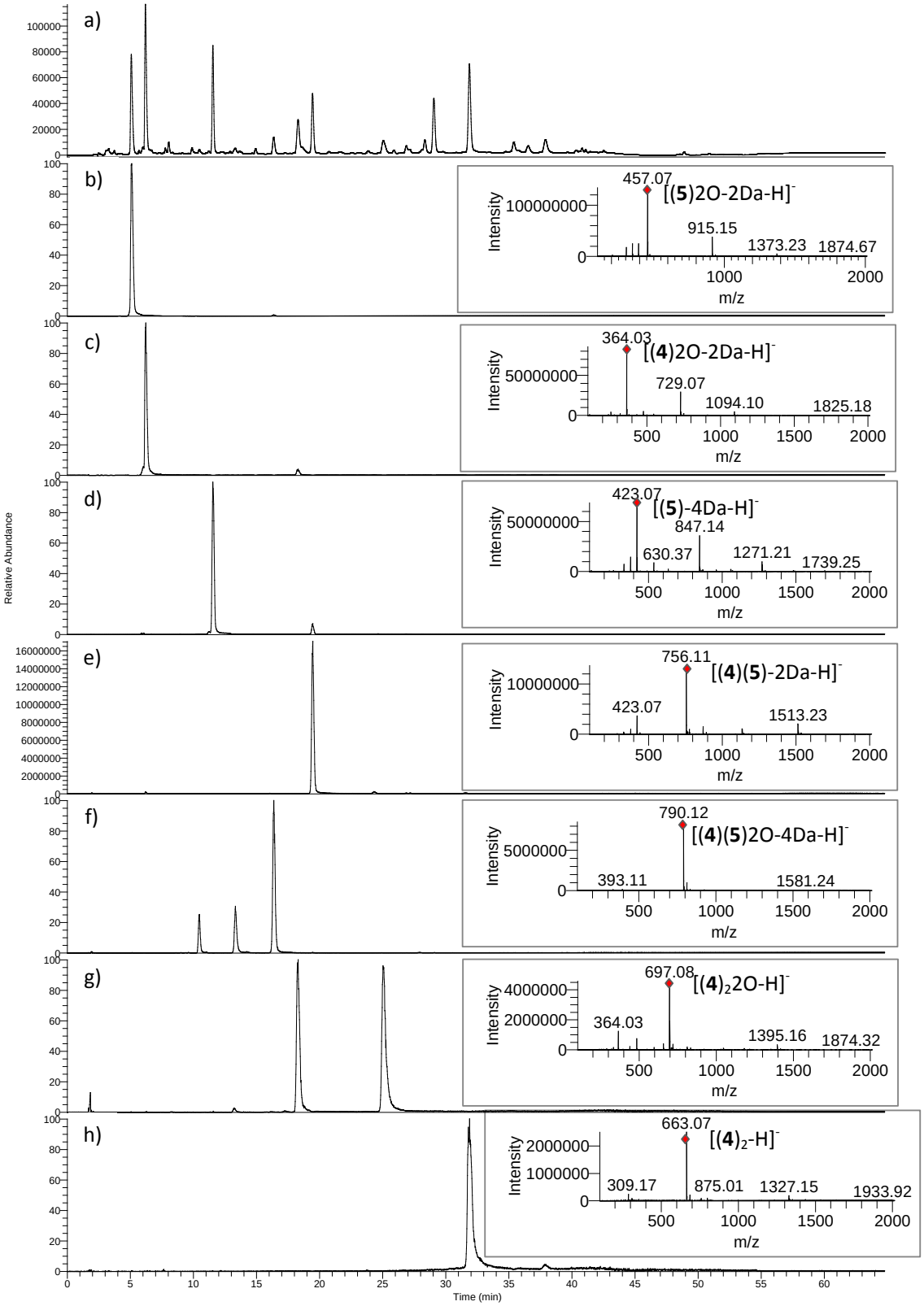

Figure 6.30: HPLC-MS analyses of a DCL prepared in 50.0 mM borate buffer (pH 8.4) and made from equimolar amounts of building blocks **4** and **5** and template **6.49** (6.0 mM in total). (a) HPLC-UV chromatogram at 280 nm (λ_{ref} = 550 nm); (b) Extracted ion chromatogram (negative ion mode) corresponding to monocharged over-oxidized monomer minus two daltons [(**5**)2O-2Da] (456.5-457.5) with (insert) ESI-MS spectra [m/z 200-2000] summed over the 5.02-5.27 min retention time window, corresponding to monomer [(**5**)2O-2Da], showing [((**5**)2O-2Da)-H]$^-$ m/z = 457.07 (expected = 457.09); (c) Extracted ion chromatogram (negative ion mode) corresponding to monocharged over-oxidized monomer minus two daltons [(**4**)2O-2Da] (363.5-364.5) with (insert) ESI-MS spectra [m/z 200-2000] summed over the 6.11-6.36 min retention time window, corresponding to monomer [(**4**)2O-2Da], showing [(**4**)2O-2Da-H]$^-$ m/z = 364.03 (expected = 364.05); (d) Extracted ion chromatogram (negative ion mode) corresponding to monocharged monomer minus four daltons [(**5**)-4Da] (422.5-423.5) with (insert) ESI-MS spectra [m/z 200-2000] summed over the 11.47-11.67 min retention time window, corresponding to monomer [(**5**)-4Da], showing [(**5**)-4Da-H]$^-$ m/z = 423.07 (expected = 423.09); (e) Extracted ion chromatogram (negative ion mode) corresponding to monocharged linear dimer minus four daltons [(**4**)(**5**)-4Da] (755.5-756.5) with (insert) ESI-MS spectra [m/z 200-2000] summed over the 6.12-6.34 min retention time window, corresponding to linear dimer [(**4**)(**5**)-4Da], showing [(**4**)(**5**)-4Da -H]$^-$ m/z = 756.11 (expected = 756.14); (f) Extracted ion chromatogram (negative ion mode) corresponding to monocharged over-oxidized linear dimer minus two daltons [(**4**)(**5**)2O-2Da] (789.5-790.5) with (insert) ESI-MS spectra [m/z 200-2000] summed over the 10.34-10.57, 13.23-13.46 and 16.25-16.49 min retention time windows, corresponding to linear dimer [(**4**)(**5**)2O-2Da], showing [(**4**)(**5**)2O-2Da-H]$^-$ m/z = 790.12 (expected = 790.14); (g) Extracted ion chromatogram (negative ion mode) corresponding to monocharged over-oxidized linear homodimer minus two daltons [(**4**)$_2$2O-2Da] (696.5-697.5) with (insert) ESI-MS spectra [m/z 200-2000] summed over the 18.14-18.40 and 24.79-25.42 min retention time windows, corresponding to linear dimer [(**4**)$_2$2O-2Da], showing [(**4**)$_2$2O-2Da-H]$^-$ m/z = 697.08 (expected = 697.10); (h) Extracted ion chromatogram (negative ion mode) corresponding to monocharged linear homodimer minus two daltons [(**4**)$_2$-2Da] (664.5-665.5) with (insert) ESI-MS spectra [m/z 200-2000] summed over the 31.6-32.11 min retention time window, corresponding to linear dimer [(**4**)$_2$-H$_2$], showing [(**4**)$_2$-H$_2$-H]$^-$ m/z = 663.07 (expected = 663.09).

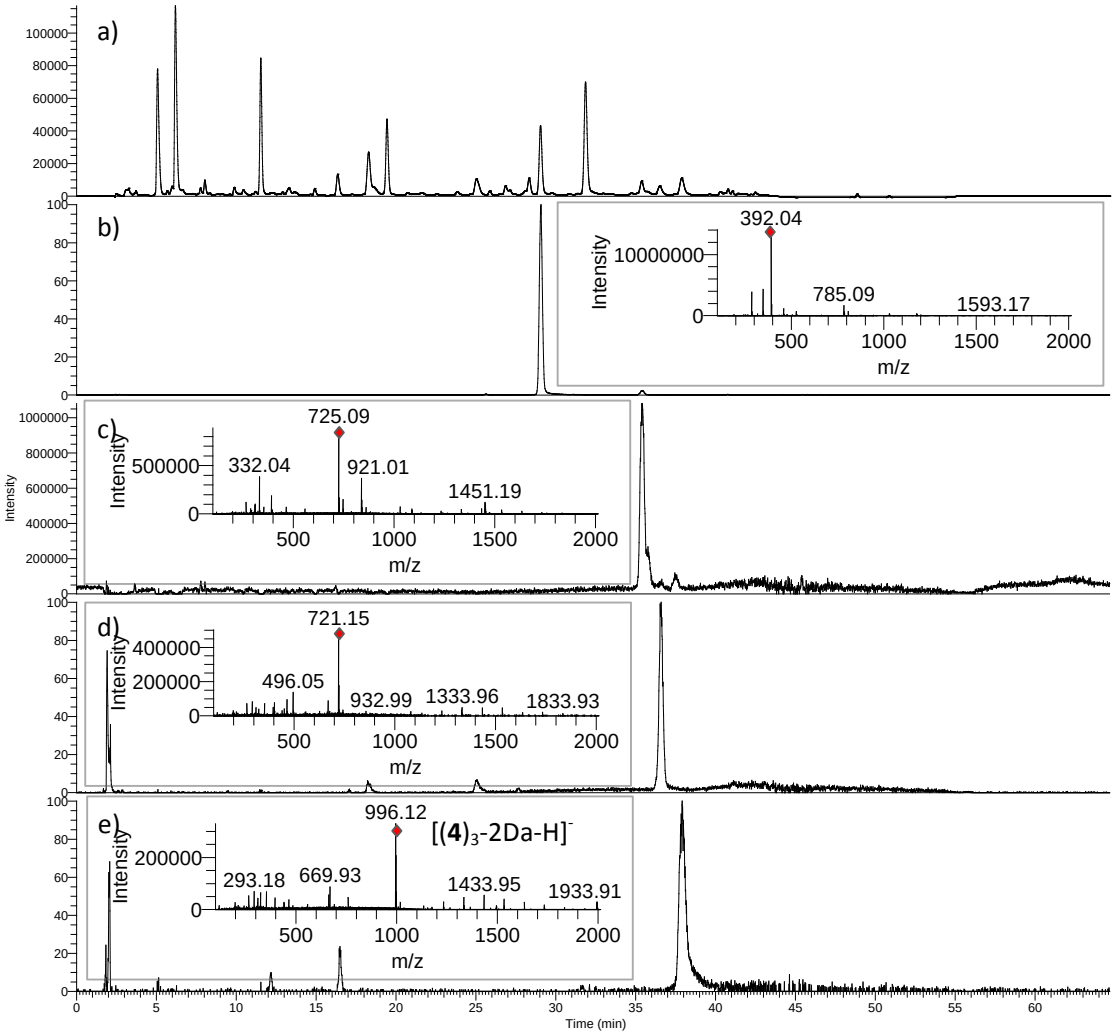

Figure 6.31: HPLC-MS analyses of a DCL prepared in 50.0 mM borate buffer (pH 8.4) and made from equimolar amounts of building blocks **4** and **5** and template **6.49** (6.0 mM in total). (a) HPLC-UV chromatogram at 280 nm (λ_{ref} = 550 nm); (b) Extracted ion chromatogram (negative ion mode) corresponding to an undefined singly charged product (391.5-392.5) with m/z = 392.04; (c) Extracted ion chromatogram (negative ion mode) corresponding to an undefined singly charged product (724.5-725.5) with m/z = 725.09; (d) Extracted ion chromatogram (negative ion mode) corresponding to an undefined singly charged product (720.5-721.5) with m/z = 721.15; (e) Extracted ion chromatogram (negative ion mode) corresponding to monocharged cyclic trimer minus four daltons [(**4**)$_3$-2Da] (995.5-996.5) with (insert) ESI-MS spectra [m/z 200-2000] summed over the 37.6-38.28 min retention time window, corresponding to cyclic trimer [(**4**)$_3$-2Da], showing [(**4**)$_3$-2Da-H]$^-$ m/z = 996.12 (expected = 996.15).

6.5 Conclusion and outlook

DCLs formed from cysteine functionalized building blocks in water have been widely reported,[26-34] yet investigations into more diverse amino acid functionalization of building blocks in water have not been frequently reported. In this chapter, the DCL behavior of building blocks that contain a flat hydrophobic surface as a central core and flexible hydrophilic amino acid side chains, *i.e.* valine residues, have been studied in water. Moreover, the behavior of these DCLs was compared with the behavior of DCLs formed from the same building blocks that were not functionalized with amino acids.

To conclude, the amino acid side chains have a crucial role in the type of the formed products, DCL distribution and library response to templates. The resulting receptors carrying flexible residues potentially capable of molecular recognition are somewhat more responsive to guests and this may lead to better guest binding.[27] Moreover, intramolecular interactions seem to occur between the amino-acid side chains of the macrocycles and these may reinforce the macrocycle-guest binding.[48,65] Comparing the DCL compositions of valine functionalized macrocycles prepared in aqueous media with different ionic strengths may highlight the possible occurrence of the intramolecular interactions. The intramolecular interactions between the hydrophobic parts of valine residues are stronger in solvents of higher ionic strengths. Therefore these interactions may shift the equilibrium more towards the formation of the macrocycles with increased amino-acid functionalization in solvents of higher ionic strengths.[60] Moreover, host-guest binding analyses (*e.g.* ITC) in aqueous media with different ionic strengths may reveal the possible reinforcement of guest binding by intramolecular interaction, and may be valuable.

The slow oxidation rates observed for the amino acids derivatized dithiols **4** and **5** has resulted in DCL systems with product distributions that probably did not reach thermodynamic control within the timescale of the experiments. The slow oxidation rate may also have promoted the overoxidation side reaction of these two building blocks. This is in line with our consideration that the thiol overoxidation (side) reaction is slowed down by the presence of a good template promoting the formation of oligomers and therefore the disulfide formation.[55,57] Alfonso *et al.*[60] have reported that the use of DMSO as co-solvent promotes thiol building block oxidation and reduces the reaction time for the disulfide formation. However, this approach has not been applied to our systems but could remedy the undesirable side reactions. Suggested methods for overcoming the slow oxidation rates of the two building blocks are discussed in the outlook chapter.

The amino-acid functionalized macrocycles which showed loss of dalton pairs could be eventually isolated using preparative HPLC and analyzed by proton NMR to reveal the source of mass unit losses.

6.6 Experimental section

6.6.1 General Points

Chemicals were purchased from Sigma-Aldrich, Alfa, Bachem or Fluka and used without further purification. Building blocks **1**, **2** and **3** were re-synthesized following the protocols reported in the literature.[59,61,63] NMR analyses were performed using a Bruker instrument. Chemical shifts, δ, are cited in part per million (ppm) and coupling constants, *J*, are cited in Hz. NMR Spectra were recorded at 300 K. Elemental analyses were performed using a EuroEA3000-CHNS0-analyser Series from Euro Vector. Details of specialized analytical equipments are provided in the sections dealing with the respective analyses.
For experiment in which a buffer was used, a 50 mM borate buffer solution pH 8.4 was prepared by dissolving boric acid (H_3BO_3) in doubly distilled water. The pH was adjusted by addition of an appropriate volume of a 1 M solution of KOH and pH was monitored using a pH meter.

6.6.2 DCL preparations

Stock solutions of single building blocks **1**, **2**, **3**, **4** and **5** and the used templates were freshly prepared at 10.0 mM concentration by dissolving the appropriate amount of the building block and the template in 50 mM borate buffer pH 8.4. The pH was readjusted to 8.4 by addition of an appropriate volume of a 1.0 M solution of KOH.
For the untemplated DCLs made from 2.0 mM of individual building blocks (**1** to **5**), 40 µl of the stock solutions of the building blocks (10 mM) were combined to 160 µl of a borate buffer solution (50 mM, pH 8.4).
For the templated DCLs made from 2.0 mM of individual building blocks (**1** to **5**) and 2.0 mM of the individual templates, 40 µl of the stock solutions of the building blocks (10 mM) and 40 µl of the stock solutions of the templates (10 mM) were combined to 120 µl of a borate buffer solution (50 mM, pH 8.4).
The DCL mixtures were allowed to oxidize and equilibrate by stirring for 4 days in closed vials at room temperature. For DCLs that were diluted with DMSO, each of the vials was manually shaken immediately before taking 3 µl samples using an Eppendorf pipette. These 3 µl solutions were diluted with 200% volume DMSO in HPLC vials immediately prior to HPLC-UV analyses.

6.6.3 HPLC and HPLC-MS analysis conditions

HPLC analyses were performed using an Agilent 1100 series HPLC equipped with a UV detector. Acetonitrile was purchased from Biosolve. Water was doubly distilled. Formic acid was purchased from Sigma-Aldrich.
HPLC analyses were performed using a reversed phase column (Kromasil C8, 4.6 x 150 mm, 5 µm), a HPLC sample diluted with 200% volume DMSO, an injection volume of 3 µL, a flow rate of 1 mL/min of acetonitrile in doubly distilled water (both containing 0.1% formic acid) at 318 K and following the HPLC gradient described below:

Time (min)	Acetonitrile (%)
0	30
5	40

30	70
35	70
40	95
50	95
55	30

The UV chromatograms shown were obtained at a wavelength of 260 nm with a reference of 360 nm.

HPLC-MS conditions

HPLC-MS analyses were performed using a HPLC-MS from Thermo Scientific coupled to an Orbitrap Mass Spectrometer (LTQ Orbitrap XL series). Acetonitrile was purchased from Biosolve. Water was doubly distilled. Formic acid was purchased from Sigma-Aldrich.
HPLC-MS analyses were performed using a reversed phase column (Kromasil C8, 4.6 x 150 mm, 5 µm), an injection volume of 9 µL, a flow rate of 1 mL/min of acetonitrile in doubly distilled water (both containing 0.1% formic acid) at 318 K and following the HPLC gradient shown above.

The UV chromatograms shown were obtained at a wavelength of 280 nm with a reference of 550 nm. The use of a splitter (1:5) for the LC-MS brought to the MS a flow of 0.2 mL/min and the samples were analyzed following the LC-MS parameters described below (negative mode): Capillary temperature: 325 °C; sheath gas flow: 30 arbitrary units (AU); aux. gas flow rate: 10 (AU); sweep gas flow: 10 (AU); ionization spray voltage: 4.2 kV; capillary voltage: -44 V; tube lens: -150.93 V.

6.6.4 DCL made from building block 5

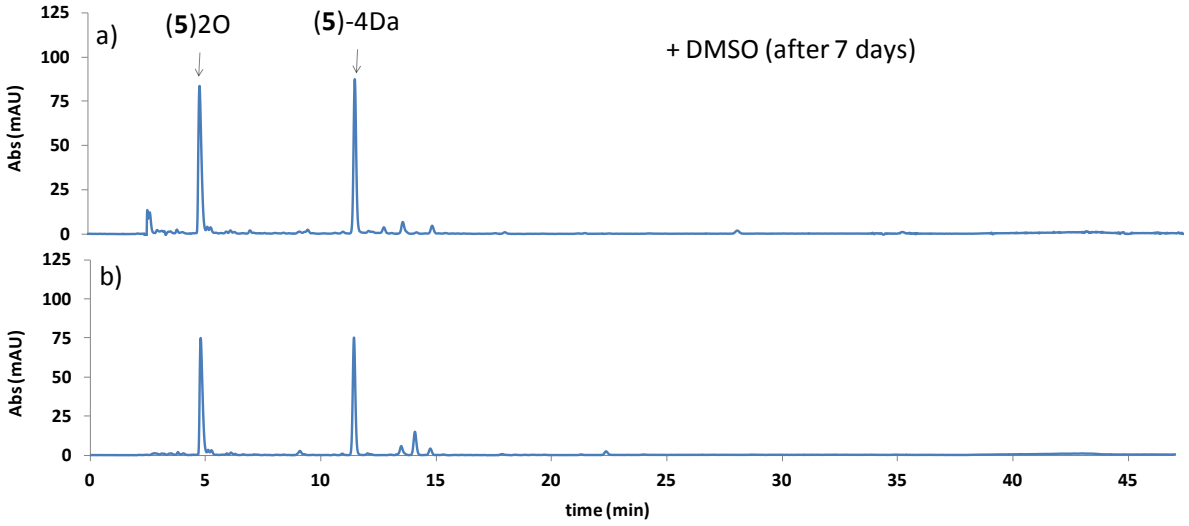

Figure 6.32: HPLC-UV analyses (λ_{abs} = 280 nm and λ_{ref} = 550 nm) of a DCL made from 2.0 mM of building block **5** in 50 mM borate buffer at pH 8.4; a) after adding 200 volume % DMSO immediately prior to the analysis and (b) without DMSO dilution.

6.6.5 Synthesis of building blocks 4 and 5

3,7-Bis-tritylsulfanylnaphthalene-2-carboxylic acid 6.39[64]

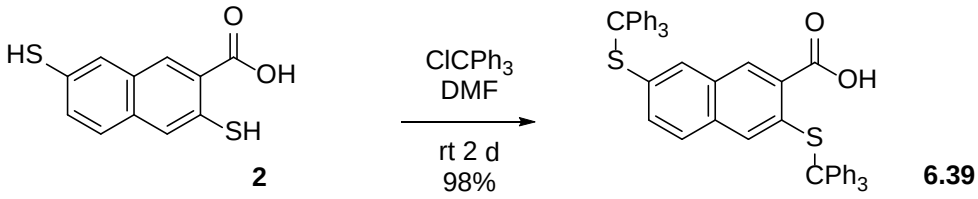

Anhydrous DMF (10 mL) was thoroughly degassed with N_2 and added to a flask containing 3,7-dimercaptonaphthalene-2-carboxylic acid (364 mg, 1.54 mmol) and trityl chloride (948 mg, 3.40 mmol). The mixture was heated until the solution was bright yellow and stirred at room temperature for 48 hours. Water (400 mL) was added to the solution and the product was extracted with diethyl ether (600 mL). The extracts were dried over Na_2SO_4, filtered and the solvent evaporated. The residue was washed with hexane to give 1.09 g (98%) of a yellow powder. ^{1}H NMR ($CDCl_3$, 400 MHz): δ 8.1 (s, 1H), 7.30-6.92 (m, 35H). ^{13}C NMR (DMSO, 100 MHz): δ 167.40, 143.73, 143.15, 134.51, 133.24, 132.49, 131.83, 131.69, 129.77, 129.67, 129.39, 128.76, 128.01, 127.93, 127.51, 127.13, 126.94, 126.62, 125.78, 70.86, 70.32 Decomposition temperature: 200-202 ˚C. HRMS: $(M-H)^-$ found: 720.20730 (expected: 720.2157).

(R)-2-[(3,7-Bis-tritylsulfanyl-naphthalene-2-carbonyl)-amino]-3-methyl butanoic acid tert-butyl ester[65] 6.41

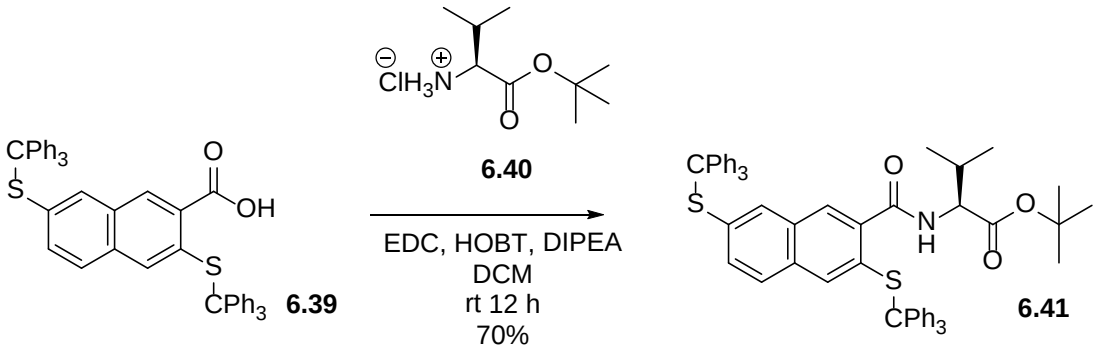

3,7–Bis-tritylsulfanylnaphthalene-2-carboxylic acid (1.0 g, 1.38 mmol) and hydroxybenzotriazole (HOBT, 244 mg, 1.81 mmol) were dissolved in 50 mL of anhydrous DCM. The solution was cooled to 0ºC to produce a yellow suspension. EDC (0.319 mL, 1.80 mmol) was added and the mixture stirred for one hour at which point it was fully dissolved. D-Valine *tert*-butyl ester hydrochloride **6.40** (0.721 g, 3.44 mmol) in 15 mL of anhydrous DCM and diisopropylethyl amine (DIPEA, 1.14 mL, 6.55 mmol) were added (as a single solution) dropwise to the solution. The solution was then stirred for 12 hours at room temperature. The solution was diluted with 20 mL of DCM and washed with 100 mL of 1 M HCl, 100 mL of $NaHCO_3$ and 100 mL NaCl. The organic layer was dried over Na_2SO_4, filtered and evaporated to a solid. The crude product was then purified by column chromatography using a 1:6 mixture of ethylacetate and hexane to give 0.845 g (70%) of a foaming white solid (R_f = 0.59 EtOAc/Hept 1:4). ^{1}H NMR ($CDCl_3$, 400 MHz): δ 7.54-6.73 (m,

35H), 4.58-4.54 (m, 1H), 2.14-2.19 (m, 1H), 1.48 (s, 9H), 0.95 (d, *J* = 6.8 Hz, 3H), 0.91 (d, *J* = 6.8 Hz, 3H). ^{13}C NMR ($CDCl_3$, 100 MHz): δ 170.9, 167.5, 144.4, 144.0, 136.3, 133.5, 133.4, 133.3, 132.3, 132.1, 132.0, 132.0, 130.7, 130.2, 130.0, 127.8, 127.0, 126.9, 126.5, 82.0, 72.1, 58.3, 31.7, 28.1, 18.9, 18.1. Decomposition temperature: 94-95 ˚C. HRMS: $(M+Na)^+$ found: 898.3378 (expected: 898.3359).

(R)-2-[(3,7-Bis-sulfanyl-naphthalene-2-carbonyl)-amino]-3-methyl butanoic acid[66] 4

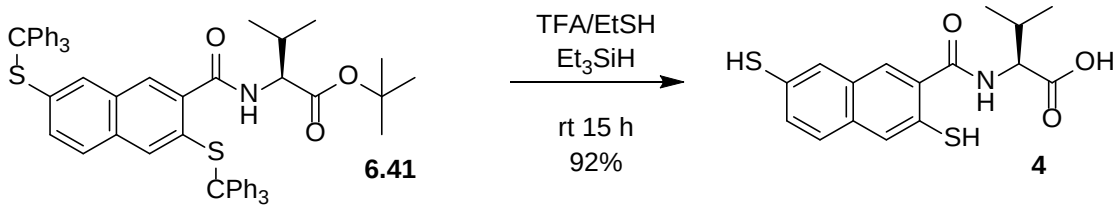

The protected building block **6.41** (85 mg, 0.097 mmol) was dissolved in 2 mL of EtSH under N_2. Degassed TFA (2 mL) was then added and the solution was stirred overnight under N_2 at room temperature. Et_3SiH (0.3 mL, 1.88 mmoL) was added to the solution. The solution was stirred for a further 45 minutes before evaporating it to a residue. The residue was then redissolved in 100 mL (9:1) methanol/water (degassed) and washed with 4 x 20 mL heptane. The methanol was evaporated to give 30 mg (92%) of an off-white powder. ^{1}H NMR (DMSO, 400 MHz): δ 8.72 (d, 1H), 7.87 (d, 1H), 7.82 (s, 1H), 7.67 (d, 1H), 7.44 (d, 1H), 5.68 (s, 1H), 5.33 (s, 2H), 4.32 (t, 1H), 2.21-2.16 (m, 1H), 0.99 (d, 6H). ^{13}C NMR (CD_3OD, 100 MHz): δ 173.3, 173.2, 133.7, 131.8, 129.1, 128.0, 127.3, 127.3, 126.8, 126.6, 126.1, 110.0, 58.5, 30.3, 18.4, 17.3. Decomposition temperature: 120-122 ˚C. HRMS: $(M-H)^-$ found: 334.0566 (expected: 334.0572).

2,5–Bis-tritylsulfanyl-terephthalic acid[64] 6.45

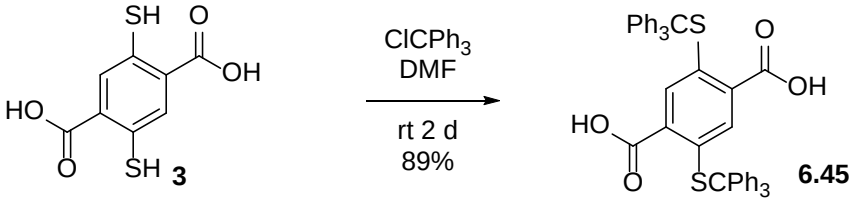

Anhydrous DMF (dimethylformamide, 5 mL) was thoroughly degassed with N_2 and added to a flask containing 2,5-dimercaptoterephthalic acid **3** (0.1 g, 0.43 mmol) and trityl chloride (0.26 mg, 0.95 mmol). The mixture was heated until the solution was bright yellow and stirred at room temperature for 48 hours. Water (150 mL) was added to the solution and the product was extracted with diethyl ether (200 mL). The extracts were dried over Na_2SO_4, filtered and the solvent was evaporated. The residue was washed with hexane to give 0.27 g (89%) of a yellow powder. ^{1}H NMR (DMSO, 400 MHz): δ 7.16-7.28 (m, 30H), 7.11 (s, 2H). ^{13}C NMR (DMSO, 100 MHz) (the product is hardly soluble in any solvent): δ 162.2, 143.1, 129.6, 127.9, 127.8, 127.5, 127.1, 114.6. Decomposition temperature: 410-411 ˚C. HRMS: $(M-H)^-$ found: 713.1814 (expected: 713.1821).

(R,R)-2-[(2,5-Bis-tritylsulfanyl-benzene-1,4-bis-carbonyl)-bis-amino]-3-bis(3-methyl butanoic acid *tert*-butyl ester)[65] 6.47

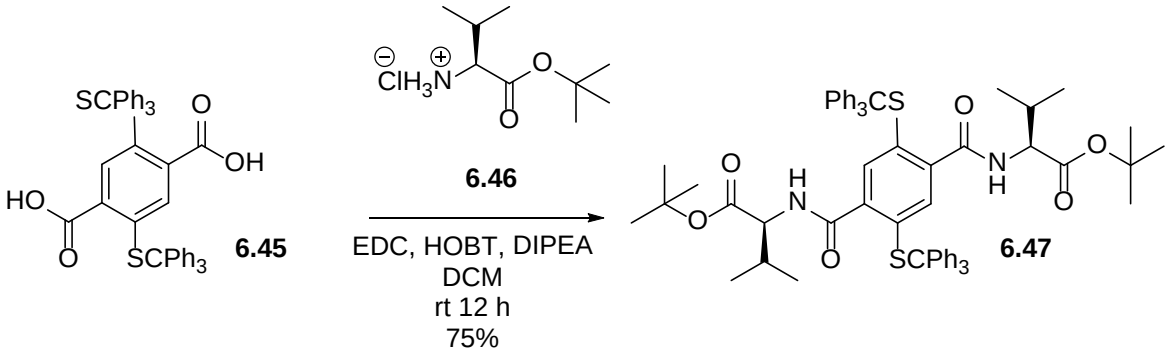

2,5–Bis-tritylsulfanyl terephthalic acid (1.0 g, 1.40 mmol) and hydroxybenzotriazole (HOBT, 0.49 g, 3.64 mmol) were dissolved in 40 mL of anhydrous DCM. The solution was cooled to 0ºC to produce a yellow suspension. EDC (0.64 mL, 3.64 mmol) was added and the mixture was stirred for one hour at which point it was fully dissolved. D-Valine *tert*-butyl ester hydrochloride **6.46** (0.76 g, 3.64 mmol) dissolved in 10 mL of anhydrous DCM and diisopropylethyl amine (DIPEA, 1.84 mL, 10.60 mmol) were added (as a single solution) dropwise to the solution. The solution was then stirred for 12 hours at room temperature. The solution was diluted with 20 mL of DCM and washed with 100 mL of 1 M HCl, 100 mL of $NaHCO_3$ and 100 mL NaCl. The organic layer was dried over Na_2SO_4, filtered and evaporated to a give a solid. The crude product was then purified by column chromatography using a 1:4 mixture of ethyl acetate and hexane to give 1.075 g (75%) of a foaming white solid (R_f = 0.50 EtOAc/Hept 1:4). ^{1}H NMR ($CDCl_3$, 400 MHz): δ 7.30-7.21 (m, 30H), 6.79 (s, 2H), 5.71 (d, *J* = 9.6 Hz, 2H), 4.40-4.36 (m, 2H), 2.05-1.97 (m, 2H), 1.42 (s, 18H), 0.77 (d, *J* = 7.0 Hz, 6H), 0.66 (d, *J* = 7.0 Hz, 6H). ^{13}C NMR ($CDCl_3$, 100 MHz): δ 170.8, 166.8, 143.9, 137.7, 133.2, 130.3, 130.2, 128.1, 127.2, 82.0, 71.3, 57.8, 32.0, 28.2, 19.0, 18.0. Decomposition temperature: 157-159 ˚C. HRMS: $(M+Na)^+$ found: 1047.4425 expected (1047.4411).

(R,R)-2-[(2,5-Dimercapto-benzene-1,4-bis-carbonyl)-bis-amino]-3-bis(3-methyl butanioc acid[66] 5

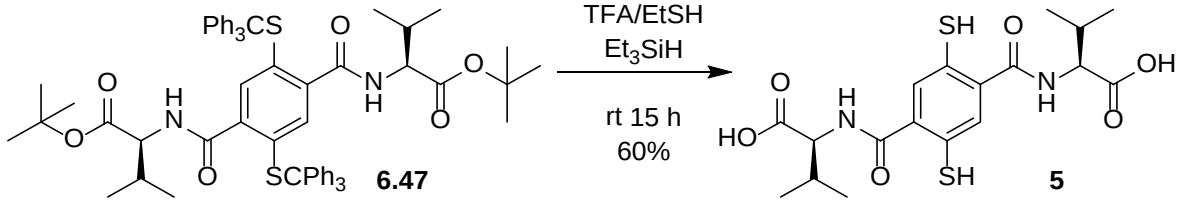

The protected building block **6.47** (200 mg, 0.20 mmol) was dissolved in 3 mL of EtSH under N_2. Degassed TFA (3 mL) was then added and the solution was stirred overnight under N_2 at room temperature. Et_3SiH (0.3 mL, 1.88 mmoL) was added to the solution. The solution was stirred for a further 45 minutes before evaporating it to a residue. The residue was then redissolved in 100 mL (9:1) methanol/water (degassed) and washed with 4 x 20 mL heptane. The methanol was evaporated to give 50 mg (60%) of an off-white powder. ^{1}H NMR (DMSO, 400 MHz): δ 8.65 (brs, 2H), 7.50 (s, 2H), 4.26 (t, *J* = 4.3 Hz, 2H), 2.17-2.10 (m, 2H), 0.95 (d, *J* = 6.6 Hz, 12H). Decomposition temperature: 164-166 ˚C. HRMS: $(M-H)^-$

found: 427.0992 (expected: 427.1003).

6.7 References

[1] (a) Moghimi, A.; Maddah, B.; Yari, A.; Shamsipur, M.; Boostani, M.; Fall Rastegar, M.; Ghaderi, A. R. *J. Mol. Struct.* **2005**, *752*, 68. (b) Metzger, A.; Gloe, K.; Stephan, H.; Schmidtchen, F. P. *J. Org. Chem.* **1996**, *61*, 2051. (c) Tsubaki, K.; Tanaka, H.; Morikawa, H.; Fuji, K. *Tetrahedron* **2003**, *59*, 3195. (d) Yi, Y. R.; Kim, K.-S.; Helal, A.; Kim, H.-S. *Supramol. Chem.* **2013**, *25*, 16.

[2] Hofstetter, O.; Hofstetter, H.; Schurig, V.; Wilchek, M.; Green, B. S. *J. Am. Chem. Soc.* **1998**, *120*, 3251.

[3] Famulok, M.; Szostak, J. W. *J. Am. Chem. Soc.* **1992**, *114*, 3990.

[4] Li, C.; Ma, J.; Zhao, L.; Zhang, Y.; Yu, Y.; Shu, X.; Li, J.; Jia, X. *Chem. Commun.* **2013**, *49*, 1924.

[5] Sessler, J. L.; Andrievsky, A. *Chem. A Eur. J.* **1998**, *4*, 159.

[6] Imai, H.; Misawa, K.; Munakata, H.; Uemori, Y. *Chem. Pharm. Bull.* **2008**, *56*, 1470.

[7] Späth, A.; König, B. *Beilstein J. Org. Chem.* **2010**, *6*, 32.

[8] As this chapter only focuses on the synthesis of non-peptidic amino acid derived macrocycles using DCC, the author review here natural and synthetic macrocycles reported in the literature and containing non-peptidic amino acids.

[9] Andavan, G. S. B.; Lemmens-Gruber, R. *Mar. Drugs* **2010**, *8*, 810.

[10] Panda, D.; Himes, R. H.; Moore, R. E.; Wilson, L.; Jordan, M. A. *Biochem.* **1997**, *36*, 12948.

[11] Kase, H.; Kaneko, M.; Yamada, K. *J. Antibiot.* **1987**, 40, 450.

[12] Park, M. K.; Park, J. H.; Cho, J. H.; Park, J. K.; Han, Y. N.; Han, B. H. *Arch. Pharm. Res.* **1991**, *14*, 103.

[13] Gibson, S. E.; Lecci, C. *Angew. Chem. Int. Ed. Engl.* **2006**, *45*, 1364.

[14] (a) Späth, A.; König, B. *Tetrahedron* **2009**, *65*, 690. (a) Mandl, C. P.; König, B. *J. Org. Chem.* **2005**, *70*, 670. (b) Voyer, N.; Deschenes, D.; Bernier, J.; Roby, J. *J. Chem. Soc., Chem. Commun.* ***1992,*** 664. (c) Zinic, M.; Frkanec, L.; Skaric, V.; Trafon, J.; Gokel, G. W. *Chem. Commun*. **1990**, 1726.

[15] (a) Ueno, A. *Supramol. Sci.* **1996**, *3*, 31. (b) Ikeda, H.; Nakamura, M.; Ise, N.; Oguma, N.; Nakamura, A.; Ikeda, T.; Toda, F.; Ueno, A. *J. Am. Chem. Soc.* **1996**, *118*, 10980. (c) Clark, J. L.; Peinado, J.; Stezowski, J. J.; Vold, R. L.; Huang, Y.; Hoatson, G. L. *J. Phys. Chem. B* **2006**, *110*, 26375. (d) Ashton, P. R.; Königer, R.; Stoddart, J. F.; Alker, D.; Harding, V. D. *J. Org. Chem.* **1996**, *61*, 903.

[16] (a) Sansone, F.; Barboso, S.; Casnati, A.; Fabbi, M.; Pochini, A.; Ugozzoli, F.; Ungaro, R. *European J. Org. Chem.* **1998**, *1998*, 897. (b) Nagasaki, T.; Tajiri, Y.; Shinkai, S. *Recl. Trav. Chim. Pays-Bas* **1993**, *112*, 407. (c) Sansone, F.; Barboso, S.; Casnati, A.; Sciotto, D.; Ungaro, R. *Tetrahedron Lett.* **1999**, *40*, 4741.

[17] Casnati, A.; Fabbi, M.; Pelizzi, N.; Pochini, A.; Sansone, F.; Unguro, R.; Di Modugno, E.; Tarzia, G. *Bioorg. Med. Chem. Lett.* **1996**, *6*, 2699.

[18] Ranganathan, D.; Samant, M. P.; Nagaraj, R.; Bikshapathy, E. *Tetrahedron Lett.* **2002**, *43*, 5145.

[19] Gavin, J. A.; Garcia, M. E.; Benesi, A. J.; Mallouk, T. E. *J. Org. Chem.* **1998**, *63*, 7663.

[20] Ranganathan, D. *Acc. Chem. Res.* **2001**, *34*, 919.

[21] Wagler, T. R.; Fang, Y.; Burrows, C. J. *J. Org. Chem.* **1989**, *54*, 1584.

[22] Wang, S.-J.; Ruan, W.-J.; Zhao, X.-J.; Luo, D.-B.; Zhu, Z.-A. *Chin. J. Chem.* **2005**, *23*, 44.

[23] Ruan, W.-J.; Zhao, X.-J.; Wang, S.-J.; Zhang, Y.-H.; Zhang, Z.-H.; Nan, J.; Zhu, Z.-A.; Wang, J.-G.; Ma, Y. *Chin. J. Chem.* **2005**, *23*, 1381.

[24] Dowden, J.; Edwards, P. D.; Flack, S. S.; Kilburn, J. D. *Chem. A Eur. J.* **1999**, *5*, 79.

[25] Hopkins, R. B.; Hamilton, A. D. *J. Chem. Soc. Chem. Commun.* **1987**, 171.

[26] Postma, T. M.; Galloway, W. R. J. D.; Cougnon, F. B. L.; Pantos, G. D.; Stokes, J. E.; *Synlett*. **2013**, 24, 765.

[27] Au-Yeung, H. Y.; Pengo, P.; Pantoş, G. D.; Otto, S.; Sanders, J. K. M. *Chem. Commun.* **2009**, 419.

[28] Au-Yeung, H. Y.; Cougnon, F. B. L.; Otto, S.; Pantoş, G. D.; Sanders, J. K. M. *Chem. Sci.* **2010**, *1*, 567.

[29] Au-Yeung, H. Y.; Pantos, G. D.; Sanders, J. K. M. *Proc. Natl. Acad. Sci. U. S. A.* **2009**, *106*, 10466.

[30] Cougnon, F. B. L.; Jenkins, N. A.; Pantoş, G. D.; Sanders, J. K. M. *Angew. Chem. Int. Ed.* **2012**, *124*, 1472.

[31] Cougnon, F. B. L.; Ponnuswamy, N.; Jenkins, N. A.; Pantoş, G. D.; Sanders, J. K. M. *J. Am. Chem. Soc.* **2012**, *134*, 19129.
[32] West, K. R.; Bake, K. D.; Otto, S. *Org. Lett.* **2005**, *7*, 2615.
[33] Stefankiewicz, A. R.; Sambrook, M. R.; Sanders, J. K. M. *Chem. Sci.* **2012**, *3*, 2326.
[34] Ponnuswamy, N.; Cougnon, F. B. L.; Clough, J. M.; Pantoş, G. D.; Sanders, J. K. M. *Science* **2012**, *338*, 783.
[35] Cousins, G. R. L.; Poulsen, S.-A.; Sanders, J. K. M. *Chem. Commun.* **1999**, 1575.
[36] Roberts, S. L.; Furlan, R. L. E.; Otto, S.; Sanders, J. K. M. *Org. Biomol. Chem.* **2003**, *1*, 1625
[37] Furlan, R. L.; Ng, Y. F.; Otto, S.; Sanders, J. K. *J. Am. Chem. Soc.* **2001**, *123*, 8876.
[38] Lam, R. T. S.; Belenguer, A.; Roberts, S. L.; Naumann, C.; Jarrosson, T.; Otto, S.; Sanders, J. K. M. *Science* **2005**, *308*, 667.
[39] Cousins, G. R. L.; Furlan, R. L. E.; Ng, Y.-F.; Redman, J. E.; Sanders, J. K. M. *Angew. Chem. Int. Ed. Engl.* **2001**, *40*, 423.
[40] Chung, M.-K.; Severin, K.; Lee, S. J.; Waters, M. L.; Gagné, M. R. *Chem. Sci.* **2011**, *2*, 744.
[41] Voshell, S. M.; Lee, S. J.; Gagné, M. R. *J. Am. Chem. Soc.* **2006**, *128*, 12422.
[42] Bulos, F.; Roberts, S. L.; Furlan, R. L. E.; Sanders, J. K. M. *Chem. Commun.* **2007**, 3092.
[43] Liu, J.; West, K. R.; Bondy, C. R.; Sanders, J. K. M. *Org. Biomol. Chem.* **2007**, *5*, 778.
[44] Houk, K. N.; Leach, A. G.; Kim, S. P.; Zhang, X. *Angew. Chem. Int. Ed. Engl.* **2003**, *42*, 4872.
[45] Otto, S. *Dalton Trans.* **2006**, 2861.
[46] Hubbard, B. K.; Walsh, C. T. *Angew. Chem. Int. Ed. Engl.* **2003**, *42*, 730.
[47] Mackay, J. P.; Gerhard, U.; Beauregard, D. A.; Williams, D. H.; Westwell, M. S.; Searle, M. S. *J. Am. Chem. Soc.* **1994**, *116*, 4581.
[48] Rodriguez-Docampo, Z.; Pascu, S. I.; Kubik, S.; Otto, S. *J. Am. Chem. Soc.* **2006**, *128*, 11206.
[49] Dawson, R. Data for biochemical research, 1959.
[50] K. R. West, R. F. Ludlow, P. Besenius, P. T. Corbett, P. A. G. Cormack, D. C. Sherrington, S. Otto, *J. Am. Chem. Soc*., **2008**, *130*, 10834-10835.
[51] Beeren, S. R.; Sanders, J. K. M. *Chem. Sci.* **2011**, *2*, 1560.
[52] Beeren, S. R.; Sanders, J. K. M. *J. Am. Chem. Soc.* **2011**, *133*, 3804.
[53] Newman, M. S.; Karnes, H. A. *J. Org. Chem.* **1966**, *31*, 3980-3984.
[54] Lloyd-Jones, G.C.; Moseley, J.D.; Renny, J.S. *Synth.* **2008**, 661-689.
[55] Molecular Networks: From Dynamic Combinatorial Libraries to Complex Systems. PhD Thesis, University of Cambridge 2008. R. Frederick Ludlow.
[56] Field, L.; Engelhard, P. R. *J. Org. Chem.* **1970**, 35, 3647.
[57] West, K. R. Molecular encapsulation through disulfide dynamic combinatorial chemistry. PhD thesis, University of Cambridge, England, **2006**.
[58] (a) Oae, S.; Takata, T.; Kim, Y. H. *Tetrahedron* **1981**, *37*, 37. (b) Takata, T.; Kim, Y. H.; Oae, S. *Tetrahedron Lett.* **1979**, *20*, 821. (c) Kice, J. L.; Rogers, T. E. *J. Am. Chem. Soc.* **1974**, *96*, 8009.
[59] K. R. West, R. F. Ludlow, P. T. Corbett, P. Besenius, F. M. Mansfeld, P. A. G. Cormack, D. C. Sherrington, J. M. Goodman, M. C. A. Stuart and S. Otto*. J. Am. Chem. Soc.*, **2008**, 130, 10835.
[60] (a) Atcher, J.; Moure, A.; Alfonso, I. *Chem. Commun.* **2013**, *49*, 487. (b) Atcher, J.; Alfonso, I. *RSC Adv.* **2013**, *3*, 25605.
[61] Hamieh, S.; Ludlow, R. F.; Perraud, O.; West, K. R.; Mattia, E.; Otto, S. *Org. Lett.* **2012**, *14*, 5404.
[62] Schanker, L. S.; Shore, P. A.; Brodie, B. B.; Hogben, C. A. *J. Pharmacol. Exp. Ther.* **1957**, *120*, 528.
[63] L. Vial, R. F. Ludlow, J. Leclaire, R. Perez-Fernandez and S. Otto. *J. Am. Chem. Soc.*, **2006**, *128*, 10253.
[64] Rudolph, J.; Theis, H.; Hanke, R.; Endermann, R.; Johannsen, L.; Geschke, F. U. *J. Med. Chem.* **2001**, *44*, 619-626.
[65] Montalbetti, C.; Falque, V. *Tetrahedron* **2005**, *61*, 10827-10852.
[66] Pearson, D. A.; Blanchette, M.; Baker, M. L.; Guindon, C. A. *Tetrahedron Lett.* **1989**, *30*, 2739-2742.

Chapter 7: Outlook

Identifying good binders

In chapter 5, an attempt to fit the host–guest binding constants using DCLFit revealed that most of the host-guest binding curves were defined by only a few data points at the beginning of the curves and many in the plateau regions. While this meant that deriving reliable binding affinities from the binding curves is impractical, it indicated that the macrocyclic hosts have very high affinities towards the α,ω-diamines guests.
Such a result was expected given that the polycationic polyamine spermine was previously found to bind to a macrocyclic host from the DCL with a high affinity of 10^7 M^{-1}. Binding involved the central two ammonium ions and four methylene units of the guest that were located inside the host cavity.
Therefore, it may be valuable to isolate the amplified macrocycles using preparative HPLC and then measure their binding affinities towards α,ω-diamines using (displacement) isothermal titration calorimetry (ITC). During the ITC analyses, nicotine, tyramine and ephedrine could serve as weaker competitive guests given their relatively modest binding affinities ranging from 10^3-10^4 M^{-1} towards the macrocyclic hosts.
These experiments may show the capability of the designed DCL to produce receptors effective at molecular recognition, and allow assessing host-guest selectivity, which until now is expressed only at the host amplification levels.
Moreover, it may be valuable to study the binding of cationic guest molecules featuring voluminous hydrophobic moieties such as compounds **7.1**, **7.2** and **7.3** (Figure 7.1) to the macrocyclic hosts. Such guest molecules have been reported by Isaac and co-workers to bind CB[*7*] with ultra high binding affinities in water,[1] and may allow the maximization of the induced-dipole interactions with the inner host cavities and the ion–dipole and salt bridge interactions with the carboxylate groups of the hosts, resulting in high binding strengths. This will shed more light on the binding capabilities of our easily accessible macrocyclic hosts.

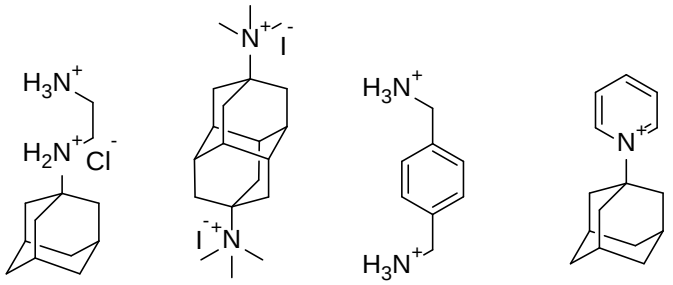

7.1 **7.2** **7.3** **7.4**

Figure 7.1: Structure of ammonium ion guests **7.1**, **7.2**, **7.3** and **7.4** which bind with high binding affinities to CB[*7*], ranging from 10^9-10^{17} M^{-1} in water, and which represent template candidates for the DCL system described in chapter 3.

Towards libraries of amino-acid functionalized macrocycles at thermodynamic equilibrium

In chapter 6, the derivatization of building blocks with amino acid residues was proposed as a simple method to increase the structural diversity of the corresponding DCLs. However, building up amino-acid functionalized DCLs was hampered by the slow oxidation rate of

both dithiol building blocks which resulted in DCLs which did not fully reach equilibrium and the formation of side products.
Two hypotheses were considered for explaining the slow oxidation rate. It may be the result of the decrease in the building block nucleophilicities after they were derivatized with amino acids, or it may be due to the steric hindrance caused by the bulky amino-acid substituents adjacent to the sulfur atoms, or both the effects may be occurring.
Comparing the oxidation rate of the building block that is derived from 2,5-dimercaptoterephthalic acid, in which thiols and carboxylic acid groups are in ortho position with respect to each other, with the oxidation rate of building block **6** that may be obtained from the previously synthesized 3,5-dimercaptoterephthalic acid[2] (Figure 7.2) may reveal which of the two hypotheses is more likely and may be valuable. Moreover, the peptide functionalized building block **7** reported by our group[3] has also shown a relatively slow oxidation rate and this was overcome by the use of sodium perborate as oxidant resulting in the rapid production of DCLs of macrocycles.[4] Furthermore, amino-acid functionalized building block **8** which should be easily accessible from the reported building block **1**[5] features benzene moieties substituted by electron withdrawing and donating groups and may be valuable for DCL studies.

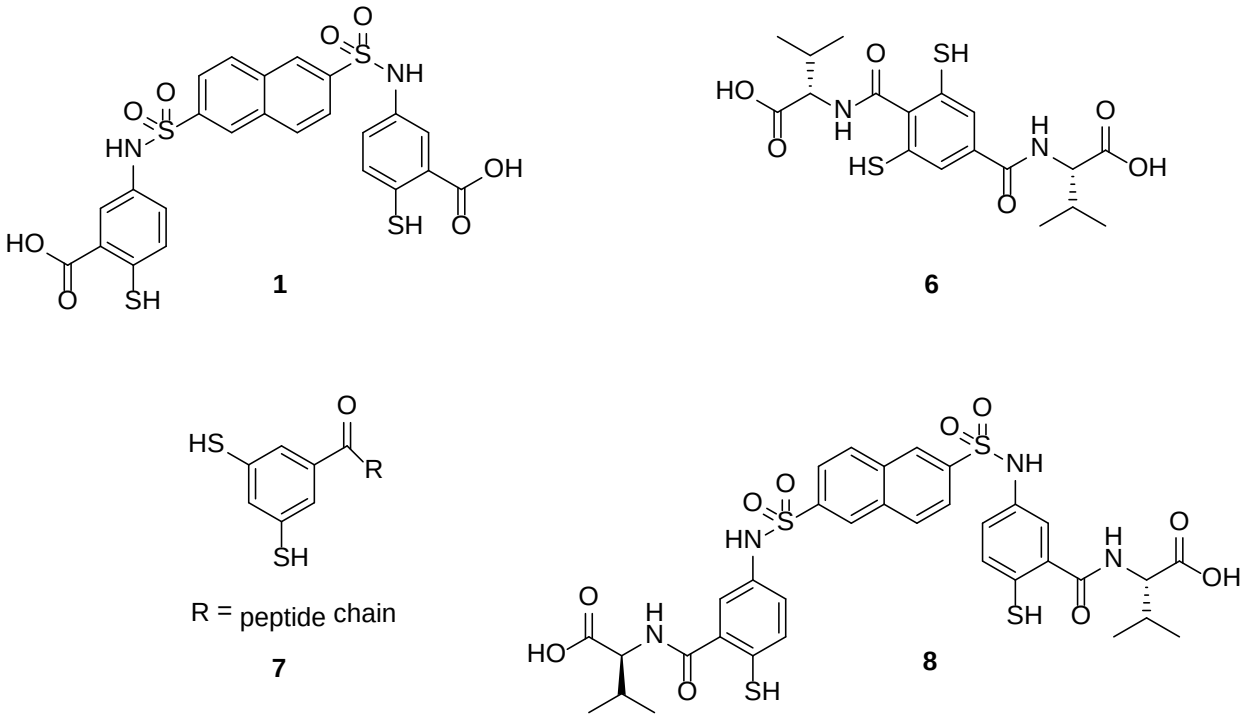

Figure 7.2: Structures of building blocks **6** derived from 3,5-dimercaptoterephthalic acid, peptide functionalized **7** and **8** derived from building block **1**.

Assessing molecular similarity using DCC

Assessing molecular similarity using DCC is a novel concept recently investigated by our group as a potentially useful tool in the drug discovery process.[6,7] Briefly, this concept centers on a systems approach to compare the external template effects on a DCL, in order to evaluate the possible similarity between the templates or effector molecules. Here the emphasis is on the multiple simultaneous molecular recognition events ideally involving

many receptors occurring upon templating, instead of focusing only on the individual library member-template interactions. The extent of the interaction between an effector and a particular library member (*e.g.* a host) provides information about the structure of this effector. However, this is only very limited information in comparison with the simultaneous interactions of the multiple library members with the effector. These interactions may provide more comprehensive descriptions of the molecular structure of the effector. In a standard experiment, a range of different classes of effectors are added as individual templates to a DCL. The DCLs are analyzed using LC-MS resulting in a multidimensional dataset made of amplification factors of all (detectable) library members. After, the data are subjected to multivariate analysis that gives a graph in which effectors with similar properties are ideally clustered. To predict the unknown activity of an effector, the latter is added to the DCL, which will classify it based on its similarity to the effectors with known biological activities.

The DCL system described in chapters 3 and 4 was able to discriminate between a range of organic ammonium ions in terms of sizes, lengths and number of cationic charges under near physiological conditions, after considering only the individual host-guest binding. Some of these templates belong to different classes of neurotransmitters while others were reported as potential drugs and the rest are with unknown biological activities. Thus, it may be valuable to investigate the ability of this DCL to assess the similarity between the templates by following the same systems approach mentioned above. Moreover, functionalizing the two dithiol building blocks forming this DCL with amino-acid residues has resulted in a more responsive (albeit not very clean) DCL, as described in chapter 6. This will enrich the multidimensional dataset made of amplification factors when using such a DCL for assessing molecular similarity, which may be valuable.

References

[1] Cao, L.; Šekutor, M.; Zavalij, P. Y.; Mlinarić-Majerski, K.; Glaser, R.; Isaacs, L. *Angew. Chemie* **2014**, *126*, 1006.
[2] Saggiomo, V. unpublished results
[3] Carnall, J. M. A.; Waudby, C. A.; Belenguer, A. M.; Stuart, M. C. A.; Peyralans, J. J.-P.; Otto, S. *Science* **2010**, *327*, 1502.
[4] Malakoutikhah, M.; Peyralans, J. J.-P.; Colomb-Delsuc, M.; Fanlo-Virgós, H.; Stuart, M. C. A.; Otto, S. *J. Am. Chem. Soc.* **2013**, *135*, 18406.
[5] Hamieh, S.; Ludlow, R. F.; Perraud, O.; West, K. R.; Mattia, E.; Otto, S. *Org. Lett*. **2012**, 14, 5404.
[6] Molecular Networks: From Dynamic Combinatorial Libraries to Complex Systems. PhD Thesis, University of Cambridge 2008. R. Frederick Ludlow.
[7] Saggiomo, V.; Hristova, Y. R.; Ludlow, R. F.; Otto, S. *J. Syst. Chem.* **2013**, *4*, 2.

Summary

Synthetic receptors for organic ammonium ions from disulfide DCLs

The first chapter shed some light on the biological importance of the molecular recognition of organic ammonium ions, and discussed the different types of the interactions involved in the recognition process in biological and aqueous and organic synthetic media. It also discussed the geometrical features of a successful synthetic receptor for these types of compounds by referring to key examples from the literature. It summarized the difficulties associated with obtaining synthetic receptors that are able to recognize organic ammonium ions in water at neutral pH. Typically, low binding affinities of these receptors, in comparison with those of proteins, were observed. The difficulties of design and synthesis and the modest binding affinity associated with obtaining a receptor through conventional chemistry were addressed. The use of external template effects in disulfide DCC was introduced as an alternative approach to conventional chemistry for obtaining synthetic receptors that are able to work in near physiological medium. Key examples of obtaining selective synthetic receptors for organic ammonium ions using disulfide DCC were discussed.

An example of successful use of an external template effect in disulfide DCC to obtain a synthetic receptor

The second chapter showed that external template effects in DCC, as an alternative approach to conventional chemistry, can be successfully used to obtain a synthetic receptor. Following this approach, carefully designed receptor fragments were able to generate a DCL of potential receptors from which nicotine, after its addition to the library, selected its (ideally) best receptor in water at neutral pH. Although the affinity of the selected nicotine receptor is lower by several orders of magnitude than those of biological nicotine receptors, this affinity was comparable to those of synthetic nicotine receptors reported so far, which have been obtained through conventional chemistry, such as the cyclophane-based receptor reported by Dougherty. The receptor we developed was obtained with 40 % yield, which is higher than that of Dougherty-type cyclophane the yield of which amounted to 18 %. ^{1}H NMR studies and CPK models of the nicotine-receptor complex suggested that only the pyridine moiety of nicotine is located within the cavity of the receptor. This notion was further supported by the invariabillity of the binding constants of the complex measured at different pHs. The binding mainly involved only the pyridine part of the guest and was driven by hydrophobic and π-π interactions, which explains the modest binding affinity obtained.

Extending the reductionist manner of using external template effects

The third chapter extended the use of external template effects in DCC. It described a carefully designed DCL of which nearly all of its members can be selectively amplified after being exposed to a range of specific templates. This showed that the selection potential in a DCL is not monopolized by one or two members but can be propagated to all of the library members. It also showed that a dynamic system is able to narrow the gap between its individual synthetic constituents and those of a biological system, not only in terms of the binding strength but also in terms of the number of functions that both systems are capable to exhibit.

A size selective DCL

The studied DCL was made from two dithiol building blocks and composed of six disulfide macrocycles featuring continuously increasing sizes and decreasing anionic charges, in addition to two different catenanes. When exposed to any of 30 organic ammonium ion templates of different sizes, shapes and numbers of cationic groups, the DCL amplified one or two macrocyclic hosts from among the six potential receptors, featuring similar cavity sizes and charges. Most of the chosen templates have biological activities and are subjects of research interest to many supramolecular chemists.

Quantification of the DCL composition

The oligomeric macrocycles are mostly constructed from a combination of four units of the two building blocks. The amplification factor *AF* was normalized to AF_n to compare the amplification between the DCL members. With *AF* being the proportion of the concentration of a given library member in the presence of a template relative to its concentration before template addition, and AF_n being the proportion of the increase (or decrease) in concentration of a library member relative to the maximum increase in concentration that this member can reach, upon templating. AF_n values range from -1 to +1 and allowed comparison of the amplification between the DCL members.

A DCL of synthetic receptors for a specific family of compounds

Chapter 4 is the continuation of the work presented in chapter 3. The research here centered on a DCL of synthetic receptors capable of binding a specific family of homologous guest molecules by adaptation to the different sizes and conformations of these guests.
We focused on aliphatic α,ω-diamines that differ in the length (n) of their alkane chain which ranged from 2 to 9 methylene units.
Aliphatic α,ω-diamines were individually added, as templates, to the DCL at a low ratio of template to total building block concentration in order to amplify the best binders. Comparing the effects of templates on the DCL revealed that the shorter templates with n = 2-7 amplified one macrocycle while the longer ones with n = 8-9 amplified another larger macrocycle. Comparing the effects of template additions on individual DCL members revealed that five individual templates of increasing lengths amplified five macrocycles of increasing sizes. Such length-size selectivity in amplification has not been reported thus far in DCC.

Estimation of host-guest binding strengths from the different product distributions of a DCL

In chapter 5, a fitting program (DCLFit) whereby quantitative information about host-guest affinities could be determined directly from the equilibrium concentration, was applied to study the DCL described in chapter 3. The program that had proven to work in a simple, experimental DCL, also was able to cope with a quite complex DCL composed of eight macrocyclic receptors, some of which consisted of multiple isomers. It generated reliable estimations of equilibrium constants for binding of the amplified oligomers to four individual templates, where the fitted concentrations correlated with the experimental ones obtained from their HPLC-UV peak areas. Moreover, reliably fitted binding constants were in close agreement with experimental ones obtained from ITC. Besides, the reported affinity constants were found to be the highest reported so far for synthetic receptors to biologically active molecules such as tyramine, ephedrine and nicotine.

Host amplifications correlate with host-guest binding strengths at subtoichiometric template concentration

The data from the fitted binding affinities of the library members towards four different templates was compared with the host amplification data. The comparison confirmed our previous computational finding that the host amplification factors (AFs) correlate with the host-guest binding affinities at substoichiometric template concentrations (relative to the DCL member concentrations).

The extent of host-guest binding strengths that DCLFit can reliably estimate for a disulfide DCL system is limited to approximately 10^5 M^{-1}

To obtain a reliable host-guest binding curve from which reliable binding affinities could be derived, the values of the latter should be in the same range of the reciprocal host concentrations. In a disulfide based DCL, the DCL member concentrations should not be much lower than mM concentration to make sure that the thiol oxidation rate is slower than that of disulfide exchange, so that the product distribution is under thermodynamic control. Therefore, the reliable range of affinity constants that DCLFit can estimate for a disulfide DCL system appears limited to 10^3-10^4 M^{-1}. Another factor that might limit the reliability of fitted binding affinities is the detection limit of the HPLC-UV system used to measure the concentrations of the DCL members.

Functionalization of a building block with natural amino acids in a DCL system

On attempt to diversify our existing set of building blocks, chapter 6 describes their derivatization with natural amino acids. We employed well-established peptide coupling methods that in principle allows the building blocks to acquire a wide range of molecular recognition properties as a large range of commercially available amino acids can be introduced. This method also allows the DCL to acquire additional diversity, solubility, chiral centers, flexibility or rigidity. Moreover, while many have reported the use of cysteine functionalized building blocks in water, very few have investigated more diverse amino acid functionalization of building blocks in water, which makes this work interesting.

Overall effects of substituting the carboxylic acid groups of the building blocks with valine residues

In chapter 6, the behavior of DCLs made from benzene or naphthalene derived dithiol building blocks which feature flat hydrophobic surfaces as central cores and carboxylic acid groups were compared with that of DCLs made from the same building blocks to which a valine residue had been coupled. Also, DCLs made from the combination of valine functionalized building blocks and those that were left unmodified have been studied. Valine side chains had a crucial role in the types of products that were formed, DCL distributions and library responses to templates. Moreover, the resulting macrocyclic hosts are somewhat more responsive to guests after substituting the carboxylic acids with the valine residues, and this may lead to better guest binding.[1] Intramolecular interactions seemed to occur between the flexible valine side chains of the macrocyclic hosts and these could potentially reinforce the host-guest binding under certain circumstances.[2] Unfortunately, also undesirable side reactions were observed upon introducing the valine residues.

References

[1] Au-Yeung, H. Y.; Pengo, P.; Pantoş, G. D.; Otto, S.; Sanders, J. K. M. *Chem. Commun.* **2009**, 419.
[2] (a) Otto, S. *Dalton Trans.* **2006**, 2861. (b) Hubbard, B. K.; Walsh, C. T. *Angew. Chem. Int. Ed. Engl.* **2003**, *42*, 730. (c) Mackay, J. P.; Gerhard, U.; Beauregard, D. A.; Williams, D. H.; Westwell, M. S.; Searle, M. S. *J. Am. Chem. Soc.* **1994**, *116*, 4581. (d) Rodriguez-Docampo, Z.; Pascu, S. I.; Kubik, S.; Otto, S. *J. Am. Chem. Soc.* **2006**, *128*, 11206.

Samenvatting

Synthetische receptoren voor organische ammonium-ionen uit disulfide dynamische combinatoriële bibliotheken

Het eerste hoofdstuk belichtte het biologische belang van de moleculaire herkenning van organische ammonium ionen, en besprak de verschillende soorten van interacties die betrokken zijn bij het herkenningsproces in biologische en waterige en organische synthetische media. Het besprak ook de geometrische kenmerken van een succesvolle synthetische receptor voor deze typen samenstellingen door te refereren aan belangrijke voorbeelden uit de literatuur. Het vatte samen welke moeilijkheden verbonden zijn aan het verkrijgen van synthetische receptoren die in staat zijn om organische ammonium-ionen te herkennen in water bij een neutrale pH. Doorgaans werd een lage bindingsaffiniteit van deze receptoren, in vergelijking met die van eiwitten, gevonden. De moeilijkheden bij het ontwerpen en synthetiseren en de matige bindingsaffiniteit die geassocieerd zijn met het verkrijgen van een receptor door middel van conventionele chemie kwamen aan de orde. Het gebruik van externe sjabloon effecten in disulfide dynamische combinatoriële chemie (DCC) werd geïntroduceerd als een alternatieve benadering voor de conventionele chemie voor het verkrijgen van synthetische receptoren die in staat zijn te functioneren in een bij benadering fysiologisch medium. Belangrijke voorbeelden van het verkrijgen van synthetische receptoren voor organische ammonium-ionen met gebruik van DCC werden besproken.

Een voorbeeld van succesvol gebruik van een extern sjabloon effect in disulfide-DCC om een synthetische receptor te verkrijgen.

Het tweede hoofdstuk liet zien dat externe sjabloon/template effecten in DCC, als alternatieve benadering voor conventionele chemie, succesvol kan worden toegepast om een synthetische receptor te verkrijgen. Door deze benadering te volgen, waren zorgvuldig ontworpen receptor fragmenten in staat om een dynamische combinatoriële bibliotheek (DCB) van potentiële receptoren te genereren, waaruit nicotine, nadat het aan de bibliotheek werd toegevoegd, zijn (idealiter) beste receptor selecteerde in water bij neutrale pH. Alhoewel de affiniteit van de geselecteerde nicotine receptor meerdere orden van grootte lager is dan die van biologische receptoren, was de affiniteit vergelijkbaar met die van synthetische nicotine receptoren die tot nu toe beschreven zijn, en welke verkregen zijn door middel van conventionele chemie, zoals de op cyclofaan gebaseerde receptor beschreven door Dougherty. De receptor die wij ontwikkelden werd verkregen met een 40% opbrengst, wat hoger is dan de opbrengst van het Dougherty-type cyclofaan welke 18% bedroeg. ^{1}H NMR studies en CPK modellen van het nicotine-receptor complex suggereerden dat enkel de pyridine helft zich in de holte van de receptor bevindt. Dit idee werd verder ondersteund door de onveranderlijkheid van de bindingsconstanten van het complex gemeten bij verschillende pH's. De binding betrof voornamelijk het pyridine-gedeelte van de gast en werd gedreven door hydrofobe en π-π-interacties, hetgeen de matige verkregen bindingsaffiniteit verklaart.

Uitbreiding van het gebruik van externe sjabloon effecten.

Het derde hoofdstuk breidde het gebruik van externe sjabloon effecten in DCC uit. Het beschreef een zorgvuldig ontworpen DCB waarvan bijna alle leden selectief kunnen worden versterkt na blootstelling aan een reeks specifieke sjablonen. Dit liet zien dat het selectiepotentieel in een DCB niet gemonopoliseerd wordt door één of twee leden, maar

over alle bibliotheekleden kan worden verspreid. Het liet ook zien dat een dynamisch systeem in staat is om de afstand tussen zijn individuele synthetische bestanddelen en die van een biologisch systeem te verkleinen, niet alleen op het vlak van bindingssterkte maar ook wat betreft het aantal functies die beide systemen in staat zijn te vertonen.

Een grootte selectieve DCB

De bestudeerde DCB werd gemaakt van twee dithiolbouwstenen en samengesteld uit zes disulfide macrocycli met continu toenemende grootten en afnemende anion lading, alsmede twee verschillende catenanen. Wanneer achtereenvolgens blootgesteld aan een van 30 organische ammoniumionsjablonen met verschillende grootten, vormen en aantallen cationgroepen, versterkte de DCB één of twee macrocyclische gastheren uit de zes potentiële receptoren, met vergelijkbare holtegrootte en lading. De meeste van de gekozen sjablonen hebben biologische activiteiten en zijn van interesse voor vele supramoleculair scheikundigen.

Het kwantificeren van de DCB samenstelling.

De macrocycli zijn meestal opgebouwd uit een combinatie van vier bouwstenen. De amplificatie factor (AF) werd genormaliseerd tot AF_n om de amplificatie tussen de DCB-leden te vergelijken. Waarbij AF de verhouding is van de concentratie van een gegeven bibliotheeklid in de aanwezigheid van een sjabloon ten opzichte van zijn concentratie voor toevoeging van de sjabloon, en AF_n de verhouding is van de toename (of afname) in concentratie van een bibliotheeklid ten opzichte van de maximale toename in concentratie die dit bibliotheeklid kan bereiken, bij sjabloontoevoeging. AF_n-waarden variëren van -1 tot +1 en maakten vergelijking van de amplificatie tussen verschillende DCB leden mogelijk.

Een DCB van synthetische receptoren voor een specifieke familie van gastmoleculen.

Hoofdstuk 4 is het vervolg op het werk gepresenteerd in hoofdstuk 3. Het onderzoek richtte zich hier op een DCB van synthetische receptoren die in staat zijn om een specifieke familie van homologe gastmoleculen te binden door aanpassing aan de verschillende grootten en conformaties van deze gasten.
We richtten ons op alifatische α,ω-diamines welke verschillen in de lengte (n) van hun alkaanketen variërend van 2 tot 9 methyleeneenheden.
Alifatische α,ω-diamines werden individueel toegevoegd, als sjablonen, aan de DCB in een lage verhouding van sjabloon ten opzichte van de totale bouwsteenconcentratie teneinde de beste binders te amplificeren. Vergelijking van de effecten van de sjablonen op de DCB toonde dat de kortere sjablonen, met n = 2-7, één macrocyclus amplificeerden, terwijl de langere, met n = 8-9, een andere langere macrocyclus amplificeerden. Vergelijking van de effecten van sjabloontoevoegingen op individuele DCB-leden liet zien dat vijf individuele sjablonen met toenemende lengtes vijf macrocycli van toenemende grootte amplificeerden. Dergelijke lenge-grootte-selectiviteit in amplificatie is niet eerder beschreven in DCC.

Inschatten van gastheer-gast bindingsterktes op basis van de verschillende productdistributies van een DCB.

In hoofdstuk 5 werd een computerprogramma (DCLFit), waarmee kwantitatieve informatie over gastheer-gast-affiniteit direct vanuit de evenwichtconcentraties kon worden bepaald, toegepast om de in hoofdstuk 3 beschreven DCB te bestuderen. Het programma dat had bewezen te werken in een simpele, experimentele DCB, bleek ook in staat om te gaan met

een redelijk complexe DCB samengesteld uit acht macrocyclische receptoren, waarvan sommige bestonden uit verschillende isomeren. Het genereerde betrouwbare schattingen van evenwichtsconstanten voor het binden van de geamplificeerde oligomeren aan vier individuele sjablonen, waarbij de geschatte concentraties correleerden met de experimentele concentraties, verkregen uit hun HPLC-UV piekopppervlakten. Bovendien waren de ingeschatte bindingconstanten in nauwe overeenstemming met experimentele waarden, verkregen middels microcalorimetrie. Daarnaast bleek dat de gerapporteerde bindingconstanten de hoogste zijn die tot nu toe beschreven zijn voor synthetische receptoren voor biologisch actieve moleculen zoals tyramine, ephedrine en nicotine.

Gastheer-amplificatie correleert met gastheer-gast bindingssterkte bij substoichiometrische sjabloonconcentratie.

De gegevens van de ingeschatte bindingsaffiniteiten van de bibliotheekleden jegens vier verschillende sjablonen werd vergeleken met de gegevens van gastheer-amplificatie. De vergelijking bevestigde onze eerdere rekenkundige bevinding dat de gastheer-amplificatiefactoren (AF's) correleren met de gastheer-gast-bindingsaffiniteit bij subtoichiometrische sjabloon/template concentraties (relatief ten opzichte van de DCB-lid-concentraties).

De omvang van gastheer-gast bindingssterktes die DCLFit betrouwbaar kan inschatten voor een disulfide DCB-systeem is gelimiteerd tot ongeveer 10^5 M^{-1}

Om een betrouwbare gastheer-gast bindingscurve te verkrijgen waaraan betrouwbare bindingsaffiniteiten kunnen worden afgeleid, zouden de waarden van deze laatste in hetzelf de bereik moeten liggen als die van de wederzijdse gastheerconcentraties. In een op disulfide gebaseerde DCL, zouden de DCL-lid-concentraties niet lager moeten zijn dan een mM-concentratie om er zeker van te zijn dat de thiol oxidatiesnelheid langzamer is dan de snelheid van de disulfideuitwisseling, zodat de productdistributie onder thermodynamische controle is. Daarom lijkt het betrouwbare bereik van evenwichtsconstanten die DCLFit kan inschatten gelimiteerd te zijn tot 10^3-10^4 M^{-1}. Een andere factor die mogelijk de betrouwbaarheid van de ingeschatte bindingsaffiniteiten limiteert is de detectielimiet van het HPLC-UV-systeem dat gebruikt wordt om de concentraties van de DCB-leden te meten.

Functionalisering van een bouwsteen met natuurlijke aminozuren in een DCL-systeem.

In een poging om onze set bouwstenen te diversifiëren, beschrijft hoofdstuk 6 hun derivatisering met natuurlijke aminozuren. We gebruikten hiervoor bekende peptide koppelingsmethoden die het in principe mogelijk maken dat de bouwstenen een breed bereik aan moleculaire herkenningseigenschappen verwerven, aangezien een breed bereik aan commercieel beschikbare aminozuren geïntroduceerd kan worden. Deze methode maakt het ook mogelijk dat de DCB extra diversiteit, oplosbaarheid, chirale centra, flexibiliteit of rigiditeit verwerft. Bovendien, terwijl velen het gebruik van met cysteïne gefunctionaliseerde bouwstenen in water hebben beschreven, hebben slechts zeer weinigen andere aminozuurfunctionalisatie in water onderzocht, hetgeen dit werk interessant maakt.

Effecten van het vervangen van carbonzuurgroepen van de bouwstenen met valineresiduen.

In hoofdstuk 6, werd het gedrag van DCB's gemaakt van uit benzeen of naftaleen gederivatiseerde dithiolbouwstenen, welke gekenmerkt worden door vlakke hydrofobe oppervlakten carbonzuurgroepen, vergeleken met dat van DCB's gemaakt van dezelfde bouwstenen waaraan een valineresidu was gekoppeld. Ook werden DCB's, gemaakt van een combinatie van met valine gefunctionaliseerde bouwstenen en niet-gemodificeerde bouwstenen, bestudeerd. Valinezijketens speelden een cruciale rol in de typen producten die werden gevormd, in DCB-distributies en in bibliotheek-respons op sjablonen. Bovendien zijn de resulterende macrocyclische gastheren wat meer responsief op gasten na vervanging van de carbonzuren door valineresiduen, en dit leidt mogelijk tot betere gastbinding.[1] Intramoleculaire interacties tussen de flexibele valine-zijketens van de macrocyclische gastheren zijn in principe mogelijk en deze zouden potentieel de gastheer-gast-binding kunnen versterken onder bepaalde omstandigheden.[2] Helaas traden ook ongewenste bijreacties op de introductie van de valine-residuen op.

Referenties

[1] Au-Yeung, H. Y.; Pengo, P.; Pantoş, G. D.; Otto, S.; Sanders, J. K. M. *Chem. Commun.* **2009**, 419.
[2] (a) Otto, S. *Dalton Trans.* **2006**, 2861. (b) Hubbard, B. K.; Walsh, C. T. *Angew. Chem. Int. Ed. Engl.* **2003**, *42*, 730. (c) Mackay, J. P.; Gerhard, U.; Beauregard, D. A.; Williams, D. H.; Westwell, M. S.; Searle, M. S. *J. Am. Chem. Soc.* **1994**, *116*, 4581. (d) Rodriguez-Docampo, Z.; Pascu, S. I.; Kubik, S.; Otto, S. *J. Am. Chem. Soc.* **2006**, *128*, 11206.

Synthèse

La chimie combinatoire dynamique (CCD) est une approche nouvelle et attractive pour générer et cribler des bibliothèques combinatoires dynamiques (BCD) de composés et ce, en une seule étape. La BCD est adaptable grâce aux interconnexions, covalentes ou non-covalentes, réversible entre ses composés, ce qui induit la sélection et l'amplification, idéalement, du composé (récepteur ou ligand) de meilleure affinité en présence d'une cible moléculaire (modèle).

Le thème général de cette thèse est le développement de récepteurs synthétiques pour des ions ammonium capables de travailler dans des conditions proches des conditions physiologiques (dans l'eau a pH = 7), en utilisant la CCD de ponts disulfures.

Le premier chapitre explique l'importance de ce développement et les difficultés associées à l'utilisation de l'approche conventionnelle itérative: conception, synthèse et test. Ensuite, il introduit les effets de l'ajout d'une cible moléculaire (modèle) à une BCD de composés générés par la formation et l'échange de ponts disulfures à partir de briques de construction de dithiols. Ces effets peuvent être utilisés comme une approche alternative et supérieure à la chimie conventionnelle pour obtenir des récepteurs pour des cibles choisies capables de travailler dans un milieu proche du milieu physiologique.

Le deuxième chapitre présente une utilisation réussie de cette approche pour développer un récepteur synthétique pour la nicotine. Le récepteur développé présente une constante d'affinité avec la nicotine comparable à celle des récepteurs déjà rapportés en littérature, et, est obtenue avec un rendement relativement meilleur. Le troisième chapitre décrit la conception d'une BCD de composés macrocycliques, à partir de deux briques de construction de dithiols. La quasi-totalité de membres macrocycliques de cette BCD peut être amplifiée avec une sélectivité basée sur une complémentarité récepteur-cible de taille, après avoir été exposée à trente ions ammonium comme cibles moléculaires. Le quatrième chapitre montre que les oligomères macrocycliques peuvent être amplifiés, avec une sélectivité basée sur une complémentarité cible-récepteur de longueur-taille, après avoir été exposé à des diamines α-ω aliphatiques de longueurs différentes.

Dans le cinquième chapitre, un programme d'ajustement (DCLFit) a été utilisé avec succès pour estimer de manière fiable les constantes d'affinités entre les composés de la BCD qui sont amplifiés et quatre cibles choisies. Les constantes d'affinités estimées étaient en accord étroit avec celles obtenues par calorimétrie isotherme à titrage (CIT), et se sont révélées être les plus élevées par rapport à celles de récepteurs synthétiques rapportés par la littérature à ce jour.

Le sixième chapitre décrit la dérivation des briques de construction de la BCD, rapportées en chapitre trois, avec des acides aminés naturels pour permettre à la BCD d'acquérir une diversité additionnelle, des centres asymétriques, des motifs supplémentaires de reconnaissance moléculaire, une rigidité ou une flexibilité. Les chaînes latérales de valine introduites lors de la dérivation ont joué un rôle crucial dans les types de produits formés, résultant en des nouvelles distributions et réponses des BCD aux cibles moléculaires ajoutées. Des réactions secondaires indésirables ont également été observées lors de l'introduction des résidus de valine.

Acknowledgements

For every story there is an end, and even for this story that sometimes seemed to never end, now the end has come. For sure I would not have been able to achieve this on my own and therefore this is the place to thank all the people that helped me along the way.

First I would like to thank Sijbren, my promoter, for giving me the chance to be in his group and allowing me the time to learn, improve and acquire new skills. I came for the job interview from Strasbourg, where I was doing an internship in ECPM. My English (being my third language) was a bit awkward and my chemistry knowledge was not the best. Sijbren looked past all that and saw how motivated I was and decided to grant me this opportunity. He motivated me to start reading English books, attend English language courses along with the chemistry courses that were part of my PhD studies. Sijbren's office door was always open for me to discuss my different projects; he always prompted me to look forward to the next step of the project and questioned me about "the what, how and why" of the projects. It will be difficult to mention all Sijbren's contributions and to fully capture his impact on me, but when seeing where I started and to where I have arrived now, I cannot see other than achievements and personal development, a big part of which I owe to Sijbren. I am glad to have worked with a big name in the field of dynamic combinatorial chemistry and my experience with him will surely bring me much good. Dank je wel, Sijbren and I hope that my motivation has fulfilled your expectations.

There are many of my lab mates in Sijben's group I would like to thank. I will now mention those people in chronological order of the time at which I met them. It is interesting to mention that I was the first to start in Sijbren's group in Groningen while Sijbren, at that time, was still in Cambridge together with Hugo, a PhD student, and Jerome, a former postdoc.

Jerome was the first to arrive from Sijbren's Cambridge group to Groningen. He helped me by teaching me how to use, assemble, disassemble and fix HPLC machines, explaining things to me many times even in French. Thanks Jerome for all the scientific discussions we have gone through, particularly those concerning Thursday morning presentations and development of the project we were both working on. Your help is appreciated and surely not forgotten.

The next person to arrive in the group was Hugo. Besides being a valuable colleague, he soon became a very good friend and a person with whom I could share everything. He has the rare quality of being able to combine science and social skills. And therefore I am very happy that he too achieved his PhD and I can say congratulations Hugo, not only for your professional achievements but also for becoming the father of a beautiful daughter. Thank you also for being the paranymph of my PhD ceremony and I am glad to be your paranymph also.

Thanks a lot to Jianwei, a former PhD student; I will never forget your wise words "Life is easy, they make it complicated".

Manuel, a former Postdoc, also helped me a lot in the beginning of the project of amino acid functionalized building blocks by sharing with me his experience in synthetic chemistry. Manuel, although the project did not work as we wished, but if you read chapter 6 now, you can see that it proposes a valuable explanation and possible solutions for the problems we encountered at that time.

I would like to sincerely thank Piotr Nowak, a PhD student. Piotr is a person who is ready to help from 10 am (or a bit later) until 2 am (and sometimes until the next day). From Piotr I learned the real meaning of generosity that goes beyond material things; discussing science, fixing equipment, improving presentations, offering ideas for the projects of others. The list is much longer but these are just some of his many academic hobbies that come to my mind. I have worked with him on the fitting program named DCLFit and learned a lot from his computer skills. I am really proud to know this person that rarely takes long holidays and says in his wise words “lets works now, later we will sleep for long”. Piotr, I applaud you for the list of qualities you possess and also would like to thank you for being my paranymph.

Vittorio, a former postdoc, has contributed to my scientific development by our daily extensive discussions about the results of my experiments (before discussing these with Sijbren) and development of the project. Vittorio, thank you also for improving presentations for conferences and also within the university and sorry for the many scientific discussions that I started at 5 pm, when Ilaria was awaiting you at home.

I would like to thank Elio, PhD student, for all the LC-MS he has performed for me. I appreciate the time he spent working on this, often after 6 pm when HPLC’s were available. Elio, I respect in you your honesty and directness and I am not surprised that you received so many good job offers. And also, I would like to thank you for the swimming techniques you taught me.

Jan, a postdoc, I would like to thank for improving my Thursday morning presentations and Andrea, a postdoc, for her support when I was dealing with the hard times of writing. I appreciated how she always tried to simplify the obstacles I was facing.

I would like also to thank again Andrea, Piotr, Jan, Asish (a postdoc) and Ivica for proofreading my long chapters. Thank you guys for having the patience for this; particularly chapter 6 which was a big task for Andrea.

I would like to thank Morteza, a former postdoc, for the nice time we spent together in Groningen, the football matches we have played along with Hugo and the swimming techniques he taught me. I would like to thank him for his support during the hard times of my thesis and the fruitful political discussions we always had and in which we never reached to an agreement.

My acknowledgements would not be complete without the mentioning of my PhD colleagues Shuo, Mathieu, Giulia, Boris, David, Meniz, Yigit and Jeffery and postdocs Andras, Gael, Yang and my student Abhinandan.

I would like to express my gratitude to the technical support team. Thanks to Monique Smith and great thanks to Theodora Tiemersma-Wegman for their assistance with HPLC and HPLC-MS analyses. I would like to express my gratitude to Wim Kruizinga and Pieter van der Meulen for their assistance with NMR experiments and to Hans van der Velde for his assistance with analytical experiments. Thanks also to our department secretaries: Hilda Biemold, Tineke Kalter-Meuken and Annette Witter-Waalkens.

I would like to thank the reading committee for taking the time and effort to read my work: Prof. Wesley Brown, from the University of Groningen, Prof. Stephan Kubik from Kaiserslautern University of Technology and Prof. Aldrik Velder from Wageningen

University. Thank you Prof. Brown for your comments and advices about the thesis and the PhD ceremony. I appreciate your modesty; for many PhD students in the department you are counted as a colleague. Prof. Velder and Prof. Kubik were part of the DCC Marie-Curie research training network to which I belonged and therefore I thank them for the contribution they have made to my personal development. Professor Kubik, thank you for your kindness and Professor Velder for your warm welcome and for the activities you organized at the side of the conference in Twente.

I would like to thank Abdelsamad, a technical account manager at the university whom I was lucky to meet just after finishing my job interview with Sijbren. Thank you Abdelsamad for welcoming me into Groningen, giving me detailed information about Groningen and its districts suitable for shopping and for living accommodation, all this in French. Meeting you at that time gave me the feeling that I would not be living abroad in Groningen.

From outside the university, I would like to express my deep appreciation to Akbel for her support during the writing times and her friendship that I am really proud of.
I would like to gratefully thank Chirine and Mazen for their nice company. You were like my Lebanese family in Groningen; thanks for calling every weekend to check on me and for the several dinner invitations that I still need to reciprocate. Thanks also to Jihan who also was part of my family in Groningen, and congratulations to her for becoming a mother of a beautiful baby girl. Also to Marjolijn thank you for the nice company and the moral support and to Ali for being proud of me simply because we were born in the same country. I greet you for your spontaneity.

Last but not least and before thanking my family I would like to express my gratitude to Dr. Maria Bouman, surgeon in UMCG hospital, for her infinity less support. Thanks Maria for standing up for me in the difficult moments I have passed through during the last months of writing without waiting thanking words or reciprocation. I greet in you all meaning of respect. Thank you also for your help in translating the summary and abstract of the thesis to the Dutch language but also for the proofreadings you have made. My list of thanking words to you is endless and your acts of kindness will never be wasted.

For my family, I think there are not enough words to describe my sincere feelings towards you. Thank you Salman Hamieh, my father, for your generosity and support from the time I traveled to France to prepare my master and for internships up to now. I sincerely hope that I have met your expectations. Your words after each telephone discussion while I was abroad were: “Okay, now what is next?” And next will hopefully be something that will make you proud. Thanks to my mother, Dam el Hana Zeiater for your kindness. You motivated me to continue school at a time when many people left it because of the war and see now how your efforts were fruitful. I am not good at writing thanking words to you and so my (only) hope is to concretize my sincere feeling towards you into more achievements, as this is how you like to be thanked.

I dedicate this thesis to these two very special people, my father and my mother.

Curriculum Vitae

Saleh Hamieh was born in Taraya, Bekaa valley, Lebanon. He started his university studies in the medical analysis department of the Saint Joseph University (USJ) -Beirut and later he switched to the department of chemistry of the Lebanese University where he received his Bachelor of Science in General Chemistry. He then joined Prof. M. Martino in SPCMIB Laboratory (Synthèse des Molecules d'Intérêts Biologiques) in the Paul Sabatier University (UPS) – Toulouse, France, for a 9 months research training period. He published his first paper with Martino's group, which concerned the use of the DOSY technique as a powerful tool for drug quality control. In 2007 he obtained his Master's Degree in Chemistry specializing in the interface Chemistry-Biology research area of the same University. His master project in the Laboratoire de Chimie de Coordination, CNRS, was on the subject of the synthesis of a new anti-tuberculosis agent. Later he attended a training in the ECPM (Ecole de Chimie, Materiaux et Polymers) Strasbourg-France in the LPCB laboratory (Laboratoire de physico-chimie bioinorganique) dealing with complexation of pyoverdine by biologically interesting metals. Afterwards he worked a short period for Ameeron Company in KSA, Khobar. In 2009, Saleh joined the research group of Prof. Sijbren Otto and started his PhD funded by the Marie Curie Network. He mainly worked on developing synthetic receptors for bioactive ammonium-ion molecules using dynamic combinatorial chemistry. During his PhD studies, Saleh supervised a (BSc) research student in a project entitled "synthesis of amino acid functionalized dithiol molecules as new building blocks in DCC", and assisted in teaching the practical course "Organic Chemistry I", for (second-year) BSc students in the Pharmacy and Life Science departments. Saleh is fully trilingual in English, French and Arabic and has a modest proficiency in the Dutch language.

Author's published papers:

A „dial-a-receptor" Dynamic Combinatorial Library
Hamieh, S.; Saggiomo, V.; Nowak, P.; Mattia, E.; Ludlow, R. F.; Otto, S. *Angew. Chem. Int. Ed*. **2013**, *52*, 12368 –12372.

A Synthetic Receptor for Nicotine from a Dynamic Combinatorial Library
Hamieh, S.; Ludlow, R. F.; Perraud, O.; West, K. R.; Mattia, E.; Otto, S. *Org. Lett.* **2012**, *14*, 5404–7.

Transient Substrate-Induced Catalyst Formation in a Dynamic Molecular Network
Fanlo-Virgós, H.; Alba, A.-N. R.; Hamieh, S.; Colomb-Delsuc, M.; Otto, S. *Angew. Chemie Int. Ed.* **2014**, *53*, 11346-11350.

Analysis of illegally manufactured formulations of tadalafil (Cialis®) by 2D DOSY, ^{1}H NMR and Raman spectroscopy
Trefi, S.; Routaboul, C.; Hamieh, S.; Gilard, V.; Malet-Martino, M.; Martino, R. *J. Pharm. Biomed. Anal.* **2008**, *47*, 103–113.